# Exploration and engineering of acetyl-CoA and succinyl-CoA metabolism in Saccharomyces cerevisiae

Baldi, N.

**DOI**
10.4233/uuid:5a458cb4-b825-4fb1-a212-391891b4eda6

**Publication date**
2021

**Document Version**
Final published version

**Citation (APA)**
Baldi, N. (2021). *Exploration and engineering of acetyl-CoA and succinyl-CoA metabolism in Saccharomyces cerevisiae*. [Dissertation (TU Delft), Delft University of Technology]. https://doi.org/10.4233/uuid:5a458cb4-b825-4fb1-a212-391891b4eda6

**Important note**
To cite this publication, please use the final published version (if applicable).
Please check the document version above.

# Exploration and engineering of acetyl-CoA and succinyl-CoA metabolism in *Saccharomyces cerevisiae*

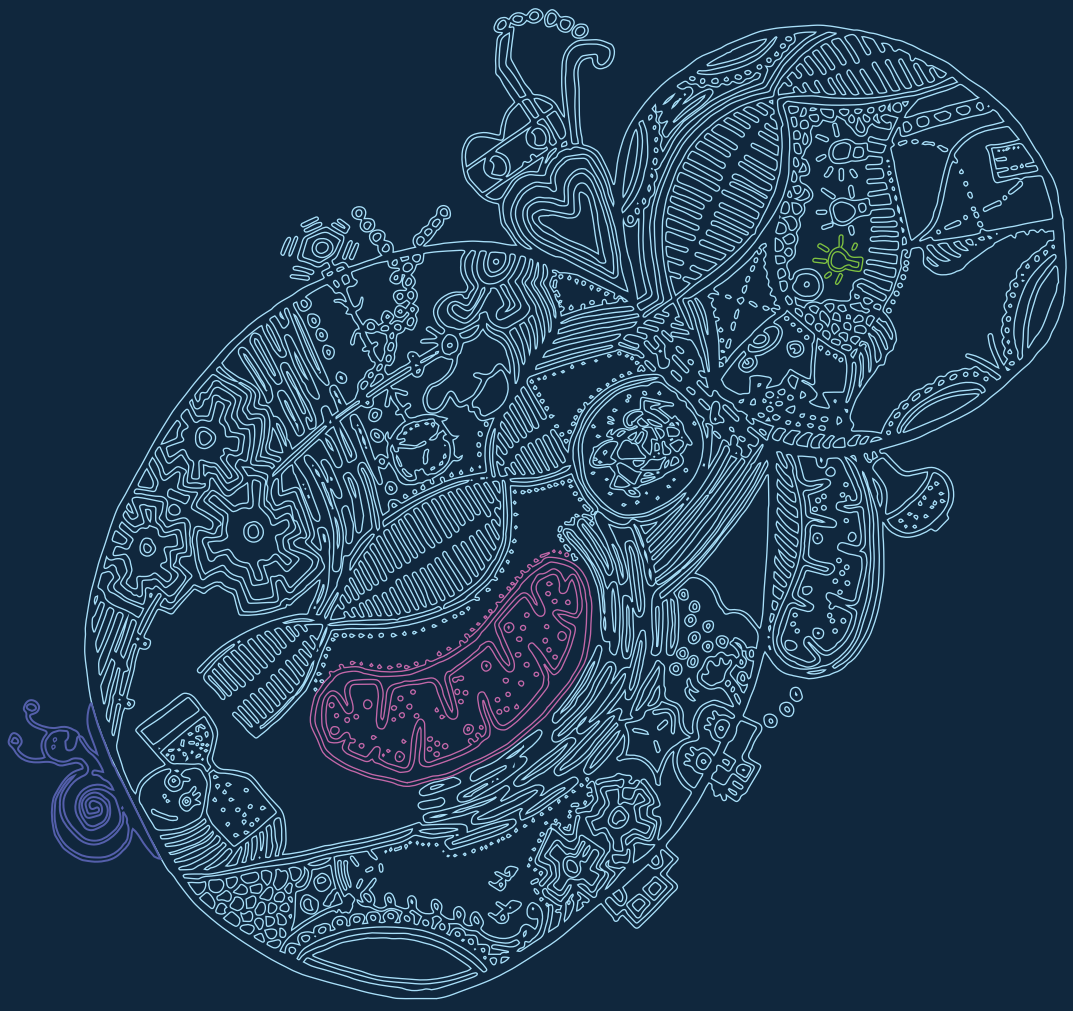

Nicolò Baldi

# Exploration and engineering of acetyl-CoA and succinyl-CoA metabolism in *Saccharomyces cerevisiae*

Dissertation
for the purpose of obtaining the degree of doctor
at Delft University of Technology
by the authority of the Rector Magnificus Prof.dr.ir. T.H.J.J. van der Hagen,
chair of the Board for Doctorates,
to be defended publicly on
Friday 11 June 2021 at 10:00 o'clock

by

**Nicolò BALDI**

Master of Science in Biotechnology,
Wageningen University and Research, the Netherlands
born in Rome, Italy

This dissertation has been approved by the promotor and copromotor.

Composition of the doctoral committee:

| | |
|---|---|
| Rector Magnificus | chairperson |
| Prof.dr. J.T. Pronk | Delft University of Technology, promotor |
| Dr.ir. R. Mans | Delft University of Technology, copromotor |

Independent members:

| | |
|---|---|
| Prof.dr. P.A.S. Daran-Lapujade | Delft University of Technology |
| Prof.dr.ir. A.J.A. van Maris | KTH Royal Institute of Technology, Sweden |
| Prof.dr.ir. R. van Kranenburg | Wageningen University and Research |
| Dr. C.E. Paul | Delft University of Technology |

Other member:

| | |
|---|---|
| Dr.ir. L. Wu | DSM |

Reserve member:

| | |
|---|---|
| Prof.dr. F. Hollmann | Delft University of Technology |

The research presented in this thesis was performed at the Department of Biotechnology, Faculty of Applied Sciences, Delft University of Technology, The Netherlands. This work was performed within the BE-Basic R&D Program (https://www.be-basic.org/), which was granted a FES subsidy from the Dutch Ministry of Economic Affairs, Agriculture and Innovation (EL&I). Research was performed in BE-Basic Flagship 10 in collaboration with Amyris (Emeryville CA, USA) and DSM (Delft, The Netherlands).

**Cover:** Marijke Luttik
**Layout:** Proefschriftmaken || www.proefschriftmaken.nl
**Printed by:** Proefschriftmaken || www.proefschriftmaken.nl
**ISBN:** 978-94-6423-270-7

An electronic version of this thesis is available at http://repository.tudelft.nl

# Table of contents

# Samenvatting

In de afgelopen decennia is biotechnologie steeds prominenter aanwezig in onze samenleving. In supermarkten liggen naast biotechnologische basisproducten zoals bier, brood en wijn ook wasmiddelen met enzymen en zepen met biotechnologisch geproduceerde geuren, die allemaal verpakt kunnen zijn in plastic dat geproduceerd is uit organisch afval. In de medische wereld zijn door gebruik van biotechnologie nieuwe moleculen ontwikkeld en op de markt gebracht die gericht zijn op het behandelen van de meest slopende ziektes: van diabetes tot malaria. Daardoor zijn duizenden levens gered.

De inleiding, **hoofdstuk één** van dit proefschrift, begint met het maken van een schets van hoe, samen met aanvullende technologieën, microbiologische biotechnologie kan bijdragen tot het bestrijden van klimaatverandering. In deze context zijn er al biotechnologische producten geïntroduceerd in de energie- en chemische grondstoffenmarkt, maar vanwege het kostenconcurrentievermogen van petrochemicaliën wordt het gebruik van biogebaseerde brandstoffen en chemicaliën beperkt. De economische haalbaarheid van een biotechnologisch proces wordt sterk beïnvloed door drie essentiële aspecten: titer (productconcentratie), snelheid en opbrengst. In de microbiologische biotechnologie is een van de belangrijkste factoren die invloed heeft op deze prestatie-indicatoren de beschikbaarheid, in het gekozen organisme, van de benodigde moleculen voor productroutes. In eukaryotische celfabrieken zoals gisten en andere schimmels zijn worden heterologe routes voor productvorming over het algemeen tot expressie gebracht in het cytosol. Deze cytosolische localisatie kan de toegankelijkheid van de productroutes voor moleculair bouwstenen beperken, als deze gemaakt worden in andere delen in de cel. Dit proefschrift focust op de energiekosten en beschikbaarheid in het cytosol van twee belangrijke biosynthetische bouwstenen, acetyl-CoA en succinyl-CoA, in de gist *Saccharomyces cerevisiae*, die veel gebruikt wordt in grootschalige industriële processen.

Er wordt in het algemeen aangenomen dat succinyl-CoA exclusief aanwezig in de mitochondriën van *S. cerevisiae*. In tegenstelling hiertoe kan acetyl-CoA gesynthetiseerd worden in zowel het cytosol als de mitochondriën, waarbij verschillende mechanismen

betrokken zijn. Zowel de hieruit voortkomende verschillende energiekosten voor de synthese van acetyl-CoA in deze celcompartimenten, als de gevolgen voor de vorming van het industrieel product, worden besproken in **hoofdstuk één**. Dit hoofdstuk beschrijft ook eerdere pogingen om deze energiekosten te beperken en de uitdagingen die men is tegengekomen bij het bereiken van dit doel.

**Hoofdstuk twee** beschrijft de implementatie van een nieuwe katabole route in de *S. cerevisiae* en de toename van haar capaciteit door middel van laboratorische evolutie. In deze gist kost synthese van cytosolisch acetyl-CoA uit pyrodruivenzuur twee mol ATP per mol acetyl-CoA. Om de ATP die gebruikt is in dit proces te regenereren, is dissimilatie van het substraat nodig, wat de opbrengst beperkt van producten die uit cytosolisch acetyl-CoA worden gemaakt. In eerder onderzoek werd deze van nature aanwezige ATP-consumerende route voor de synthese van cytosolisch acetyl-CoA vervangen door een ATP-onafhankelijke route via een heteroloog pyruvaatdehydrogenase (PDH) dat in het gistcytosol tot expressie werd gebracht. De resulterende stam kon cytosolisch acetyl-CoA synthetiseren in een tempo dat snelle groei mogelijk maakte, maar voor productvorming zou een nog veel hogere synthesesnelheid nodig zijn. Het onderzoek dat gepresenteerd wordt in hoofdstuk twee focust op een metabole ontwerpstrategie om de pyruvaatdissimilatie om te leiden door een heteroloog tot expressie gebracht PDH. Daartoe werden de *S. cerevisiae* pyruvaatdecarboxylase-genen (*PDC1*, *PDC5* en *PDC6*) en een gen dat codeert voor een essentiële subunit van het natuurlijke mitochondriële PDH (*PDA1*) verwijderd en een cytosolisch PDH tot expressie gebracht. De ontworpen stam kon niet onmiddellijk groeien op koolstofbronnen waarvan de stofwisseling via pyruvaat verloopt. Daarom werden evolutie-experimenten in het lab gebruikt om extra mutaties te selecteren, die het mogelijk zouden maken om het heterologe, cytosolische PHD te gebruiken als enig mechanisme voor pyruvaatdissimilatie. Geëvolueerde stammen lieten groeisnelheden op lactaat, een substraat dat exclusief wordt gedissimileerd via pyruvaat, zien van maximaal 0.15 $h^{-1}$. Het opnieuw bepalen van de DNA-volgorde van de genomen van geëvolueerde stammen gaf geen volledige verklaring voor voor het onderliggende moleculaire mechanisme dat verantwoordelijk was voor hun snelle groei. Hoewel in meerdere evolutie-lijnen een mutatorfenotype optrad dat interpretatie van de geaccumuleerde mutaties moeilijker maakte, kon uit deze analyse toch een rol van de beschikbaarheid van intramitochondrieel acetyl-CoA afgeleid worden.

**Hoofdstuk drie** beschrijft het eerste experimentele bewijs voor de synthese van cytosolisch succinyl-CoA in *S. cerevisiae*. Om de cytosolische synthese van dit metaboliet mogelijk te maken, werden de structurele genen voor alle drie de subunits van het *Escherichia coli* α-ketoglutaraatdehydrogenase (αKGDH) complex tot expressie gebracht in *S. cerevisiae*. Tegelijkertijd werd een *E. coli*-enzym tot expressie gebracht om lipoylering van het αKGDH-complex, wat nodig is voor enzymatische activiteit, mogelijk te maken. Kolomchromatografie met scheiding op molecuulgrootte en massaspectrometrie toonden aan dat het αKGDH-complex alle subunits bevatte en dat het dezelfde grootte had als in *E. coli*. Functionele expressie van het heterologe complex bleek uit de toename van de αKGDH-activiteit in de cytosolische fractie van gistcelhomogenaten. De cytosolische activiteit van het

αKGDH-complex werd *in vivo* getest door het maken van een reporterstam waarin het metaboliet 5-aminolevulinezuur gesynthetiseerd kon worden uit cytosolisch, maar niet uit mitochondrieel, succinyl-CoA. Daartoe werd *HEM1*, het gen dat codeert voor het mitochondrieel enzym 5-aminolevuliniczuur (ALA) synthase, dat succinyl-CoA omzet, verwijderd en vervangen door een bacterieel ALA synthase dat in het cytosol tot expressie werd gebracht. In de resulterende stam hing de complementatie van ALA auxotrofie af van de activering van het αKGDH-complex door de toevoeging van lipoinezuur. Deze functionele expressie van een bacterieel αKGDH-complex in gist vormt een belangrijke stap naar efficiënte productie, met gistcultures, van verbindingen zoals 1,4-butanediol en 4-aminobutyraat, waarvan de productroutes succinyl-CoA gebruiken als bouwsteen.

In het onderzoek verricht in **hoofdstuk twee**, werd melkzuur gebruikt als koolstofbron in de groeimedia. Losstaand van dit gebruik is melkzuur een product van belang in industriële biotechnologie met toepassingen in de voedselindustrie, in de medische wereld en in polymeerscheikunde. Hoewel de routes die dit organische zuur met het centraal koolstofmetabolisme verbinden goed bekend zijn, is de export van melkzuur uit microbiële cellen tot dusver nog onvolledig begrepen. In voorafgaand onderzoek leidde laboratoriumevolutie van een *S. cerevisiae*-stam waaruit de belangrijke carbonzuurtransporter Jen1 was verwijderd, tot de ontdekking dat een eiwit dat betrokken is bij transport van acetaat (Ady2), ook lactaat kan transporteren. Het in **hoofdstuk 4** beschreven onderzoek laat zien dat een stam die geen van beide transporters bezit, na laboratoriumevolutie weer lactaat kon consumeren. Bepaling van de DNA-volgorde van het hele genoom van verschillende bracht aan het licht dat twee *ADY2* homologen (*ATO2* en *ATO3*) waren gemuteerd in verschillende geëvolueerde cellijnen. Het introduceren van deze mutaties in een niet-geëvolueerde stam en een daaropvolgende fysiologische karakterisering liet zien dat de betreffende varianten van Ato2 en Ato3 efficiënt melkzuur de cel in konden transporteren. Modellering van de 3D-structuren van Ady2, Ato2 en Ato3 liet zien dat mutaties die efficiënt transport van melkzuur mogelijk maakten, vaak leidden tot verandering van een van de drie aminozuren die de hydrofobe constrictie van het anionkanaal vormen. Wij stellen voor dat een verwijding van deze constrictie in deze transporters gefaciliteerde diffusie van melkzuur mogelijk maakte.

# Summary

In the past decades, biotechnology has become ever more prominent in our society. On supermarket shelves, biotechnological staple products such beer, bread and wine are accompanied by enzyme-containing detergents and soaps with biotechnologically produced fragrances, all of which are possibly packaged with bio-derived plastics. In the medical field, new molecules aimed at treating the most debilitating diseases known to humanity, from diabetes to malaria, have been developed and commercialized using biotechnology, saving thousands of lives in the process.

The introductory Chapter 1 of this thesis starts by outlining how, together with other complementary technologies, microbial biotechnology can contribute to combating climate change. In this context, biotechnological products have already entered the energy and commodity chemicals markets, although cost-competitiveness with their conventional petrochemical counterparts is still limiting the widespread use of bio-based fuel and chemicals. The economic feasibility of a biotechnological process is strongly influenced by three critical aspects of product formation: titer, rate and yield. In microbial biotechnology, one of the key factors affecting these performance indicators is the availability, in the organism of choice, of precursor molecules for product pathways. In eukaryotic cell factories such as yeasts and other fungi, heterologous product pathways are usually expressed in the cytosol. This cytosolic localization may limit access to precursors that are generated in other cellular compartments. This dissertation focuses on the energetic cost and cytosolic availability of acetyl-CoA and succinyl-CoA, two key biosynthetic precursors, in the yeast *Saccharomyces cerevisiae*, which is used in many large-scale industrial processes.

In *Saccharomyces cerevisiae* succinyl-CoA is generally assumed to be exclusively localized in the mitochondria. In contrast, acetyl-CoA can be synthetized in the cytosol as well as in the mitochondria, albeit by different mechanisms. The different energetic costs for the synthesis of cytosolic acetyl-CoA in these two compartments, as well as its repercussions on industrial product formation, are discussed in **Chapter 1**. This Chapter also describes

previous attempts at reducing said energetic cost, and the challenges encountered in achieving this goal.

**Chapter 2** describes the implementation of a novel catabolic route in *S. cerevisiae* and the increase of its capacity by laboratory evolution. In this yeast, synthesis of the cytosolic acetyl-CoA pool comes at the cost of two moles of ATP per mole of acetyl-CoA formed. To regenerate the ATP invested in this conversion, substrate dissimilation is required, which effectively limits the yield of acetyl-CoA derived products. In previous work, this native, ATP-consuming pathway for cytosolic acetyl-CoA synthesis was replaced by an ATP-independent route via a heterologous pyruvate dehydrogenase (PDH) expressed in the yeast cytosol. While the resulting strain was able to synthesize cytosolic acetyl-CoA at a rate that enabled rapid growth, a much higher synthesis rate would be required for product synthesis. The research presented in Chapter 2 first focused on a metabolic engineering strategy to completely redirect pyruvate dissimilation through the heterologously expressed PDH. To this end, the *S. cerevisiae* pyruvate decarboxylase genes and (*PDC1*, *PDC5*, *PDC6*) and a gene encoding an essential subunit of the native, mitochondrial PDH (*PDA1*) were deleted, and a cytosolic PDH was expressed. The engineered strain could not immediately grow directly on carbon sources whose metabolism converged at pyruvate. Therefore, laboratory evolution was used to select for additional mutations that would allow the heterologous pathway to serve as sole mechanism for pyruvate dissimilation. Evolved strains exhibited growth rates on lactate, a substrate that is exclusively dissimilated via pyruvate, of up to 0.15 $h^{-1}$. Resequencing of the genomes of evolved strains did not allow for a complete resolution of the molecular mechanism underlying their fast growth. However, despite the emergence, in multiple evolution lines, of a mutator phenotype that complicated interpretation of the accumulated mutations, a possible role of the intramitochondrial acetyl-CoA pool could be inferred.

In **Chapter 3***,* the first experimental proof for the synthesis of cytosolic succinyl-CoA in *Saccharomyces cerevisiae* is described. To enable cytosolic synthesis of this metabolite, the structural genes for all three subunits of the *Escherichia coli* α-ketoglutarate dehydrogenase (αKGDH) complex were expressed in *S. cerevisiae*. The *E. coli* lipoic-acid scavenging enzyme was co-expressed to enable cytosolic lipoylation of the αKGDH complex, which is required for its enzymatic activity. Size-exclusion chromatography and mass spectrometry indicated that the heterologously expressed αKGDH complex contained all subunits and that its size was the same as in *E. coli*. Functional expression of the heterologous complex was evident from increased αKGDH activity in the cytosolic fraction of yeast cell homogenates. In vivo cytosolic activity of the αKGDH complex was tested by constructing a reporter strain in which the essential metabolite 5-aminolevulinic acid could only be synthetized from cytosolic, and not mitochondrial, succinyl-CoA. To this end *HEM1*, which encodes the succinyl-CoA-converting mitochondrial enzyme 5-aminolevulinic acid (ALA) synthase, was deleted and a bacterial ALA synthase was expressed in the cytosol. In the resulting strain, complementation of ALA auxotrophy depended on activation of the αKGDH complex by lipoic acid addition. Functional expression of a bacterial αKGDH complex in yeast represents

a vital step towards efficient yeast-based production of compounds such as 1,4-butanediol and 4-aminobutyrate, whose product pathways use succinyl-CoA as a precursor.

In the research performed in Chapter 2, lactic acid was extensively used as the carbon source in the growth media. Apart from this use, lactic acid is a product of interest in industrial biotechnology, with uses in food industry, in medicine and in polymer chemistry. Although the pathways connecting this organic acid to the central carbon metabolism are well known, its export from microbial cells remains elusive. In previous work, adaptive laboratory evolution of a *S. cerevisiae* strain lacking the major carboxylic acid transporter *JEN1,* led to the identification of a gene involved in acetate transport (*ADY2*), which was also able to transport lactate. Our work in **Chapter 4** shows that a strain lacking both these transporters can, by means of adaptive laboratory evolution, be evolved to consume lactate. Whole genome sequencing of different colony isolates revealed that two *ADY2* homologues (*ATO2* and *ATO3*) were mutated across multiple evolution lines. Reverse engineering of these mutations and subsequent physiological characterization showed that these transporters were able to efficiently transport lactic acid into the cell. Modeling of the 3D structures of *ADY2*, *ATO2* and *ATO3* revealed that mutations allowing efficient transport of lactic acid often occur in one of three amino acid residues that comprise the hydrophobic constriction of the anion channel. We propose that an increased size of the constriction present in these transporters may allow for facilitated diffusion of lactic acid.

# 1.
# General introduction

Scientific research articles presume the reader to be knowledgeable of the concepts and vocabulary used in the field. As scientific literature is most often directed at peers, a technical, unambiguous writing style helps in unequivocally communicating experimental results and in avoiding unnecessary repetition. It does, however, tend to make scientific works unfriendly and difficult to grasp for the general public. While the use of a technical vocabulary is necessary for a description of the technical details of this work, sections 1.1, 1.2, 1.3 and 1.4 of this introductory chapter have mostly been written in layman's terms, with the intention to make them accessible for a broader audience. Before delving into specific technical details, these sections outline a huge societal challenge that scientists around the world are trying to address, and the role biotechnology plays in it.

## 1.1 Consequences of climate change

Today, climate change is the single biggest threat facing humanity. Avoiding an increase of the average global temperature of over 1.5 °C, relative to the average temperature of the past 150 years, is widely held to be crucial to avoid extensive irreparable damage (Stocker et al., 2013). In 2019, the average global temperature was already 0.95 °C above the 20$^{th}$ century average (NOAA, 2019).

Climate change will not only cause damage to the natural environment, but also socio-economic disruption and, ultimately, loss of human lives (Masson-Delmotte et al., 2018; Reuveny, 2007). Melting of the polar caps will cause flooding of low-lying, often densely populated, areas (McMillan et al., 2014) and higher global average temperatures will de-stabilize local habitats, causing animal migration towards higher latitudes and altitudes (Hill et al., 2011) and species extinction (Sala et al., 2000; Thomas et al., 2004). Severe weather events, flooding and droughts will increase, both in intensity and frequency, with an ever larger negative impact on crop yields (Rosenzweig and Parry, 1994). As a still growing world population seeks to get out of poverty, food supply will not be able to meet the expected demand by 2050 (Lobell et al., 2008; Lobell et al., 2011). By 2050, an estimated 25 million to 1 billion people will have fled low laying coastal regions from rising sea levels (Brown, 2009; Clark et al., 2016) and between 25 and 36 countries will lose 10 % or more of their coastal areas (Marzeion and Levermann, 2014). As the northern polar cap shrinks, new waterways will open up for trade, and new areas will be available for the exploitation of natural resources. These situations have the potential of exacerbating geopolitical tensions between countries already at odds over maritime and land boundaries (WEF, 2020).



## 1.2 Causes of climate change

The scientific community virtually unanimously recognizes the anthropogenic (i.e. caused by human activity) increase of the atmospheric concentrations of greenhouse gases as single biggest contributor to the current increase of global average temperatures (Metz et al., 2001). Greenhouse gases act by reflecting infrared radiation (heat) emitted from earth back to the surface (much like the way in which a greenhouse keeps warmth in – hence the name). Different gases, including carbon dioxide ($CO_2$), methane ($CH_4$) and nitrous oxide ($N_2O$) have the potential to cause this effect, with $CO_2$ being the biggest contributor to the current climate change. Over the past 800,000 years, the global average $CO_2$ concentration in the Earth's atmosphere ranged between 175 and 300 parts per million (ppm)[1] (Bereiter et al., 2015). However, since the industrial revolution of the 19$^{th}$ century, this concentration steadily increased, reaching 408 ppm in 2018 (Figure 1). Over this time period, fossil resources were increasingly used for the production of fuels and commodity chemicals. The latter are chemicals used as precursors for the production of different goods that are

1 Parts per million (ppm) is the accepted unit to measure the concentration of carbon dioxide in the atmosphere. 175 ppm corresponds to 0.34 grams of $CO_2$ per cubic meter of air ($g \cdot m^{-3}$), 300 ppm corresponds to 0.58 $g \cdot m^{-3}$, and 408 ppm to 0.79 $g \cdot m^{-3}$.

used on a very large scale, such as plastics. Fuel burning for power generation and goods production were therefore at the basis of a massive release of $CO_2$ into the atmosphere.

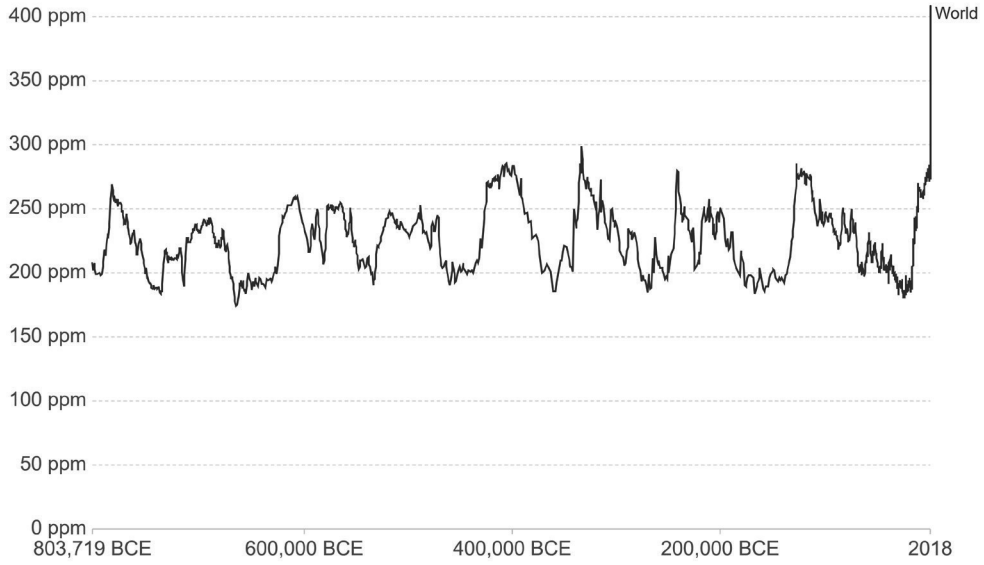


**Figure 1** Global average long-term atmospheric concentration of carbon dioxide ($CO_2$) measured in parts per million (ppm). Adapted from: ourworldindata.org/co2-and-other-greenhouse-gas-emissions. Data source: Bereiter et al. (2015)

Accumulation of $CO_2$ in the atmosphere is a direct consequence of the hugely different rates at which $CO_2$ is formed or converted to fossil fuels (van Maris et al., 2006) (Figure 2). In the past few centuries, mankind has used fossil resources for power generation at an ever-increasing rate, thereby rapidly releasing $CO_2$ into the atmosphere. Fossil resources have themselves been formed from $CO_2$, but this process is extremely slow. It starts with the fixation (capture) of $CO_2$ by plants and algae to yield biomass (organic matter in living or dead organisms). This biomass can then sediment and fossilize, thus trapping carbon from the atmosphere to underground reservoirs. While the fixation of $CO_2$ by plants and algae is a relatively fast process, the subsequent sedimentation and fossilization of biomass can take millions of years. This disparity in rates lies at the root of the current climate problem.

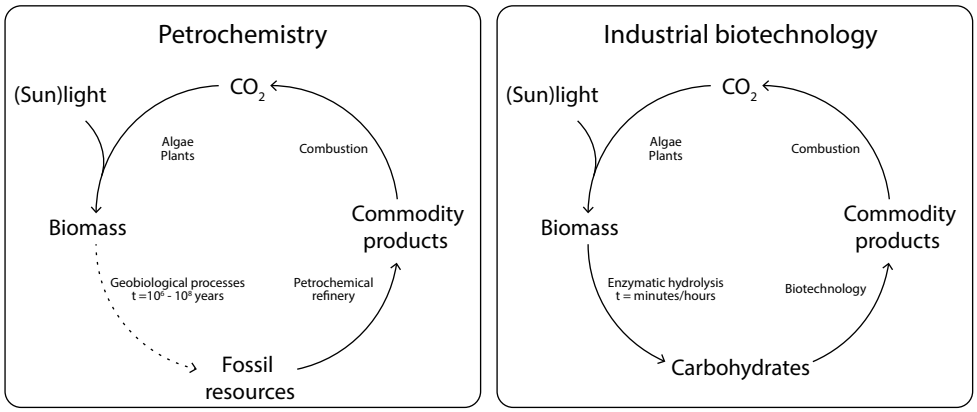


**Figure 2** Carbon cycle of commodity products. Left: Petrochemical material streams. Right: Industrial biotechnology streams. $10^6$: 1 million years. $10^8$: 100 million years. Adapted from van Maris et al. (2006)



To avoid the warming effects caused by a further increase of atmospheric $CO_2$, the use of fossil resources should be reduced to zero before 2050 (Rogelj et al., 2018). In order to achieve that, strategies are urgently needed to replace fossil-based processes for chemical production and power generation with renewable ones.

## 1.3 Strategies to abate carbon dioxide emissions

To meet the energy demand of a still growing human population, and at the same time reduce $CO_2$ emissions, implementation of new technology for power generation and production of materials will have to go hand in hand with behavioral changes.

Reducing or eliminating $CO_2$ emissions will inevitably require changes in life style, as new policies and technologies often require decades before their implementation at a national level, while behavioral shifts have the potential to be rapidly implemented (Pacala and Socolow, 2004). A European household produces between 8 and 10 tons of $CO_2$ per year per person, while in the US this value fluctuates between 12 and 16 tons of $CO_2$. Within these carbon budgets, the proportions are roughly equivalent: 30 % derives from transportation, 30 % from utilities (electricity and gas) and 20-30 % from production and consumption of food, with the remaining 10-20 % derived from tangible products (Jones and Kammen, 2011; Ottelin et al., 2019). In this context, behavioral changes such reducing meat consumption, living without a car and avoiding air travel have the potential of reducing yearly per capita emission by 30 to 50%.

At present, we are observing a shift in regards to power generation. The energy obtained from solar and wind power plants is, thanks to the development of new technologies, becoming more and more affordable. In many parts of the world, its cost is currently on par with fossil-

derived energy (Comello et al., 2018). These forms of renewable energies, together with the use of non-$CO_2$ emitting technologies such as geothermal facilities, hydroelectric dams and nuclear power plants, have the potential to eliminate $CO_2$ production for power generation.

There is also an increasing trend of replacing traditional, gasoline-based road vehicles with electric ones. While this shift is possible for short-range transport by road, it is not currently applicable for long-range road transport, shipping and, in particular, aviation, due to the low energy density of electric batteries[2]. To avoid using fossil-based fuels for these modes of transport, biotechnological processes have been developed in which sugars from fast growing plants (sugar cane and corn) can be converted into liquid transport fuels (biofuels). These biomass-derived fuels have the potential to very strongly reduce net $CO_2$ emissions relative to conventional fossil-based transport fuels. At first glance, this may seem peculiar, since the amount of $CO_2$ released upon combustion of biofuels is roughly equal to the amount emitted by an energy-equivalent amount of fossil-derived fuel. However, the amount of $CO_2$ released from biofuels is then again incorporated in the plants and crops used to produce the biofuels in the first place, thereby dramatically shortening its retention time in the atmosphere by several thousand folds. As an illustration, when biofuels are produced from fast-growing plants such as corn or sugar cane, the $CO_2$ will already be fixed in next growth season and completely bypass the slow fossilization process (see Figure 2, “Industrial biotechnology”). It has to be noted that this ‘zero-net-emission scenario’ does not include the $CO_2$ generated during the production of fertilizers, nor any $CO_2$ emitted when land is repurposed for the cultivation of suitable crops (Fargione et al., 2008). Both these factors, as well as the $CO_2$ production associated with of transport and processing of raw materials and products, need to be taken into account in ultimately achieving net-zero carbon emission biofuels production.

About 80 % of extracted crude oil is processed to yield fuels, either for electricity generation in power plants, or for use in the transport sector (Alfke et al., 2007; U.S. Energy Information Administration, 2020). The remaining 20 % is used for the synthesis of hundreds of different products, from car tires to plastics. For the latter, durability is both a desired characteristic and an environmental threat. If not properly disposed, plastic has the potential to pollute the environment for hundreds or even thousands of years, in addition to the environmental damage already caused by the $CO_2$ released from its production in the first place. It has been estimated that, in 2010 alone, 275 million tons of plastic were released in the ocean (Jambeck et al., 2015), where its resilience will cause harm to aquatic species, but also wildlife and, possibly, humans (Thompson et al., 2009). In addition, with its primary market being packaging, in which the package itself is destined for immediate disposal, plastic pollution is destined to increase (Jambeck et al., 2015).

To reduce carbon emissions and address environmental concerns, biotechnology has, in recent years, started developing compounds that may be used for plastic production (Baek

2 One kilogram of gasoline contains between 27- and 47-fold more energy than a fully charged one-kilogram battery.

et al., 2016; Getachew and Woldesenbet, 2016). As in the case for biofuels, the abatement in $CO_2$ emission would come from the use of fast-growing plants to produce sugars, which would then be converted into plastics via biotechnological processes (bioplastics). An additional advantage is that some (but not all) types of bioplastics are biodegradable[3], with a half-life ranging from a few months to a decade (Bagheri et al., 2017). Furthermore, the basic building blocks of biodegradable bioplastics are naturally occurring molecules in living organisms thus leading to reduced toxicity problems when bioplastics are degraded in the environment.

The two illustrated examples, biofuels and bioplastics, show how biotechnology can provide solutions to our current climate challenges. However, biotechnology alone cannot solve the climate challenge. To avoid disastrous consequences of climate change, carbon emission will have to drop to zero before 2050 (Rogelj et al., 2018). To achieve that goal, an integrated approach, involving different technologies for renewable power generation, sustainable agricultural practices and better material use is needed.



## 1.4 Industrial biotechnology

In the context of this thesis, industrial biotechnology refers to the use of microorganisms (bacteria, yeasts and fungi) to make products. Millennia before the term 'industrial biotechnology' was used, mankind already used microorganisms to make a wide range of products (Liu et al., 2018), with beer and wine brewing (Michel et al., 1992) and bread making (Bell et al., 2001) as main examples of early biotechnological processes. These latter applications are examples of microbial fermentation processes, in which a substrate (the sugars present in either wort, grape must or dough) is converted into a product (ethanol in wine and beer, and leavening bubbles of carbon dioxide in bread) by means of 'cell factories' (microorganisms).

Since the introduction, four decades ago, of techniques to precisely change the genetic information (DNA) of microorganisms ('genetic modification' or 'genetic engineering'), it has become possible to extend the range of products of microorganisms beyond their natural capabilities. This approach has become a cornerstone of industrial biotechnology, both for expanding its product range to include compounds ranging from life-saving drugs to aviation fuels and for improving the efficiency and rate of product formation.

Today, genetically modified microbial cell factories are used in industry to produce a wide range of products, from simple bulk compounds such as ethanol (Argueso et al., 2009; Moyses et al., 2016) and succinic acid (Otero et al., 2013; Raab et al., 2010), to highly complex molecules such as antibiotics (Awan et al., 2017; van der Beek and Roels, 1984) and sugar substitutes (Olsson et al., 2016) (Figure 3).

3 Biodegradation: naturally occurring breakdown of materials by microorganisms.

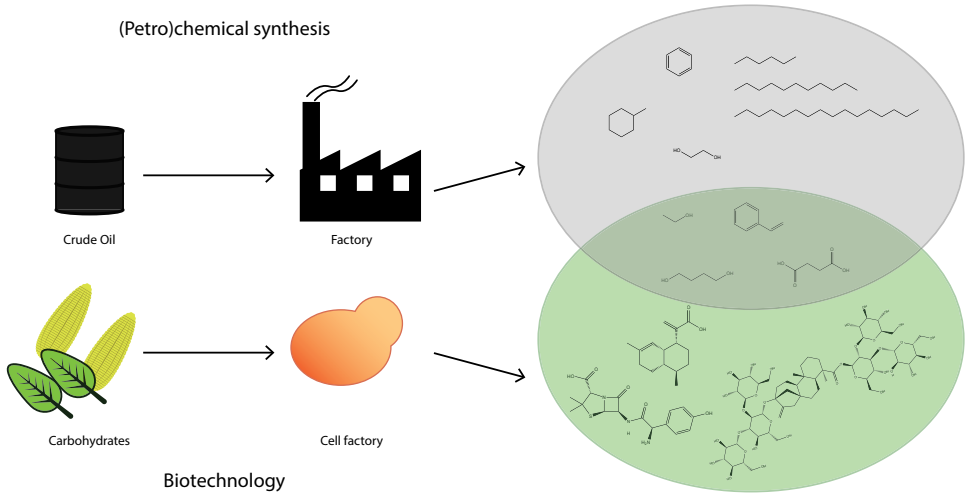


**Figure 3** Spectrum of molecules attainable using either petrochemical synthesis or biotechnology. Grey circle, small molecules produced from petro-chemical synthesis. Green circle: complex molecules produced in industrial biotechnology. The product spectra of the two fields overlap.

Apart from replacing molecules currently derived from fossil resources, biotechnological processes can be used to improve the sustainability and economics of the production of compounds that are derived from natural resources. An early example includes the production of human growth hormone (hGH), which is used for treatment of growth disorders in children. Until the early 1980's, isolation of hGH from donor brains conferred a risk of contamination with the deadly Creutzfeld-Jacob disease (Brown et al., 1985; Powell-Jackson et al., 1985). This risk was completely eliminated by producing hGH in a genetically engineered *Escherichia coli* bacterium, into which the human gene for hGH was introduced (Flodh, 1986). A more recent example is the biosynthesis of artemisinic acid, a precursor for the potent antimalarial drug artemisinin. This compound naturally occurs in the plant *Artemisia annua*, from which it can be extracted to produce malaria therapeutics (Miller and Su, 2011). However, growth requirements, the year-long life cycle, the minute quantities of the active compound present in the plant and the lack of adequate chemical synthesis routes for this compound (Covello, 2008), caused the supply of the drug to always fall short of global demand, especially in economically underdeveloped areas (Hale et al., 2007; Rodrigues et al., 2019). This issue was addressed by very extensive genetic engineering[4] of the yeast *Saccharomyces cerevisiae* (baker's yeast) to enable it to produce artemisinic acid from sugar (Mercke et al., 2000; Ro et al., 2006). After efficient production in yeast, artemisinic acid could then be chemically converted to the drug artemisinin. In doing so,

4 Genetic engineering: modification of the genetic makeup of an organism in order to change its characteristics. The genetic makeup (or 'genome') is the collection of instructions (or 'genes') needed for the organism to function. The genome is stored within the organism itself in the form of DNA. Different modifications can be performed: a gene (or part thereof) can be copied or removed; a change can be made within a gene; a gene from a different organism can be transferred to a new host.

production of the drug was made independent of the harvest of the plant it originally derived from, thus making it both more available and affordable (Rodrigues et al., 2019).

Every year, thousands of new biologically derived molecules are discovered in nature (Pye et al., 2017), each of which may have an industrial or pharmaceutical application. As many of these molecules are too complex to be chemically synthetized in an economically feasible manner, biotechnology offers an opportunity to tap nature's potential, and to bring new industrially relevant compounds to the market or to provide new drugs for the treatment of diseases.

## 1.5 *Saccharomyces cerevisiae* as a production platform



Yeasts are unicellular fungi that, for many centuries, have been used for the production of fermented foods and beverages. In the context of industrial biotechnology, yeasts are used for the production of hundreds of products, in many cases after genetic modification to introduce and optimize biochemical pathways that naturally occur in other organisms (Rebello et al., 2018). *Saccharomyces cerevisiae* is currently the yeast with the broadest product spectrum, which has been enabled by an extremely well developed set of molecular biology tools for genetic modification (Mattanovich et al., 2014). Although progress in yeast research is increasingly enabling similar genetic access and industrial applications in non-*Saccharomyces* ('non-conventional') yeast species (Rebello et al., 2018), *S. cerevisiae* has an impressive record of being the first. It was the first eukaryotic organism whose genome was sequenced (Goffeau et al., 1996), the first eukaryotic organism used for the production of heterologous proteins (Hitzeman et al., 1981) and it continues to be the organism responsible for the production of the largest-volume product of industrial biotechnology (ethanol, now > 100 Mton/year) (Gombert and van Maris, 2015; Mussatto et al., 2010).

Expanding the product range and improving the stoichiometry and kinetics of product formation by *S. cerevisiae* (and other microorganisms) has been greatly aided by the development of new DNA-sequencing technology, DNA-synthesis platforms and molecular biology tools. Over the past two decades, sequencing technologies such as Illumina and Nanopore have brought the costs for sequencing yeast and fungal genomes down from millions to just over a hundred dollars per sample (Wetterstrand, 2020). The costs for custom synthesis of DNA sequences have also dropped drastically, and are now in the range of 0.05 – 0.20 € per base pair (Hughes and Ellington, 2017). Recombinant DNA technologies have been used since the 1980's for the modification of microbial genomes, first with the use of restriction enzymes, then with the development of now common molecular biology techniques such as the polymerase chain reaction (PCR) and the establishment of cre-loxP system for genome engineering (Morange, 2000). In the past decade, the discovery of the mechanisms behind the CRISPR system (Brouns et al., 2008), and subsequently the use of Cas9 (CRISPR-associated protein 9) for genome engineering (DiCarlo et al., 2013; Jinek et al., 2012; Mans et al., 2015) has revolutionized the field by allowing for multiple, extremely

precise genome edits to be simultaneously performed in a wide range of organisms, including *S. cerevisiae* and other yeasts.

### 1.5.1 Current *S. cerevisiae* product spectrum

In the context of industrial biotechnology, *S. cerevisiae* is best known, as mentioned above, for ethanol production to be used as biofuel, where it can be used directly or blended with conventional gasoline for use in the automotive industry. While not yet on the market, Lanzatech has recently obtained approval for commercialization of ethanol-derived jet fuel (LanzaTech, 2018). In their process, ethanol is chemically converted to medium/long-chain hydrocarbons, which can be blended up to 50 % with regular jet fuel, substantially reducing carbon emission from one of the least sustainable forms of transport (Eagan et al., 2019; LanzaTech, 2019). The low energy density (by weight) of ethanol has brought academic and industrial scientists to attempt production of other alcohols, such as butanol or isobutanol (Branduardi et al., 2013; Lan and Liao, 2013; Steen et al., 2008). Industrial production of isobutanol has been demonstrated by GEVO, which uses *S. cerevisiae* as a production host (Ryan, 2019). Recently, farnesene, a sesquiterpene, has been produced by Amyris (Meadows et al., 2016). After production by engineered *S. cerevisiae*, this hydrocarbon can be chemically hydrogenated to farnesane, whose applicability as a transport fuel has been demonstrated in practice (Renninger and Mcphee, 2008).

Organic acids, such as pyruvic, lactic, and succinic acid, which find applications in the food, pharmaceutical and chemical industry and in the manufacturing of solvents and polymers, may also be produced with *S. cerevisiae* (Abbott et al., 2009b). Industrial processes for the production of succinic acid using baker's yeast are currently established (Verwaal et al., 2007), while other acids are produced in a variety of hosts (Sauer et al., 2008). The main advantage in using *S. cerevisiae* for organic acid production is its tolerance to low pH, which allows the production of the free acid rather than its salt, thus simplifying downstream processing and reducing costs.

In addition to ethanol, farnesene and organic acids, production of a large and rapidly growing number of other complex molecules by engineered *S. cerevisiae* strains has been demonstrated. Products of interest include the flavonoid naringenin (Koopman et al., 2012), the drug precursor artemisinic acid (Ro et al., 2006) and flavor and fragrance precursors such as phenyl-ethanol (Hassing et al., 2019) and geraniol (Oswald et al., 2007). The power of modern yeast genetic modification techniques is illustrated by a study of Galanie et al. (2015), who demonstrated the successful engineering of *S. cerevisiae* for the biosynthesis of opioids, in a process which required the insertion of 13 heterologous genes and the modification of several steps in the native yeast central carbon metabolism.

### 1.5.2 Strategies for strain improvement

In any biotechnological process, titer, rate and yield (TRY) are critical factors in determining its economic feasibility. In the case of bulk or commodity chemicals, the cost of the substrate

account for the majority of the cost of the product (Kumar and Murthy, 2011), which implies that yield of product on substrate (Y) is of crucial importance in determining economic viability. Further optimization can be achieved by accelerating product formation (R) and its concentration in the fermentation broth (T). Improved rate and titer help to minimize the scale and costs of cultivation vessels, and a high titer also helps to recover product from microbial cultures. When profit margins are narrow, even small improvement of the titer, rate, and yield (TRY) of a bioprocess can have large relative impact on its economic profitability. For the production of (very) high added-value molecules, such as pharmaceuticals, costs of feedstock and fermentation infrastructure are often of lower importance, and the ease of recovering a pure compound, which is often related to the product titer (T) is generally much more important than the rate of product formation or its yield on substrate.

With rare exceptions, wild-type microorganisms do not produce a metabolite of interest in industrially relevant quantities. Therefore, in order to improve the characteristics of the strain of interest, three strategies are often applied: random mutagenesis (also known as classical strain improvement), metabolic engineering and adaptive laboratory evolution.



'Classical' strain improvement refers to the iterative application of rounds of random mutagenesis with chemical mutagens or irradiation, screening and selection of the best performing mutants. In the absence of an easily identifiable phenotype (e.g., production of a colored compound) application of this technique often requires an infrastructure capable of screening from tens of thousands newly generated strains. One of the first massive applications of this approach started immediately after the second world war, when strains of the antibiotic producing fungus *Penicillium* (Fleming, 1929) were mutagenized for the production of the life-saving new antibiotic penicillin (van der Beek and Roels, 1984). In this example, the use of this technique yielded a several thousand-fold improvement in antibiotic production. Mutagenesis and selection, which can now be intensified and automatic by application of robotics, continues to be an important technique in modern biotechnology. 'Classical' strain improvement finds application when the molecular or genetic basis of a relevant trait is not known, or when genetic engineering tools are not available. Selection of the best performing strain (often without the use of mutagenic factors) has also been applied in the food industry, where consumer acceptance issues preclude the use of genetic modification. The power of this improvement technique has been amplified by the option to re-sequence the entire genome of better performing strains, thereby allowing the identification of causal mutations (Herrgård and Panagiotou, 2012; Oud et al., 2012).

Metabolic engineering is defined as the rational, targeted genetic modification of a microorganism aimed at improving its metabolic characteristics for industrial application (Bailey, 1991). With the exception of beer, wine and bread, the previously mentioned examples for the production of chemicals in *S. cerevisiae* are examples of metabolic engineering, in which the metabolism of this yeast was engineered either for the production of a metabolite of interest, or for the improvement of the availability of precursors and

cofactors of the central carbon metabolism. Contrary to classical strain improvement, this approach requires a deep knowledge and understanding of the organism being modified, and molecular biology tools are needed in order to perform the intended modifications.

Adaptive laboratory evolution, also referred to as 'evolutionary engineering' refers to the use of specific cultivation strategies to establish a selection pressure for the isolation of mutants with desired phenotypes (Dragosits and Mattanovich, 2013; Sauer, 2001). This technique, in a similar fashion to classical strain improvement, is used when a clear metabolic engineering target cannot immediately be identified, and it is often used in combination with the other two approaches. In contrast to random mutagenesis, the best performing strain is isolated by means of an applied selection pressure, thus bypassing the need for intensive screening facilities. Moreover, adaptive laboratory evolution allows for the accumulation of subsequent mutations that provide a selective advantage under the selected cultivation regime. Re-sequencing of single colony isolates from parallel evolution lines can then elucidate the molecular mechanism of the obtained phenotype. The use of parallel evolution lines is often a necessity to discriminate between causal and random, non-deleterious mutations.

Adaptive laboratory evolution of *S. cerevisiae* has been applied for the selection of phenotypes such as resistance to toxic compounds, ability to consume non-native substrates and implementation of alternative catabolic pathways (for a detailed review see Mans et al. (2018)). Selection for improved production of anabolic products, whose synthesis requires a net input of energy, is challenging, as improved production often causes a metabolic burden which could be selected against. Successful examples of the implementation of adaptive laboratory evolution aimed at anabolic product formation include the isolation of a *S. cerevisiae* strain engineered for the production of β-carotene. This organism was challenged with increasing concentration of hydrogen peroxide. As β-carotene is a potent antioxidant, strains overproducing this compound have a selective advantage under oxidative stress, and thus survive harsher and harsher conditions (Reyes et al., 2014). In another elegant example, strains of *Yarrowia lipolytica* exhibiting a higher lipid content were selected on the basis on increased buoyancy (Liu et al., 2015). Both examples show how the design of the experimental conditions plays a key role in the successful selection of a phenotype of interest.

In contrast to metabolic engineering, and alike classical strain improvement, adaptive laboratory evolution does not *per se* require deep knowledge of the metabolism of the organism of interest, nor has the need of molecular biology tools. Both of those come into play at the step of reverse engineering (Oud et al., 2012), that is, inserting the newly found mutations in the parental strain, in order to elucidate the molecular mechanism leading to the observed phenotype.

## 1.6 Engineering precursor supply

The metabolism of any living organism is organized around a set of 12 molecules (glucose-1-phosphate, glucose-6-phosphate, erythrose-4-phosphate, ribose-5-phosphate, dihydroxyacetone-phosphate, 3-phosphoglycerate, phosphoenolpyruvate, pyruvate, acetyl-Coenzyme A, oxaloacetate, α-ketoglutarate and succinyl-Coenzyme A), which can act as precursors for the synthesis of all other metabolites found within the cell (Noor et al., 2010). To economize use of substrate and cellular energy, regulation mechanisms have evolved in order to synthetize only the necessary amount required for growth. When considered from this perspective, metabolic regulation has evolved to avoid wasting precious resources (Metallo and Vander Heiden, 2013).

Product pathways for the synthesis of industrially relevant metabolites tap into cellular pools of these metabolic intermediates, whose availability can therefore limit rate of formation and yield of the product of interest (Nielsen and Keasling, 2016). Similarly, these process indicators are also impacted by the metabolic route used for the synthesis of precursors. Some of the metabolites are synthetized in different cellular compartments, using distinct metabolic routes which differ in their use of cofactors and ATP consumption, and thereby impact the maximum attainable product yield. Therefore, while the mere introduction of the set of genes encoding enzymes required for conversion of precursors into product (the 'product pathway') often leads to measurable product formation, it is in general not sufficient to achieve titers, rates and yields that are required for economically feasible industrial processes. In metabolic engineering strategies, it is therefore essential to take into account the availability of key precursors and cofactors of the reactions involved in their synthesis. In the past decade, nearly all scientific literature in which microorganisms were successfully engineered for non-native product formation integrated research on pathway expression and precursor supply (reviews for *S. cerevisiae*, non-conventional hosts and bacteria can be found in Lian et al. (2018), Sun and Alper (2020) and Calero and Nikel (2019), respectively).

In the past years, numerous engineering efforts have been made to enable the synthesis of new 'drop-in' biofuels. Metabolic engineering strategies for yeast-based production of non-native alcohols such as n-butanol (Atsumi et al., 2008; Lee et al., 2008) and isobutanol (Chen et al., 2011; Smith et al., 2010) and other alcohols derived from the 2-ketoacid pathway have been intensively explored, as well as pathways for fatty acids/isoprenoids derived fuels (Chandran et al., 2011; Steen et al., 2010). In most cases, production of these molecules requires efficient supply of the precursor molecule acetyl-CoA. In microbial cell factories, this precursor affects yield, and productivities for the synthesis of a wide range of compounds of interest.

## 1.7 Acetyl-CoA

Acetyl-CoA is one of the 12 essential metabolic precursors for biomass formation (Noor et al., 342 2010). In native yeast metabolism, compounds synthesized from this precursor include

fatty acids, sterols and multiple amino acids, while acetyl-CoA is also used as acetyl-donor for the acetylation of histones and other proteins (Flikweert et al., 1999; Flikweert et al., 1997; Henriksen et al., 2012; Takahashi et al., 2006). The synthesis of several major classes of industrially relevant products whose production in yeast is actively explored, including fatty acids, isoprenoid- and flavonoid-derived products and n-butanol, start with acetyl-CoA as a building block. In *S. cerevisiae*, acetyl-CoA can be synthesized either in the mitochondria or in the cytosol (Figure 4) and, due to the impermeability of the mitochondrial membrane for coenzyme-A (Flikweert et al., 1999; Van den Berg and Steensma, 1995), this molecule is only available for use in product pathways in the compartment in which it has been generated.

Mitochondrial synthesis of acetyl-CoA is mediated by the pyruvate dehydrogenase complex, a multi-subunit, thiamine- and lipoate-dependent enzyme complex with a molecular weight of up to 2 million Daltons (2 MDa) (Patel and Roche, 1990). The concerted action of its subunits enables the decarboxylation and oxidation of pyruvate, the reduction of $NAD^+$ to NADH and the formation of a thioester bond to form acetyl-CoA. Alternatively, mitochondrial acetyl-CoA can be synthetized by the mitochondrial enzyme Ach1, which transfers the CoA group from succinyl-CoA to acetate, thereby generating acetyl-CoA and succinate (Buu et al., 2003). This acetyl-CoA can then either be used to fuel the TCA cycle, or as a precursor for the biosynthesis of mitochondrial fatty acids and as a precursor for amino acids derived from α-ketoglutarate..

Cytosolic synthesis of acetyl-CoA is mediated by the concerted action of three separate enzymes: pyruvate decarboxylase, acetaldehyde dehydrogenase and acetyl-CoA synthetase. This pathway, known as the pyruvate-dehydrogenase bypass, is used to provide cytosolic acetyl-CoA for fatty acid, lysine and terpenoid biosynthesis, as well as for histone acetylation (Pronk et al., 1996; van Rossum et al., 2016a). Additionally, this pool is used by malate synthase, part of the glyoxylate cycle, to replenish intermediates of the TCA cycle when growing on ethanol or acetate (Kornberg, 1966). The last step of the pathway, the activation of acetate to acetyl-CoA, is thermodynamically unfavorable, with a $\Delta G^{o'}$ of + 47.1 ± 1.0 kJ $mol^{-1}$ (Flamholz et al., 2012). The synthesis is therefore driven forward by the hydrolysis of ATP to AMP, which lowers the total change in Gibb's free energy under biochemical standard conditions of the overall reaction to – 4.5 ± 0.8 kJ $mol^{-1}$. The pyrophosphate ($PP_i$) formed in this reaction is further hydrolyzed to phosphate and the formation of one mole of cytosolic acetyl-CoA in native *S. cerevisiae* cells therefore uses the energetic equivalent of two moles of ATP hydrolyzed to ADP. In *S. cerevisiae*, two acetyl-CoA synthetase isoenzymes can catalyze this reaction. *ACS1* is expressed during growth on ethanol or acetate (De Virgilio et al., 1992) and in glucose-limited cultures (van den Berg et al., 1996), while *ACS2* is required for growth at high glucose concentrations (de Jong-Gubbels et al., 1997; van den Berg and Steensma, 1995). A deletion mutant lacking both genes is not viable unless an alternative pathway for cytosolic acetyl-CoA biosynthesis is introduced (Kozak et al., 2014a). Apart from their difference in expression, these isoenzymes also have different kinetic characteristics (Table 1), with Acs1 having a lower $K_m$ for acetate than Acs2 (van den Berg et al., 1996).

**Table 1** Kinetic properties of acetyl-coenzyme A synthetases in cell extracts of glucose-limited, aerobic chemostat cultures of *S. cerevisiae*. Table adapted from van den Berg et al. (1996).

| | $V_{max}$ (mM) | $K_m$ acetate (mM) | $K_m$ ATP (mM) |
|---|---|---|---|
| Acs1 | 1.10 ± 0.01 | 0.32 ± 0.01 | 1.4 ± 0.0 |
| Acs2 | 0.34 ± 0.01 | 8.8 ± 0.5 | 1.3 ± 0.1 |

The absence, in bacterial proteins, of N-terminal sequences that would direct them to a specific cellular compartment in eukaryotic cells, often results in their localization in the cytosol when expressed in eukaryotic organisms (Kozak et al., 2014b). As demonstrated in a study on isobutanol production in *S. cerevisiae* (Avalos et al., 2013), it is possible to transfer product pathways to the mitochondrial matrix. This does, however, require the engineering of every protein of the pathway, and transport of substrates and products in and out of the mitochondrion. In practice, heterologous product pathways are still predominantly expressed in the cytosol, where they only have access to cytosolic pools of acetyl-CoA and other precursors. In such scenarios, the ATP requirement of the native 'pyruvate-dehydrogenase bypass' pathway for acetyl-CoA synthesis in *S. cerevisiae* can have a huge impact on the maximum attainable product yields for pathways starting at acetyl-CoA. As an example, the biosynthesis of farnesene requires 9 cytosolic acetyl-CoA molecules for each mole of farnesene. Consequently, this would require an input 18 ATP just to generate the precursor for a single molecule of product. If this ATP cost would be eliminated it could, when coupled with an ameliorated cofactor usage, increase the yield of farnesene on glucose by 25 % (when compared to the maximum pathway yield attainable using the native *S. cerevisiae* metabolic network) (Meadows et al., 2016). This example clearly demonstrates the industrial relevance of ATP-independent sources of acetyl-CoA in the yeast cytosol.



## 1.8 Alternative pathways for cytosolic acetyl-CoA biosynthesis

Several metabolic engineering strategies for decreasing or eliminating the ATP costs of cytosolic acetyl-CoA synthesis in *S. cerevisiae* have been explored, whose energetic requirements are summarized in Table 2. In this table, the energetics cost for precursor synthesis is indicated as the cost of ATP per acetyl-CoA formed from glucose. Under these conditions, the native ACS pathway has a cost of 1 ATP per acetyl-CoA formed, as the ATP generated from the conversion of glucose to pyruvate is also taken into account.

**Table 2** Energetics of different pathways for the biosynthesis of cytosolic acetyl-CoA from glucose. The indicated stoichiometries are based on their combination with a yeast-type Embden-Meyerhof glycolysis and energy-independent uptake of glucose. ACS – acetyl-CoA synthetase, PK and PTA – xylulose-5-phosphate phosphoketolase and phosphate acetyltransferase, PFL – pyruvate-formate lyase, with or without formate dehydrogenase (FDH), ACL – ATP-citrate lyase, A-ALD – acetylating acetaldehyde dehydrogenase, PDH – pyruvate dehydrogenase, CAR – carnitine shuttle (using the native PDH). Table adapted from Kozak et al., (2014b). Literature references refer to studies in which these pathways, which originate from different organisms, have been functionally expressed in *S. cerevisiae*.

| Pathway | ATP/Acetyl-CoA | NAD(P)H/Acetyl-CoA | Reference |
|---|---|---|---|
| ACS | -1 | 2 | (Shiba et al. 2007) |
| PK, PTA[a] | -1/2 | 2 | (Sonderegger et al., 2004) |
| PK, PTA[b] | -1/3 | 0 | (Sonderegger et al., 2004) |
| ACL | 0 | 1 + 1 mitochondrial | (Rodriguez et al., 2016; Tang et al., 2013) |
| PFL | 0 (includes export of formate) | 1 | (Kozak et al., 2014a) |
| PFL, FDH | 1 | 2 | (Kozak et al., 2014a) |
| A-ALD | 1 | 2 | (Kozak et al., 2014a; Kozak et al., 2016) |
| PDH | 1 | 2 | (Kozak et al., 2014b) |
| CAR (mitochondrial PDH) | 1 | 1 + 1 mitochondrial | (van Rossum et al., 2016b) |

### 1.8.1 Xylulose-5-phosphate phosphoketolase and phosphate acetyltransferase pathway

An alternative pathway for the biosynthesis of cytosolic acetyl-CoA was first explored by Sonderegger et al. (2004), who expressed *Bifidobacterium lactis* phosphoketolase (PK) and *Bacillus subtilis* phosphate acetyltransferase (PTA) in *S. cerevisiae* (Figure 4). In this system, xylulose-5-phosphate is split in glyceraldehyde-3-phosphate and acetyl-phosphate by the introduced phosphoketolase. The resulting acetyl-phosphate is then substrate of the heterologous phosphate acetyltransferase which converts it to acetyl-CoA, whereas glyceraldehyde-3-phosphate continues through glycolysis and is converted to acetyl-CoA via the native acetyl-CoA synthetase. The ATP cost for the PK-PTA pathway depends on how the initial molecule xylulose-5-phosphate is generated. If generated from glucose-6-phosphate via the oxidative pentose phosphate pathway, the ATP cost via this route is 0.5 ATP per acetyl-CoA. If, however, xylulose-5-phosphate is produced via the non-oxidative pentose phosphate pathway (starting at fructose-6-phosphate and glyceraldehyde-3-phosphate), and the glyceraldehyde-3-phosphate generated by the PK can be recycled to produce fructose-6-phosphate, which reduces the ATP cost to 1/3 ATP per acetyl-CoA.

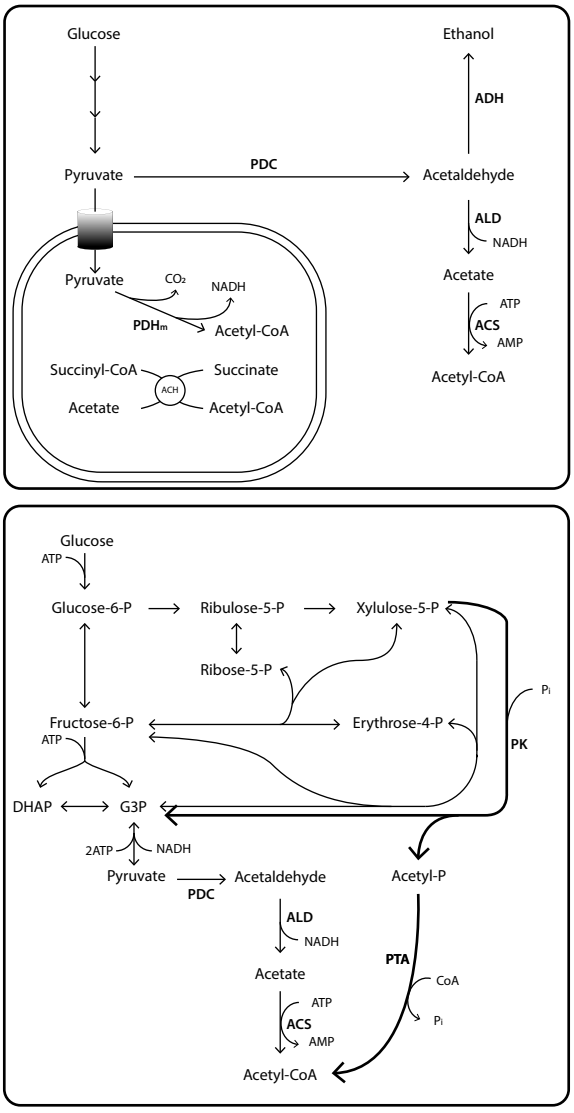


**Figure 4** Top panel: native *S. cerevisiae* metabolism for acetyl-CoA formation. Bottom panel: engineered *S. cerevisiae* metabolism for acetyl-CoA synthesis derived from the pentose phosphate pathway. Abbreviations: PDC, pyruvate decarboxylase. ADH, alcohol dehydrogenase. ALD, acetaldehyde dehydrogenase. ACS, acetyl-CoA synthetase. PDHm, mitochondrial pyruvate dehydrogenase. ACH, acetyl-CoA hydrolase. PK, phosphoketolase. PTA, phosphotransacetylase. DHAP, dihydroxyacetone phosphate. G3P, glyceraldehyde-3-phosphate. Metabolic reactions have been simplified for clarity.

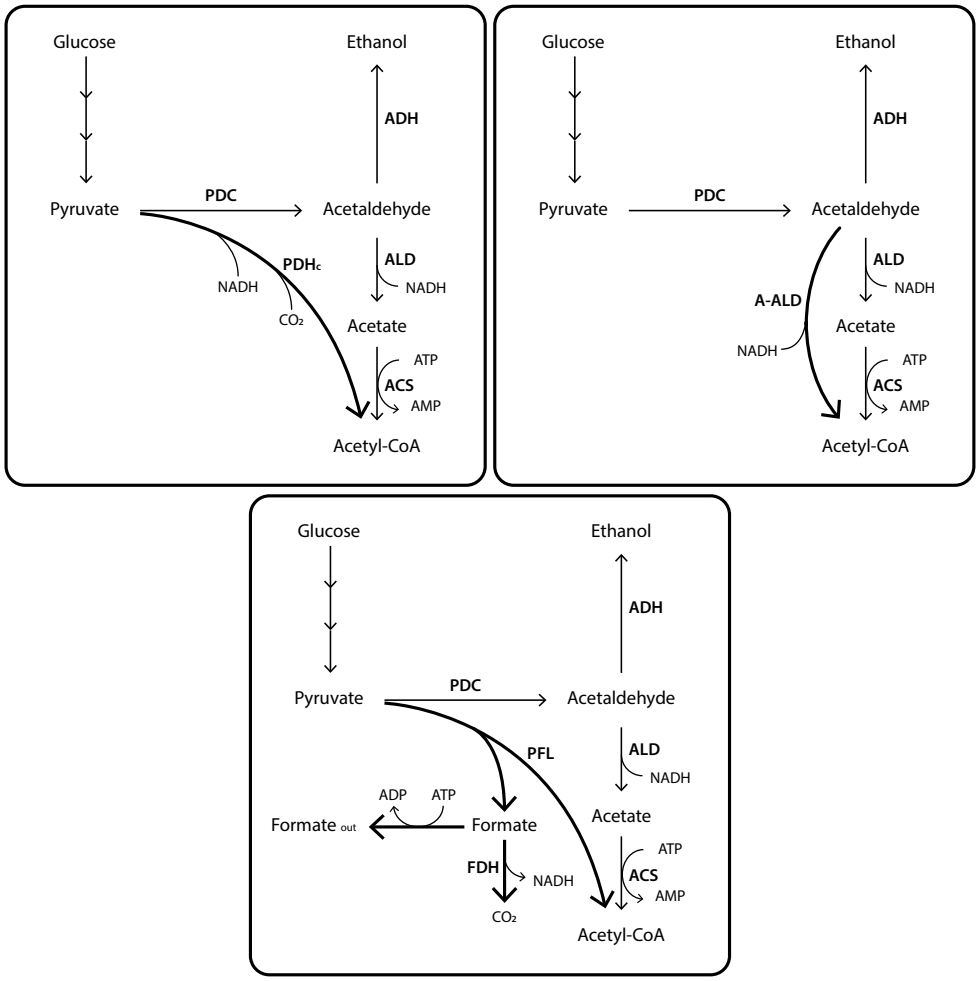


**Figure 5** Alternative reactions requiring cytosolic metabolites for acetyl-CoA formation. Abbreviations: PDC, pyruvate decarboxylase. ADH, alcohol dehydrogenase. ALD, acetaldehyde dehydrogenase. ACS, acetyl-CoA synthetase. PDHc, cytosolic pyruvate dehydrogenase. A-ALD, acetylating acetaldehyde dehydrogenase. PFL, pyruvate-formate lyase. FDH, formate dehydrogenase. Metabolic reactions have been simplified for clarity.

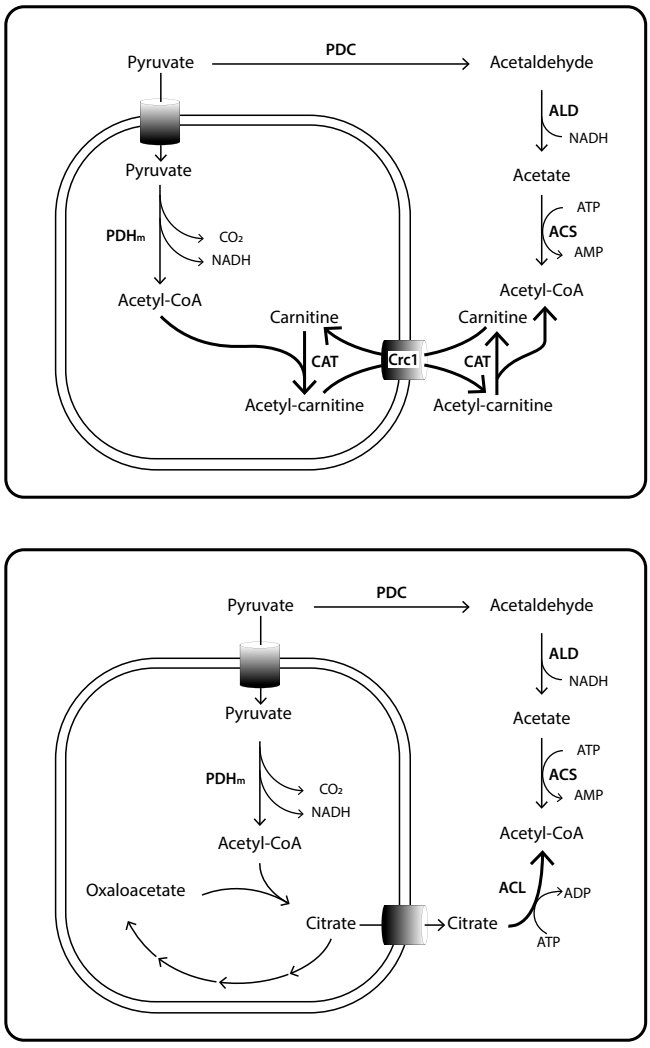


**Figure 6** Alternative reactions for cytosolic acetyl-CoA formation requiring the activity of the native pyruvate dehydrogenase complex. Abbreviations: PDC, pyruvate decarboxylase. ALD, acetaldehyde dehydrogenase. ACS, acetyl-CoA synthetase. PDHm, mitochondrial pyruvate dehydrogenase. CAT, carnitine acetyl-transferase. Crc1, mitochondrial carnitine carrier. ACL, ATP-citrate lyase. Metabolic reactions have been simplified for clarity.

### 1.8.2 Pyruvate-formate lyase

Pyruvate – formate lyase (PFL) is an enzyme that predominantly occurs in bacteria and which catalyzes the ATP-independent conversion of pyruvate and coenzyme-A to acetyl-CoA and formic acid (Figure 5) (Waks and Silver, 2009). Kozak et al. (2014a) showed that expression of *E. coli* Pfl allowed growth on glucose of an *acs1Δ acs2Δ S. cerevisiae* strain, at 74% of the specific growth rate observed for the reference (*ACS1*, *ACS2*) strain. Applicability of this metabolic engineering strategy is limited by the oxygen sensitivity of the pyruvate formate lyase, which implies that growth of engineered strains is restricted to anaerobic or oxygen-limited conditions. Additionally, it is assumed that organic acid export may come at a cost of 1 ATP per molecule of acid (Abbott et al., 2009a; van Maris et al., 2004). When taking into account ATP-dependent formate export, the synthesis of acetyl-CoA from glucose via a PFL yields 0 ATP per acetyl-CoA formed. The expression of a formate dehydrogenase, which oxidizes formate to $CO_2$, with concomitant production of NADH, could in principle make formate export unnecessary, thus restoring the net ATP yield of 1 ATP per cytosolic acetyl-CoA formed.

### 1.8.3 Acetylating acetaldehyde dehydrogenase

The use of an acetylating acetaldehyde dehydrogenase for cytosolic acetyl-CoA synthesis in engineered *S. cerevisiae* was first published by Kozak et al. (2014a) (Figure 5). This enzyme converts, in a single step, acetaldehyde to acetyl-CoA, thus conserving the energy released in the oxidation of acetaldehyde and using it to drive the energy-intensive formation of the thioester bond. As the energetically expensive step of the acetyl-CoA synthetase is bypassed, this route yields, on glucose grown cultures, 1 ATP per acetyl-CoA formed. Expression of the *EutE* gene from *E. coli* in a *S. cerevisiae* strain lacking the acetaldehyde dehydrogenase genes (*ald2Δ*, *ald3Δ*, *ald4Δ*, *ald5Δ*, *ald6Δ*) allowed for aerobic growth on glucose at 82% of the growth rate of the reference strain ($0.27 \pm 0.00$ $h^{-1}$ and $0.33 \pm 0.00$ $h^{-1}$, respectively). While this enzyme was able to sustain anabolic requirements of acetyl-CoA in glucose-grown cultures, growth on ethanol, which should require the entire catabolic flux to run through this pathway, was only observed at very low rates after laboratory evolution (Kozak et al., 2016).

### 1.8.4 Pyruvate dehydrogenase

An alternative way for acetyl-CoA biosynthesis was explored by Kozak et al. (2014b) and Lian and Zhao (2016) (Figure 5). In the work from these independent groups, a bacterial pyruvate dehydrogenase complex was expressed in order to complement an otherwise lethal *acs1Δ, acs2Δ* deletion. The choice of a bacterial enzyme was motivated by the fact that bacterial proteins lack mitochondrial localization sequences and would not require 'clipping' of eukaryotic sequences by additional genetic modifications. This strategy was initiated to generate acetyl-CoA from pyruvate in the yeast cytosol by the same oxidative decarboxylation reaction that occurs in eukaryotic mitochondria. Compared to the previously mentioned strategies, use of the pyruvate dehydrogenase complex has several potential advantages. In contrast to PFL, it is not sensitive to oxygen, allowing it to operate under both aerobic and anaerobic conditions. Furthermore, NADH and $CO_2$ are formed, rather than formic acid, thus

obviating the need for organic acid export. In addition, the NADH formed is available as a reducing equivalent for the biosynthesis of highly reduced products. When compared to the A-ALD, there are also several advantages in using a cytosolic pyruvate dehydrogenase. The reaction catalyzed by the A-ALD has a standard Gibbs free energy change ($\Delta G^{o\prime}$) of 0.1 ± 2.4 kJ $mol^{-1}$ or 1.1 ± 2.4 kJ $mol^{-1}$ when using $NAD^+$ or $NAPD^+$, respectively. These near-zero values indicate that direction of the reaction strongly depends on concentrations of reactants and products, and could therefore lead to an accumulation of acetaldehyde. In contrast, the reaction catalyzed by the pyruvate dehydrogenase complex has a $\Delta G^{o\prime}$ of -35.5 ± 6.4 kJ $mol^{-1}$, similar to the one observed for pyruvate decarboxylase (-35.4 ± 6.5 kJ $mol^{-1}$), thus driving the reaction towards acetyl-CoA formation. Like the A-ALD, the use of a cytosolic PDH bypasses the ATP-consuming ACS reaction, thus yielding 1 ATP per acetyl-CoA on glucose grown cultures.

**1.8.5 ATP-citrate lyase**

The use of a heterologously expressed ATP-citrate lyase as the pathway for the biosynthesis of cytosolic acetyl-CoA in *S. cerevisiae* has been explored by and Rodriguez et al. (2016) and, previously, by Tang et al., (2013) (Figure 6). In their work, formation of a cytosolic acetyl-CoA was mediated by the activity of cytosolically expressed ATP citrate lyase, which hydrolyses citrate to oxaloacetate and acetyl-CoA, using one ATP to drive the reaction. The formation of citrate required, in turn, the activity of the mitochondrial pyruvate dehydrogenase and citrate synthase, thus coupling the cytosolic and mitochondrial acetyl-CoA pools. Compared to the PDH bypass, acetyl-CoA formation from glucose via this system has a net ATP cost of 0 (2 ATPs formed in glycolysis, and 2 ATPs used to convert citrate to acetyl-CoA). A pitfall of this system is its reliance on the mitochondrial pyruvate dehydrogenase and citrate synthase, whose *in vivo* activity is strongly reduced in the presence of glucose, due to the transcriptional repression of these genes in the presence of this carbon source. In addition, activity of the pyruvate dehydrogenase complex is inhibited by glucose-induced phosphorylation (Gey et al., 2008), thus limiting the applicability of this strategy to conditions in cultures exposed to high glucose concentrations.

**1.8.6 Carnitine shuttle**

In mammals (Vaz and Wanders, 2002) and in some yeasts (Strijbis et al., 2009), acetyl-CoA moieties can be transported between intracellular compartments by means of the carnitine shuttle. This system is used during growth on fatty acids, as β-oxidation occurs in the peroxisomes, and the produced acetyl-CoA moiety has to be transferred to the mitochondria to fuel the TCA cycle (Bieber, 1988; Hiltunen et al., 2003; Kawamoto et al., 1979; Vaz and Wanders, 2002). As previously mentioned, CoA-containing molecules cannot readily cross organelle membranes (van Roermund et al., 1995), and must therefore be transported. To this end, the acyl group is transferred to carnitine, and the resulting acyl-carnitine can then be transported into the mitochondria. Before the discovery of the PDH bypass, it was thought that this system would be required for the formation of cytosolic aceyl-CoA (Kohlhaw and Tan-Wilson, 1977). However, it was later shown that the carnitine shuttle operates in a unidirectional manner, shuttling acyl moieties from the peroxisome

and cytosol to the mitochondria (van Maris et al., 2003), despite the reaction being mechanistically and thermodynamically reversible ($\Delta G^{o'}$ -1.1 ± 2.9 kJ $mol^{-1}$ in the direction of acetyl-L-carnitine formation). Subsequent metabolic engineering and adaptive laboratory evolution experiments have shown that this system can be engineered to transfer acetyl-CoA from the mitochondrion to the cytosol in glucose grown cultures (van Rossum et al., 2016b) (Figure 6). Using this strategy, the ATP cost for cytosolic acetyl-CoA formation was reduced, as this molecule would be supplied by the mitochondrial pyruvate dehydrogenase and then transferred out by the carnitine shuttle. However, as *S. cerevisiae* lacks the required biosynthetic pathway for carnitine biosynthesis (Swiegers et al., 2001), this system would rely on the supplementation of carnitine, which might increase the overall costs of the bioprocess.

As in the case of the overexpression of a citrate lyase, the use of a carnitine shuttle for the supplementation of cytosolic acetyl-CoA requirements relies on the formation of intramitochondrial acetyl-CoA, mediated by the native pyruvate dehydrogenase (van Rossum et al., 2016b). This enzyme is strongly (but not completely) repressed during growth on glucose (Bowman et al., 1992; Gey et al., 2008), and could thus limit the flux of acetyl-CoA needed for a feasible product pathway. Unlike the ATP-citrate lyase pathway, acetyl-CoA formation in the cytosol is mediated by a shuttle, and not by the ATP-dependent conversion of citrate, thus yielding a net 1 ATP per acetyl-CoA formed in glucose grown cultures.

**1.9 Succinyl-CoA**

Succinyl-CoA, the thioester of succinic acid and coenzyme A is, like acetyl-CoA, also one of the 12 key metabolites required for biomass formation by living cells (Dickinson et al., 1986). In eukaryotes, succinyl-CoA is synthesized in the mitochondria by means of the α-ketoglutarate dehydrogenase complex or by the succinate-CoA ligase (Bard et al., 1974). In addition to its role as an intermediate in catabolism via the TCA cycle, it is required in yeast anabolism as the starting metabolite for the synthesis of 5-aminolevulinic acid, the first committed precursor in heme biosynthesis (Weinert et al., 2013) (Figure 7). Contrary to the well-established native pathway for cytosolic synthesis of acetyl-CoA in *S. cerevisiae*, no mechanisms for cytosolic succinyl-CoA formation have, to date, been reported in this yeast. This observation is puzzling since clear evidence for succinylation of cytosolic proteins in eukaryotic organisms (Martin and Williams, 2003) suggests availability of a cytosolic succinyl-CoA pool to act as succinyl donor for this post-translational modification process.

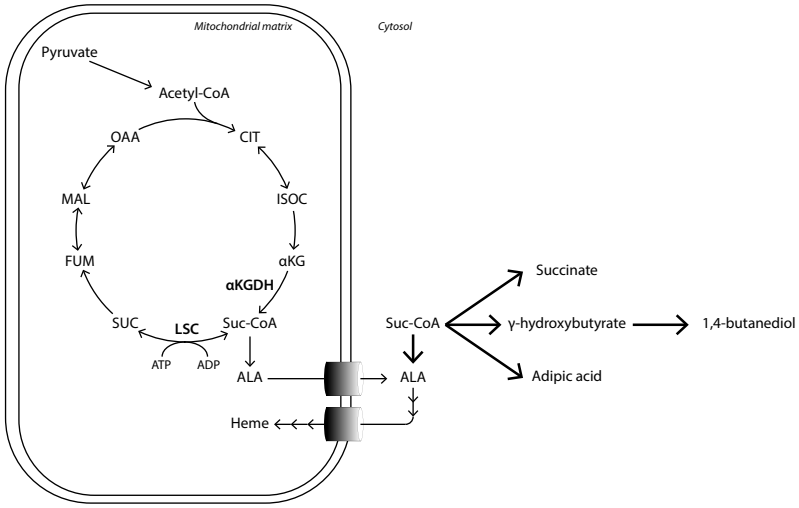


**Figure 7** Succinyl-CoA formation in *S. cerevisiae* and possible products. Abbreviations: OAA, oxaloacetate. CIT, citrate. ISOC, isocitrate. αKG, alpha-ketoglutarate. Suc-CoA, succinyl-CoA. SUC, succinate. FUM, fumarate. MAL, malate. αKGDH, alpha-ketoglutarate dehydrogenase. LSC, succinate-CoA ligase. Metabolic reactions have been simplified for clarity.

Industrially relevant compounds, such as γ-hydroxybutyric acid, 1,4-butanediol, 5-aminolevulinic acid (ALA) and adipic acid can all be synthetized from succinyl-CoA (Figure 7). γ-hydroxybutyric acid can be used as a precursor for polyhydroxybutyrate, a compostable bioplastic which currently finds applications in medicine as an internal suture material (Martin and Williams, 2003; Karidurаganavar et al., 2014), and whose production has been previously engineered in *E. coli* (Le Meur et al., 2013). 1,4-butanediol, a commodity chemical for the production of plastics, polyesters and spandex fibers, has been produced in engineered *E. coli* (Yim et al., 2011), but not in yeast. At first used as an herbicide (Rebeiz et al., 1984), it was discovered that 5-aminolevulinic acid would readily accumulate in cancer cells, where it is converted in protoporphyrin IX (Kennedy et al., 1990). Upon exposure with an appropriate light source (violet-blue light, wavelength 395-415 nm) this molecule emits a red fluorescence, thus aiding the surgeon in the localization of the tumor (Kaneko (1998), reviewed by Sasaki et al. (2002)). Apart from this diagnostic use, ALA is also used as a treatment for some types of skin cancer: upon application, cancerous cells are irradiated with specific laser radiation, which causes the accumulated protoporphyrin to produce singlet oxygen molecules. The damage caused by this reactive oxygen species causes irreparable cellular damage which, ultimately, kills the tumor (Kennedy et al., 1990). This versatile, non-proteinogenic amino acid has been produced in different hosts (reviewed in Liu et al. (2014)). Adipic acid is the most common industrial dicarboxylic acid (Musser, 2000), which is the precursor for the synthesis of nylon. Recently, Cheong et al. (2016) showed that it is possible to produce this molecule in *E. coli*, thereby opening up research lines

towards bio-based production of nylon from renewable resources. With the exception of 5-aminolevulinic acid, which can be natively produced by several algae (Beale, 1970; Sasaki et al., 1995), all the succinyl-CoA-derived compounds mentioned above have been produced in prokaryotic organisms. The confinement of succinyl-CoA to the mitochondria have so far precluded the use of eukaryotic hosts, including yeasts, for production of these compounds. Establishment of an *S. cerevisiae* platform with an energy-efficient, cytosolic pathway for succinyl-CoA production could therefore be highly relevant for yeast biotechnology.

## Scope and outline of this thesis

Efficient, economically feasible production of high-energy molecules, such as long-chain alcohols and fatty acids, is required for a successful transition towards a biobased economy. Currently, economically viable production of these metabolites in *S. cerevisiae* is precluded by a limited availability and high metabolic cost of key cytosolic precursors needed for their synthesis. The goal of the research presented in this thesis was to explore strategies for improving the production of two such precursors, acetyl-CoA and succinyl-CoA, in the yeast cytosol.

Chapter 1 gives a general introduction on the current climate challenge, and describes how biotechnology may help to reduce output of greenhouse gases associated with the production of chemicals and transport fuels. In addition, the product spectrum of *S. cerevisiae* is described, together with the general engineering strategies that can be used to expand and improve product formation by this yeast. The chapter then introduces the two product precursors, acetyl-CoA and succinyl-CoA, on which the experimental research described in this thesis was focused.

Chapter 2 describes the engineering, characterization and genome data analysis of engineered *S. cerevisiae* strains in which a cytosolically expressed, bacterial pyruvate dehydrogenase (PDH) complex is the sole enzyme responsible for formation of acetyl-CoA from pyruvate. Metabolic engineering approaches alone did not enable growth solely relying on this introduced pathway. Therefore, adaptive laboratory evolution experiments were devised and successfully applied to select evolved strains in which acetyl-CoA production was strictly dependent on the heterologously expressed PDH complex. Whole-genome sequencing revealed, in multiple independent lines, the emergence of mutator phenotypes, which suggested that multiple, simultaneous mutations had to occur for the establishment of the improved phenotype. Analysis of the complex genotypes of the evolved strains suggested possible explanations for the observed phenotype, which challenged some current hypotheses on the regulation of genes involved in central carbon metabolism.

ATP-efficient production of succinyl-CoA in the yeast cytosol could open up new pathways towards compounds such as 1,4-butanediol, 4-hydroxybutyrate and 5-aminolevulinic acid. Chapter 3 explores a strategy to accomplish cytosolic synthesis of succinyl-CoA in *S. cerevisiae* by functional expression of a bacterial α-ketoglutarate dehydrogenase complex. Experiments

with cell homogenates indicated the cytosolic expression and assembly of a functional α-ketoglutarate dehydrogenase complex in the engineered yeast strains. In addition, *in vivo* experiments showed that the heterologous pathway could fully complement an introduced auxotrophy for 5-aminolevulinic acid, thus indicating the presence of a usable pool of succinyl-CoA in the cytosol of *S. cerevisiae*. This work is the first evidence for the production of cytosolic succinyl-CoA and opens up *S. cerevisiae* for the production of relevant industrial compounds that are currently not yet produced in this host.

The research described in Chapter 2 made intensive use of lactate-grown cultures for laboratory evolution of yeast strains with genetic modifications in pyruvate metabolism. Based on earlier research, it was anticipated that some of the mutations in evolved strains might be related to lactate transport rather than to pyruvate metabolism. As a parallel research line, Chapter 4 therefore focused on the application of adaptive laboratory evolution to identify genes and alleles that could, potentially, contributed to improved transport of lactic acid in *S. cerevisiae*. To this end, a strain in which the *JEN1* and *ADY2* lactate transporter genes were deleted, was evolved for consumption of lactic acid. This research line, which led to the identification of new lactate transporters, showed the power of laboratory evolution experiments in identifying relevant phenotypes and genetic plasticity.

## References

Abbott, D. A., van den Brink, J., Minneboo, I. M., Pronk, J. T., van Maris, A. J., 2009a. Anaerobic homolactate fermentation with *Saccharomyces cerevisiae* results in depletion of ATP and impaired metabolic activity. FEMS Yeast Res. 9, 349-57. DOI: https://doi.org/10.1111/j.1567-1364.2009.00506.x

Abbott, D. A., Zelle, R. M., Pronk, J. T., van Maris, A. J., 2009b. Metabolic engineering of *Saccharomyces cerevisiae* for production of carboxylic acids: current status and challenges. FEMS Yeast Res. 9, 1123-36. DOI: https://doi.org/10.1111/j.1567-1364.2009.00537.x

Alfke, G., Irion, W. W., Neuwirth, O. S., 2007. Oil Refining. Ullmann's Encyclopedia of Industrial Chemistry.

Argueso, J. L., Carazzolle, M. F., Mieczkowski, P. A., Duarte, F. M., Netto, O. V., Missawa, S. K., Galzerani, F., Costa, G. G., Vidal, R. O., Noronha, M. F., Dominska, M., Andrietta, M. G., Andrietta, S. R., Cunha, A. F., Gomes, L. H., Tavares, F. C., Alcarde, A. R., Dietrich, F. S., McCusker, J. H., Petes, T. D., Pereira, G. A., 2009. Genome structure of a *Saccharomyces cerevisiae* strain widely used in bioethanol production. Genome Res. 19, 2258-70. DOI: https://doi.org/10.1101/gr.091777.109

Atsumi, S., Cann, A. F., Connor, M. R., Shen, C. R., Smith, K. M., Brynildsen, M. P., Chou, K. J., Hanai, T., Liao, J. C., 2008. Metabolic engineering of *Escherichia coli* for 1-butanol production. Metab Eng. 10, 305-11. DOI: https://doi.org/10.1016/j.ymben.2007.08.003

Avalos, J. L., Fink, G. R., Stephanopoulos, G., 2013. Compartmentalization of metabolic pathways in yeast mitochondria improves the production of branched-chain alcohols. Nat Biotechnol. 31, 335-41. DOI: https://doi.org/10.1038/nbt.2509

Awan, A. R., Blount, B. A., Bell, D. J., Shaw, W. M., Ho, J. C. H., McKiernan, R. M., Ellis, T., 2017. Biosynthesis of the antibiotic nonribosomal peptide penicillin in baker's yeast. Nat Commun. 8, 15202. DOI: https://doi.org/10.1038/ncomms15202

Baek, S. H., Kwon, E. Y., Kim, Y. H., Hahn, J. S., 2016. Metabolic engineering and adaptive evolution for efficient production of D-lactic acid in *Saccharomyces cerevisiae*. Appl Microbiol Biotechnol. 100, 2737-48. DOI: https://doi.org/10.1007/s00253-015-7174-0

Bagheri, A. R., Laforsch, C., Greiner, A., Agarwal, S., 2017. Fate of So-Called Biodegradable Polymers in Seawater and Freshwater. Glob Chall. 1, 1700048. DOI: https://doi.org/10.1002/gch2.201700048

Bailey, J. E., 1991. Toward a science of metabolic engineering. Science. 252, 1668-75. DOI: https://doi.org/10.1126/science.2047876

Bard, M., Woods, R. A., Haslam, J. M., 1974. Porphyrin mutants of *Saccharomyces cerevisiae*: Correlated lesions in sterol and fatty acid biosynthesis. Biochemical and Biophysical Research Communications. 56, 324-330. DOI: https://doi.org/10.1016/0006-291x(74)90845-6

Beale, S. I., 1970. The biosynthesis of d-aminolevulinic acid in *Chlorella*. Plant Physiol. 45, 504-6. DOI: https://doi.org/10.1104/pp.45.4.504

Bell, P. J., Higgins, V. J., Attfield, P. V., 2001. Comparison of fermentative capacities of industrial baking and wild-type yeasts of the species *Saccharomyces cerevisiae* in different sugar media. Lett Appl Microbiol. 32, 224-9. DOI: https://doi.org/10.1046/j.1472-765x.2001.00894.x

Bereiter, B., Eggleston, S., Schmitt, J., Nehrbass-Ahles, C., Stocker, T. F., Fischer, H., Kipfstuhl, S., Chappellaz, J., 2015. Revision of the EPICA Dome C CO2 record from 800 to 600 kyr before present. Geophysical Research Letters. 42, 542-549. DOI: https://doi.org/10.1002/2014gl061957

Bieber, L. L., 1988. Carnitine. Annu Rev Biochem. 57, 261-83. DOI: https://doi.org/10.1146/annurev.bi.57.070188.001401

Bowman, S. B., Zaman, Z., Collinson, L. P., Brown, A. J., Dawes, I. W., 1992. Positive regulation of the *LPD1* gene of *Saccharomyces cerevisiae* by the *HAP2/HAP3/HAP4* activation system. Mol Gen Genet. 231, 296-303. DOI: https://doi.org/10.1007/BF00279803

Branduardi, P., Longo, V., Berterame, N. M., Rossi, G., Porro, D., 2013. A novel pathway to produce butanol and isobutanol in *Saccharomyces cerevisiae*. Biotechnol Biofuels. 6, 68. DOI: https://doi.org/10.1186/1754-6834-6-68

Brouns, S. J., Jore, M. M., Lundgren, M., Westra, E. R., Slijkhuis, R. J., Snijders, A. P., Dickman, M. J., Makarova, K. S., Koonin, E. V., van der Oost, J., 2008. Small CRISPR RNAs guide antiviral defense in prokaryotes. Science. 321, 960-4. DOI: https://doi.org/10.1126/science.1159689

Brown, O., 2009. Migration, climate change and the environment: A complex nexus. Geneve: IOM Policy Brief. December.

Brown, P., Gajdusek, D. C., Gibbs Jr, C., Asher, D. M., 1985. Potential epidemic of Creutzfeldt–Jakob disease from human growth hormone therapy. New England Journal of Medicine. 313, 728-731. DOI: https://doi.org/10.1056/NEJM198509193131205

Buu, L. M., Chen, Y. C., Lee, F. J., 2003. Functional characterization and localization of acetyl-CoA hydrolase, Ach1p, in *Saccharomyces cerevisiae*. J Biol Chem. 278, 17203-9. DOI: https://doi.org/10.1074/jbc.M213268200

Calero, P., Nikel, P. I., 2019. Chasing bacterial chassis for metabolic engineering: a perspective review from classical to non-traditional microorganisms. Microb Biotechnol. 12, 98-124. DOI: https://doi.org/10.1111/1751-7915.13292

Chandran, S. S., Kealey, J. T., Reeves, C. D., 2011. Microbial production of isoprenoids. Process Biochemistry. 46, 1703-1710. DOI: https://doi.org/10.1016/j.procbio.2011.05.012

Chen, X., Nielsen, K. F., Borodina, I., Kielland-Brandt, M. C., Karhumaa, K., 2011. Increased isobutanol production in *Saccharomyces cerevisiae* by overexpression of genes in valine metabolism. Biotechnol Biofuels. 4, 21. DOI: https://doi.org/10.1186/1754-6834-4-21

Cheong, S., Clomburg, J. M., Gonzalez, R., 2016. Energy- and carbon-efficient synthesis of functionalized small molecules in bacteria using non-decarboxylative Claisen condensation reactions. Nat Biotechnol. 34, 556-61. DOI: https://doi.org/10.1038/nbt.3505

Clark, P. U., Shakun, J. D., Marcott, S. A., Mix, A. C., Eby, M., Kulp, S., Levermann, A., Milne, G. A., Pfister, P. L., Santer, B. D., Schrag, D. P., Solomon, S., Stocker, T. F., Strauss, B. H., Weaver, A. J., Winkelmann, R., Archer, D., Bard, E., Goldner, A., Lambeck, K., Pierrehumbert, R. T., Plattner, G.-K., 2016. Consequences of twenty-first-century policy for multi-millennial climate and sea-level change. Nature Climate Change. 6, 360-369. DOI: https://doi.org/10.1038/nclimate2923

Comello, S., Reichelstein, S., Sahoo, A., 2018. The road ahead for solar PV power. Renewable and Sustainable Energy Reviews. 92, 744-756. DOI: https://doi.org/10.1016/j.rser.2018.04.098

Covello, P. S., 2008. Making artemisinin. Phytochemistry. 69, 2881-5. DOI: https://doi.org/10.1016/j.phytochem.2008.10.001

de Jong-Gubbels, P., van den Berg, M. A., Steensma, H. Y., van Dijken, J. P., Pronk, J. T., 1997. The *Saccharomyces cerevisiae* acetyl-coenzyme A synthetase encoded by the *ACS1* gene, but not the *ACS2*-encoded enzyme, is subject to glucose catabolite inactivation. FEMS microbiology letters. 153, 75-81. DOI: https://doi.org/10.1111/j.1574-6968.1997.tb10466.x

De Virgilio, C., Bürckert, N., Barth, G., Neuhaus, J. M., Boller, T., Wiemken, A., 1992. Cloning and disruption of a gene required for growth on acetate but not on ethanol: The acetyl-coenzyme a synthetase gene of *Saccharomyces cerevisiae*. Yeast. 8, 1043-1051. DOI: https://doi.org/10.1002/yea.320081207

DiCarlo, J. E., Norville, J. E., Mali, P., Rios, X., Aach, J., Church, G. M., 2013. Genome engineering in *Saccharomyces cerevisiae* using CRISPR-Cas systems. Nucleic Acids Res. 41, 4336-43. DOI: https://doi.org/10.1093/nar/gkt135

Dickinson, J. R., Roy, D. J., Dawes, I. W., 1986. A mutation affecting lipoamide dehydrogenase, pyruvate dehydrogenase and 2-oxoglutarate dehydrogenase activities in *Saccharomyces cerevisiae*. Journal. 204, 103-107.

Dragosits, M., Mattanovich, D., 2013. Adaptive laboratory evolution -- principles and applications for biotechnology. Microb Cell Fact. 12, 64. DOI: https://doi.org/10.1186/1475-2859-12-64

Eagan, N. M., Kumbhalkar, M. D., Buchanan, J. S., Dumesic, J. A., Huber, G. W., 2019. Chemistries and processes for the conversion of ethanol into middle-distillate fuels. Nature Reviews Chemistry. 3, 223-249. DOI: https://doi.org/10.1038/s41570-019-0084-4

Fargione, J., Hill, J., Tilman, D., Polasky, S., Hawthorne, P., 2008. Land clearing and the biofuel carbon debt. Science. 319, 1235-8. DOI: https://doi.org/10.1126/science.1152747

Flamholz, A., Noor, E., Bar-Even, A., Milo, R., 2012. eQuilibrator--the biochemical thermodynamics calculator. Nucleic Acids Res. 40, D770-5. DOI: https://doi.org/10.1093/nar/gkr874

Fleming, A., 1929. On the Antibacterial Action of Cultures of a Penicillium, with Special Reference to Their Use in the Isolation of *B. influenzae.* British Journal of Experimental Pathology. 10, 226-236.

Flikweert, M. T., de Swaaf, M., van Dijken, J. P., Pronk, J. T., 1999. Growth requirements of pyruvate-decarboxylase-negative *Saccharomyces cerevisiae*. FEMS Microbiol Lett. 174, 73-9. DOI: https://doi.org/10.1111/j.1574-6968.1999.tb13551.x

Flikweert, M. T., van Dijken, J. P., Pronk, J. T., 1997. Metabolic responses of pyruvate decarboxylase-negative *Saccharomyces cerevisiae* to glucose excess. Appl Environ Microbiol. 63, 3399-404. DOI: https://doi.org/10.1128/AEM.63.9.3399-3404.1997

Flodh, H., 1986. Human growth hormone produced with recombinant DNA technology: development and production. Acta Paediatr Scand Suppl. 325, 1-9. DOI: https://doi.org/10.1111/j.1651-2227.1986.tb10356.x

Galanie, S., Thodey, K., Trenchard, I. J., Filsinger Interrante, M., Smolke, C. D., 2015. Complete biosynthesis of opioids in yeast. Science. 349, 1095-100. DOI: https://doi.org/10.1126/science.aac9373

Getachew, A., Woldesenbet, F., 2016. Production of biodegradable plastic by polyhydroxybutyrate (PHB) accumulating bacteria using low cost agricultural waste material. BMC research notes. 9, 1-9. DOI: https://doi.org/10.1186/s13104-016-2321-y

Gey, U., Czupalla, C., Hoflack, B., Rodel, G., Krause-Buchholz, U., 2008. Yeast pyruvate dehydrogenase complex is regulated by a concerted activity of two kinases and two phosphatases. J Biol Chem. 283, 9759-67. DOI: https://doi.org/10.1074/jbc.M708779200

Goffeau, A., Barrell, B. G., Bussey, H., Davis, R. W., Dujon, B., Feldmann, H., Galibert, F., Hoheisel, J. D., Jacq, C., Johnston, M., Louis, E. J., Mewes, H. W., Murakami, Y., Philippsen, P., Tettelin, H., Oliver, S. G., 1996. Life with 6000 genes. Science. 274, 546, 563-7. DOI: 10.1126/science.274.5287.546

Gombert, A. K., van Maris, A. J., 2015. Improving conversion yield of fermentable sugars into fuel ethanol in 1st generation yeast-based production processes. Curr Opin Biotechnol. 33, 81-6. DOI: https://doi.org/10.1016/j.copbio.2014.12.012

Hale, V., Keasling, J. D., Renninger, N., Diagana, T. T., 2007. Microbially derived artemisinin: a biotechnology solution to the global problem of access to affordable antimalarial drugs. Am J Trop Med Hyg. 77, 198-202. DOI: https://doi.org/10.4269/ajtmh.2007.77.198

Hassing, E. J., de Groot, P. A., Marquenie, V. R., Pronk, J. T., Daran, J. G., 2019. Connecting central carbon and aromatic amino acid metabolisms to improve de novo 2-phenylethanol production in *Saccharomyces cerevisiae*. Metab Eng. 56, 165-180. DOI: https://doi.org/10.1016/j.ymben.2019.09.011

Henriksen, P., Wagner, S. A., Weinert, B. T., Sharma, S., Bacinskaja, G., Rehman, M., Juffer, A. H., Walther, T. C., Lisby, M., Choudhary, C., 2012. Proteome-wide analysis of lysine acetylation suggests its broad regulatory scope in *Saccharomyces cerevisiae*. Mol Cell Proteomics. 11, 1510-22. DOI: https://doi.org/10.1074/mcp.M112.017251

Herrgård, M., Panagiotou, G., 2012. Analyzing the genomic variation of microbial cell factories in the era of "New Biotechnology". Computational and structural biotechnology journal. 3, e201210012. DOI: https://doi.org/10.5936/csbj.201210012

Hill, J. K., Griffiths, H. M., Thomas, C. D., 2011. Climate change and evolutionary adaptations at species' range margins. Annu Rev Entomol. 56, 143-59. DOI: https://doi.org/10.1146/annurev-ento-120709-144746

Hiltunen, J. K., Mursula, A. M., Rottensteiner, H., Wierenga, R. K., Kastaniotis, A. J., Gurvitz, A., 2003. The biochemistry of peroxisomal beta-oxidation in the yeast *Saccharomyces cerevisiae*. FEMS microbiology reviews. 27, 35-64. DOI: https://doi.org/10.1016/S0168-6445(03)00017-2

Hitzeman, R. A., Hagie, F. E., Levine, H. L., Goeddel, D. V., Ammerer, G., Hall, B. D., 1981. Expression of a human gene for interferon in yeast. Nature. 293, 717-22. DOI: https://doi.org/10.1038/293717a0

Hughes, R. A., Ellington, A. D., 2017. Synthetic DNA Synthesis and Assembly: Putting the Synthetic in Synthetic Biology. Cold Spring Harb Perspect Biol. 9, a023812. DOI: https://doi.org/10.1101/cshperspect.a023812

Jambeck, J. R., Geyer, R., Wilcox, C., Siegler, T. R., Perryman, M., Andrady, A., Narayan, R., Law, K. L., 2015. Marine pollution. Plastic waste inputs from land into the ocean. Science. 347, 768-71. DOI: https://doi.org/10.1126/science.1260352

Jinek, M., Chylinski, K., Fonfara, I., Hauer, M., Doudna, J. A., Charpentier, E., 2012. A programmable dual-RNA–guided DNA endonuclease in adaptive bacterial immunity. science. 337, 816-821. DOI: https://doi.org/10.1126/science.1225829

Jones, C. M., Kammen, D. M., 2011. Quantifying carbon footprint reduction opportunities for US households and communities. Environmental science & technology. 45, 4088-4095. DOI: https://doi.org/10.1021/es102221h

Kaneko, S., 1998. Photodynamic diagnosis using 5-ALA-preliminary report. J. Iwamizawa Municipal General Hospital. 24, 71-79.

Kariduraganavar, M. Y., Kittur, A. A., Kamble, R. R., 2014. Polymer Synthesis and Processing. In: Kumbar, S. G., Laurencin, C. T., Deng, M., Eds.), Natural and Synthetic Biomedical Polymers. Elsevier, Oxford, pp. 1-31.

Kawamoto, S., Tanaka, A., Fukui, S., 1979. Yeast peroxisomes (microbodies): structure, function and application. Seikagaku. 51, 1009-22.

Kennedy, J. C., Pottier, R. H., Pross, D. C., 1990. Photodynamic therapy with endogenous protoporphyrin IX: basic principles and present clinical experience. J Photochem Photobiol B. 6, 143-8. DOI: https://doi.org/10.1016/1011-1344(90)85083-9

Kohlhaw, G. B., Tan-Wilson, A., 1977. Carnitine acetyltransferase: candidate for the transfer of acetyl groups through the mitochondrial membrane of yeast. J Bacteriol. 129, 1159-61. DOI: https://doi.org/10.1128/JB.129.2.1159-1161.1977

Koopman, F., Beekwilder, J., Crimi, B., van Houwelingen, A., Hall, R. D., Bosch, D., van Maris, A. J., Pronk, J. T., Daran, J. M., 2012. De novo production of the flavonoid naringenin in engineered *Saccharomyces cerevisiae*. Microb Cell Fact. 11, 155. DOI: https://doi.org/10.1186/1475-2859-11-155

Kornberg, H. L., 1966. The role and control of the glyoxylate cycle in *Escherichia coli*. Biochem J. 99, 1-11. DOI: https://doi.org/10.1042/bj0990001

Kozak, B. U., van Rossum, H. M., Benjamin, K. R., Wu, L., Daran, J. M., Pronk, J. T., van Maris, A. J., 2014a. Replacement of the *Saccharomyces cerevisiae* acetyl-CoA synthetases by alternative pathways for cytosolic acetyl-CoA synthesis. Metab Eng. 21, 46-59. DOI: https://doi.org/10.1016/j.ymben.2013.11.005

Kozak, B. U., van Rossum, H. M., Luttik, M. A., Akeroyd, M., Benjamin, K. R., Wu, L., de Vries, S., Daran, J. M., Pronk, J. T., van Maris, A. J., 2014b. Engineering acetyl coenzyme A supply: functional expression of a bacterial pyruvate dehydrogenase complex in the cytosol of *Saccharomyces cerevisiae*. mBio. 5, e01696-14. DOI: https://doi.org/10.1128/mBio.01696-14

Kozak, B. U., van Rossum, H. M., Niemeijer, M. S., van Dijk, M., Benjamin, K., Wu, L., Daran, J. M., Pronk, J. T., van Maris, A. J., 2016. Replacement of the initial steps of ethanol metabolism in *Saccharomyces cerevisiae* by ATP-independent acetylating acetaldehyde dehydrogenase. FEMS Yeast Res. 16, fow006. DOI: https://doi.org/10.1093/femsyr/fow006

Kumar, D., Murthy, G. S., 2011. Impact of pretreatment and downstream processing technologies on economics and energy in cellulosic ethanol production. Biotechnol Biofuels. 4, 27. DOI: https://doi.org/10.1186/1754-6834-4-27

Lan, E. I., Liao, J. C., 2013. Microbial synthesis of n-butanol, isobutanol, and other higher alcohols from diverse resources. Bioresour Technol. 135, 339-49. DOI: https://doi.org/10.1016/j.biortech.2012.09.104

LanzaTech, Jet Fuel Derived from Ethanol Now Eligible for Commercial Flights. 2018.

LanzaTech, LanzaTech Moves Forward on Sustainable Aviation Scale Up in the USA and Japan. 2019.

Le Meur, S., Zinn, M., Egli, T., Thöny-Meyer, L., Ren, Q., 2013. Poly (4-hydroxybutyrate)(P4HB) production in recombinant *Escherichia coli*: P4HB synthesis is uncoupled with cell growth. Microbial cell factories. 12, 123. DOI: https://doi.org/10.1186/1475-2859-12-123

Lee, S. Y., Park, J. H., Jang, S. H., Nielsen, L. K., Kim, J., Jung, K. S., 2008. Fermentative butanol production by *Clostridia*. Biotechnol Bioeng. 101, 209-28. DOI: https://doi.org/10.1002/bit.22003

Lian, J., Mishra, S., Zhao, H., 2018. Recent advances in metabolic engineering of *Saccharomyces cerevisiae*: New tools and their applications. Metab Eng. 50, 85-108. DOI: https://doi.org/10.1016/j.ymben.2018.04.011

Lian, J., Zhao, H., 2016. Functional reconstitution of a pyruvate dehydrogenase in the cytosol of *Saccharomyces cerevisiae* through lipoylation machinery engineering. ACS Synth Biol. 5, 689-97. DOI: https://doi.org/10.1021/acssynbio.6b00019

Liu, L., Pan, A., Spofford, C., Zhou, N., Alper, H. S., 2015. An evolutionary metabolic engineering approach for enhancing lipogenesis in *Yarrowia lipolytica*. Metab Eng. 29, 36-45. DOI: https://doi.org/10.1016/j.ymben.2015.02.003

Liu, L., Wang, J., Rosenberg, D., Zhao, H., Lengyel, G., Nadel, D., 2018. Fermented beverage and food storage in 13,000 y-old stone mortars at Raqefet Cave, Israel: Investigating Natufian ritual feasting. Journal of Archaeological Science: Reports. 21, 783-793. DOI: https://doi.org/10.1016/j.jasrep.2018.08.008

Liu, S., Zhang, G., Li, X., Zhang, J., 2014. Microbial production and applications of 5-aminolevulinic acid. Appl Microbiol Biotechnol. 98, 7349-57. DOI: https://doi.org/10.1007/s00253-014-5925-y

Lobell, D. B., Burke, M. B., Tebaldi, C., Mastrandrea, M. D., Falcon, W. P., Naylor, R. L., 2008. Prioritizing climate change adaptation needs for food security in 2030. Science. 319, 607-10. DOI: https://doi.org/10.1126/science.1152339

Lobell, D. B., Schlenker, W., Costa-Roberts, J., 2011. Climate trends and global crop production since 1980. Science. 333, 616-20. DOI: https://doi.org/10.1126/science.1204531

Mans, R., Daran, J. G., Pronk, J. T., 2018. Under pressure: evolutionary engineering of yeast strains for improved performance in fuels and chemicals production. Curr Opin Biotechnol. 50, 47-56. DOI: https://doi.org/10.1016/j.copbio.2017.10.011

Mans, R., van Rossum, H. M., Wijsman, M., Backx, A., Kuijpers, N. G., van den Broek, M., Daran-Lapujade, P., Pronk, J. T., van Maris, A. J., Daran, J. M., 2015. CRISPR/Cas9: a molecular Swiss army knife for simultaneous introduction of multiple genetic modifications in *Saccharomyces cerevisiae*. FEMS Yeast Res. 15. DOI: https://doi.org/10.1093/femsyr/fov004

Martin, D. P., Williams, S. F., 2003. Medical applications of poly-4-hydroxybutyrate: a strong flexible absorbable biomaterial. Biochemical Engineering Journal. 16, 97-105. DOI: https://doi.org/10.1016/s1369-703x(03)00040-8

Marzeion, B., Levermann, A., 2014. Loss of cultural world heritage and currently inhabited places to sea-level rise. Environmental Research Letters. 9, 034001. DOI: https://doi.org/10.1088/1748-9326/9/3/034001

Masson-Delmotte, V., Zhai, P., Pörtner, H.-O., Roberts, D., Skea, J., Shukla, P. R., Pirani, A., Moufouma-Okia, W., Péan, C., Pidcock, R., Connors, S., Matthews, J. B. R., Chen, Y., Zhou, X., Gomis, M. I., Lonnoy, E., Maycock, T., Tignor, M., T., W., IPCC, 2018: Summary for Policymakers. In: Global Warming of 1.5°C. An IPCC Special Report on the impacts of global warming of 1.5°C above pre-industrial levels and related global greenhouse gas emission pathways, in the context of strengthening the global response to the threat of climate change, sustainable development, and efforts to eradicate povert. IPCC, 2018.

Mattanovich, D., Sauer, M., Gasser, B., 2014. Yeast biotechnology: teaching the old dog new tricks. Microb Cell Fact. 13, 34. DOI: https://doi.org/10.1186/1475-2859-13-34

McMillan, M., Shepherd, A., Sundal, A., Briggs, K., Muir, A., Ridout, A., Hogg, A., Wingham, D., 2014. Increased ice losses from Antarctica detected by CryoSat-2. Geophysical Research Letters. 41, 3899-3905. DOI: https://doi.org/10.1002/2014gl060111

Meadows, A. L., Hawkins, K. M., Tsegaye, Y., Antipov, E., Kim, Y., Raetz, L., Dahl, R. H., Tai, A., Mahatdejkul-Meadows, T., Xu, L., Zhao, L., Dasika, M. S., Murarka, A., Lenihan, J., Eng, D., Leng, J. S., Liu, C. L., Wenger, J. W., Jiang, H., Chao, L., Westfall, P., Lai, J., Ganesan, S., Jackson, P., Mans, R., Platt, D., Reeves, C. D., Saija, P. R., Wichmann, G., Holmes, V. F., Benjamin, K., Hill, P. W., Gardner, T. S., Tsong, A. E., 2016. Rewriting yeast central carbon metabolism for industrial isoprenoid production. Nature. 537, 694-697. DOI: https://doi.org/10.1038/nature19769

Mercke, P., Bengtsson, M., Bouwmeester, H. J., Posthumus, M. A., Brodelius, P. E., 2000. Molecular cloning, expression, and characterization of amorpha-4,11-diene synthase, a key enzyme of artemisinin biosynthesis in *Artemisia annua* L. Arch Biochem Biophys. 381, 173-80. DOI: https://doi.org/10.1006/abbi.2000.1962

Metallo, C. M., Vander Heiden, M. G., 2013. Understanding metabolic regulation and its influence on cell physiology. Mol Cell. 49, 388-98. DOI: https://doi.org/10.1016/j.molcel.2013.01.018

Metz, B., Davidson, O., Swart, R., Pan, J., 2001. Climate change 2001: mitigation: contribution of Working Group III to the third assessment report of the Intergovernmental Panel on Climate Change. Cambridge University Press.

Michel, R. H., McGovern, P. E., Badler, V. R., 1992. Chemical evidence for ancient beer. Nature. 360, 24-24. DOI: https://doi.org/10.1038/360024b0

Miller, L. H., Su, X., 2011. Artemisinin: discovery from the Chinese herbal garden. Cell. 146, 855-8. DOI: https://doi.org/10.1016/j.cell.2011.08.024

Morange, M., 2000. A history of molecular biology. Harvard University Press.

Moyses, D. N., Reis, V. C., de Almeida, J. R., de Moraes, L. M., Torres, F. A., 2016. Xylose Fermentation by *Saccharomyces cerevisiae*: Challenges and Prospects. Int J Mol Sci. 17, 207. DOI: https://doi.org/10.3390/ijms17030207

Mussatto, S. I., Dragone, G., Guimaraes, P. M., Silva, J. P., Carneiro, L. M., Roberto, I. C., Vicente, A., Domingues, L., Teixeira, J. A., 2010. Technological trends, global market, and challenges of bio-ethanol production. Biotechnol Adv. 28, 817-30. DOI: https://doi.org/10.1016/j.biotechadv.2010.07.001

Musser, M. T., 2000. Adipic Acid. Ullmann's Encyclopedia of Industrial Chemistry.

Nielsen, J., Keasling, J. D., 2016. Engineering Cellular Metabolism. Cell. 164, 1185-1197. DOI: https://doi.org/10.1016/j.cell.2016.02.004

NOAA, N. C. f. E. I., State of the Climate: Global Climate Report for Annual 2019. NOAA, National Centers for Environmental Information, 2019.

Noor, E., Eden, E., Milo, R., Alon, U., 2010. Central carbon metabolism as a minimal biochemical walk between precursors for biomass and energy. Mol Cell. 39, 809-20. DOI: https://doi.org/10.1016/j.molcel.2010.08.031

Olsson, K., Carlsen, S., Semmler, A., Simon, E., Mikkelsen, M. D., Moller, B. L., 2016. Microbial production of next-generation stevia sweeteners. Microb Cell Fact. 15, 207. DOI: https://doi.org/10.1186/s12934-016-0609-1

Oswald, M., Fischer, M., Dirninger, N., Karst, F., 2007. Monoterpenoid biosynthesis in *Saccharomyces cerevisiae*. FEMS Yeast Res. 7, 413-21. DOI: https://doi.org/10.1111/j.1567-1364.2006.00172.x

Otero, J. M., Cimini, D., Patil, K. R., Poulsen, S. G., Olsson, L., Nielsen, J., 2013. Industrial systems biology of *Saccharomyces cerevisiae* enables novel succinic acid cell factory. PLoS One. 8, e54144. DOI: https://doi.org/10.1371/journal.pone.0054144

Ottelin, J., Heinonen, J., Nässén, J., Junnila, S., 2019. Household carbon footprint patterns by the degree of urbanisation in Europe. Environmental Research Letters. 14, 114016. DOI: https://doi.org/10.1088/1748-9326/ab443d

Oud, B., van Maris, A. J., Daran, J. M., Pronk, J. T., 2012. Genome-wide analytical approaches for reverse metabolic engineering of industrially relevant phenotypes in yeast. FEMS Yeast Res. 12, 183-96. DOI: https://doi.org/10.1111/j.1567-1364.2011.00776.x

Pacala, S., Socolow, R., 2004. Stabilization wedges: solving the climate problem for the next 50 years with current technologies. Science. 305, 968-72. DOI: https://doi.org/10.1126/science.1100103

Patel, M. S., Roche, T. E., 1990. Molecular biology and biochemistry of pyruvate dehydrogenase complexes. FASEB J. 4, 3224-33. DOI: https://doi.org/10.1096/fasebj.4.14.2227213

Powell-Jackson, J., Weller, R. O., Kennedy, P., Preece, M. A., Whitcombe, E. M., Newsom-Davis, J., 1985. Creutzfeldt-Jakob disease after administration of human growth hormone. Lancet. 2, 244-6. DOI: https://doi.org/10.1016/s0140-6736(85)90292-2

Pronk, J. T., Yde Steensma, H., Van Dijken, J. P., 1996. Pyruvate metabolism in *Saccharomyces cerevisiae*. Yeast. 12, 1607-33. DOI: https://doi.org/10.1002/(sici)1097-0061(199612)12:16<1607::aid-yea70>3.0.co;2-4

Pye, C. R., Bertin, M. J., Lokey, R. S., Gerwick, W. H., Linington, R. G., 2017. Retrospective analysis of natural products provides insights for future discovery trends. Proc Natl Acad Sci U S A. 114, 5601-5606. DOI: https://doi.org/10.1073/pnas.1614680114

Raab, A. M., Gebhardt, G., Bolotina, N., Weuster-Botz, D., Lang, C., 2010. Metabolic engineering of *Saccharomyces cerevisiae* for the biotechnological production of succinic acid. Metab Eng. 12, 518-25. DOI: https://doi.org/10.1016/j.ymben.2010.08.005

Rebeiz, C., Montazer-Zouhoor, A., Hopen, H., Wu, S., 1984. Photodynamic herbicides: 1. Concept and phenomenology. Enzyme and microbial technology. 6, 390-396. DOI:

Rebello, S., Abraham, A., Madhavan, A., Sindhu, R., Binod, P., Karthika Bahuleyan, A., Aneesh, E. M., Pandey, A., 2018. Non-conventional yeast cell factories for sustainable bioprocesses. FEMS Microbiol Lett. 365, fny222. DOI: https://doi.org/10.1093/femsle/fny222

Renninger, N. S., Mcphee, D. J., Fuel compositions comprising farnesane and farnesane derivatives and method of making and using same. Google Patents, 2008.

Reuveny, R., 2007. Climate change-induced migration and violent conflict. Political Geography. 26, 656-673. DOI: https://doi.org/10.1016/j.polgeo.2007.05.001

Reyes, L. H., Gomez, J. M., Kao, K. C., 2014. Improving carotenoids production in yeast via adaptive laboratory evolution. Metab Eng. 21, 26-33. DOI: https://doi.org/10.1016/j.ymben.2013.11.002

Ro, D. K., Paradise, E. M., Ouellet, M., Fisher, K. J., Newman, K. L., Ndungu, J. M., Ho, K. A., Eachus, R. A., Ham, T. S., Kirby, J., Chang, M. C., Withers, S. T., Shiba, Y., Sarpong, R., Keasling, J. D., 2006. Production of the antimalarial drug precursor artemisinic acid in engineered yeast. Nature. 440, 940-3. DOI: https://doi.org/10.1038/nature04640

Rodrigues, M. F. F., Sousa, I. M. O., Vardanega, R., Nogueira, G. C., Meireles, M. A. A., Foglio, M. A., Marchese, J. A., 2019. Techno-economic evaluation of artemisinin extraction from *Artemisia annua* L. using supercritical carbon dioxide. Industrial Crops and Products. 132, 336-343. DOI: https://doi.org/10.1016/j.indcrop.2019.02.049

Rodriguez, S., Denby, C. M., Van Vu, T., Baidoo, E. E., Wang, G., Keasling, J. D., 2016. ATP citrate lyase mediated cytosolic acetyl-CoA biosynthesis increases mevalonate production in *Saccharomyces cerevisiae*. Microb Cell Fact. 15, 48. DOI: https://doi.org/10.1186/s12934-016-0447-1

Rogelj, J., Shindell, D., Jiang, K., Fifita, S., Forster, P., Ginzburg, V., Handa, C., Kheshgi, H., Kobayashi, S., Kriegler, E., 2018. Mitigation pathways compatible with 1.5 C in the context of sustainable development.

Rosenzweig, C., Parry, M. L., 1994. Potential impact of climate change on world food supply. Nature. 367, 133-138. DOI: https://doi.org/10.1038/367133a0

Ryan, C., An overview of GEVO's biobased isobutanol production process. 2019.

Sala, O. E., Chapin, F. S., 3rd, Armesto, J. J., Berlow, E., Bloomfield, J., Dirzo, R., Huber-Sanwald, E., Huenneke, L. F., Jackson, R. B., Kinzig, A., Leemans, R., Lodge, D. M., Mooney, H. A., Oesterheld, M., Poff, N. L., Sykes, M. T., Walker, B. H., Walker, M., Wall, D. H., 2000. Global biodiversity scenarios for the year 2100. Science. 287, 1770-4. DOI: https://doi.org/10.1126/science.287.5459.1770

Sasaki, K., Watanabe, K., Tanaka, T., Hotta, Y., Nagai, S., 1995. 5-Aminolevulinic acid production by *Chlorella* sp. during heterotrophic cultivation in the dark. World J Microbiol Biotechnol. 11, 361-2. DOI: https://doi.org/10.1007/BF00367123

Sasaki, K., Watanabe, M., Tanaka, T., Tanaka, T., 2002. Biosynthesis, biotechnological production and applications of 5-aminolevulinic acid. Appl Microbiol Biotechnol. 58, 23-9. DOI: https://doi.org/10.1007/s00253-001-0858-7

Sauer, M., Porro, D., Mattanovich, D., Branduardi, P., 2008. Microbial production of organic acids: expanding the markets. Trends Biotechnol. 26, 100-8. DOI: https://doi.org/10.1016/j.tibtech.2007.11.006

Sauer, U., 2001. Evolutionary engineering of industrially important microbial phenotypes. Metabolic engineering. Springer, pp. 129-169.

Shiba, Y., Paradise, E. M., Kirby, J., Ro, D. K., Keasling, J. D., 2007. Engineering of the pyruvate dehydrogenase bypass in *Saccharomyces cerevisiae* for high-level production of isoprenoids. Metab Eng. 9, 160-8. DOI: https://doi.org/10.1016/j.ymben.2006.10.005

Smith, K. M., Cho, K. M., Liao, J. C., 2010. Engineering *Corynebacterium glutamicum* for isobutanol production. Appl Microbiol Biotechnol. 87, 1045-55. DOI: https://doi.org/10.1007/s00253-010-2522-6

Sonderegger, M., Schumperli, M., Sauer, U., 2004. Metabolic engineering of a phosphoketolase pathway for pentose catabolism in *Saccharomyces cerevisiae*. Appl Environ Microbiol. 70, 2892-7. DOI: https://doi.org/10.1128/aem.70.5.2892-2897.2004

Steen, E. J., Chan, R., Prasad, N., Myers, S., Petzold, C. J., Redding, A., Ouellet, M., Keasling, J. D., 2008. Metabolic engineering of *Saccharomyces cerevisiae* for the production of n-butanol. Microb Cell Fact. 7, 36. DOI: https://doi.org/10.1186/1475-2859-7-36

Steen, E. J., Kang, Y., Bokinsky, G., Hu, Z., Schirmer, A., McClure, A., Del Cardayre, S. B., Keasling, J. D., 2010. Microbial production of fatty-acid-derived fuels and chemicals from plant biomass. Nature. 463, 559-62. DOI: https://doi.org/10.1038/nature08721

Stocker, T. F., Qin, D., Plattner, G.-K., Tignor, M., Allen, S. K., Boschung, J., Nauels, A., Xia, Y., Bex, V., Midgley, P. M., 2013. Climate change 2013: The physical science basis. Contribution of working group I to the fifth assessment report of the intergovernmental panel on climate change. 1535.

Strijbis, K., van Roermund, C. W., Hardy, G. P., van den Burg, J., Bloem, K., de Haan, J., van Vlies, N., Wanders, R. J., Vaz, F. M., Distel, B., 2009. Identification and characterization of a complete carnitine biosynthesis pathway in *Candida albicans*. FASEB J. 23, 2349-59. DOI: https://doi.org/10.1096/fj.08-127985

Sun, L., Alper, H. S., 2020. Non-conventional hosts for the production of fuels and chemicals. Curr Opin Chem Biol. 59, 15-22. DOI: https://doi.org/10.1016/j.cbpa.2020.03.004

Swiegers, J. H., Dippenaar, N., Pretorius, I. S., Bauer, F. F., 2001. Carnitine-dependent metabolic activities in *Saccharomyces cerevisiae*: three carnitine acetyltransferases are essential in a carnitine-dependent strain. Yeast. 18, 585-95. DOI: https://doi.org/10.1002/yea.712

Takahashi, H., McCaffery, J. M., Irizarry, R. A., Boeke, J. D., 2006. Nucleocytosolic acetyl-coenzyme a synthetase is required for histone acetylation and global transcription. Mol Cell. 23, 207-17. DOI: https://doi.org/10.1016/j.molcel.2006.05.040

Tang, X., Feng, H., Chen, W. N., 2013. Metabolic engineering for enhanced fatty acids synthesis in *Saccharomyces cerevisiae*. Metab Eng. 16, 95-102. DOI: https://doi.org/10.1016/j.ymben.2013.01.003

Thomas, C. D., Cameron, A., Green, R. E., Bakkenes, M., Beaumont, L. J., Collingham, Y. C., Erasmus, B. F., De Siqueira, M. F., Grainger, A., Hannah, L., Hughes, L., Huntley, B., Van Jaarsveld, A. S., Midgley, G. F., Miles, L., Ortega-Huerta, M. A., Peterson, A. T., Phillips, O. L., Williams, S. E., 2004. Extinction risk from climate change. Nature. 427, 145-8. DOI: https://doi.org/10.1038/nature02121

Thompson, R. C., Moore, C. J., vom Saal, F. S., Swan, S. H., 2009. Plastics, the environment and human health: current consensus and future trends. Philos Trans R Soc Lond B Biol Sci. 364, 2153-66. DOI: https://doi.org/10.1098/rstb.2009.0053

U.S. Energy Information Administration, Oil and petroleum products explained 2020.

van den Berg, M. A., de Jong-Gubbels, P., Kortland, C. J., van Dijken, J. P., Pronk, J. T., Steensma, H. Y., 1996. The two acetyl-coenzyme A synthetases of *Saccharomyces cerevisiae* differ with respect to kinetic properties and transcriptional regulation. J Biol Chem. 271, 28953-9. DOI: https://doi.org/10.1074/jbc.271.46.28953

van den Berg, M. A., Steensma, H. Y., 1995. *ACS2*, a *Saccharomyces cerevisiae* gene encoding acetyl-coenzyme A synthetase, essential for growth on glucose. Eur J Biochem. 231, 704-13. DOI: https://doi.org/10.1111/j.1432-1033.1995.tb20751.x

van der Beek, C. P., Roels, J. A., 1984. Penicillin production: biotechnology at its best. Antonie Van Leeuwenhoek. 50, 625-39. DOI: https://doi.org/10.1007/BF02386230

van Maris, A. J., Abbott, D. A., Bellissimi, E., van den Brink, J., Kuyper, M., Luttik, M. A., Wisselink, H. W., Scheffers, W. A., van Dijken, J. P., Pronk, J. T., 2006. Alcoholic fermentation of carbon sources in biomass hydrolysates by *Saccharomyces cerevisiae*: current status. Antonie Van Leeuwenhoek. 90, 391-418. DOI: https://doi.org/10.1007/s10482-006-9085-7

van Maris, A. J., Luttik, M. A., Winkler, A. A., van Dijken, J. P., Pronk, J. T., 2003. Overproduction of threonine aldolase circumvents the biosynthetic role of pyruvate decarboxylase in glucose-limited chemostat cultures of *Saccharomyces cerevisiae*. Appl Environ Microbiol. 69, 2094-9. DOI: https://doi.org/10.1128/aem.69.4.2094-2099.2003

van Maris, A. J., Winkler, A. A., Porro, D., van Dijken, J. P., Pronk, J. T., 2004. Homofermentative lactate production cannot sustain anaerobic growth of engineered *Saccharomyces cerevisiae*: possible consequence of energy-dependent lactate export. Appl Environ Microbiol. 70, 2898-905. DOI: https://doi.org/10.1128/aem.70.5.2898-2905.2004

van Roermund, C. W., Elgersma, Y., Singh, N., Wanders, R. J., Tabak, H. F., 1995. The membrane of peroxisomes in *Saccharomyces cerevisiae* is impermeable to NAD(H) and acetyl-CoA under in vivo conditions. EMBO J. 14, 3480-6.

van Rossum, H. M., Kozak, B. U., Niemeijer, M. S., Duine, H. J., Luttik, M. A., Boer, V. M., Kotter, P., Daran, J. M., van Maris, A. J., Pronk, J. T., 2016a. Alternative reactions at the interface of glycolysis and citric acid cycle in *Saccharomyces cerevisiae*. FEMS Yeast Res. 16. DOI: https://doi.org/10.1093/femsyr/fow017

van Rossum, H. M., Kozak, B. U., Niemeijer, M. S., Dykstra, J. C., Luttik, M. A., Daran, J. M., van Maris, A. J., Pronk, J. T., 2016b. Requirements for Carnitine Shuttle-Mediated Translocation of Mitochondrial Acetyl Moieties to the Yeast Cytosol. mBio. 7, e00520-16. DOI: https://doi.org/10.1128/mBio.00520-16

Vaz, F. M., Wanders, R. J., 2002. Carnitine biosynthesis in mammals. Biochem J. 361, 417-29. DOI: https://doi.org/10.1042/0264-6021:3610417

Verwaal, R., Wu, L., Damveld, R. A., Sagt, C. M. J., Succinic acid production in a eukaryotic cell In: WIPO, (Ed.). Dsm Ip Assets B.V., 2007.

Waks, Z., Silver, P. A., 2009. Engineering a synthetic dual-organism system for hydrogen production. Appl Environ Microbiol. 75, 1867-75. DOI: https://doi.org/10.1128/AEM.02009-08

WEF, World Economic Forum 2007-2020, Global Risks Reports. World Economic Forum, 2020.

Weinert, B. T., Scholz, C., Wagner, S. A., Iesmantavicius, V., Su, D., Daniel, J. A., Choudhary, C., 2013. Lysine succinylation is a frequently occurring modification in prokaryotes and eukaryotes and extensively overlaps with acetylation. Cell Rep. 4, 842-51. DOI: https://doi.org/10.1016/j.celrep.2013.07.024

Wetterstrand, K. A., DNA Sequencing Costs: Data from the NHGRI Genome Sequencing Program (GSP) Vol. 2020, www.genome.gov/sequencingcostsdata, 2020.

Yim, H., Haselbeck, R., Niu, W., Pujol-Baxley, C., Burgard, A., Boldt, J., Khandurina, J., Trawick, J. D., Osterhout, R. E., Stephen, R., Estadilla, J., Teisan, S., Schreyer, H. B., Andrae, S., Yang, T. H., Lee, S. Y., Burk, M. J., Van Dien, S., 2011. Metabolic engineering of *Escherichia coli* for direct production of 1,4-butanediol. Nat Chem Biol. 7, 445-52. DOI: https://doi.org/10.1038/nchembio.580

# 2.

# Complete redirection of pyruvate dissimilation in *Saccharomyces cerevisiae* via a cytosolic pyruvate-dehydrogenase complex

Nicolò Baldi, Demi van Duuren, Marcel van den Broek,
Jack T. Pronk and Robert Mans

Department of Biotechnology, Delft University of Technology,
van der Maasweg 9, 2629 HZ Delft, The Netherlands

## ABSTRACT

Expression of a bacterial pyruvate dehydrogenase (PDH) complex in the cytosol of *Saccharomyces cerevisiae* can provide sufficient cytosolic acetyl-CoA for biosynthesis, while lowering the ATP-requirement for synthesis of this industrially relevant precursor molecule. To explore and extend the capacity of this pathway, we engineered *S. cerevisiae* to completely redirect pyruvate dissimilation via a cytosolic PDH complex. After eliminating native pyruvate-decarboxylase and mitochondrial PDH activities in a strain expressing a bacterial PDH complex in the cytosol, a two-stage laboratory evolution approach was applied to enable and accelerate growth on L-lactate. Growth of evolved strains on L-lactate strictly depended on the cytosolic PDH complex and estimated rates of cytosolic acetyl-CoA production through the PDH complex were three-fold higher than previously reported. Whole-genome sequencing revealed high numbers of mutations in three independently evolved cell lines. The inferred mutator phenotypes of these strains complicated interpretation of sequence data and suggested that multiple mutations contributed to the evolved phenotype. All evolved strains showed mutations in genes encoding subunits of the heterologous PDH complex and loss-of-function mutations in *ACS1*, which encodes a high-affinity acetyl-CoA synthetase isoenzyme. The latter observation, together with a positive impact of carnitine addition on growth rates, identified availability of mitochondrial acetyl-CoA as critical factor in strains that depended on a cytosolic PDH complex for pyruvate dissimilation. While the genetic basis for the phenotype of the evolved strains was not fully resolved, this work provides a basis for further research into compartmentation of acetyl-CoA metabolism and to improve functionality of bacterial PDH complexes in industrial yeast strains.

## 1. INTRODUCTION

Biotechnological processes are used to industrially produce compounds ranging from bulk chemicals such as (cellulosic) ethanol and succinic acid to specialty chemicals such as sweeteners (Mikkelsen et al., 2018; Zhao et al., 2019), pharmaceuticals and their precursors (Ro et al., 2006). Several important products of microbial biotechnology, including those consisting of or derived from fatty acids (Qiao et al., 2017), isoprenoids (Meadows et al., 2016) and flavonoids (Rodriguez et al., 2017), require acetyl-Coenzyme A (acetyl-CoA) as a biosynthetic precursor. Found in all living organisms, acetyl-CoA participates in a multitude of reactions in yeast metabolism: it fuels the TCA cycle, is a precursor for the synthesis of lipids, sterols, N-acetylglucosamine and lysine (Flikweert et al., 1999; Flikweert et al., 1996) and acts as acetyl-donor for protein acetylation (Henriksen et al., 2012; Takahashi et al., 2006) .

In the industrial yeast *Saccharomyces cerevisiae*, acetyl-CoA can be synthesized from pyruvate via two distinct pathways. In the mitochondria, the pyruvate dehydrogenase (PDH) complex oxidatively decarboxylates pyruvate to acetyl-CoA and thereby feeds the TCA cycle. Since the mitochondrial inner membrane is impermeable to acetyl-CoA, an alternative route of acetyl-CoA synthesis is required to feed cytosolic pathways for synthesis of lysine, lipids and sterols and for protein acetylation (Flikweert et al., 1999; Takahashi et al., 2006; van den Berg and Steensma, 1995). In wild-type *S. cerevisiae*, cytosolic acetyl-CoA is formed by the concerted action of three cytosolic enzymes, which together constitute the 'PDH bypass' (Holzer and Goedde, 1957): pyruvate decarboxylase (Pdc1,5,6), acetaldehyde dehydrogenase (Ald2,3,4,5,6) and acetyl-CoA synthetase (Acs1,2).



The cytosolic formation of acetyl-CoA from pyruvate requires three distinct conversions: decarboxylation of pyruvate ($\Delta G^{o\prime}$ -40.3 ± 3.6 kJ mol$^{-1}$), pyridine-nucleotide dependent oxidation of acetaldehyde ($\Delta G^{o\prime}$ -47.0 ± 2.6 kJ mol$^{-1}$) and activation of acetate with coenzyme A ($\Delta G^{o\prime}$ +47.1 ± 1.0 kJ mol$^{-1}$) (Flamholz et al., 2012; Noor et al., 2012; Noor et al., 2014; Noor et al., 2013). When these reactions are combined by the mitochondrial PDH complex, the free-energy change of the first two steps is used to drive the complete reaction, resulting in an overall $\Delta G^{o\prime}$ of -40.2 kJ mol$^{-1}$ (the calculated change in free energy of the oxidative reactions assumes the use of the NAD+/NADH couple as an electron acceptor/donor). When pyruvate conversion to acetyl-CoA occurs in the cytosol, the change in free energy of the pyruvate decarboxylase and acetaldehyde dehydrogenase reactions is dissipated and an input of free energy is required to 'push' activation of acetate to acetyl-CoA (Figure 1). Since Acs1 and Acs2 convert ATP to AMP and the pyrophosphate generated in this reaction is hydrolyzed, the net ATP cost of acetate activation to acetyl-CoA is equivalent to the conversion of 2 ATP to 2 ADP (Pronk et al., 1994). The different ATP stoichiometries of cytosolic and mitochondrial acetyl-CoA synthesis strongly affect the product yields of acetyl-CoA derived compounds produced in *S. cerevisiae*. For example, biosynthesis of a single molecule of the sesquiterpene farnesene in genetically engineered *S. cerevisiae* requires 9 molecules of cytosolic acetyl-CoA. When synthesized via the native cytosolic PDH bypass, formation of this amount of acetyl-CoA comes a net cost of 18 ATP and, as a result, a complete molecule of glucose has to be respired to generate the ATP required for the acetyl-CoA synthetase reaction (Meadows et al., 2016; van Rossum et al., 2016b).

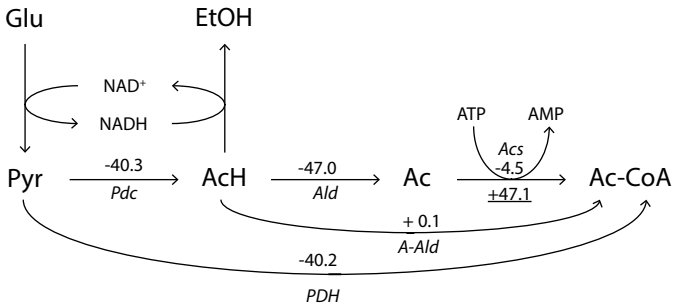


**Figure 1** Gibbs free energy change for different routes for acetyl-CoA formation from pyruvate. The change in Gibbs free energy ($\Delta G^{o\prime}$, in kJ $mol^{-1}$) is indicated in the numbers above the arrows. The values calculated for the direct conversion of pyruvate and acetaldehyde to acetyl-CoA assume the concomitant reduction of $NAD^+$. The underlined value for the conversion of acetate to acetyl-CoA indicates the change in $\Delta G^{o\prime}$ for ATP-independent conversion. Abbreviations: Glu: glucose. Pyr: pyruvate. AcH: acetaldehyde. EtOH: ethanol. Ac: acetate. Ac-CoA: acetyl coenzyme A. Pdc: pyruvate decarboxylase. Ald: acetaldehyde dehydrogenase. Acs: acetyl-CoA synthetase. A-Ald: Acetylating acetaldehyde dehydrogenase. PDH: pyruvate dehydrogenase complex and lipoylation machinery.

Several metabolic engineering strategies have been tested to reduce or eliminate ATP requirements for cytosolic acetyl-CoA synthesis from pyruvate in *S. cerevisiae* (reviewed by van Rossum et al. (2016b)). A bacterial pyruvate-formate lyase (PFL), which converts pyruvate to formate and acetyl-CoA, was previously expressed in *S. cerevisiae* (Kozak et al., 2014a). While the PFL reaction itself does not require an input of free energy, ATP was inferred to be required for export of formate. Alternatively, the native pyruvate decarboxylase reaction can be linked to a heterologous acetylating acetaldehyde dehydrogenase (A-ALD) (Kozak et al., 2014a; Kozak et al., 2016). A-ALD catalyses the oxidative, $NAD^+$-dependent conversion of acetaldehyde and CoA to acetyl-CoA. Both PFL and A-ALD combine formation of the energy-rich thioester with another reaction (decarboxylation of pyruvate for PFL, and acetaldehyde oxidation for A-ALD), resulting in $\Delta G^{o\prime}$s of -21.2 ± 3.0 and 0.1 ± 2.4 kJ $mol^{-1}$, respectively, for the overall reactions. Under some conditions, the near-zero $\Delta G^{o\prime}$ of the A-ALD reaction has been implicated in acetaldehyde toxicity in engineered strains (Kozak et al., 2014a; Kozak et al., 2016).

ATP-independent formation of cytosolic acetyl-CoA in yeast can also be accomplished by heterologous expression of a bacterial PDH complex in the yeast cytosol. PDH complexes consist of three catalytic subunits: pyruvate dehydrogenase (E1, in some organisms consisting of E1α and E1β proteins), dihydrolipoyl transacetylase (E2) and dihydrolipoyl dehydrogenase. Thiamine pyrophosphate (TPP) is involved as a cofactor in the decarboxylation reaction, while covalently E2-bound lipoic acid shuttles the substrate along the different catalytic domains (Bunik, 2003; Graham and Perham, 1990). TPP is available in the yeast cytosol, where it acts as cofactor for transketolase and pyruvate decarboxylase (Hohmann and Meacock, 1998). Lipoic acid is only present in yeast mitochondria, where it is synthetized from octanoyl-acyl-carrier-protein (octanoyl-ACP), an intermediate of fatty acid biosynthesis (Schonauer et al., 2009). Kozak et al. (2014b) showed that combined expression of bacterial PDH complex

subunits and lipoylation enzymes fully complemented the acetyl-CoA requirement of an *S. cerevisiae acs1Δ acs2Δ* double mutant for growth.

The goals of this work were to investigate if a heterologously expressed cytosolic PDH complex can provide more cytosolic acetyl-CoA than the small amount needed for biosynthesis in glucose-grown *S. cerevisiae* cultures and to explore options to increase its *in vivo* capacity. To address these issues, we engineered *S. cerevisiae* to fully redirect pyruvate dissimilation through cytosolic PDH complex and characterized the resulting strains. Subsequently, laboratory evolution on medium containing L-lactate as sole carbon source was used to select mutants with a higher *in vivo* flux through cytosolic PDH complex. Whole-genome sequencing and functional analysis of mutated alleles was then applied to investigate the molecular basis for improved growth of evolved strains.

## 2. MATERIALS AND METHODS

### 2.1 Strains and maintenance

The *S. cerevisiae* strains used in this study (Table 2) share the CEN.PK genetic background (Entian and Kötter, 2007). Stock cultures of *S. cerevisiae* were grown aerobically in 500 mL shake flasks containing 100 mL synthetic medium (SM) (Verduyn et al., 1992) or YP medium (10 g $L^{-1}$ Bacto yeast extract, 20 g $L^{-1}$ Bacto peptone) supplemented with the appropriate carbon source. When needed, cultures were supplied with DL-lipoic acid (Sigma-Aldrich, St. Louis, MO, USA) to a final concentration of 100 µg $L^{-1}$. Stock cultures of *E. coli* XL1-Blue Subcloning Grade Competent Cells (Agilent Genomics, Santa Clara, CA, USA) were grown in LB medium (5 g $L^{-1}$ Bacto yeast extract, 10 g $L^{-1}$ Bacto tryptone, 10 g $L^{-1}$ NaCl) supplemented with 100 mg $L^{-1}$ ampicillin. Media were autoclaved at 121 °C for 20 min. Temperature-sensitive media supplements (vitamins and lipoic acid) and antibiotics were filter sterilized and added to the autoclaved media prior to use. Media containing 2-(N-morpholino) ethanesulfonic acid hydrate (MES-hydrate) were not autoclaved, but filter sterilized. For yeast strain storage, glycerol was added to grown cultures to a final concentration of 30 % v/v and 1 mL aliquots were stored at -80°C.

### 2.2 Molecular biology techniques

Phusion high-fidelity DNA Polymerase (Thermo Fisher Scientific, Waltham, MA, USA) was used for PCR amplification for cloning purposes. Diagnostic PCR was performed with DreamTaq PCR Master Mix (2X) (Thermo Fisher Scientific). Manufacturers' protocols were followed, except for the use of a lower primer concentration (0.2 µM instead of 0.5 µM). Desalted oligonucleotide primers were used, except for primers binding to coding regions, which were PAGE purified (Sigma-Aldrich). For PCR analysis of yeast colonies, genomic DNA was isolated as described by Lõoke et al. (2011). Commercial kits for DNA extraction and purification were used for small-scale DNA isolation (Sigma-Aldrich), PCR cleanup (Sigma-Aldrich), and gel extraction (Zymo Research, Irvine, CA, USA). Restriction analysis of constructed plasmids was performed using FastDigest restriction enzymes (Thermo Scientific). Gibson assembly of linear DNA fragments was performed using NEBuilder HiFi DNA Assembly Master Mix

(New England Biolabs, Ipswich, MA, USA) following the manufacturer's recommendations, but using a reduced reaction volume of 5 µL. Transformation of chemically competent *E. coli* XL1-Blue was performed according to the manufacturer's protocol.

### 2.3 Plasmid construction

Plasmids and oligonucleotide primers used in this study are listed in Table 1 and in Supplementary Table 1, respectively. Plasmid pUDR070 was constructed by Gibson assembly of two linear fragments, both obtained via PCR amplification of plasmid pROS13 using primers 7716-7593 (for the *PDC5*-gRNA_2µ_*PDC6*-gRNA insert) and 6005 (for the plasmid backbone), as previously described by Mans et al. (2015). Plasmid pUDR622 was constructed by Gibson assembly of two linear fragments, both obtained via PCR amplification of plasmid pROS12 using primer 16001 (for the *ACS1*-gRNA_2µ_*ACS1*-gRNA insert) and 6005 (for the plasmid backbone). Plasmid pUDR677 was constructed by Gibson assembly of two linear fragments, both obtained via PCR amplification of plasmid pROS12 using primer 16814 (for the *ACS2*-gRNA_2µ_*ACS2*-gRNA insert) and 6005 (for the plasmid backbone). Plasmid pUDR704 was constructed by Gibson assembly of two linear fragments, both obtained via PCR amplification of plasmid pROS12 using primers 6178 and 7713 (for the *PDC1-gRNA_2µ_MTH1*-gRNA insert) and 6005 (for the plasmid backbone).

**Table 1:** Plasmids used in this study.

| Name | Relevant characteristic | Origin |
|---|---|---|
| pUD301 | *pTPI1-pdhA-tTEF1* | (Kozak et al., 2014) |
| pUD302 | *pTDH3-pdhB-tCYC1* | (Kozak et al., 2014) |
| pUD303 | *pADH1-aceF-tPGI1* | (Kozak et al., 2014) |
| pUD304 | *pTEF1-lpd-tADH1* | (Kozak et al., 2014) |
| pUD305 | *pPGK1-lplA-tPMA1* | (Kozak et al., 2014) |
| pUD306 | *pPGI1-lplA2-tPYK1* | (Kozak et al., 2014) |
| pROS12 | *hphNT1* gRNA-*CAN1* gRNA-*ADE2* | (Mans et al., 2015) |
| pROS13 | *kanMX* gRNA-*CAN1* gRNA-*ADE2* | (Mans et al., 2015) |
| pUDR070 | *kanMX* gRNA-*PDC5* gRNA-*PDC6* | This work |
| pUDR047 | *hphNT1* gRNA-*PDA1* | (van Rossum et al., 2016a) |
| pUDR471 | *kanMX* gRNA-SynPAM *(2x)* | (Perli et al., 2020) |
| pUDR622 | *hphNT1* gRNA-*ACS1* | This work |
| pUDR677 | *hphNT1* gRNA-*ACS2* | This work |
| pUDR704 | *hphNT1* gRNA-*PDC1* gRNA-*MTH1* | This work |

### 2.4 Strain construction

*S. cerevisiae* strains were transformed with the LiAc/ssDNA method (Gietz and Woods, 2002). The transformation mixture was plated on YP plates with either glucose (20 g $L^{-1}$) or a mixture of glycerol and ethanol (1 % v/v each) as carbon source. Hygromycin B or G418 were added at a final concentration of 200 mg $L^{-1}$. Gene deletions and integrations were performed as described previously (Mans et al., 2015). Expression cassettes for heterologous genes

were flanked by 60 bp short homology repeats (SHRs) for assembly and genomic integration (Kuijpers et al., 2013).

Strain IMX808 was constructed by transforming the Cas9 expressing strain IMX585 with plasmid pUDR07 and two double stranded repair fragments, obtained by annealing oligonucleotides 7717 with 7718 and 7935 with 7936. Strain IMX1135 was constructed by transforming strain IMX808 with plasmid pUDR047 and a double stranded repair fragment obtained by annealing oligonucleotides 6157 and 6158. Strain IMK964 was constructed by transforming strain IMX585 with plasmid pUDR622 and a double stranded repair fragment obtained by annealing oligonucleotides 16587 and 16588.

Expression cassettes for chromosomal integration of the *Enterococcus faecalis* pyruvate dehydrogenase and lipoylation genes were prepared as follows. The cassette containing the *Ef_pdhA* ORF was amplified from plasmid pUD301 using primers 5654 and 9967; the cassette containing the *Ef_pdhB* ORF was amplified from plasmid pUD302 using primers 3277 and 7338; the cassette containing the *Ef_aceF* ORF was amplified from plasmid pUD303 with primers 3284 and 9969; the cassette containing the *Ef_lpd* ORF was amplified from plasmid pUD304 using primers 5652 and 5653; the cassette containing the *Ef_lplA* ORF was amplified from plasmid pUD305 using primers 5663 and 5661 and the cassette containing the *Ef_lplA2* ORF was amplified from plasmid pUD306 using primers 3285 and 2686. Primers 9967 and 9969 contain homology to sequences flanking *PDC1* to enable integration of the cassette at this locus in *S. cerevisiae* IMX1191. For the integration at the *ACS2* locus, these primers were substituted with primers 7426 and 7356, respectively. Strain IMX1135 was co-transformed with the expression cassettes designed to integrate in *PDC1* and pUDR704, yielding strain IMX1191. In parallel, co-transformation strain of IMK964 with the *ACS2*-targeting set of fragments and pUDR677 yielded strain IMX2361.

Strain IMG011 was constructed by transforming strain IMX2361 with pUDR471, targeting an introduced synthetic target site in the *ACS1* locus, together with a fragment PCR-amplified from IMS660 using primers 16585 and 16586. Strains IMG012, IMG013, IMG014, IMG015 and IMG016 were constructed following the same approach, with repair fragments originating from strains IMS974, IMS978, IMS980, IMS982 and CEN.PK113-7D, respectively. After transformation, gRNA expression plasmids were removed by growing strains on non-selective media. Throughout this paper, the cluster of expression cassettes for *E. faecalis* PDH complex subunits and lipoylation enzymes (*pADH1-aceF-tPGI1 pPGI1-lplA2-tPYK1 pPGK1-lplA-tPMA1 pTDH3-pdhB-tCYC1 pTEF1-lpd-tADH1 pTPI1-pdhA-tTEF1*) is referred to as {PDHL} (Kozak et al., 2014b).

**Table 2** *Saccharomyces cerevisiae* strains used in this study. {PDHL} denotes a chromosomally integrated cluster of expression cassettes for *E. faecalis* genes encoding PDH complex subunits and lipoylation proteins: *pADH1-aceF-tPGI1 pPGI1-lplA2-tPYK1 pPGK1-lplA-tPMA1 pTDH3-pdhB-tCYC1 pTEF1-lpd-tADH1 pTPI1-pdhA-tTEF1*.

| | Parental strain | Relevant genotype | Origin |
|---|---|---|---|
| CEN.PK113-7D | | Prototrophic reference, *MAT*a | (Entian and Kötter, 2007) |
| IMX585 | CEN.PK113-7D | *MAT*a *can1Δ::cas9-natNT2* | (Mans et al., 2015) |
| IMX808 | IMX585 | *MAT*a *can1Δ::cas9-natNT2, pdc5Δ, pdc6Δ* | This study |
| IMX1135 | IMX808 | *MAT*a *can1Δ::cas9-natNT2, pdc5Δ, pdc6Δ, pda1Δ* | This study |
| IMX1191 | IMX1135 | *MAT*a *can1Δ::cas9-natNT2, pdc5Δ, pdc6Δ, pda1Δ, MTH1ΔT, pdc1Δ::*{PDHL} | This study |
| IMK964 | IMX585 | *MAT*a *can1Δ::cas9-natNT2 acs1Δ::synPAM* | This study |
| IMX2361 | IMK964 | *MAT*a *can1Δ::cas9-natNT2 acs1Δ::synPAM, acs2Δ::*{PDHL} | This study |
| IMG011 | IMX2361 | *MAT*a *can1Δ::cas9-natNT2 ACS1$^{C1753T}$, acs2Δ::*{PDHL} | This study |
| IMG012 | IMX2361 | *MAT*a *can1Δ::cas9-natNT2 ACS1$^{G1090A,\ C1753T}$, acs2Δ::*{PDHL} | This study |
| IMG013 | IMX2361 | *MAT*a *can1Δ::cas9-natNT2 ACS1$^{C1752A,\ C1753T}$, acs2Δ::*{PDHL} | This study |
| IMG014 | IMX2361 | *MAT*a *can1Δ::cas9-natNT2 ACS1$^{G1747A,\ C1753T}$, acs2Δ::*{PDHL} | This study |
| IMG015 | IMX2361 | *MAT*a *can1Δ::cas9-natNT2 ACS1$^{G692T,\ C1753T}$, acs2Δ::*{PDHL} | This study |
| IMG016 | IMX2361 | *MAT*a *can1Δ::cas9-natNT2 ACS1, acs2Δ::*{PDHL} | This study |
| IMS657 | | Single colony isolate from chemostat evolution 1 | This study |
| IMS659 | | Single colony isolate from chemostat evolution 1 | This study |
| IMS660 | | Single colony isolate from chemostat evolution 2 | This study |
| IMS662 | | Single colony isolate from chemostat evolution 2 | This study |
| IMS775 | | Population of chemostat evolution 1 evolved in shake flasks on L-lactate. Single colony isolate from evolution line 2 | This study |
| IMS776 | | Population of chemostat evolution 1 evolved in shake flasks on L-lactate with carnitine addition. Single colony isolate from evolution line 1 | This study |
| IMS778 | | Population of chemostat evolution 1 evolved in shake flasks on L-lactate with carnitine addition. Single colony isolate from evolution line 2 | This study |
| IMS805 | | Population of chemostat evolution 1 evolved in shake flasks on L-lactate. Single colony isolate from evolution line 1 | This study |
| IMS971 | IMS660 | IMS660 evolved in shake flasks on L-lactate. Single colony isolate from evolution line 1 | This study |
| IMS974 | IMS660 | IMS660 evolved in shake flasks on L-lactate. Single colony isolate from evolution line 2 | This study |
| IMS976 | IMS660 | IMS660 evolved in shake flasks on L-lactate. Single colony isolate from evolution line 3 | This study |
| IMS978 | IMS662 | IMS662 evolved in shake flasks on L-lactate. Single colony isolate from evolution line 1 | This study |
| IMS980 | IMS662 | IMS662 evolved in shake flasks on L-lactate. Single colony isolate from evolution line 2 | This study |
| IMS982 | IMS662 | IMS662 evolved in shake flasks on L-lactate. Single colony isolate from evolution line 2 | This study |

**2.5 Media and cultivation**

Shake-flask cultures of *S. cerevisiae* strains were grown at 30 °C in 500 mL flasks containing 100 mL synthetic medium (Verduyn et al., 1992) with either 20 g $L^{-1}$ glucose, 7.2 g $L^{-1}$ lactic acid or a mixture of ethanol and glycerol (1 g $L^{-1}$ each) as the carbon source. Cultures were grown in an Innova incubator shaker (New Brunswick Scientific, Edison, NJ, USA) set at 200 rpm. Alternatively, strains were grown at 30 °C in a Growth-Profiler system (EnzyScreen, The Netherlands) equipped with 24-well plates with a working volume of the wells of 1 mL, set at 250 rpm. Media were supplemented with lipoic acid at a concentration of 100 µg $L^{-1}$. With the exception of L-lactate containing media, the initial pH was set at 6.0. When using L-lactate as a carbon source, the initial pH was set at 4.0 to limit the effects of alkalization during growth. The pH of solid media was set at 6 for all carbon sources.

Carbon-limited chemostat cultivation was performed at 30 °C in 2 L laboratory bioreactors (Applikon, Delft, The Netherlands) with a working volume of 1 L. SM was supplemented with a mixture of 6 g $L^{-1}$ L-lactic acid (67 mM) and 1.15 g $L^{-1}$ ethanol (25 mM), yielding a total carbon concentration of 250 mM. Media were additionally supplemented with 0.2 g $L^{-1}$ Pluronic PE6100 antifoam (BASF) and lipoic acid. The latter compound was added as a 50 g $L^{-1}$ solution in ethanol to a concentration of 500 µg $L^{-1}$. Each chemostat culture was preceded by a batch cultivation phase on the same medium. When a rapid decrease of $CO_2$ production indicated carbon source exhaustion in the batch culture, chemostat cultivation was initiated at a dilution rate of 0.05 $h^{-1}$. Culture pH was maintained at 5.0 by automatic addition of 2 M KOH. Bioreactors were sparged with 500 mL $min^{-1}$ air and stirred at 800 rpm to ensure fully aerobic conditions (dissolved oxygen concentration > 80% of air saturation). Laboratory evolution was performed by serial transfer in shake flasks containing 100 mL SM with L-lactate as sole carbon source (pH 4). To limit culture alkalinization due to L-lactate consumption, they were buffered with 25 mM MES (2-(N-morpholino)ethanesulfonic acid). When indicated, L-carnitine was supplemented to a concentration of 0.2 mM. After cultures had reached stationary phase, a 1 mL aliquot of culture was transferred to a new flask. After 15 transfers, corresponding to approximately 100 generations, the evolution was stopped and single colony isolates were taken.

**2.6 Analytical methods**

Optical density of cultures at 660 nm was measured with a Libra S11 spectrophotometer (Biochrom, Cambridge, United Kingdom). Metabolite concentrations in culture supernatants and media were analyzed using an Agilent 1260 Infinity HPLC system equipped with an Aminex HPX-87H ion exchange column, operated at 60 °C with 5 mM $H_2SO_4$ as mobile phase at a flow rate of 0.600 mL $min^{-1}$.

**2.7 Whole-genome sequencing**

*S. cerevisiae* IMX1191 and derived single colony isolates were grown at 30 °C in 500 mL SM containing ethanol and glycerol (1 % v/v each). Genomic DNA was isolated from stationary-phase cultures using the Qiagen 100/G kit (Qiagen, Hilden, Germany) according to the manufacturer's instructions. DNA concentrations were estimated with a Qubit® Fluorometer

2.0 (Thermo Fisher Scientific). Strains IMX1191, IMS657, IMS659, IMS660 and IMS662 were sequenced by Novogene Bioinformatics Technology Co., Ltd (Yuen Long, Hong Kong) on a HiSeq 2500 (Illumina, San Diego, CA, USA) with 150 bp paired-end reads using TruSeq PCR-free library preparation (Illumina). *S. cerevisiae* strains IMS775, IMS776, IMS778, IMS805, IMS971, IMS974, IMS976, IMS978, IMS980 and IMS982 were sequenced in-house on a MiSeq sequencer (Illumina) with 300 bp paired-end reads using TruSeq PCR-free library preparation (Illumina). For all strains, reads were mapped onto the *S. cerevisiae* CEN.PK113-7D reference genome (Salazar et al., 2017) using the Burrows–Wheeler Alignment tool (BWA) and further processed using SAMtools and Pilon for variant calling (Li and Durbin, 2010; Li et al., 2009; Walker et al., 2014).

## 3. RESULTS

### 3.1 Replacement of native pyruvate dissimilation by a cytosolic PDH complex eliminates growth of *S. cerevisiae* on glucose, pyruvate and -lactate.

To redirect the entire metabolic flux from pyruvate to acetyl-CoA in *S. cerevisiae* through a heterologously expressed cytosolic PDH complex (Figure 2), native genes required for this conversion were deleted. Activity of the native, mitochondrial PDH complex was eliminated by deleting *PDA1*, which encodes its essential E1 subunit (Wenzel et al., 1992). In addition, all three structural genes encoding pyruvate decarboxylase isoenzymes (*PDC1,5,6*) (Hohmann, 1991; Hohmann and Cederberg, 1990) were disrupted. An internal deletion in *MTH1* was also introduced, as it enables growth of pyruvate-decarboxylase negative strains on glucose (Oud et al., 2012). Combined with the integration of a set of expression cassettes encoding subunits of the *Enterococcus faecalis* PDH complex, as well as two *E. faecalis* lipoylation enzymes (*pdhA*, *pdhB*, *aceF*, *lpd*, *lplA* and *lplA2*, together referred to as {PDHL}), this yielded strain IMX1191.

*S. cerevisiae* IMX1191 grew well on ethanol, but did not grow on SM containing either glucose, pyruvate, L-lactate or glycerol as sole carbon sources. Except for ethanol, these substrates all require conversion of pyruvate to acetyl-CoA for their dissimilation. These results suggested that, in strain IMX1191, the cytosolic PDH complex could not support a sufficiently high rate of pyruvate dissimilation to sustain growth on glucose or 3-carbon substrates. Consistent with this hypothesis, L-lactate and ethanol were co-consumed in cultures of strain IMX1191 grown on SM supplemented with both L-lactic acid and ethanol (1 % v/v of each substrate; Supplementary Figure 4).

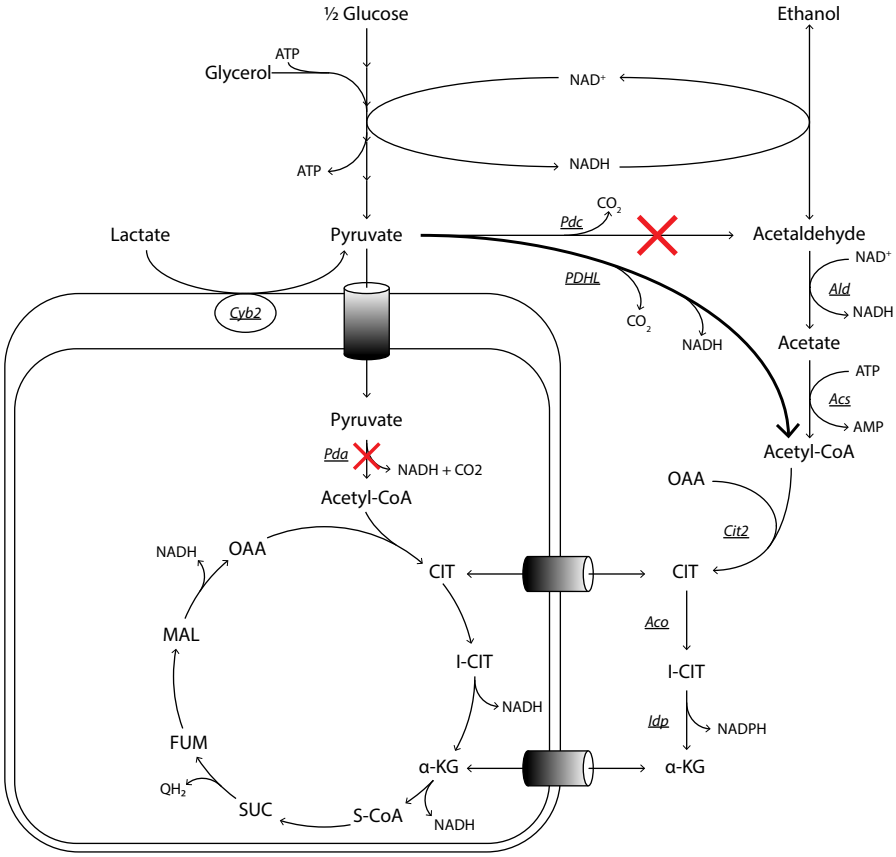


**Figure 2** Simplified overview of central carbon metabolism in *S. cerevisiae*, highlighting the modifications introduced in strain IMX1191 (*pda1Δ, pdc1Δ, pdc5Δ, pdc6Δ*, {PDHL}) to completely re-route pyruvate dissimilation via cytosolic acetyl-CoA. Red crosses indicate deletions in *PDC1,5,6* (Pdc) and *PDA1* (Pda). The thick line labeled PDHL represents the conversion enabled the heterologously expressed, cytosolic pyruvate dehydrogenase complex. Abbreviations: Pdc, pyruvate decarboxylase; PDHL, heterologous pyruvate dehydrogenase; Ald, acetaldehyde dehydrogenase; Acs, acetyl-CoA synthetase; Cyb2, lactate dehydrogenase; Cit2, cytosolic citrate synthase; Aco, aconitase; Idp, isocitrate dehydrogenase; Pda, mitochondrial pyruvate dehydrogenase; OAA, oxaloacetate; CIT, citrate; I-CIT, isocitrate; α-KG, α-ketoglutarate; S-CoA, succinyl-CoA; SUC, succinate; FUM, fumarate; MAL, malate.

### 3.2 Laboratory evolution in carbon-limited chemostat cultures enables growth of IMX1191 on L-lactate as sole carbon source

To investigate the inability of strain IMX1191 to grow on L-lactate, whose dissimilation requires conversion of pyruvate to acetyl-CoA, we applied laboratory evolution in duplicate chemostat cultures (reactors L and R, Figure 3A). These cultures were grown at a dilution rate of 0.05 $h^{-1}$ on SM containing 25 mM ethanol and 67 mM L-lactate. Lactate rather than glucose was used in view of the reported overproduction of pyruvate by glucose-grown cultures of pyruvate-decarboxylase-negative *S. cerevisiae* (van Maris et al., 2004). Concentrations of 25 mM ethanol and 67 mM L-lactate were chosen to provide a selective advantage to spontaneous mutants able to consume L-lactate with a reduced requirement for co-consumption of ethanol. Culture performance was monitored via the $CO_2$ concentration in the exhaust gas (Supplementary Figure 1) and by regular measurements of residual ethanol and L-lactate concentrations in the cultures (Supplementary Figure 2). Throughout the experiments, the residual ethanol concentration in the cultures remained below 0.2 mM. Concentrations of L-lactate and pyruvate progressively decreased and reached values below 1 mM after 1100 h (corresponding to 79 generations). To further increase the selective pressure on L-lactate dissimilation via cytosolic PDH, concentrations of ethanol and L-lactate in the medium feed were then changed to 5 mM and 80 mM, respectively. After a further 250 h (corresponding to a total number of 97 generations), concentrations of ethanol, pyruvate and L -lactate were below detection limit and the cultures were terminated. The evolved populations only grew on SM plates with 80 mM L-lactate as sole carbon source when supplied with 100 µg $L^{-1}$ lipoic acid. This result indicated that growth of the evolved culture still depended on activity of the cytosolic PDH complex (Supplementary Figure 3).

Single-cell isolates from both reactors were obtained by plating on SM with L-lactate as sole carbon source and supplemented with lipoic acid. This yielded strains IMS657 and IMS659 from reactor L, and strains IMS660 and IMS662 from reactor R (Figure 3A). Strains IMS657 and IMS659 exhibited a specific growth rate of 0.03 $h^{-1}$ (Supplementary Figure 5) on SM with L-lactate as sole carbon source without a significant lag phase, whereas growth of strains IMS660 and IMS662 was only observed after prolonged (6 weeks) incubation. Addition of 0.2 mM L-carnitine, which enables import of cytosolic acetyl-CoA into *S. cerevisiae* mitochondria (Bieber, 1988; Hiltunen et al., 2003), increased both the specific growth rate and the final optical density of strains IMS657 and IMS659, indicating a possible limitation in mitochondrial acetyl-CoA availability (Supplementary Figure 5).

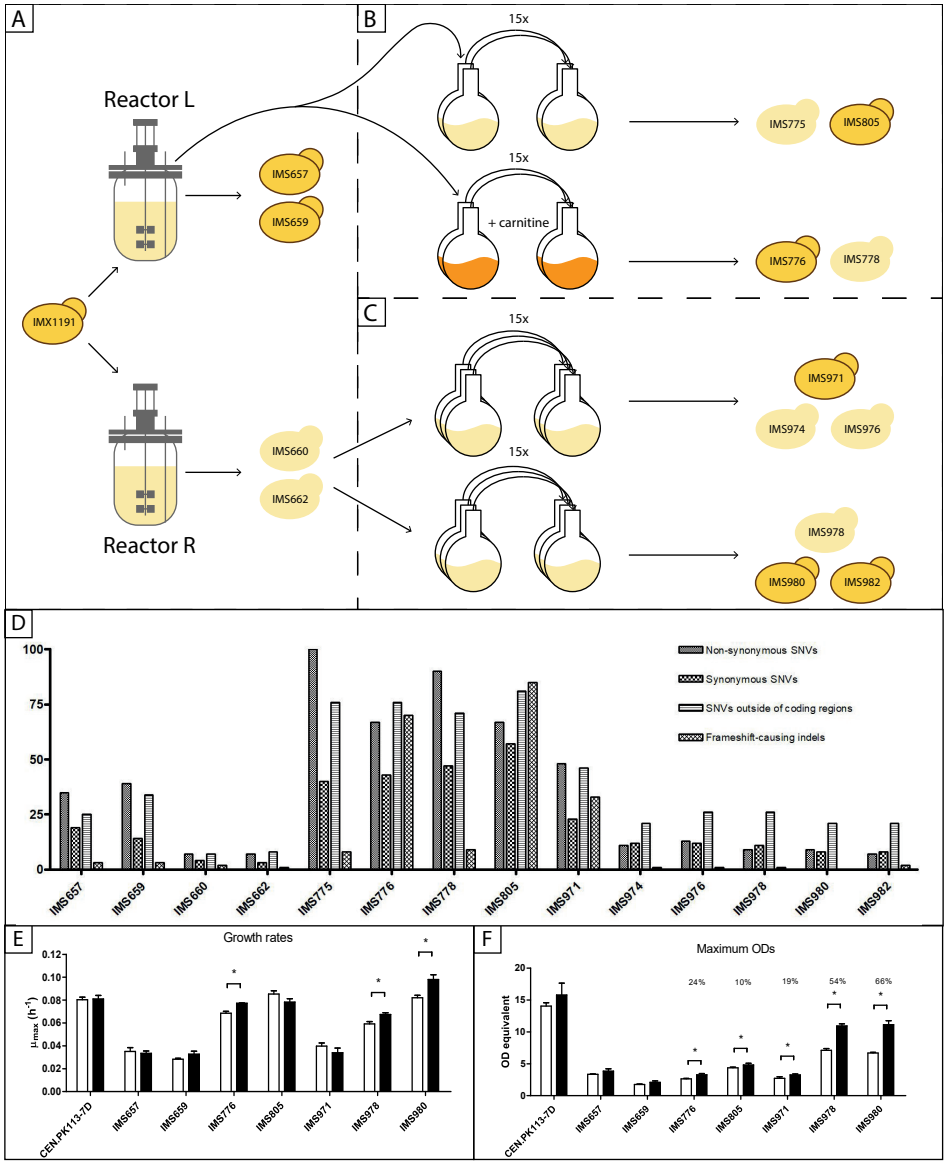


**Figure 3** Schematic overview of the strategy used for the evolution of *S. cerevisiae* strain IMX1191 (*pda1Δ, pdc1Δ, pdc5Δ, pdc6Δ*, {PDHL}) for (improved) growth in medium containing L-lactate and the mutant strains obtained. Panel A: chemostat evolution for improved affinity on lactic acid; the two reactors and the single colony isolates obtained at the end of the evolution from each reactor are shown. Highlighted strains have been characterized (see panels E and F). Panel B&C: evolution for higher specific growth rates in sequential batches in shake flasks containing medium with L-lactic acid as sole carbon source. The evolutions in panel B were performed in duplicate and 0.2 mM carnitine was added to one of the evolutions. For both evolutions in panel B, the inoculum consisted of the evolved population from reactor L. The evolutions in panel C were performed in triplicate and the inoculum were the single colony isolate strains IMS660 and IMS662. At the end of each of the evolution experiments, a single colony isolate was taken. Panel D: number of SNVs and indels found in the single colony isolates. Panel E&F: growth rates (E) and final optical densities (F) of the isolated strains. White bars represent cultures grown in synthetic media with L-lactic acid as sole carbon source, while black bars represent cultures grown in the same media supplemented with 0.2 mM carnitine. Asterisks indicate a significant difference between the two conditions (student t-test, $p < 0.05$). For each strain, the percentage increase in final optical density is indicated.

### 3.3 Laboratory evolution for faster growth on L-lactate

To select for higher fluxes through the cytosolic PDH, two parallel laboratory evolution approaches were chosen. In a first approach, to maximize genetic heterogeneity of the initial population, a sample of the complete evolved culture from bioreactor L was used as inoculum for four parallel serial transfer experiments in shake flask cultures grown on L-lactic acid. In view of its beneficial effects on growth of strains IMS657 and IMS659 on L-lactate, 0.2 mM of L-carnitine was included in two of the four experiments (Figure 3, panel B). In a second approach, single colony isolates IMS660 and IMS662 derived from bioreactor R were used to inoculate three serial transfer experiments each on L-lactate (Figure 3, panel C). The objective of this approach was to facilitate differentiation between mutations that occurred during chemostat selection and serial transfer in subsequent genome sequencing experiments. After 15 transfers (approximately 100 generations), the serial transfer experiments were terminated and single colony isolates obtained by plating on SM with the same supplements used in the shake flasks.

Surprisingly, even after prolonged incubation, none of the evolved isolates grew when frozen stocks were used to inoculate shake flasks on SM with L-lactate as sole carbon source (pH 4). After plating on solid SM-lactate and transfer to liquid medium, 7 out of 14 strains grew after 14 days. Biomass of these strains (IMS657, IMS659, IMS776, IMS805, IMS971, IMS978 and IMS980) was used to determine specific growth rates SM with L-lactate as sole carbon source, both with and without addition of L-carnitine (Figure 3 E&F). Specific growth rates of the strains ranged from 0.03 $h^{-1}$ to 0.10 $h^{-1}$ (Figure 3, panel E). Specific growth rates of evolved strains IMS657 and IMS659 (both 0.03 $h^{-1}$) were below the dilution rate of the chemostat in which their ancestors had evolved (0.05 $h^{-1}$). This result may reflect different cultivation conditions in the chemostats and the serial transfer experiments (e.g. presence or absence of pH control and substrate concentration). Addition of L-carnitine had a significant impact on the final optical density for all strains except IMS657 and IMS659, with increases in final optical density of up to 64% (Figure 3, panel F).

### 3.4 Whole-genome *sequencing* reveals emergence of mutator phenotypes.

To identify the genetic basis of the evolved phenotypes, the genomes of the obtained single colony isolates were sequenced. No large structural variations (chromosomal duplications/ rearrangements) were found, but multiple single-nucleotide variations (SNVs), deletions and insertions were identified in all isolates. Analysis of the chemostat-derived strains indicated five-fold more mutations in strains IMS657 and IMS659 than in strains IMS660 and IMS662 (Figure 3A and 3D). This large difference was tentatively attributed to a 'mutator phenotype' caused by a single-nucleotide deletion in *MSH6*, a gene involved in DNA mismatch repair (Marsischky et al., 1996), which was observed in the chemostat-evolved strains IMS657 and IMS659. Genome sequence analysis of the derived evolved strains IMS775, IMS776, IMS778 and IMS805 revealed 67 to 100 non-synonymous SNVs in coding regions (Supplementary Table 2), a number far higher than other reports of laboratory evolution with a comparable number of generations (Ho et al., 2017; Papapetridis et al., 2018; Perli et al., 2020; Strucko et al., 2018; Verhoeven et al., 2018; Verhoeven et al., 2017). Of these strains, IMS775 and

IMS778 contained 90 to 100 SNVs and 20 to 25 indels. They also contained the indel in *MSH6* that was present in the chemostat-evolved single-cell isolates IMS657 and IMS659. However, in IMS776 and IMS805, *MSH6* remained intact, indicating that these isolates had evolved from a distinct subpopulation present in the chemostat culture from which IMS657 and IMS695 had been obtained. Surprisingly, a high incidence of SNVs and indels was also identified in strain IMS971. This strain was evolved from strain IMS660, which was derived from the other bioreactor and did show a high number of mutations after chemostat evolution (Supplementary Table 2).

### 3.5 Evolved strains contain mutations in genes encoding PDH complex subunits

To identify mutations responsible for the accelerated growth on L-lactate, we first focused on mutations in the genes encoding subunits of the *E. faecalis* PDH. All evolved strains carried non-synonymous SNVs in at least one of the genes encoding its two E1α and E1β subunits (*pdhA* and *pdhB*, respectively; Table 3). In addition, strains IMS776 and IMS805 carried a mutation in *lplA2*, one of the two genes required for the lipoylation of the complex. The Protein Variation Effect Analyzer (PROVEAN) tool (Choi, 2012; Choi and Chan, 2015; Choi et al., 2012) flagged all substitutions on the subunit E1α (PdhA), as well as two substitutions found on E1β (V292F and P192L) as deleterious for protein function.



**Table 3** Mutations found in three (PdhA, PdhB, LplA2) of the subunits of the heterologous pyruvate dehydrogenase complex. Mutations highlighted in bold are predicted to affect protein function, as analysed by the Protein Variation Effect Analyzer (PROVEAN) tool. All strains were obtained from single, independent evolution lines, with the exceptions of the couples IMS657-IMS659 and IMS660-IMS662, which were isolated from two independent chemostat evolution lines. A graphic overview of the lineages of the strains can be found in Figure 3.

| | | | Mutations (protein level) | | |
|---|---|---|---|---|---|
| **Evolved strain** | **Parental** | **Evolution type** | **PdhA** | **PdhB** | **LplA2** |
| IMS657 | IMX1191 | Chemostat | | V292F | |
| IMS659 | | | | V292F | |
| IMS660 | | | **G175S** | | |
| IMS662 | | | **G175S** | | |
| IMS775 | Population from chemostat L | Sequential batches | **T268N** | **V292F** | |
| IMS776 | | | **T174I** | **V292F** | E325G |
| IMS778 | | | **T268N** | **V292F** | |
| IMS805 | | | **T174I** | **V292F** | E325G |
| IMS971 | IMS660 | Sequential batches | **G175S** | **P192L** | |
| IMS974 | | | **G175S** | | |
| IMS976 | | | **G175S** | | |
| IMS978 | IMS662 | Sequential batches | **G175S** | E190Q | |
| IMS980 | | | **G175S** | A188V | |
| IMS982 | | | **G175S** | S293A | |

### 3.6 *ADH1* and *ACS1* carry mutations in independent evolution lines

Further analysis focused on genes that showed mutations in independently evolved strains. A SNV in *ADH1*, which caused a premature stop codon at amino acid 148 of Adh1, was found in all isolates derived from the chemostat evolution experiment. This SNV ultimately resulted in the loss of the NADH binding domain, thereby most likely causing the protein to be inactive. Genome sequencing of the evolved strains identified a common loss-of-function mutation in *ADH1*, which encodes a major isoenzyme of cytosolic $NAD^+$-dependent alcohol dehydrogenase whose expression is upregulated under fermentative growth conditions (Denis et al., 1983). This mutation already occurred during the initial chemostat phase of the evolution experiments. Since the chemostat cultures were grown on mixtures of L-lactate and ethanol, the *adh1* mutation may primarily have affected ethanol utilization. Since we could not find a plausible role of Adh1 in redirection of respiratory pyruvate metabolism in the evolved strains, we did not further explore its role.

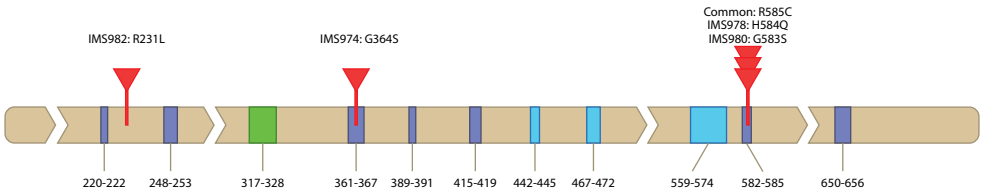


**Figure 4** Schematic overview of the amino-acid sequence of Acs1 and of mutations found in evolved *S. cerevisiae* strains. Colored areas indicate regions containing amino acids involved in the catalytic mechanism. Regions without relevant residues were cropped. Purple areas: CoA binding. Light blue areas: AMP (ATP) binding. Green area: acyl-activating enzyme consensus sequence. Red flags indicate mutated sites. The strain name, and the associated mutation, is indicated. The substitution R585C, already present in the chemostat evolved strains IMS660 and IMS662, is shared by strains IMS971, IMS974, IMS976, IMS978, IMS980 and IMS982, which were obtained after further evolution in serial transfer experiments.

The chemostat-derived strains IMS660 and IMS662 showed a mutation in *ACS1* (R585C), which encodes a high-affinity acetyl-CoA synthetase reported to be required for growth on non-fermentable carbon sources (De Virgilio et al., 1992; van den Berg et al., 1996) (Figure 2). The R585C mutation falls within the ATP binding site of the protein and was retained among all strains evolved from IMS660 and IMS660 in serial-transfer experiments (Figure 3C). Four of these further evolved strains contained additional mutations in *ACS1*. Strain IMS974 carried the additional mutation G364S, which falls between a residue involved in acetate binding (I366) and a residue involved in CoA binding (G361). In strains IMS978, IMS980 and IMS982, Acs1 carried the mutations H584Q, G583S and R231L, respectively. The residues at position 583 and 584 are part of the active site involved in CoA binding and the residue at position 231 is situated close to residues involved in the catalytic mechanism (Figure 4). The high incidence of mutations in *ACS1* suggested an important role of Acs1 activity in redirection of pyruvate dissimilation through a cytosolic PDH.

### 3.7 Mutations in *ACS1* cause loss of function

To investigate functionality of the evolved *ACS1* alleles, we introduced them in strain IMK964 (*acs1Δ::synPAM*) tested the ability of the resulting strains to grow on acetate, for which Acs1 was previously described to be essential (De Virgilio et al., 1992). However, in contrast with results presented in these earlier studies, even an *acs1Δ* strain that was used as negative control grew on acetate (Figure 5, strain IMK964). To circumvent this problem, we used strain IMX2361 in which both *ACS1* and *ACS2* were inactivated and the *E. faecalis* PDH complex and lipoylation enzymes were expressed. In this strain, growth on glucose is lipoic-acid dependent, as acetyl-CoA cannot be synthesized via the PDH bypass due to absence of Acs1 and Acs2 (Kozak et al. 2014b). After introduction of the wild-type and evolved alleles of *ACS1* in strain IMX2361, the resulting strains IMG011 to IMG016 were tested for growth on several carbon sources on solid media (Figure 5). Strain IMG016, expressing the native *ACS1* allele, readily grew on acetate or ethanol as sole carbon source. In contrast, none of the strains expressing the evolved *ACS1* alleles were able to do so. This result indicated that the Acs1 variants in the evolved strains had an insufficient *in vivo* activity to sustain growth on these C2-compounds.

To test their ability to sustain the much lower anabolic cytosolic acetyl-CoA requirements, the same set of strains was grown on L-lactate, supplemented with either ethanol or acetate for cytosolic acetyl-CoA synthesis via Acs1. Using L-lactate as the sole carbon source, and in the absence of lipoic acid, strain IMK964 (*acs1Δ ACS2*) showed a severe growth defect, while strain IMX2361 (*acs1Δ acs2Δ* {PDHL} did not grow at all (Figure 5). This is in line with the notion that, of the two *S. cerevisiae* acetyl-CoA synthetases, Acs1 is the largest contributor to the formation of cytosolic acetyl-CoA during growth on non-fermentable carbon sources (van den Berg et al., 1996). The inability of IMX2361 to grow on this medium can be explained from its requirement for lipoic acid, to activate the heterologous PDH complex and thus to synthesize cytosolic acetyl-CoA. Among the set of congenic strains carrying the different *ACS1* alleles, IMG016 (*ACS1*$^{wt}$) grew well on L-lactate while, of the strains carrying evolved *ACS1* alleles, only IMG011 (*ACS1*$^{R585G}$) exhibited very slow growth on this carbon source (Figure 5). Supplementation of acetate or ethanol to SM-lactate plates fully restored growth of strain IMK964 (*acs1Δ ACS2*), while strains expressing the evolved *ACS1* alleles remained unable to grow. This included strain IMG011, whose weak growth on SM-lactate, did not occur with, in addition to L-lactate, the medium was supplemented with either acetate or ethanol (Figure 5). This result may reflect an inhibitory effect of the latter substrates on L-lactate consumption. Strain IMG011 showed improved growth on SML when lipoic acid was supplied, suggesting that low activities of the Acs1$^{R585G}$ variant and the *E. faecalis* PDH complex acted synergistically.

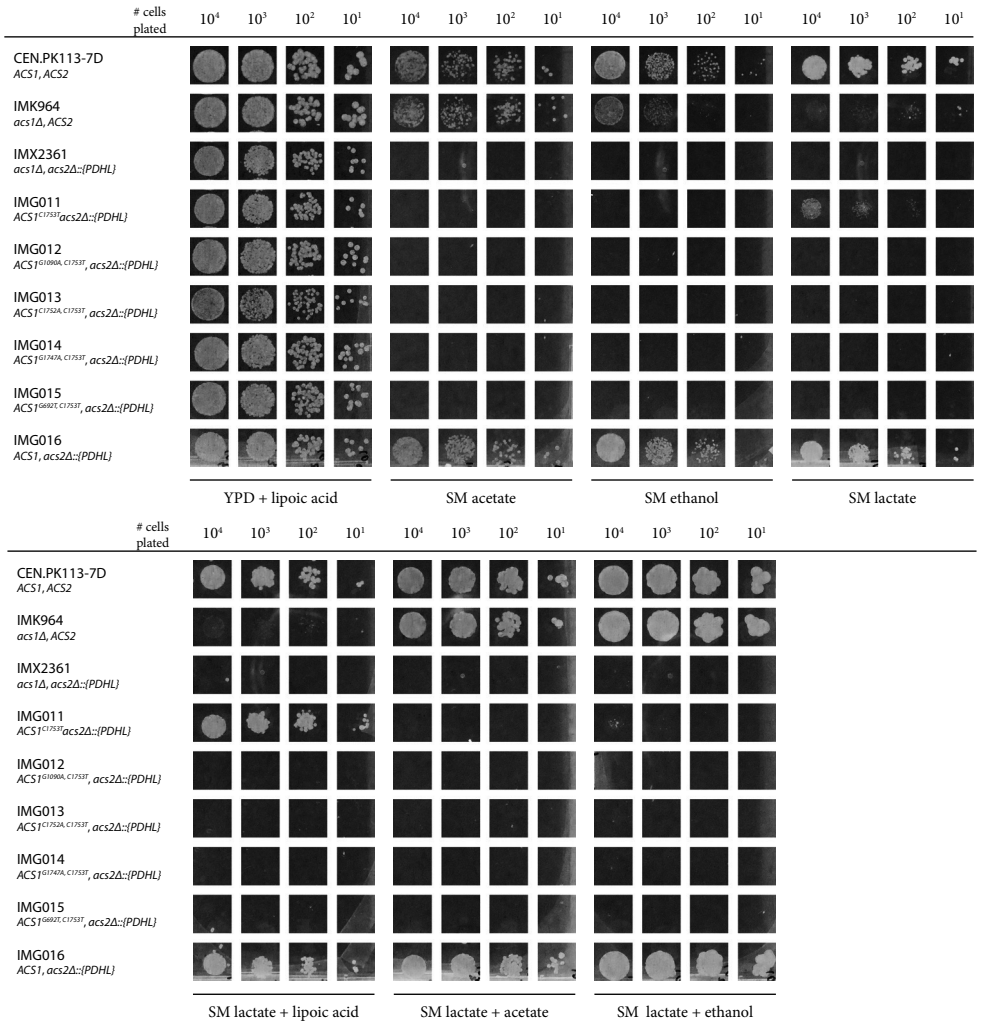


**Figure 5** Spot plate assay of different *S. cerevisiae* strains, in order to verify the functionality of different evolved *ACS1* alleles. The genotype of each strain is indicated on the left-hand side of the figure. {PDHL} denotes a cluster of gene cassettes for the expression of a cytosolic pyruvate dehydrogenase and lipoylation machinery. Growth was tested on solid synthetic media (SM) with different carbon sources. Complex YPD media supplemented with lipoic acid was used as a positive control. SM acetate and SM ethanol plates were used to test the ability of the different alleles of *ACS1* to carry a catabolic flux. SM lactate + acetate and SM lactate + ethanol plates were used to test the ability of the different alleles of *ACS1* to carry an anabolic flux. The remaining plates were used as controls. All carbon sources were added at a final concentration of 10 g $L^{-1}$ each, with the exception of glucose, which had a concentration of 20 g $L^{-1}$ in the YPD plate. When indicated, lipoic acid was supplemented at a final concentration of 100 µg $L^{-1}$. SM plates were incubated for 5 days, while the YPD plate was incubated for 2 days.

## 4. DISCUSSION

The present study demonstrates how a combination of targeted metabolic engineering and laboratory evolution enabled the complete redirection of pyruvate dissimilation in *S. cerevisiae* via a cytosolically expressed PDH complex. After eliminating native pathways for conversion of pyruvate to acetyl-CoA in a strain expression a cytosolic PDH complex, no growth was observed on three- and six-carbon substrates. A two-stage laboratory evolution strategy was successfully applied to first select for growth on L-lactate as sole carbon source and subsequently for faster growth.

One of the goals of this study was to explore whether the *in vivo* flux through a cytosolically expressed PDH complex could be increased beyond the value of 0.41 mmol (g biomass)$^{-1}$ h$^{-1}$ observed for an *S. cerevisiae* strain in which PDH complex only provided cytosolic acetyl-CoA for biosynthesis (Kozak et al., 2014a). The evolved strain strains grew on L-lactate at specific growth rates of up to 0.10 h$^{-1}$. Based on a stoichiometric analysis of yeast metabolism in L-lactate-grown cultures (Cortassa et al., 1995) and a P/O ratio for NADH of 1 (Joseph-Horne et al., 2001), the estimated specific rate of oxidative lactate metabolism in these cultures was 1.15 mmol (g biomass)$^{-1}$ h$^{-1}$. This estimated flux through the cytosolic PDH complex is almost three-fold higher than calculated for the strain described by (Kozak et al., 2014b). We were unable find biomass-specific rates of cytosolic acetyl-CoA production in industrial strains in the literature. However, based on reported volumetric oxygen consumption rates, process stoichiometry (Meadows et al., 2016) and culture optical densities in high-cell-density cultures (Knoll et al., 2007; Riesenberg and Guthke, 1999; Wang et al., 2007), we estimate that turn-over rates of cytosolic acetyl-CoA in an industrial farnesene-producing *S. cerevisiae* were two- to five-fold higher than observed in our study. However, as will be discussed below, genome sequence data from evolved strains indicated that specific growth rates of the evolved strains were not solely constrained by the capacity of the heterologous PDH complex.

Laboratory evolution experiments with other *S. cerevisiae* strains derived from the CEN.PK lineage and encompassing similar or even more generations of selective growth, typically yield 5 to 20 SNVs in coding sequences (Ho et al., 2017; Papapetridis et al., 2018; Perli et al., 2020; Strucko et al., 2018; Verhoeven et al., 2018; Verhoeven et al., 2017), and partial or full chromosomal duplications are often present (Bracher et al., 2017; Perli et al., 2020). Indels in coding regions also occur, albeit at lower frequencies (Kozak et al., 2016). In the present study, already after approximately 70 generations of laboratory evolution in chemostat cultures, substantially higher number of SNVs were found in strains IMS657 and IMS659 (Supplementary Table 2). We tentatively attributed this high incidence of mutations in these strains to a premature stop codon in *MSH6*, which encodes a component of the Msh2/Msh6 DNA mismatch repair system (Marsischky et al., 1996). The resulting predicted truncation of Msh6 caused loss of its essential ATP binding domain (Antony et al., 2006; Hess et al., 2002; Hess et al., 2006; Mazur et al., 2006; Studamire et al., 1998). High numbers of mutations, which did not coincide with a mutation in *MSH6*, were also observed in strains IMS776 and

IMS805 after fifteen serial transfers on SM-lactate and in strain IMS971, which was derived from an independent bioreactor experiment (Supplementary Table 2). We were, however, unable to identify a plausible molecular basis for the inferred mutator phenotype of these strains from DNA sequence data.

The occurrence of mutator phenotypes has been previously observed, and despite their inherent genetic instability, they often provide an advantage under selective conditions. For example, reports have shown that a strain able to mutate rapidly can quickly develop antibiotic resistance (Labat et al., 2005; Levy et al., 2004; Ren et al., 1999), or develop resistance mechanisms to phage infections (Morgan et al., 2010; Pal et al., 2007; Scott et al., 2008). Occurrence of mutator phenotypes in laboratory evolution experiments can be taken as an indication that evolved phenotype require multiple simultaneous mutations, thereby outweighing negative impacts of a high mutation load (Miller et al., 1999). Consistent with such a trade-off between the selected phenotype and negative impacts of non-related mutations, evolved strains with inferred mutator phenotypes exhibited lower specific growth rates and final biomass concentrations than the non-mutators (Figure 3 panels E and F, and Supplementary Figure 5). Although the large number of mutations in the evolved strains complicated interpretation, several observations stood out.

All evolved strains harbored mutations in genes encoding subunits of the heterologous PDH complex. This result suggested that the higher specific growth rates of these strains could at least partly be attributed to a higher *in vivo* capacity of the PDH complex itself. Analysis of these evolved alleles with PROVEAN, an algorithm that assesses whether mutations affect conserved domains of a protein (Choi and Chan, 2015), indicated that the predicted amino-acid changes in the E1α subunit of PDH complex all affected its activity. Of the amino acid changes in the E1β subunit, only $PdhB^{V292F}$ and $PdhB^{P192L}$, which occurred in the majority of the evolved strains, were predicted to affect enzyme activity, while a mutation in the lipoylation enzyme LplA2 was predicted to be neutral. Further functional analysis is required to assess how these mutations, both individually and combinatorially, affect the PDH complex kinetics, regulation and/or stability.

Evolved strains in which pyruvate dissimilation was redirected through the cytosolic PDH complex showed a variety of mutations in *ACS1*, which encodes the high affinity acetyl-CoA synthetase of *S. cerevisiae* (Figure 4). Functional complementation studies showed that a mutation that occurred during chemostat-based evolution ($Acs1^{R585G}$) already strongly decreased activity of Acs1 and was followed by additional mutations that led to a further loss of activity (Figure 5). Mutations in *ACS1* were also observed (Kozak et al. 2016) when evolving *S. cerevisiae* strains in which ethanol metabolism was entirely rerouted through and acetylating acetaldehyde dehydrogenase (acetaldehyde + $NAD^+$ + CoA → acetyl-CoA + NADH + $H^+$). We hypothesize that, in strains in which a mitochondrial PDH complex is not active in metabolism, a shortage of mitochondrial acetyl-CoA occurs. In addition, mitochondrial acetyl-CoA is an essential precursor for synthesis of lipoic acid, which is an essential cofactor of the mitochondrial 2-oxoglutarate dehydrogenase (OGDH) complex. Although lipoic acid

was included in growth media, the lipoylation system of mitochondrial enzymes cannot use free lipoate. Instead, it attaches an octanoyl group derived from mitochondrial fatty acid biosynthesis pathway to the OGDH complex, which is then modified to yield a lipoyl group (Schonauer et al., 2009).

This hypothesis that mitochondrial acetyl-CoA supply a key factor is consistent with the growth-promoting effect of carnitine on evolved strains (Figure 3, Panels E and F), since the carnitine shuttle can link cytosolic and mitochondrial acetyl-CoA pools in *S. cerevisiae*. The selection for (partial) loss-of-function mutations in *ACS1* suggests that, after rerouting pyruvate dissimilation through a cytosolic PDH complex, Acs1 protein competes for cytosolic acetate with a carnitine-independent pathway for provision of mitochondrial acetyl-CoA. In such engineered strains, cytosolic acetate could either be provided by acetyl-CoA hydrolase (Ach1) or by protein de-acetylation. Despite Ach1 being annotated as a mitochondrial enzyme (Buu et al., 2003), available data are insufficient to conclude that this protein is absent from the yeast cytosol. Simultaneous activity of Ach1 in the cytosol and mitochondrial, combined with acetate transport across the mitochondrial membrane, may enable a net transfer of acetyl-CoA units across the mitochondrial membrane. Unfortunately, despite supplementation of growth media with carnitine, attempts to delete *ACH1* in evolved strains in order to test this hypothesis were not successful.



Our results illustrate the importance of metabolic compartmentation of biosynthetic reactions and intracellular transport mechanisms in the design of metabolic engineering strategies for rerouting primary metabolism in eukaryotes. In particular, the roles of mitochondrial acetyl-CoA in *S. cerevisiae* and its supply in engineered strains require further study.

## References

Antony, E., Khubchandani, S., Chen, S., Hingorani, M. M., 2006. Contribution of Msh2 and Msh6 subunits to the asymmetric ATPase and DNA mismatch binding activities of *Saccharomyces cerevisiae* Msh2–Msh6 mismatch repair protein. DNA repair. 5**,** 153-162. DOI: https://doi.org/10.1016/j.dnarep.2005.08.016

Bieber, L. L., 1988. Carnitine. Annu Rev Biochem. 57**,** 261-83. DOI: https://doi.org/10.1146/annurev.bi.57.070188.001401

Bracher, J. M., de Hulster, E., Koster, C. C., van den Broek, M., Daran, J. G., van Maris, A. J. A., Pronk, J. T., 2017. Laboratory Evolution of a Biotin-Requiring *Saccharomyces cerevisiae* Strain for Full Biotin Prototrophy and Identification of Causal Mutations. Appl Environ Microbiol. 83. DOI: 10.1128/AEM.00892-17

Bunik, V. I., 2003. 2-Oxo acid dehydrogenase complexes in redox regulation. Eur J Biochem. 270**,** 1036-42. DOI: https://doi.org/10.1046/j.1432-1033.2003.03470.x

Buu, L. M., Chen, Y. C., Lee, F. J., 2003. Functional characterization and localization of acetyl-CoA hydrolase, Ach1p, in *Saccharomyces cerevisiae*. J Biol Chem. 278**,** 17203-9. DOI: https://doi.org/10.1074/jbc.M213268200

Choi, Y., A fast computation of pairwise sequence alignment scores between a protein and a set of single-locus variants of another protein. Proceedings of the ACM Conference on Bioinformatics, Computational Biology and Biomedicine, 2012, pp. 414-417.

Choi, Y., Chan, A. P., 2015. PROVEAN web server: a tool to predict the functional effect of amino acid substitutions and indels. Bioinformatics. 31**,** 2745-7. DOI: https://doi.org/10.1093/bioinformatics/btv195

Choi, Y., Sims, G. E., Murphy, S., Miller, J. R., Chan, A. P., 2012. Predicting the functional effect of amino acid substitutions and indels. PLoS One. 7**,** e46688. DOI: https://doi.org/10.1371/journal.pone.0046688

Cortassa, S., Aon, J. C., Aon, M. A., 1995. Fluxes of carbon, phosphorylation, and redox intermediates during growth of *Saccharomyces cerevisiae* on different carbon sources. Biotechnol Bioeng. 47**,** 193-208. DOI: 10.1002/bit.260470211

De Virgilio, C., Bürckert, N., Barth, G., Neuhaus, J. M., Boller, T., Wiemken, A., 1992. Cloning and disruption of a gene required for growth on acetate but not on ethanol: The acetyl-coenzyme A synthetase gene of *Saccharomyces cerevisiae*. Yeast. 8**,** 1043-1051. DOI: https://doi.org/10.1002/yea.320081207

Entian, K.-D., Kötter, P., 2007. 25 Yeast genetic strain and plasmid collections. Methods in Microbiology. 36**,** 629-666. DOI: https://doi.org/10.1016/S0580-9517(06)36025-4

Flamholz, A., Noor, E., Bar-Even, A., Milo, R., 2012. eQuilibrator--the biochemical thermodynamics calculator. Nucleic Acids Res. 40**,** D770-5. DOI: https://doi.org/10.1093/nar/gkr874

Flikweert, M. T., de Swaaf, M., van Dijken, J. P., Pronk, J. T., 1999. Growth requirements of pyruvate-decarboxylase-negative *Saccharomyces cerevisiae*. FEMS Microbiol Lett. 174**,** 73-9. DOI: https://doi.org/10.1111/j.1574-6968.1999.tb13551.x

Flikweert, M. T., Van Der Zanden, L., Janssen, W. M., Steensma, H. Y., Van Dijken, J. P., Pronk, J. T., 1996. Pyruvate decarboxylase: an indispensable enzyme for growth of *Saccharomyces cerevisiae* on glucose. Yeast. 12**,** 247-57. DOI: https://doi.org/10.1002/(SICI)1097-0061(19960315)12:3%3C247::AID-YEA911%3E3.0.CO;2-I

Gietz, R. D., Woods, R. A., 2002. Transformation of yeast by lithium acetate/single-stranded carrier DNA/polyethylene glycol method. Methods Enzymol. 350**,** 87-96. DOI: https://doi.org/10.1016/s0076-6879(02)50957-5

Graham, L. D., Perham, R. N., 1990. Interactions of lipoyl domains with the E1p subunits of the pyruvate dehydrogenase multienzyme complex from *Escherichia coli*. FEBS Lett. 262**,** 241-4. DOI: https://doi.org/10.1016/0014-5793(90)80200-3

Henriksen, P., Wagner, S. A., Weinert, B. T., Sharma, S., Bacinskaja, G., Rehman, M., Juffer, A. H., Walther, T. C., Lisby, M., Choudhary, C., 2012. Proteome-wide analysis of lysine acetylation suggests its broad regulatory scope in *Saccharomyces cerevisiae*. Mol Cell Proteomics. 11**,** 1510-22. DOI: https://doi.org/10.1074/mcp.M112.017251

Hess, M. T., Gupta, R. D., Kolodner, R. D., 2002. Dominant *Saccharomyces cerevisiae* msh6 mutations cause increased mispair binding and decreased dissociation from mispairs by Msh2-Msh6 in the presence of ATP. J Biol Chem. 277**,** 25545-53. DOI: https://doi.org/10.1074/jbc.M202282200

Hess, M. T., Mendillo, M. L., Mazur, D. J., Kolodner, R. D., 2006. Biochemical basis for dominant mutations in the *Saccharomyces cerevisiae MSH6* gene. Proc Natl Acad Sci U S A. 103**,** 558-63. DOI: https://doi.org/10.1073/pnas.0510078103

Hiltunen, J. K., Mursula, A. M., Rottensteiner, H., Wierenga, R. K., Kastaniotis, A. J., Gurvitz, A., 2003. The biochemistry of peroxisomal beta-oxidation in the yeast *Saccharomyces cerevisiae*. FEMS microbiology reviews. 27**,** 35-64. DOI: https://doi.org/10.1016/S0168-6445(03)00017-2

Ho, P. W., Swinnen, S., Duitama, J., Nevoigt, E., 2017. The sole introduction of two single-point mutations establishes glycerol utilization in *Saccharomyces cerevisiae* CEN.PK derivatives. Biotechnol Biofuels. 10**,** 10. DOI: 10.1186/s13068-016-0696-6

Hohmann, S., 1991. Characterization of PDC6, a third structural gene for pyruvate decarboxylase in *Saccharomyces cerevisiae*. J Bacteriol. 173**,** 7963-9. DOI: 10.1128/jb.173.24.7963-7969.1991

Hohmann, S., Cederberg, H., 1990. Autoregulation May Control the Expression of Yeast Pyruvate Decarboxylase Structural Genes Pdc1 and Pdc5. European Journal of Biochemistry. 188**,** 615-621. DOI: DOI 10.1111/j.1432-1033.1990.tb15442.x

Hohmann, S., Meacock, P. A., 1998. Thiamin metabolism and thiamin diphosphate-dependent enzymes in the yeast *Saccharomyces cerevisiae*: genetic regulation. Biochimica et biophysica acta. 1385**,** 201-19. DOI: https://doi.org/10.1016/s0167-4838(98)00069-7

Holzer, H., Goedde, H., 1957. Two paths from pyruvate to acetyl coenzyme A in yeast. Biochem. Ztschr. 329**,** 175-191. DOI:

Joseph-Horne, T., Hollomon, D. W., Wood, P. M., 2001. Fungal respiration: a fusion of standard and alternative components. Biochimica et biophysica acta. 1504**,** 179-95. DOI: 10.1016/s0005-2728(00)00251-6

Knoll, A., Bartsch, S., Husemann, B., Engel, P., Schroer, K., Ribeiro, B., Stockmann, C., Seletzky, J., Buchs, J., 2007. High cell density cultivation of recombinant yeasts and bacteria under non-pressurized and pressurized conditions in stirred tank bioreactors. J Biotechnol. 132**,** 167-79. DOI: 10.1016/j.jbiotec.2007.06.010

Kozak, B. U., van Rossum, H. M., Benjamin, K. R., Wu, L., Daran, J. M., Pronk, J. T., van Maris, A. J., 2014a. Replacement of the *Saccharomyces cerevisiae* acetyl-CoA synthetases by alternative pathways for cytosolic acetyl-CoA synthesis. Metab Eng. 21**,** 46-59. DOI: https://doi.org/10.1016/j.ymben.2013.11.005

Kozak, B. U., van Rossum, H. M., Luttik, M. A., Akeroyd, M., Benjamin, K. R., Wu, L., de Vries, S., Daran, J. M., Pronk, J. T., van Maris, A. J., 2014b. Engineering acetyl coenzyme A supply: functional expression of a bacterial pyruvate dehydrogenase complex in the cytosol of *Saccharomyces cerevisiae*. mBio. 5**,** e01696-14. DOI: https://doi.org/10.1128/mBio.01696-14

Kozak, B. U., van Rossum, H. M., Niemeijer, M. S., van Dijk, M., Benjamin, K., Wu, L., Daran, J. M., Pronk, J. T., van Maris, A. J., 2016. Replacement of the initial steps of ethanol metabolism in *Saccharomyces cerevisiae* by ATP-independent acetylating acetaldehyde dehydrogenase. FEMS Yeast Res. 16**,** fow006. DOI: https://doi.org/10.1093/femsyr/fow006

Kuijpers, N. G., Solis-Escalante, D., Bosman, L., van den Broek, M., Pronk, J. T., Daran, J. M., Daran-Lapujade, P., 2013. A versatile, efficient strategy for assembly of multi-fragment expression vectors in *Saccharomyces cerevisiae* using 60 bp synthetic recombination sequences. Microb Cell Fact. 12**,** 47. DOI: https://doi.org/10.1186/1475-2859-12-47

Labat, F., Pradillon, O., Garry, L., Peuchmaur, M., Fantin, B., Denamur, E., 2005. Mutator phenotype confers advantage in *Escherichia coli* chronic urinary tract infection pathogenesis. FEMS Immunol Med Microbiol. 44**,** 317-21. DOI: https://doi.org/10.1016/j.femsim.2005.01.003

Levy, D. D., Sharma, B., Cebula, T. A., 2004. Single-nucleotide polymorphism mutation spectra and resistance to quinolones in *Salmonella enterica* serovar Enteritidis with a mutator phenotype. Antimicrob Agents Chemother. 48**,** 2355-63. DOI: https://doi.org/10.1128/AAC.48.7.2355-2363.2004

Li, H., Durbin, R. J. B., 2010. Fast and accurate long-read alignment with Burrows–Wheeler transform. 26**,** 589-595. DOI: https://doi.org/10.1093/bioinformatics/btp698

Li, H., Handsaker, B., Wysoker, A., Fennell, T., Ruan, J., Homer, N., Marth, G., Abecasis, G., Durbin, R., Genome Project Data Processing, S., 2009. The Sequence Alignment/Map format and SAMtools. Bioinformatics. 25**,** 2078-9. DOI: https://doi.org/10.1093/bioinformatics/btp352

Lõoke, M., Kristjuhan, K., Kristjuhan, A., 2011. Extraction of genomic DNA from yeasts for PCR-based applications. Biotechniques. 50**,** 325-8. DOI: https://doi.org/10.2144/000113672

Mans, R., van Rossum, H. M., Wijsman, M., Backx, A., Kuijpers, N. G., van den Broek, M., Daran-Lapujade, P., Pronk, J. T., van Maris, A. J., Daran, J. M., 2015. CRISPR/Cas9: a molecular Swiss army knife for simultaneous introduction of multiple genetic modifications in *Saccharomyces cerevisiae*. FEMS Yeast Res. 15. DOI: https://doi.org/10.1093/femsyr/fov004

Marsischky, G. T., Filosi, N., Kane, M. F., Kolodner, R., 1996. Redundancy of *Saccharomyces cerevisiae MSH3* and *MSH6* in *MSH2*-dependent mismatch repair. Genes Dev. 10**,** 407-20. DOI: https://doi.org/10.1101/gad.10.4.407

Mazur, D. J., Mendillo, M. L., Kolodner, R. D., 2006. Inhibition of Msh6 ATPase activity by mispaired DNA induces a Msh2(ATP)-Msh6(ATP) state capable of hydrolysis-independent movement along DNA. Mol Cell. 22**,** 39-49. DOI: https://doi.org/10.1016/j.molcel.2006.02.010

Meadows, A. L., Hawkins, K. M., Tsegaye, Y., Antipov, E., Kim, Y., Raetz, L., Dahl, R. H., Tai, A., Mahatdejkul-Meadows, T., Xu, L., Zhao, L., Dasika, M. S., Murarka, A., Lenihan, J., Eng, D., Leng, J. S., Liu, C. L., Wenger, J. W., Jiang, H., Chao, L., Westfall, P., Lai, J., Ganesan, S., Jackson, P., Mans, R., Platt, D., Reeves, C. D., Saija, P. R., Wichmann, G., Holmes, V. F., Benjamin, K., Hill, P. W., Gardner, T. S., Tsong, A. E., 2016. Rewriting yeast central carbon metabolism for industrial isoprenoid production. Nature. 537**,** 694-697. DOI: https://doi.org/10.1038/nature19769

Mikkelsen, M. D., Hansen, J., Simon, E., Brianza, F., Semmler, A., Olsson, K., Carlsen, S., Düring, L., Ouspenski, A., Hicks, P., Methods for improved production of rebaudioside D and rebaudioside M. Google Patents, 2018.

Miller, J. H., Suthar, A., Tai, J., Yeung, A., Truong, C., Stewart, J. L., 1999. Direct selection for mutators in *Escherichia coli*. J Bacteriol. 181**,** 1576-84. DOI: https://doi.org/10.1128/JB.181.5.1576-1584.1999

Morgan, A. D., Bonsall, M. B., Buckling, A., 2010. Impact of bacterial mutation rate on coevolutionary dynamics between bacteria and phages. Evolution: International Journal of Organic Evolution. 64**,** 2980-2987. DOI: https://doi.org/10.1111/j.1558-5646.2010.01037.x

Noor, E., Bar-Even, A., Flamholz, A., Lubling, Y., Davidi, D., Milo, R., 2012. An integrated open framework for thermodynamics of reactions that combines accuracy and coverage. Bioinformatics. 28**,** 2037-44. DOI: https://doi.org/10.1093/bioinformatics/bts317

Noor, E., Bar-Even, A., Flamholz, A., Reznik, E., Liebermeister, W., Milo, R., 2014. Pathway thermodynamics highlights kinetic obstacles in central metabolism. PLoS Comput Biol. 10**,** e1003483. DOI: https://doi.org/10.1371/journal.pcbi.1003483

Noor, E., Haraldsdóttir, H. S., Milo, R., Fleming, R. M., 2013. Consistent estimation of Gibbs energy using component contributions. PLoS Comput Biol. 9**,** e1003098. DOI: https://doi.org/10.1371/journal.pcbi.1003098

Oud, B., Flores, C. L., Gancedo, C., Zhang, X., Trueheart, J., Daran, J. M., Pronk, J. T., van Maris, A. J., 2012. An internal deletion in *MTH1* enables growth on glucose of pyruvate-decarboxylase negative, non-fermentative *Saccharomyces cerevisiae*. Microb Cell Fact. 11**,** 131. DOI: https://doi.org/10.1186/1475-2859-11-131

Pal, C., Macia, M. D., Oliver, A., Schachar, I., Buckling, A., 2007. Coevolution with viruses drives the evolution of bacterial mutation rates. Nature. 450**,** 1079-81. DOI: https://doi.org/10.1038/nature06350

Papapetridis, I., Verhoeven, M. D., Wiersma, S. J., Goudriaan, M., van Maris, A. J. A., Pronk, J. T., 2018. Laboratory evolution for forced glucose-xylose co-consumption enables identification of mutations that improve mixed-sugar fermentation by xylose-fermenting *Saccharomyces cerevisiae*. Fems Yeast Research. 18. DOI: 10.1093/femsyr/foy056

Perli, T., Moonen, D. P. I., van den Broek, M., Pronk, J. T., Daran, J. M., 2020. Adaptive Laboratory Evolution and Reverse Engineering of Single-Vitamin Prototrophies in *Saccharomyces cerevisiae*. Appl Environ Microbiol. 86**,** e00388-20. DOI: https://doi.org/10.1128/AEM.00388-20

Pronk, J. T., Wenzel, T. J., Luttik, M. A., Klaassen, C. C., Scheffers, W. A., Steensma, H. Y., van Dijken, J. P., 1994. Energetic aspects of glucose metabolism in a pyruvate-dehydrogenase-negative mutant of *Saccharomyces cerevisiae*. Microbiology (Reading). 140 ( Pt 3)**,** 601-10. DOI: 10.1099/00221287-140-3-601

Qiao, K., Wasylenko, T. M., Zhou, K., Xu, P., Stephanopoulos, G., 2017. Lipid production in *Yarrowia lipolytica* is maximized by engineering cytosolic redox metabolism. Nat Biotechnol. 35**,** 173-177. DOI: 10.1038/nbt.3763

Ren, L., Rahman, M. S., Humayun, M. Z., 1999. *Escherichia coli* cells exposed to streptomycin display a mutator phenotype. J Bacteriol. 181**,** 1043-4. DOI: https://doi.org/10.1128/JB.181.3.1043-1044.1999

Riesenberg, D., Guthke, R., 1999. High-cell-density cultivation of microorganisms. Appl Microbiol Biotechnol. 51**,** 422-30. DOI: 10.1007/s002530051412

Ro, D. K., Paradise, E. M., Ouellet, M., Fisher, K. J., Newman, K. L., Ndungu, J. M., Ho, K. A., Eachus, R. A., Ham, T. S., Kirby, J., Chang, M. C., Withers, S. T., Shiba, Y., Sarpong, R., Keasling, J. D., 2006. Production of the antimalarial drug precursor artemisinic acid in engineered yeast. Nature. 440**,** 940-3. DOI: https://doi.org/10.1038/nature04640

Rodriguez, A., Strucko, T., Stahlhut, S. G., Kristensen, M., Svenssen, D. K., Forster, J., Nielsen, J., Borodina, I., 2017. Metabolic engineering of yeast for fermentative production of flavonoids. Bioresour Technol. 245**,** 1645-1654. DOI: https://doi.org/10.1016/j.biortech.2017.06.043

Salazar, A. N., Gorter de Vries, A. R., van den Broek, M., Wijsman, M., de la Torre Cortes, P., Brickwedde, A., Brouwers, N., Daran, J. G., Abeel, T., 2017. Nanopore sequencing enables near-complete de novo assembly of *Saccharomyces cerevisiae* reference strain CEN.PK113-7D. FEMS Yeast Res. 17. DOI: https://doi.org/10.1093/femsyr/fox074

Schonauer, M. S., Kastaniotis, A. J., Kursu, V. A., Hiltunen, J. K., Dieckmann, C. L., 2009. Lipoic acid synthesis and attachment in yeast mitochondria. J Biol Chem. 284**,** 23234-42. DOI: https://doi.org/10.1074/jbc.M109.015594

Scott, J., Thompson-Mayberry, P., Lahmamsi, S., King, C. J., McShan, W. M., 2008. Phage-associated mutator phenotype in group A streptococcus. J Bacteriol. 190**,** 6290-301. DOI: https://doi.org/10.1128/JB.01569-07

Strucko, T., Zirngibl, K., Pereira, F., Kafkia, E., Mohamed, E. T., Rettel, M., Stein, F., Feist, A. M., Jouhten, P., Patil, K. R., Forster, J., 2018. Laboratory evolution reveals regulatory and metabolic trade-offs of glycerol utilization in *Saccharomyces cerevisiae*. Metab Eng. 47**,** 73-82. DOI: 10.1016/j.ymben.2018.03.006

Studamire, B., Quach, T., Alani, E., 1998. *Saccharomyces cerevisiae* Msh2p and Msh6p ATPase activities are both required during mismatch repair. Molecular and cellular biology. 18**,** 7590-7601. DOI: https://doi.org/10.1128/mcb.18.12.7590

Takahashi, H., McCaffery, J. M., Irizarry, R. A., Boeke, J. D., 2006. Nucleocytosolic acetyl-coenzyme a synthetase is required for histone acetylation and global transcription. Mol Cell. 23**,** 207-17. DOI: https://doi.org/10.1016/j.molcel.2006.05.040

van den Berg, M. A., de Jong-Gubbels, P., Kortland, C. J., van Dijken, J. P., Pronk, J. T., Steensma, H. Y., 1996. The two acetyl-coenzyme A synthetases of *Saccharomyces cerevisiae* differ with respect to kinetic properties and transcriptional regulation. J Biol Chem. 271**,** 28953-9. DOI: https://doi.org/10.1074/jbc.271.46.28953

van den Berg, M. A., Steensma, H. Y., 1995. *ACS2*, a *Saccharomyces cerevisiae* gene encoding acetyl-coenzyme A synthetase, essential for growth on glucose. Eur J Biochem. 231**,** 704-13. DOI: https://doi.org/10.1111/j.1432-1033.1995.tb20751.x

van Maris, A. J., Geertman, J. M., Vermeulen, A., Groothuizen, M. K., Winkler, A. A., Piper, M. D., van Dijken, J. P., Pronk, J. T., 2004. Directed evolution of pyruvate decarboxylase-negative *Saccharomyces cerevisiae*, yielding a C2-independent, glucose-tolerant, and pyruvate-hyperproducing yeast. Appl Environ Microbiol. 70**,** 159-66. DOI: https://doi.org/10.1128/aem.70.1.159-166.2004

van Rossum, H. M., Kozak, B. U., Niemeijer, M. S., Dykstra, J. C., Luttik, M. A., Daran, J. M., van Maris, A. J., Pronk, J. T., 2016a. Requirements for Carnitine Shuttle-Mediated Translocation of Mitochondrial Acetyl Moieties to the Yeast Cytosol. mBio. 7**,** e00520-16. DOI: https://doi.org/10.1128/mBio.00520-16

van Rossum, H. M., Kozak, B. U., Pronk, J. T., van Maris, A. J. A., 2016b. Engineering cytosolic acetyl-coenzyme A supply in *Saccharomyces cerevisiae*: Pathway stoichiometry, free-energy conservation and redox-cofactor balancing. Metab Eng. 36**,** 99-115. DOI: https://doi.org/10.1016/j.ymben.2016.03.006

Verduyn, C., Postma, E., Scheffers, W. A., Van Dijken, J. P., 1992. Effect of benzoic acid on metabolic fluxes in yeasts: a continuous-culture study on the regulation of respiration and alcoholic fermentation. Yeast. 8**,** 501-17. DOI: https://doi.org/10.1002/yea.320080703

Verhoeven, M. D., Bracher, J. M., Nijland, J. G., Bouwknegt, J., Daran, J. M. G., Driessen, A. J. M., van Maris, A. J. A., Pronk, J. T., 2018. Laboratory evolution of a glucose-phosphorylation-deficient, arabinose-fermenting *S. cerevisiae* strain reveals mutations in GAL2 that enable glucose-insensitive L-arabinose uptake. Fems Yeast Research. 18**,** foy062. DOI: 10.1093/femsyr/foy062

Verhoeven, M. D., Lee, M., Kamoen, L., van den Broek, M., Janssen, D. B., Daran, J. G., van Maris, A. J., Pronk, J. T., 2017. Mutations in PMR1 stimulate xylose isomerase activity and anaerobic growth on xylose of engineered *Saccharomyces cerevisiae* by influencing manganese homeostasis. Sci Rep. 7**,** 46155. DOI: 10.1038/srep46155

Walker, B. J., Abeel, T., Shea, T., Priest, M., Abouelliel, A., Sakthikumar, S., Cuomo, C. A., Zeng, Q., Wortman, J., Young, S. K., Earl, A. M., 2014. Pilon: an integrated tool for comprehensive microbial variant detection and genome assembly improvement. PLoS One. 9**,** e112963. DOI: https://doi.org/10.1371/journal.pone.0112963

Wang, Z., Tan, T. W., Song, J., 2007. Effect of amino acids addition and feedback control strategies on the high-cell-density cultivation of *Saccharomyces cerevisiae* for glutathione production. Process Biochemistry. 42**,** 108-111. DOI: 10.1016/j.procbio.2006.07.008

Wenzel, T. J., van den Berg, M. A., Visser, W., van den Berg, J. A., Steensma, H. Y., 1992. Characterization of *Saccharomyces cerevisiae* mutants lacking the E1 alpha subunit of the pyruvate dehydrogenase complex. Eur J Biochem. 209**,** 697-705. DOI: 10.1111/j.1432-1033.1992.tb17338.x

Zhao, L., Wenzong, L., Wichmann, G., Khankhoje, A., DE, C. G. D. G. G., MAHATDEJKUL-MEADOWS, T., Jackson, S., Leavell, M., PLATT, D., Udp-dependent glycosyltransferase for high efficiency production of rebaudiosides. Google Patents, 2019.

## Supplementary figures

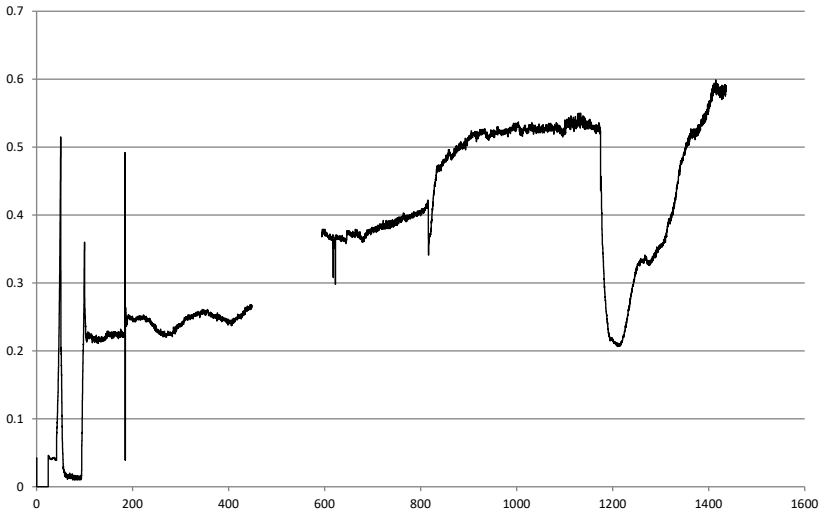


**Supplementary Figure 1** Exhaust $CO_2$ concentration from a chemostat culture of IMX1191 (*pda1Δ, pdc1Δ, pdc5Δ, pdc6Δ*, {PDHL}). From the start of the culture until approximately timepoint 1200h, the medium reservoir contained 25 mM ethanol and 67 mM lactic acid. Additionally, the growth medium contained 100 µg $L^{-1}$ of the required cofactor lipoic acid. This cultivation method was used for enabling lactate consumption. The sharp drop in the off-gas $CO_2$ concentration at 1200h coincides with the change for a more stringent media, containing 5 mM ethanol and 80mM lactic acid. Y-axis: $CO_2$ concentration (%). X-axis: time (h). A representative example of a duplicate experiment is shown.

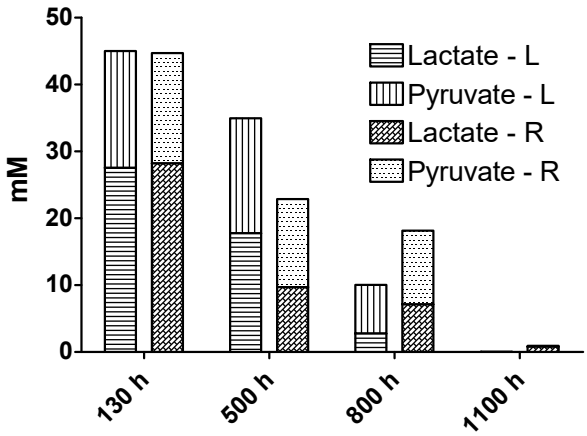


**Supplementary Figure 2** Residual carbon source concentration over time in the broth of the chemostat setups used for the evolution of IMX1191 (*pda1Δ, pdc1Δ, pdc5Δ, pdc6Δ,* {PDHL}). "L" and "R" indicate the two different bioreactor setups. In all cases, the ethanol concentration was below detection limit.

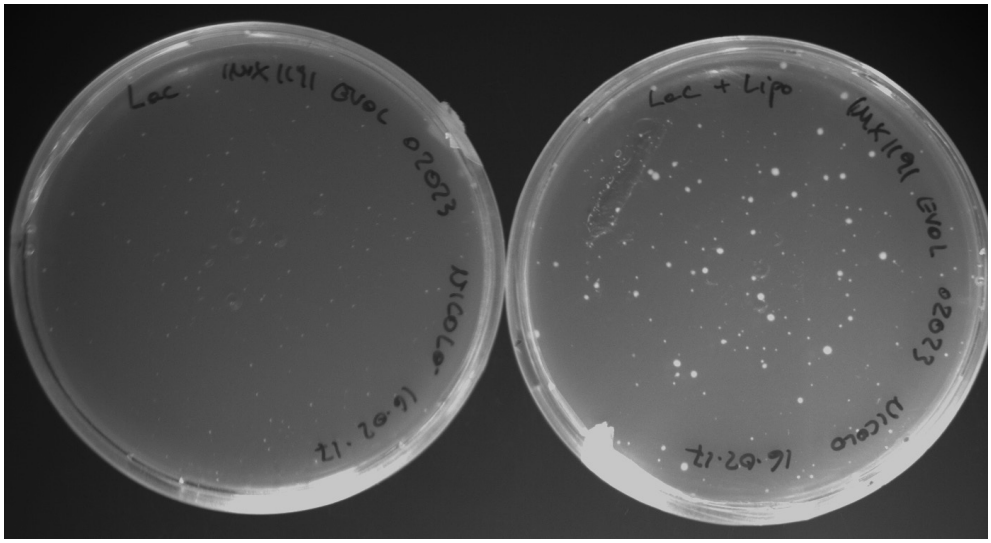


**Supplementary Figure 3** Evolved population originated from IMX1191 (*pda1Δ, pdc1Δ, pdc5Δ, pdc6Δ*, {PDHL}) after chemostat evolution. Cells were taken from the bioreactor broth and plated on solid synthetic media (SM) plates containing 80 mM lactate as sole carbon source, with (right) and without (left) supplementation of 100 µg $L^{-1}$ lipoic acid, and incubated for 5 days.



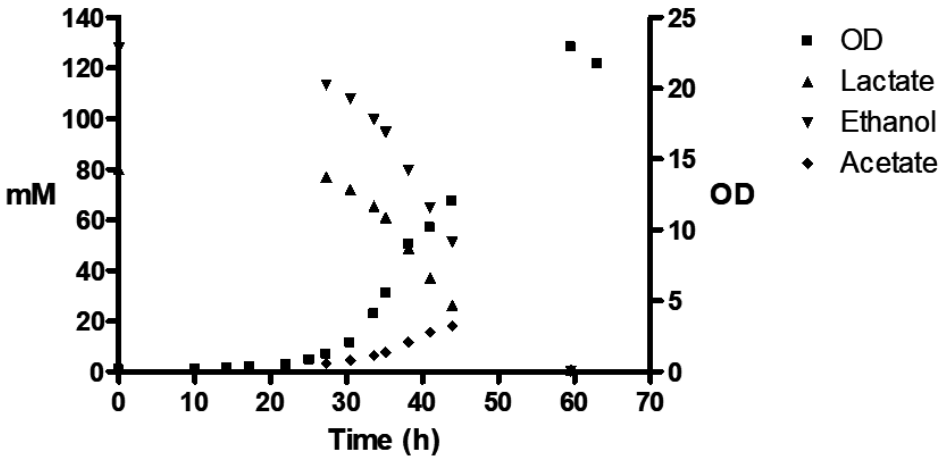


**Supplementary Figure 4** Optical density (λ = 660 nm) and metabolite concentrations in aerobic batch cultures of *S. cerevisiae* IMX1191 (*pda1Δ, pdc1Δ, pdc5Δ, pdc6Δ,* {PDHL}) grown in synthetic medium using a mixture of ethanol and lactate as carbon sources. The medium was supplemented with lipoic acid (100 µg $L^{-1}$). The same growth profile was observed when lipoic acid was omitted from the medium. A representative of a duplicate shake-flask batch culture is shown.

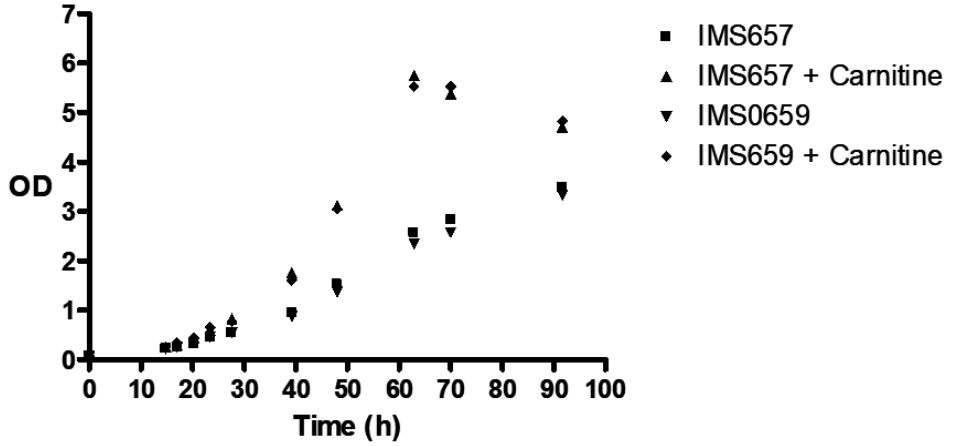


**Supplementary Figure 5** Growth profiles of single colony isolates IMS657 and IMS659 in SM medium containing 80 mM lactic acid as the sole carbon source, with and without carnitine supplementation (0.2 mM). The initial pH of the media was set at 4. All flasks were supplemented with lipoic acid (100 µg $L^{-1}$). IMS657 and IMS659 are single colony isolates derived from an evolution started with IMX1191 (*pda1Δ, pdc1Δ, pdc5Δ, pdc6Δ,* {PDHL}).

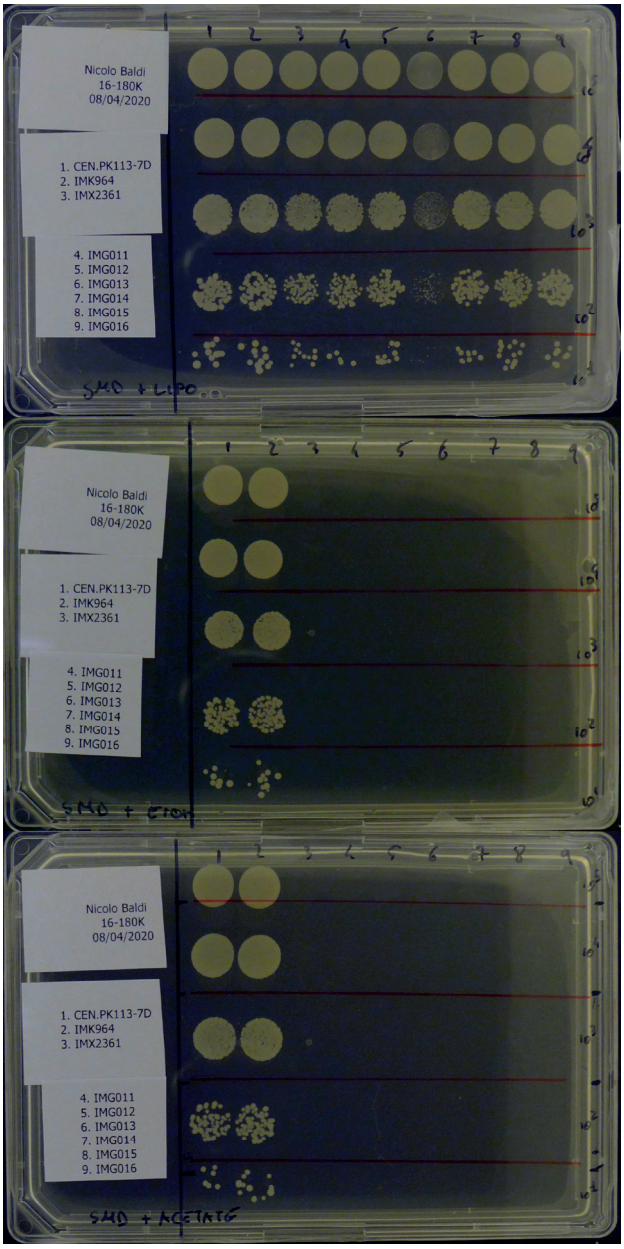


**Supplementary Figure 6** Spot plate assay showing growth of several strains on different carbon sources. Plates (from top to bottom): synthetic medium with 20 g $L^{-1}$ glucose as carbon source, supplemented with either 100 µg $L^{-1}$ lipoic acid (top panel), 1 g $L^{-1}$ ethanol (middle panel) or 1 g $L^{-1}$ acetate (bottom panel). Numbers (1-9) on the top edge of each plate indicate the plated strain: **1.** CEN.PK113-7D (prototrophic reference, *MAT*a); **2.** IMK964 (*acs1Δ*); **3.** IMX2361 (*acs1Δ, acs2Δ*, {PDHL}); **4.** IMG011 (*ACS1*$^{C1753T}$, *acs2Δ*, {PDHL}); **5.** IMG012 (*ACS1*$^{G1090A,\ C1753T}$, *acs2Δ*, {PDHL}); **6.** IMG013 (*ACS1*$^{C1752A,\ C1753T}$, *acs2Δ*, {PDHL}); **7.** IMG014 (*ACS1*$^{G1747A,\ C1753T}$, *acs2Δ*, {PDHL}); **8.** IMG015 (*ACS1*$^{G692T,\ C1753T}$, *acs2Δ*, {PDHL}); **9.** IMG016 (*ACS1, acs2Δ*, {PDHL}); The spots, from top to bottom, contained approximately $10^5$, $10^4$, $10^3$, $10^2$, $10^1$ cells. Plates were incubated for 3 days at 30 °C.

**Supplementary Table 1** Oligonucleotide primers used in this study

| Primer number | Name | Sequence 5' -> 3' | Notes |
|---|---|---|---|
| 6005 | p426 CRISP rv | GATCATTTATCTTTCACTGCGGAGAAG | pROS plasmid series construction |
| 16001 | gRNA_ACS1_pos1753 | TGCGCATGTTTCGGCGTTCGAAACTTCTCCGCAGTGAAAGATAAATGATCCAATTTCAGCGGTAGACA-GAGTTTTAGAGCTAGAAATAGCAAGTTAAAATAAGGCTAGTCCGTTATCAAC | gRNA ACS1 |
| 16587 | 16587_ACS1_rep_synPAM_f | GCAAAACCAAACATATCAAAACTACTAGAAAGACATTGCCCCACTGTGTTAGTAGAATTTCACCTAGAC-GAGGAACAACTGCCGCATCGCTACCACCACTACTTGTGAAGTCCCTGGAGT | Replacement of ACS1 with SynPAM |
| 16588 | 16588_ACS1_rep_synPAM_r | ACTCCAGGGACTTCACAAGTAGTGGTGGTAGCGATGCGGCAGTTGTTCCTCGTCTAGGTGAAATTC-TACTAACACAGTGGGGCAATGTCTTTCTAGTAGTTTTGATATGTTTGGTTTTGC | Replacement of ACS1 with SynPAM |
| 16814 | ACS2_targetRNA FW | TGCGCATGTTTCGGCGTTCGAAACTTCTCCGCAGTGAAAGATAAATGATCTTAAGATTAATCAAACGTGT-GTTTTAGAGCTAGAAATAGCAAGTTAAAATAAGGCTAGTCCGTTATCAAC | gRNA ACS2 |
| 16585 | 16585_ACS1_fw | CTGACATGCCGTGGCAAATGATTGGG | |
| 16586 | 16586_ACS1_rv | TTTGCTGGTACCTACGAGCCACACTG | |
| 7593 | pPDC6 gRNA FW ClaI | TGCGCATGTTTCGGCGTTCGAAACTTCTCCGCAGTGAAAGATAAATGATCTCCTGTAATCAAATCGATCT-GTTTTAGAGCTAGAAATAGCAAGTTAAAATAAG | |
| 7716 | PDC5_targetRNA FW | TGCGCATGTTTCGGCGTTCGAAACTTCTCCGCAGTGAAAGATAAATGATCGCCGAATATAATGAAAT-TCAGTTTTAGAGCTAGAAATAGCAAGTTAAAATAAG | |
| 7717 | PDC5_repair oligo fw | ACTTATTTCACATAATCAATCTCAAAGAGAACAACACAATACAATAACAAGAAGAACAAAGCTAATTAA-CATAAAACTCATGATTCAACGTTTGTGTATTTTTTTACTTTTGAAGGTTAT | |
| 7718 | PDC5_repair oligo rv | ATAACCTTCAAAAGTAAAAAAATACACAAACGTTGAATCATGAGTTTTATGTTAATT-AGCTTTGTTCTTCTTGTTATTGTATTGTGTTGTTCTCTTTGAGATTGATTATGTGAAATAAGT | |
| 7935 | PDC6 repair oligo FW | GTGTAGTAGTGATAAACTGGTGCTTCAATTTCTTTTTATGAATTGATCTGTATCTGCACCCATTAGTAGTG-TACTCAAAAACGAATTATTGTTGCAAATAAATAAATTTACACAGTTTG | |
| 7936 | PDC6 repair oligo RV | CAAACTGTGTAAATTTATTTATTTGCAACAATAATTCGTTTTTGAGTACACTACTAATGGGTGCAGATA-CAGATCAATTCATAAAAAGAAATTGAAGCACCAGTTTATCACTACTACAC | |
| 6157 | PDA1 repair fw | TGTTTATCTCTCTTCTGATTCCTCCACCCCTTCCTTACTCAACCGGGTAAATGTCGCATCTTAATCGTAAG-GAAAAATAAAATAATAGTGCTGTGATCGCATGATATTCTTCCCTGGAAG | |
| 6158 | PDA1 repair rv | CTTCCAGGGAAGAATATCATGCGATCACAGCACTATTATTTTATTTTTCCTTACGATTAAGATGCGA-CATTTACCCGGTTGAGTAAGGAAGGGGTGGAGGAATCAGAAGAGAGATAAACA | |
| 6178 | PDC1 gRNA | GTGCGCATGTTTCGGCGTTCGAAACTTCTCCGCAGTGAAAGATAAATGATCGAAACCGGTACCTC-CGCTTTGTTTTAGAGCTAGAAATAGCAAGTTAAAATAAG | |
| 7713 | MTH1_targetRNA FW | TGCGCATGTTTCGGCGTTCGAAACTTCTCCGCAGTGAAAGATAAATGATCTGAGAGCTACTCATTGA-TAGGTTTTAGAGCTAGAAATAGCAAGTTAAAATAAG | |

| Primer number | Name | Sequence 5' -> 3' | Notes |
|---|---|---|---|
| 7714 | MTH1 ^T deletion FW | CCGGAAAACACGATGAGTGGCAGTGATAATGCTTCTTTTCAAAGTTTGCCACTATCAATGTTTTCTGC-CCCCTCTACTGTGCACACGCAACTAACTAATGACTCTTCGTTCTCCGAATTT | |
| 7715 | MTH1 ^T deletion RV | AAATTCGGAGAACGAAGAGTCATTAGTTAGTTGCGTGTGCACAGTAGAGGGGGCAGAAAACATTGA-TAGTGGCAAACTTTGAAAAGAAGCATTATCACTGCCACTCATCGTGTTTTCCGG | |
| 5654 | D_FW_E1a | GAATTCACGCATCTACGACTG | |
| 9967 | 9967_PDC1_downstream_ tPGI1 | TATTTTTCGTTACATAAAAATGCTTATAAAACTTTAACTAATAATTAGAGATTAAATCGCGGAGGCACTAT-TACTGATGTGATTTC | |
| 7338 | pTDH3 fw ol tag I | TATTCACGTAGACGGATAGGTATAGCCAGACATCAGCAGCATACTTCGGGAACCGTAGGCATAAAAAA-CACGCTTTTTCAGTTCG | |
| 3277 | Fus Tag C rv | CTAGCGTGTCCTCGCATAGTTCTTAGATTG | |
| 3284 | Fus Tag J rv | CGACGAGATGCTCAGACTATGTGTTC | |
| 9969 | 9969_PDC1_upstream_ Ttef1_correct | TCTCAATTATTATTTTCTACTCATAACCTCACGCAAAATAACACAGTCAAATCAATCAAATTAATTTTTA-AAATTTTTACTTTTCGCGAC | |
| 5652 | C_FW_E3 | AAGCTTACGTCTCACGGATCG | |
| 5653 | D_RV_E3 | AAGCTTAATCACTCTCCATACAGGG | |
| 5661 | I_RV_LL.LA1 | TCTAGAGCCTACGGTTCCCGA | |
| 5663 | H_FW_LA1 | TCTAGAAGATTACTCTAACGCCTCAGC | |
| 3285 | Fus Tag J fw | GGCCGTCATATACGCGAAGATGTC | |
| 2686 | Tag H fusion reverse | GTCACGGGTTCTCAGCAATTCG | |
| 7356 | tPGI1 ol pACS2 | GGTTAGTGATTGTTATACACAAACAGAATACAGGAAAGTAAATCAATACAATAATAAAATTAATTTTTA-AAATTTTTACTTTTCGCGAC | |
| 7426 | tTEF1_yeast ol tACS2 | GAAAATAGAAAACAGAAAAGGAGCGAAATTTTATCTCATTACGAAATTTTTCTCATTTAAGGAGGCAC-TATTACTGATGTGATTTC | |

**Supplementary Table 2** Type and number of mutations found in evolved single colony isolates. All strains were originally derived from IMX1191 (*pda1Δ, pdc1Δ, pdc5Δ, pdc6Δ,* {PDHL}). This strain was then evolved for lactic acid consumption in two separate chemostats. Strains IMS657-IMS659 were obtained from chemostat L, while IMS660-IMS662 were obtained from chemostat R. Further evolution was then performed in sequential batches containing SM medium with lactic acid as the sole carbon source. The population of chemostat L was used to inoculate four independent flasks, which yielded IMS775, IMS776, IMS778 and IMS805, respectively. Strains IMS660 and IMS662 were inoculated each in three different flasks, for a total of six independent evolution lines, from which strains IMS971, IMS974, IMS976, IMS978, IMS980 and IMS982 were isolated. For all sequential batches a total of 15 transfers (approximately 100 generations) were performed.

| Strain | Parental | Non-synonymous SNVs | Synonymous SNVs | SNVs outside of coding regions | Indels | Indels in coding regions | Indels causing a frameshift |
|---|---|---|---|---|---|---|---|
| IMS657 | IMX1191 | 35 | 19 | 25 | 10 | 3 | 3 |
| IMS659 | IMX1191 | 39 | 14 | 34 | 10 | 3 | 3 |
| IMS660 | IMX1191 | 7 | 4 | 7 | 4 | 3 | 2 |
| IMS662 | IMX1191 | 7 | 3 | 8 | 3 | 2 | 1 |
| IMS775 | Population chemostat L | 100 | 40 | 76 | 20 | 8 | 8 |
| IMS776 | Population chemostat L | 67 | 43 | 76 | 487 | 73 | 70 |
| IMS778 | Population chemostat L | 90 | 47 | 71 | 24 | 9 | 9 |
| IMS805 | Population chemostat L | 67 | 57 | 81 | 576 | 88 | 85 |
| IMS971 | IMS660 | 48 | 23 | 46 | 301 | 37 | 33 |
| IMS974 | IMS660 | 11 | 12 | 21 | 4 | 2 | 1 |
| IMS976 | IMS660 | 13 | 12 | 26 | 4 | 2 | 1 |
| IMS978 | IMS662 | 9 | 11 | 26 | 3 | 2 | 1 |
| IMS980 | IMS662 | 9 | 8 | 21 | 2 | 1 | 0 |
| IMS982 | IMS662 | 7 | 8 | 21 | 5 | 3 | 2 |

# 3.

# Functional expression of a bacterial α-ketoglutarate dehydrogenase in the cytosol of *Saccharomyces cerevisiae*

Nicolò Baldi[a], James C. Dykstra[a], Marijke A.H. Luttik[a], Martin Pabst[a], Liang Wu[b], Kirsten R. Benjamin[c], André Vente[b], Jack T. Pronk[a], Robert Mans[a]*

[a] Department of Biotechnology, Delft University of Technology, van der Maasweg 9, 2629 HZ Delft, The Netherlands
[b] DSM Biotechnology Center, Delft, The Netherlands
[c] Amyris Inc., Emeryville, California, USA

Essentially as published in Metabolic engineering (https://doi.org/10.1016/j.ymben.2019.10.001)

## ABSTRACT

Efficient production of fuels and chemicals by metabolically engineered micro-organisms requires availability of precursor molecules for product pathways. In eukaryotic cell factories, heterologous product pathways are usually expressed in the cytosol, which may limit availability of precursors that are generated in other cellular compartments. In *Saccharomyces cerevisiae*, synthesis of the precursor molecule succinyl-Coenzyme A is confined to the mitochondrial matrix. To enable cytosolic synthesis of succinyl-CoA, we expressed the structural genes for all three subunits of the *Escherichia coli* α-ketoglutarate dehydrogenase (αKGDH) complex in *S. cerevisiae*. The *E. coli* lipoic-acid scavenging enzyme was co-expressed to enable cytosolic lipoylation of the αKGDH complex, which is required for its enzymatic activity. Size-exclusion chromatography and mass spectrometry indicated that the heterologously expressed αKGDH complex contained all subunits and that its size was the same as in *E. coli*. Functional expression of the heterologous complex was evident from increased αKGDH activity in the cytosolic fraction of yeast cell homogenates. *In vivo* cytosolic activity of the αKGDH complex was tested by constructing a reporter strain in which the essential metabolite 5-aminolevulinic acid could only be synthetized from cytosolic, and not mitochondrial, succinyl-CoA. To this end *HEM1*, which encodes the succinyl-CoA-converting mitochondrial enzyme 5-aminolevulinic acid (ALA) synthase, was deleted and a bacterial ALA synthase was expressed in the cytosol. In the resulting strain, complementation of ALA auxotrophy depended on activation of the αKGDH complex by lipoic acid addition. Functional expression of a bacterial αKGDH complex in yeast represents a vital step towards efficient yeast-based production of compounds such as 1,4-butanediol and 4-aminobutyrate, whose product pathways use succinyl-CoA as a precursor.

## 1. INTRODUCTION

Production of industrially relevant compounds with engineered microorganisms relies on introduction of heterologous product pathways as well as on changing the expression and/or sequences of native genes. Selection of a suitable production organism is based on several criteria, including native ability to synthesize the compound of interest, robustness to industrial conditions, ability to excrete the product and genetic accessibility. *Saccharomyces cerevisiae* is a popular microbial platform for production of low-molecular-weight compounds. Recent advances in genome editing technology have helped to expand its product spectrum from simple products such as succinic acid (Jansen et al., 2017) to complex pharmaceutical molecules such as artemisinic acid (Ro et al., 2006) and opioids (Galanie et al., 2015). *S. cerevisiae* is used for industrial production of, among others, farnesene, resveratrol, artemisinic acid and artificial sweeteners (Ekas et al., 2019). In *S. cerevisiae*, heterologous product pathways are usually expressed in the cytosol. Since, as in other eukaryotes, metabolism in *S. cerevisiae* is highly compartmentalized, the intracellular localization of metabolic precursors is a key aspect in the design and construction of engineered strains (Avalos et al., 2013; van Rossum et al., 2016b).

In *S. cerevisiae*, succinyl-CoA is synthesized in the mitochondria, where it is used as a substrate for 5-aminolevulinic acid synthase, which catalyses the first committed step in heme biosynthesis (Hoffman et al., 2003). Succinyl-CoA is an important precursor molecule in microbial biotechnology, as it can be reduced to succinate semialdehyde and subsequently to 4-hydroxybutyrate (4HB), which can be further converted to 4-aminobutyrate (GABA) or 1,4-butanediol (1,4-BDO) (Yim et al., 2011). GABA is used in the pharmaceutical and nutraceutical industry (Abdou et al., 2006), while 4HB and 1,4-BDO have applications as solvents or as components in polymers for medical applications (Martin and Williams, 2003; Saito et al., 1996) and compostable bioplastics (Chen et al., 2015). Microbial production of 4HB and 1,4-BDO currently uses *Escherichia coli* as a host, and titers of approximately 85 mM (4HB) and 200 mM (1,4-BDO) have been reported in microaerobic fed-batch fermentations (Yim et al., 2011). Neither the production of 4HB nor the production of 1,4-BDO via reduction of succinyl-CoA to succinate semialdehyde have hitherto been reported in *S. cerevisiae*. Exploration of yeast-based production of these commercially relevant compounds could benefit from the availability of a pathway that generates succinyl-CoA in the yeast cytosol.

Succinyl-CoA is produced by oxidative decarboxylation of α-ketoglutarate, mediated by the α-ketoglutarate dehydrogenase (αKGDH) complex. In eukaryotes, the αKGDH complex is present in the mitochondria, where it participates in the tricarboxylic acid cycle. The *S. cerevisiae* αKGDH complex is composed of three catalytic subunits: α-ketoglutarate dehydrogenase (E1, EC 1.2.4.2), dihydrolipoyl transsuccinylase (E2, EC 2.3.1.61) and dihydrolipoyl dehydrogenase (E3, EC 1.8.1.4) (Dickinson et al., 1986; Repetto and Tzagoloff, 1989; Repetto and Tzagoloff, 1990). The structural subunit E4 was identified more recently in *S. cerevisiae* (Heublein et al., 2014) and has a role in recruiting the E3 subunit to the E1-E2

core. In *S. cerevisiae*, E1, E2 and E4 are specific for the αKGDH complex, whereas E3 is shared with the pyruvate dehydrogenase complex (Pettit and Reed, 1967).

Thiamine pyrophosphate (TPP) and lipoic acid are essential cofactors for activity of the αKGDH complex. TPP is involved in the decarboxylation reaction whereas lipoic acid is covalently bound to E2 and shuttles the substrate through the different catalytic domains (Bunik, 2003; Graham and Perham, 1990). Functional expression of an αKGDH complex in the yeast cytosol will therefore require availability of both TPP and lipoic acid in this cellular compartment. TPP is present in the yeast cytosol, where it acts as cofactor for transketolase and pyruvate decarboxylase (Hohmann and Meacock, 1998). Lipoic acid is, however, only present in yeast mitochondria, where it is synthetized from octanoyl-acyl-carrier-protein (octanoyl-ACP), an intermediate of fatty acid biosynthesis (Schonauer et al., 2009). Therefore, functional expression of an αKGDH complex in the yeast cytosol is expected to require the additional introduction of cytosolic enzymes required for its lipoylation (Kozak et al., 2014).

Lipoic acid biosynthesis and attachment are best understood in *E. coli*, which harbors a *de novo* biosynthetic pathway and a scavenging pathway (Spalding and Prigge, 2010). The *de novo* synthesis pathway uses octanoyl-ACP as substrate and involves two dedicated enzymes: lipoyl(octanoyl)-ACP:protein transferase (LipB) and lipoyl synthase (LipA), of which the yeast homologs (Lip5 and Lip2, respectively) are located in the mitochondria. The *E. coli* scavenging pathway depends on a lipoate-protein ligase (LplA), which activates lipoate to lipoyl-AMP and attaches it to the target protein (Morris et al., 1995). The scavenging pathway is absent in *S. cerevisiae*, even though *LIP3*, a homolog of *E. coli lplA*, is required for *de novo* mitochondrial synthesis of lipoic acid (Schonauer et al., 2009).

The goal of the present study was explore the functional expression of a heterologous αKGDH complex in the cytosol of *S. cerevisiae*. To this end, structural genes encoding subunits of the *E. coli* αKGDH complex and the lipoic acid scavenging gene *lplA* were expressed in *S. cerevisiae*. Functional expression was tested by assaying αKGDH activity in mitochondrial and cytosolic fractions of cell extracts. Size-exclusion chromatography and mass-spectrometry were used to investigate assembly of the complex and its lipoylation status. Finally, to explore *in vivo* functionality, a 5-aminolevulinic acid (ALA) auxotrophic strain was constructed whose growth in the absence of ALA depended on cytosolic activity of the heterologously expressed αKGDH complex.

## 2. MATERIALS AND METHODS

### 2.1 Strains and maintenance

The *S. cerevisiae* strains used in this study (Table 2) share the CEN.PK113-7D genetic background (Entian and Kötter, 2007). Stock cultures of *S. cerevisiae* were grown aerobically in 500 mL shake flasks containing 100 mL synthetic medium (SM) (Verduyn et al., 1992) or YP medium (10 g $L^{-1}$ Bacto yeast extract, 20 g $L^{-1}$ Bacto peptone, 20 g $L^{-1}$ D-glucose). When needed, cultures were supplied with DL-lipoic acid (Sigma-Aldrich, St. Louis, USA) to a final concentration of 100 µg $L^{-1}$ or with 5-aminolevulinic acid (Sigma-Aldrich) to a final concentration of 50 mg $L^{-1}$. Stock cultures of *E. coli* XL1-Blue Subcloning Grade Competent Cells (Agilent Genomics, Santa Clara, USA) were grown in LB medium (5 g $L^{-1}$ Bacto yeast extract, 10 g $L^{-1}$ Bacto tryptone, 10 g $L^{-1}$ NaCl) supplemented with 100 mg $L^{-1}$ ampicillin. Media were autoclaved at 121°C for 20 min. Media supplements and antibiotics were filter sterilized and added to the media prior to use. For yeast strain storage, glycerol was added to grown cultures to a final concentration of 30% v/v and 1 mL aliquots were stored at -80°C.

### 2.2 Molecular biology techniques

Phusion High-Fidelity DNA Polymerase (Thermo Fisher Scientific, Waltham, USA) was used for PCR amplification for cloning purposes. The manufacturer's protocol was followed except for the use of a low primer concentration (0.2 µM instead of 0.5 µM). Diagnostic PCR was performed with DreamTaq PCR Master Mix (2X) (Thermo Fisher Scientific). Desalted (DST) oligonucleotide primers were used, except for primers binding to coding regions, which were PAGE purified (Sigma Aldrich). For yeast colony PCR, genomic DNA was isolated as described by Lõoke et al. (2011). Commercial kits for DNA extraction and purification were used for small-scale DNA isolation (Sigma Aldrich), PCR cleanup (Sigma Aldrich), and gel extraction (Zymo Research, Irvine, USA). Restriction analysis of constructed plasmids was performed using FastDigest restriction enzymes (Thermo Scientific). Gibson assembly of linear DNA fragments was performed using NEBuilder HiFi DNA Assembly Master Mix (New England Biolabs) in a total reaction volume of 5 µL. Transformation of chemically competent *E. coli* XL1-Blue was performed according to the manufacturer's protocol.

### 2.3 Plasmid construction

The plasmids and oligonucleotide primers used in this study are listed in Table 1 and in Supplementary Table 1, respectively. Protein sequences of *E. coli* αKGDH subunits E1 (*Ec_sucA,* accession number P0AFG3), E2 (*Ec_sucB,* P0AFG6) and E3 (*Ec_lpd,* accession number P0A9P0), lipoate protein ligase LplA (*Ec_lplA,* P32099), and of *Rhodobacter sphaeroides* 5-aminolevulinic acid synthase (*Rs_hemA*, Q04512), were used to order codon-optimized sequences from GeneArt (Regensburg, Germany). Codon usage was optimized with the GeneArt algorithm (Raab et al., 2010). Genes *Ec_sucA* and *Ec_sucB* were ordered as linear DNA fragments (GeneStrings, GeneArt), other genes were ordered in plasmids.

Plasmid pUD614 was constructed by Gibson assembly of the *Ec_sucA* ORF amplified from ordered linear DNA fragments using primers 10540 and 10541 and a vector backbone

amplified from plasmid pUD301, using primers 6486 and 10562. Plasmid pUD616 was constructed by Gibson assembly of the *Ec_sucB* ORF amplified from the ordered linear DNA fragments using primers 10542 and 10543 and a vector backbone amplified from plasmid pUD302 using primers 3628 and 6494. Plasmid pUD618 was constructed by Gibson assembly of the *Ec_lplA* ORF amplified from pUD622 using primers 10544 and 10545 and a vector backbone amplified from plasmid pUD303 using primers 4671 and 6221. The *Ec_lpd* ORF was amplified from plasmid pUD191 using primers 11303 and 11304. The obtained PCR product was used as template for amplification with primers 11219 and 10561. Plasmid pUD625 was then constructed by Gibson assembly of the *Ec_lpd* ORF, obtained as specified above, and a vector backbone amplified from plasmid pUD304 using primers 3903 and 3904. Plasmid pUD623 was constructed via Gibson assembly of the *Rs_hemA* ORF amplified from pUD482 using primers 10560 and 10561 and a vector backbone amplified from plasmid pUDE482 using primers 3904 and 10563.

Plasmid pUDR263 was constructed by Gibson assembly of a double-stranded DNA fragment, obtained by annealing the complementary single-stranded oligonucleotides 10534 and 10535, and a vector backbone amplified from plasmid pMEL11 using primers 6005 and 6006. Plasmid pUDR573 was constructed by Gibson assembly of two linear fragments, both obtained via PCR amplification of plasmid pMEL11 using primer couples 5792-5980 and 5979-7374.

**Table 1:** Plasmids used in this study.

| Name | Relevant characteristic | Origin |
|---|---|---|
| pMEL11 | 2 µm ori, *amdSYM*, *pSNR52*-gRNA.*CAN1.Y-tSUP4* | (Mans et al., 2015) |
| pUDR119 | *amdSYM* 2µm gRNA-*SGA1* | (van Rossum et al., 2016a) |
| pUDR263 | *amdSYM* 2µm gRNA-*HEM1* | This work |
| pUDR573 | *amdSYM* 2µm gRNA-*X-2* | This work |
| pUD191 | pMA-*pTPI1-Ec_lpd-tTEF1* | GeneArt, Germany |
| pUD482 | pMA-*Rs_hemA* | GeneArt, Germany |
| pUD622 | pMA-*Ec_lplA* | GeneArt, Germany |
| pUD301 | *pTPI1-pdhA-tTEF1* | (Kozak et al., 2014) |
| pUD302 | *pTDH3-pdhB-tCYC1* | (Kozak et al., 2014) |
| pUD303 | *pADH1-aceF-tPGI1* | (Kozak et al., 2014) |
| pUD304 | *pTEF1-lpd-tADH1* | (Kozak et al., 2014) |
| pUDE482 | *pTEF1*-Venus-*tENO2* | (Gorter de Vries et al., 2018) |
| pUD614 | *pTPI1-Ec_sucA-tTEF1* | This work |
| pUD616 | *pTDH3-Ec_sucB-tCYC1* | This work |
| pUD618 | pADH1-lplA-tPGI1 | This work |
| pUD623 | *pTEF1-Rs_hemA-tENO2* | This work |
| pUD625 | *pTEF1-lpd-tADH1* | This work |

### 2.4 Strain construction

*S. cerevisiae* strains were transformed with the LiAc/ssDNA method (Gietz and Woods, 2002). The transformation mixture was plated on modified SM plates, in which $(NH_4)_2SO_4$ was replaced by 0.6 g $L^{-1}$ acetamide and 6.6 g $L^{-1}$ $K_2SO_4$ (SM-Ac). Single colonies were obtained by re-streaking three times on identical plates. Counter-selection for plasmid loss was performed on SM plates containing 2.3 g $L^{-1}$ fluoroacetamide (SM-Fac) (Solis-Escalante et al., 2013). Gene deletions and integrations were performed as previously described (Mans et al., 2015). Expression cassettes were flanked by 60 bp short homology repeats (SHRs) to allow assembly of the αKGDH cluster in the X-2 intergenic locus (Mikkelsen et al., 2012), and of the *Rs_hemA* cassette in the *SGA1* locus by means of homologous recombination (Kuijpers et al., 2013).

Strain IMX1190 was constructed by transforming the Cas9 expressing strain IMX585 with plasmid pUD263 and a double stranded repair oligonucleotide obtained by annealing oligonucleotides 10536 and 10537. Strain IMX1230 was constructed by transforming strain IMX1190 with plasmid pUDR119 and a repair fragment obtained by PCR amplification of the *Rs_hemA* expression cassette from plasmid pUDE482 using primers 10710 and 10711.

Gene expression cassettes for integration of αKGDH genes were prepared as follows: the cassette containing the *Ec_sucA* ORF was amplified from plasmid pUD614 using primers 5654 and 8646; the cassette containing the *Ec_sucB* ORF was amplified from plasmid pUD616 using primers 3277 and 11186; the cassette containing the *Ec_lpd* ORF was amplified from plasmid pUD625 with primers 5652 and 5653; the cassette containing the *Ec_lplA* ORF was amplified from pUD618 using primers 3284 and 8645. The obtained fragments were co-transformed with pUDR573 into IMX1230, yielding strain IMX1401. After transformation, gRNA expression plasmids were removed by counter-selection as described above.



**Table 2** *Saccharomyces cerevisiae* strains used in this study

| Strain name | Relevant genotype [a] | Origin |
|---|---|---|
| CEN.PK113-7D | Prototrophic reference, *MAT*a | (Entian and Kötter, 2007) |
| IMX585 | *MAT*a *can1Δ::cas9-natNT2* | (Mans et al., 2015) |
| IMX1190 | *MAT*a *can1Δ::cas9-natNT2 hem1Δ* | This study |
| IMX1230 | *MAT*a *can1Δ::cas9-natNT2 hem1Δ; sga1Δ::Rs_hemA* | This study |
| IMX1401 | *MAT*a *can1Δ::cas9-natNT2 hem1Δ; sga1Δ::Rs_hemA; X2::*{αKGDH} | This study |

[a] {αKGDH}: chromosomally integrated *E. coli* α-ketoglutarate dehydrogenase cluster, *pTPI1-Ec_sucA-tTEF1 pTDH3-Ec_sucB-tCYC1 pTEF1-lpd-tADH1 pADH1-lplA-tPGI1*.

### 2.5 Media and cultivation

Shake-flask cultures were grown at 30°C in 500 mL flasks containing 100 mL synthetic medium (Verduyn et al., 1992) with 20 g $L^{-1}$ glucose (SMD) in an Innova incubator shaker (New Brunswick Scientific, Edison, NJ, USA) set at 200 rpm. When required, media were

supplemented with lipoic acid at a concentration of 100 µg $L^{-1}$, or with 5-aminolevulinic acid at a concentration of 50 mg $L^{-1}$. Glucose-limited chemostat cultivation was performed at 30°C in 2 L laboratory bioreactors (Applikon, Delft, The Netherlands) with a working volume of 1 L. For continuous cultures, synthetic medium was supplemented with 7.5 g $L^{-1}$ glucose (SMD) and 0.2 g $L^{-1}$ Pluronic PE6100 antifoam (BASF). For cultures supplemented with lipoic acid, a lipoic acid solution (50 g $L^{-1}$) in ethanol was prepared and added to the medium to a final concentration of 500 µg $L^{-1}$. Continuous cultivation was preceded by a batch culture grown under the same conditions. When a rapid decrease in the $CO_2$ production indicated glucose depletion in the batch culture, continuous cultivation was initiated at a dilution rate of 0.10 $h^{-1}$. Culture pH was maintained at 5.0 by automatic addition of 2 M KOH. Bioreactors were sparged with 500 mL $min^{-1}$ air and stirred at 800 rpm to ensure fully aerobic conditions.

Sequential batch cultivation was carried out in bioreactors as indicated above, with the exception of the glucose concentration in the medium, which was increased to 20 g $L^{-1}$. Biomass was first grown in a bioreactor on synthetic medium supplemented with 5-aminolevulinic acid. Subsequently the biomass was harvested, washed twice to remove residual 5-aminolevulinic acid, and used to inoculate new reactors, containing SMD with or without lipoic acid supplementation.

**2.6 Analytical methods**

Culture optical density at 660 nm was measured with a Libra S11 spectrophotometer (Biochrom, Cambridge, United Kingdom). Metabolite concentrations in culture supernatants and media were analyzed using an Agilent 1260 Infinity HPLC system equipped with an Aminex HPX-87H ion exchange column, operated at 60°C with 5 mM $H_2SO_4$ as mobile phase at a flow rate of 0.600 mL $min^{-1}$.

**2.7 Separation of mitochondrial and cytosolic fractions**

Separation of mitochondrial and cytosolic fractions of cell homogenates was performed as described previously (Luttik et al., 1998) with minor modifications. Zymolyase from *Arthobacter luteus* (20,000 U $g^{-1}$, AMS Biotechnology Ltd., Abingdon, United Kingdom) was used. Biomass from CEN.PK113-7D and IMX1401 was harvested from glucose-limited chemostat cultures supplemented with 500 µg $L^{-1}$ of lipoic acid. αKGDH activity was measured in the complete homogenate, as well as in the cytosolic and mitochondrial fractions. Protein concentrations of homogenates and fractions were determined using the Quick Start Bradford Protein Assay (Bio-Rad Laboratories Inc., Hercules, CA, USA) according to the supplier's manual, with bovine serum albumin (essentially fatty acid free, Sigma-Aldrich) as a standard.

**2.8 αKGDH enzymatic activity measurements**

α-Ketoglutarate dehydrogenase complex activity was tested in complete cell homogenates as well as in cytosolic and mitochondrial fractions. Prior to enzyme-activity assays, samples were dialyzed for 2 h at 4°C using a 0.5 mL Slide-A-Lyzer dialysis cassette with a 10000 molecular-weight cut-off (Thermo Fisher Scientific). The samples were dialyzed in 100 mM

potassium phosphate buffer (pH 7.5) at 500 x sample volume. Activity of the αKGDH complex was measured at 30°C in a Hitachi model U-3010 spectrophotometer (Sysmex, Norderstedt, Germany) by monitoring reduction of $NAD^+$ at 340 nm in a 1 mL reaction mixture containing 100 mM phosphate buffer (pH 8.0), 1 mM $MgCl_2$, 0.2 mM thiamine pyrophosphate, 2.5 mM $NAD^+$, 5 mM α-ketoglutaric acid (disodium salt, dehydrate), 2 mM L-cysteine hydrochloride, 0.05% (v/v) Triton X-100, and 20 to 100 µL of cell extract. The reaction was started by addition of 0.15 mM Coenzyme A (trilithium salt). All reagents were purchased from Sigma Aldrich.

**2.9 Purification of the αKGDH complex by size-exclusion chromatography**

Separation of mitochondrial and cytosolic fractions was performed as described above. Cytosolic fractions were centrifuged (4°C, 10 min at 47000 x *g*) and the supernatant was transferred to an Amicon Ultra-15 centrifugal unit (10 kDa cutoff; EMD Millipore Corporation, Billerica, MA) for protein concentration. In this step, the sorbitol-containing buffer (0.65 M sorbitol, 25 mM potassium phosphate buffer (pH 7.5), 1 mM EDTA, and 1 mM $MgCl_2$) used for cellular fractionation was replaced with chromatography buffer containing 100 mM potassium phosphate buffer (pH 7.0), 0.01% sodium azide, 5% glycerol, 0.1 mM ribosylthymine phosphate, and 0.1 mM dithiothreitol. The final volume was 10 mL. A 5 mL aliquot of the sample was applied to a HiPrep 16/60 Sephacryl S-500 HR size-exclusion chromatography column (GE Healthcare, Little Chalfont, Buckinghamshire, United Kingdom) mounted on a Bio-Rad chromatography system. Elution with chromatography buffer was performed at a flow rate of 0.5 mL $min^{-1}$. Elution of proteins was followed using the embedded spectrophotometer set at 280 nm. Fractions of 2 mL each were collected and used to measure αKGDH activity. Protein concentrations of the fractions were determined with the Quick Start Bradford protein assay. Fractions obtained from the chromatographic column were stored at -80°C.

**2.10 Proteomic analysis**

For the proteomic analysis of the size-exclusion chromatography fractions, sample preparation and HPLC-tandem mass spectrometry (MS/MS) were performed as described previously (Kozak et al., 2014; Lu et al., 2007). To analyze the post-translational modifications of the E2 subunit of the αKGDH, strain IMX1401 was grown on SMD supplemented with lipoic acid and 2.5 mg (wet weight) of biomass were harvested and quickly chilled on ice. Protein extraction was performed as previously described (Tong, 2011) with minor modifications. Prior to protein precipitation with trichloroacetic acid (Sigma Aldrich), cells were vortexed in 1.5 mL Eppendorf tubes containing 0.50 g glass beads (450-600 µm; Sigma Aldrich). Three bursts of 30 s were performed and between bursts the sample was chilled on ice for at least 30 s. After washing the sample with acetone, it was dried and resuspended in 50 µL of a 6 M urea, 200 mM ammonium bicarbonate (ABC) solution. The protein concentration was determined using a Nanodrop 2000 (Thermo Scientific) and normalized to 1 µg $mL^{-1}$ in the same solution. An aliquot of 50 µg of protein was further processed by adding 15 µL of a 10 mM dithiothreitol solution in 200 mM ABC. After incubation for 1 h at 37°C, 30 µL of a 20 mM iodoacetamide (Sigma Aldrich) solution in 200 mM ABC was added and the sample was incubated in the dark for 30 min at room temperature. The protein solution was then

diluted with ABC in order to reach a final urea concentration of 0.9 M. To digest the protein, 3 µL of the proteolytic enzyme GluC (Promega) was added to 150 µL of protein solution and digestion was performed overnight at 37°C.

The digested peptides were desalted using an Oasis HLB 96 well plate (Waters, Milford, USA) according to manufacturer protocol. The purified peptide eluate was further dried using a SpeedVac vacuum concentrator. The speed-vac dried peptide fraction was resuspended in an aqueous solution of 3% (v/v) acetonitrile and 0.1% (v/v) formic acid under careful vortexing. An aliquot corresponding to approximately 250 ng of protein digest was analyzed using a one-dimensional shot-gun proteomics approach as described by (Köcher et al., 2012) with minor modifications. Briefly, 1 µL of sample was analyzed using a nano-liquid-chromatography system consisting of an ESAY nano LC 1200, equipped with an Acclaim PepMap RSLC RP C18 separation column (50 µm x 150 mm, 2 µm, 100 Å), and an QE plus Orbitrap mass spectrometer (Thermo Scientific). The flow rate was maintained at 300 nL $min^{-1}$ over a linear gradient from 5% to 30% solvent B (in solvent A) over 90 min, and finally to 75% B over 25 min. Solvent A consisted of an aqueous solution containing 0.1% (v/v) formic acid, while solvent B consisted of 80% (v/v) acetonitrile in water and 0.1% (v/v) formic acid. The Orbitrap was operated in data depended acquisition mode acquiring peptide signals from 400-1250 m/z at 70K resolution, where the top 10 signals were isolated at a window of 2.0 m/z and fragmented using a NCE of 28. The AGC target was set to $5 \cdot 10^4$, at a max IT of 150 ms and 17.5K resolution. In addition, Parallel Reaction Monitoring (PRM) was used to screen for the expected masses of both the unmodified and the lipoylated TDKVVLE peptide. For this fragmentation spectra were continuously acquired at 17.5K resolution, $2 \cdot 10^5$ AGC target, max 100 msec IT, an isolation window of 2.0 Da and 28 NCE. To confirm complete lipoylation, a synthetic, unmodified peptide standard of sequence TDKVVLE was purchased from Genscript (Nanjing, China). A quantity of approximately 500 pg of peptide standard was injected in the LC-MS/MS system to determine retention time (Supplementary Figure 4) and fragmentation profile. Database search and data processing. Raw data were analyzed using PEAKS Studio 8.5 (Bioinformatics Solutions Inc, Waterloo, Canada) allowing 20 ppm parent ion and 0.02 Da fragment mass error tolerance. Search conditions included considering 2 missed cleavages, carbamidomethylation as fixed and K linked lipoyl (+188.03 Da), or carbamidomethylated lipoyl (+304.09 Da) groups as variable modifications. Data were analyzed against the *S. cerevisiae* protein database (Uniprot, June 2018, Tax ID 4932) where the protein sequence of dihydrolipoyllysine-residue succinyltransferase component of 2-oxoglutarate dehydrogenase complex (*sucB*, *E. coli*, P0AFG6) was added manually. Database search included the GPM crap contaminant database (https://www.thegpm.org/crap/) and a decoy fusion for determining false discovery rates. Peptide spectrum matches were filtered against 1% false discovery rate (FDR) and protein identifications with 2 or more unique peptides were considered as significant hit. Data from PRM were analysed manually for expected peptide hits.

## 3. RESULTS

### 3.1 Expression of *E. coli* α-ketoglutarate dehydrogenase genes in *S. cerevisiae* leads to increased cytosolic αKGDH activity.

To introduce a functional α-ketoglutarate dehydrogenase complex (αKGDH) in the yeast cytosol, its three subunits need to be functionally expressed and assembled in this cellular compartment. Mitochondrial targeting of the subunits of the *S. cerevisiae* αKGDH complex is mediated by N-terminal amino-acid sequences (Dudek et al., 2013). Since prokaryotic enzymes are not expected to harbour sequences that target them to yeast mitochondria, the *E. coli* genes encoding the three αKGDH subunits (*Ec_ sucA*, *Ec_sucB* and *Ec_lpd*) were selected for expression in *S. cerevisiae*. Activity of the αKGDH complex is dependent on lipoylation of the E2 subunit (Schonauer et al., 2009). Since the *S. cerevisiae* lipoylation system is confined to the mitochondrial matrix and therefore cannot lipoylate cytosolic proteins (Kozak et al., 2014), the *E. coli* gene encoding lipoate-protein ligase (*Ec_lplA*; P32099) was also expressed. All four genes were expressed from constitutive promoters as a single {αKGDH} cluster. To enable characterization of *in vivo* cytosolic αKGDH activity, the native mitochondrial 5-aminolevulinic acid (ALA) synthase gene *HEM1* was deleted and a cytosolic bacterial ALA synthase from *Rhodobacter sphaeroides* was integrated, resulting in *S. cerevisiae* strain IMX1401.

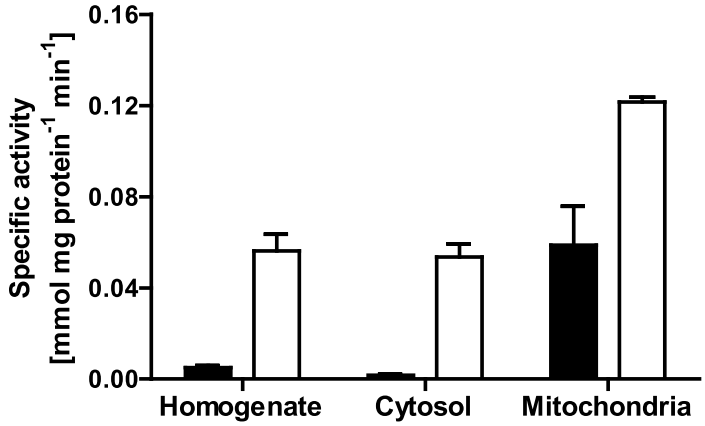


**Figure 1** α-Ketoglutarate dehydrogenase activity in complete homogenate, cytosolic and mitochondrial fractions of the reference strain *S. cerevisiae* CEN.PK113-7D (black bars) and strain IMX1401 (cytosolic αKGDH, *lplA*; white bars). The specific activity was calculated based on the protein content of the respective fraction. Yeast strains were pre-grown in aerobic, glucose-limited cultures supplemented with lipoic acid. Average and standard error were obtained from duplicate fractionation experiments for each strain.

To investigate subcellular localization and activity of the heterologously expressed *E. coli* αKGDH, cells of strain IMX1401 (*hem1Δ*; *sga1Δ::Rs_hemA*; *X2::*{αKGDH}) and of the reference strain CEN.PK113-7D were harvested from steady-state aerobic, glucose-limited

chemostat cultures supplemented with lipoic acid. Cell homogenates of these cultures were separated into cytosolic and mitochondrial fractions. For each fraction, αKGDH enzymatic activity was measured and the specific activity was calculated based on the protein content of the assayed fraction. αKGDH activity in homogenates of the reference strain *S. cerevisiae* CEN.PK113-7D was 0.005 ± 0.002 µmol (mg protein)$^{-1}$ min$^{-1}$. An over 10-fold higher activity (0.056 ± 0.015 µmol (mg protein)$^{-1}$ min$^{-1}$), representing the combined activities of the native and heterologously expressed αKGDH complexes, was observed in the homogenate of strain IMX1401 (Figure 1).

The activity of αKGDH in mitochondrial fractions of the homogenates of strains IMX1401 and CEN.PK113-7D showed a much smaller difference (0.122 ± 0.004 and 0.059 ± 0.034 µmol (mg protein)$^{-1}$ min$^{-1}$, respectively; Figure 1). As anticipated based on the mitochondrial localization of the native *S. cerevisiae* αKGDH complex, only very low αKGDH activities were observed in cytosolic fractions of the reference strain CEN.PK113-7D (0.002 ± 0.001 µmol mg (protein)$^{-1}$ min$^{-1}$). In contrast, activity in cytosolic fractions of strain IMX1401 was close to that of the total homogenates (0.054 ± 0.011 µmol (mg protein)$^{-1}$ min$^{-1}$). These results indicated that *S. cerevisiae* IMX1401 functionally expressed *E. coli* αKGDH in its cytosol.

**3.2 Size-exclusion chromatography and mass spectrometry reveal fully assembled and lipoylated αKGDH subunits in the yeast cytosol**

Proteins in the cytosolic fraction of *S. cerevisiae* IMX1401 (*hem1Δ*; *sga1Δ::Rs_hemA*; *X2::*{αKGDH}) were separated by size-exclusion chromatography. αKGDH activity was first detected after 0.12 column volume changes (29 fractions of 2 mL, column volume of 482.5 mL, Figure 2). Peak αKGDH activity was observed in fraction 32, and no activity was found beyond fraction 37. Fractions 29-31 and 32-34 were pooled (pools 1 and 2, respectively) and subjected to mass spectrometry to determine which native *S. cerevisiae* proteins co-eluted in the fractions with peak αKGDH activity and, thereby, to estimate the size of the heterologously expressed αKGDH complex. Peptides originating from each of the three structural *E. coli* αKGDH subunits were detected in pools 1 and 2, indicating that all three subunits were incorporated in the active complex. The main native *S. cerevisiae* proteins identified in the same fractions were ribosomal proteins (pool 1 and 2) and proteins of the proteasome (pool 2) (Supplementary Materials). These results indicate that the heterologous αKGDH complex is larger than the proteasome (2.4 MDa, as reported by Leggett et al. (2002) and at least as large as the ribosome (3.3 MDa, as reported by Ben-Shem et al. 2010) .

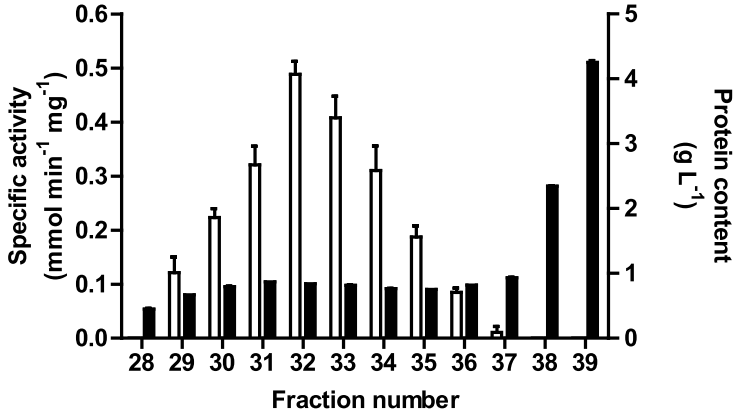


**Figure 2** α-Ketoglutarate dehydrogenase activity (white bars) and protein content (black bars) of the cytosolic fraction of a cell homogenate of *S. cerevisiae* IMX1401 (*hem1Δ, X2::hemA, sga1Δ*::{αKGDH}) in fractions obtained by size-exclusion chromatography. Averages and standard errors were obtained from duplicate measurements performed for the same sample.

To investigate the attachment of the lipoyl residue on E2 subunit of the heterologously expressed αKGDH complex, proteins were extracted from an early exponential phase culture of strain IMX1401 grown aerobically on SMD supplemented with lipoic acid. Peptides generated by digestion with GluC, a proteolytic enzyme that cleaves at the C-terminus of either aspartic or glutamic acid residues (Drapeau et al., 1972), were analysed by LC-MS/MS. Digestion yielded a peptide with the sequence TDKVVLE, which corresponded with the lipoylation target sequence of the *E. coli* E2 subunit. Mass and fragmentation profiles were coherent with a peptide of sequence TDKVVLE having a lipoic acid group attached at the target lysine (K) (Supplementary Figure 3, panel B and C), while no unmodified peptide was found (Supplementary Figure 3, panel A). The analytical capability to detect the unmodified peptide was confirmed by spiking a fully unmodified, synthetic peptide into the yeast lysate digest (Supplementary Figure 4). The synthetic peptide was readily detected, confirming that all lysine residues on the heterologously expressed *E. coli* E2 subunit were indeed correctly lipoylated.



### 3.3 5-aminolevulinic acid auxotrophy of a *hem1Δ* strain is complemented by cytosolic expression of *E. coli* α-ketoglutarate dehydrogenase and *Rhodobacter sphaeroides* aminolevulinic acid synthase.

To test whether expression of *E. coli* αKGDH supports *in vivo* synthesis of succinyl-CoA in the yeast cytosol, its activity was connected to that of a cytosolically expressed heterologous enzyme that uses succinyl-CoA as a substrate. In *S. cerevisiae*, the heme precursor 5-aminolevulinic acid (ALA) is formed from succinyl-CoA and glycine in a condensation reaction catalyzed by the mitochondrial pyridoxal-5'-phosphate-dependent ALA-synthase Hem1 (Gollub et al., 1977; Moretti et al., 1993; Volland and Felix, 1984) (Figure 3). Deletion of *HEM1* renders *S. cerevisiae* auxotrophic for ALA, which can be taken up from the medium by the GABA permease Uga4 (Garcia et al., 1997).

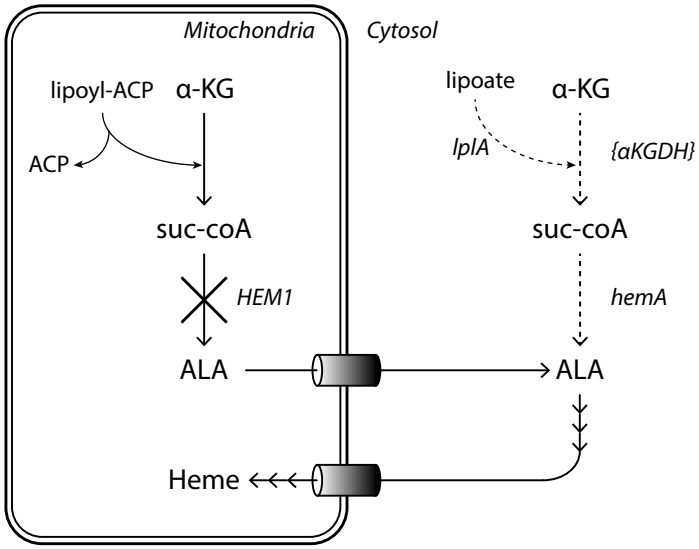


**Figure 3** Biosynthesis of 5-aminolevulinic acid (ALA) in *Saccharomyces cerevisiae*. Solid lines represent the native pathway for ALA biosynthesis. Dashed lines indicate a heterologous ALA synthesis pathway, which is dependent on cytosolic αKGDH activity and able to complement deletion of *hem1*. αKG: α-ketoglutarate; suc-CoA: succinyl-CoA; suc: succinate; ALA: 5-aminolevulinic acid; ACP: acyl carrier protein; {αKGDHm}: native α-ketoglutarate dehydrogenase enzyme complex;{αKGDH}: heterologous α-ketoglutarate dehydrogenase complex

Deletion of *HEM1* in the Cas9-expressing *S. cerevisiae* reference strain IMX585 (Mans et al., 2015) yielded strain IMX1190. The specific growth rate of this *hem1Δ* strain on SMD supplemented with 50 mg $L^{-1}$ aminolevulinic acid was only slightly lower than that of the reference strain IMX585 (0.36 ± 0.00 $h^{-1}$ versus 0.38 ± 0.00 $h^{-1}$). Upon transfer to SMD without ALA supplementation, the *hem1Δ* strain continued to grow for approximately 5 further generations until growth arrest. This residual growth was attributed to carry-over of ALA or derived metabolites with the inoculum. Consistent with this notion, no growth was observed over a period of 200 h after transfer of biomass from this culture to a second culture on SMD without ALA. This observation confirmed the ALA auxotrophy of strain IMX1190 (Supplementary Figure 1).

Integration of a heterologous, bacterial ALA synthase gene (*Rs_hemA*) from *Rhodobacter sphaeroides* in the genome of IMX1190 yielded strain IMX1230 (*hem1Δ, Rs_hemA*). Strain IMX1230 showed the same growth arrest upon ALA depletion as strain IMX1190 (Figure 4). The observation that expression of *Rs_hemA* alone did not restore growth of a *hem1Δ* strain was attributed to the absence of succinyl-CoA, a substrate of the encoded ALA synthase, in the yeast cytosol.

Strain IMX1401 contained a deletion of the native mitochondrial ALA synthase gene *HEM1* and overexpression of a cytosolic bacterial ALA synthase. Therefore, ALA biosynthesis in IMX1401 was dependent on the cytosolic availability of the substrate succinyl-CoA. To

investigate if *in vivo* cytosolic αKGDH activity could indeed support sufficient succinyl-CoA production to enable growth without ALA supplementation, strains IMX1401 (*hem1Δ, Rs_hemA*, {αKGDH}) and IMX1230 (*hem1Δ, Rs_hemA*) were grown in sequential bioreactor batch cultures (Figure 5 and Supplementary Figure 2, respectively). The first bioreactor batch culture was grown on SMD supplemented with ALA to allow for biomass formation. Upon glucose depletion, biomass was harvested, washed three times with sterile water to remove external ALA and used to inoculate duplicate bioreactor cultures on SMD with and without lipoic acid.

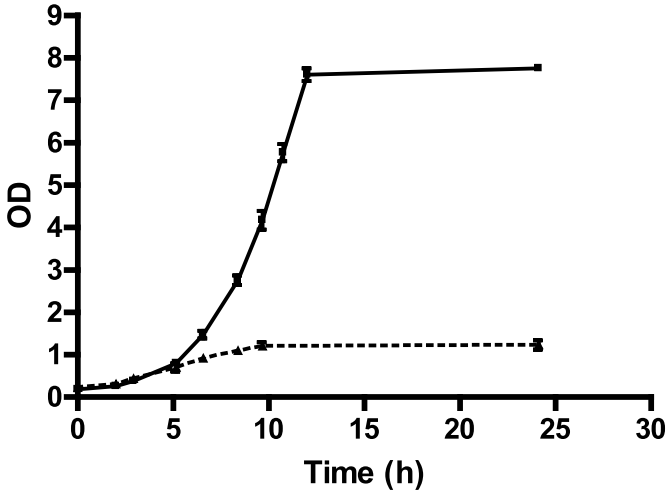


**Figure 4** Growth of *S. cerevisiae* IMX1230 (*hem1Δ, sga1Δ::Rs_hemA*), lacking the native 5-aminolevulinic acid synthase (Hem1) and expressing a heterologous ALA synthase from *Rhodobacter sphaeroides* (HemA). Cells were pre-grown in SMD supplemented with ALA, harvested, washed three times and inoculated in SMD either in the presence (solid line) or in the absence (dotted line) of 5-aminolevulinic acid (ALA). Data are represented as average and standard error of measurements on duplicate growth experiments.

When strain IMX1401 (*hem1Δ*, *Rs_hemA*, {αKGDH}) was transferred to SMD without ALA and lipoic acid, no growth was observed over 40 h (Figure 5, Panel B). In contrast, during four sequential batches of strain IMX1401 on SMD without ALA but with lipoic acid (Figure 5, panel A), its specific growth rate (0.37 ± 0.00 $h^{-1}$, estimated from $CO_2$ production profiles) was almost identical to that of ALA-supplemented cultures (0.38 $h^{-1}$). The requirement of externally added lipoic acid for complementation of the ALA auxotrophy in strain IMX1401 (*hem1Δ, αKGDH, Rs_hemA*), combined with the inability of IMX1230 (*hem1Δ, Rs_hemA*) to grow in the presence of lipoic acid demonstrated *in vivo* αKGDH activity in the yeast cytosol, coupled to a heterologously expressed succinyl-CoA requiring enzyme.

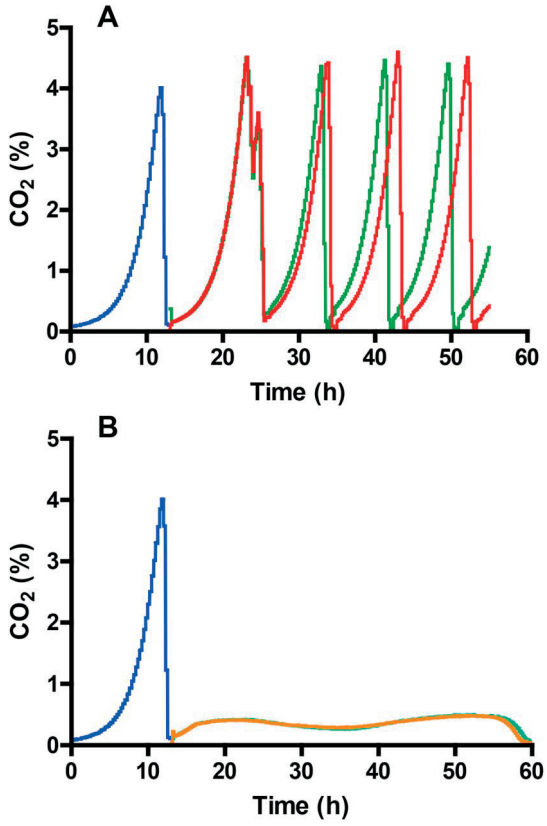


**Figure 5** Sequential bioreactor batch cultures of strain IMX1401 (*hem1Δ, Rs_hemA,* {αKGDH}). Growth was monitored by the $CO_2$ concentration in the exhaust gas of the cultures. Blue lines indicate $CO_2$ profiles of an initial batch culture on SMD supplemented with 50 mg $L^{-1}$ 5–aminolevulinic acid (ALA). Biomass grown in this culture was used as inoculum for subsequent bioreactor experiments without ALA supplementation. Panel A: cultivation on SMD supplemented with 100 µg $L^{-1}$ lipoic acid (red and green lines); Panel B: cultivation on SMD without supplementation (light green and orange lines). Except for the ALA-supplemented culture, duplicate cultures were run for each experimental condition.

## 4. DISCUSSION

This study demonstrates the expression, assembly and *in vivo* activity of a bacterial α-ketoglutarate dehydrogenase complex in the cytosol of *S. cerevisiae*.

To test *in vivo* activity of the heterologous αKGDH complex, we used a strain in which synthesis of 5-aminolevulinic acid, the first committed precursor for heme biosynthesis, depended on cytosolic succinyl-CoA. Heme is required for functionality of the respiratory chain, the biosynthesis of sterols and as a cofactor for methionine biosynthesis. Since, especially during fermentative growth, only minute amounts of heme are required for these roles (Hanna et al., 2016), the tester strain was expected to be very sensitive to

traces of cytosolic succinyl-CoA. The inability of strain IMX1230 (*hem1Δ*; *sga1Δ::Rs_hemA*) to grow without 5-aminolevulinic acid supplementation therefore confirmed that native supply cannot support efficient production of compounds that require cytosolic succinyl-CoA as a precursor. Although presence of cytosolic succinyl-CoA has not been described in *S. cerevisiae*, this compound has been proposed as succinyl donor for protein succinylation, which would require its availability outside of the mitochondria (Weinert et al., 2013; Zhang et al., 2010). The yeast strains described in this study provide an interesting platform for studies into the source of succinyl moieties for protein succinylation in *S. cerevisiae*.

Size-exclusion chromatography (Figure 2) combined with mass spectrometry showed that the heterologously expressed αKGDH co-eluted with *S. cerevisiae* proteasome and ribosome subunits (Supplementary Materials). The *S. cerevisiae* proteasome and ribosome have reported masses of 2.4 MDa and 3.3 MDa, respectively (Leggett et al., 2002; Ben-Shem et al., 2010). Our results are therefore in good agreement with the expected size of a fully assembled *E. coli* αKGDH complex, which has been described as 2.5-2.8 MDa according to Angelides and Hammes (1979) or 4.2 MDa based on the subunit stoichiometry described by Izard et al. (1999).

Expression of the *E. coli* αKGDH in the yeast cytosol provides a cytosolic source of succinyl-CoA, and thereby offers new possibilities for design and construction of yeast cell factories for industrially relevant compounds such as γ-aminobutyric acid, γ-hydroxybutyric acid, 5-aminolevulinic acid and 1,4-butanediol. Complementation of the ALA auxotrophy of an especially designed tester strain provides a proof of principle for succinyl-CoA synthesis in the yeast cytosol. The specific cytosolic αKGDH activity of the engineered strain IMX1401 was 0.056 ± 0.015 μmol (mg protein)$^{-1}$ min$^{-1}$, while the activity of this enzyme in *E. coli* has been reported at 0.03 ± 0.00 μmol (mg protein)$^{-1}$ min$^{-1}$ (Li et al., 2006; Veit et al., 2007). Although the αKGDH activities between the native host and the engineered strain are comparable, further research is needed to assess and if necessary improve *in vivo* capacity of the heterologously expressed αKGDH complex to enable efficient production of succinyl-CoA derived chemicals. Furthermore, while dependency on lipoate supplementation was useful for checking *in vivo* activity of the heterologously expressed αKGDH complex, industrial application can benefit from a published metabolic engineering strategy for lipoic acid synthesis in the cytosol of *S. cerevisiae* (Lian and Zhao, 2016).

Previously, ATP-independent production of cytosolic acetyl-CoA, which is crucial for yeast-based production of a wide range of industrially relevant compounds (de Kok et al., 2012; van Rossum et al., 2016b), has been achieved by cytosolic expression of bacterial pyruvate dehydrogenase complexes, whose size is similar to that of *E. coli* αKGDH (Kozak et al., 2014; Lian and Zhao, 2016). This concept was then used to couple acetyl-CoA synthesis via such a heterologously expressed pyruvate dehydrogenase complex to production of the polyketide tri-acetic acid lactone (Cardenas and Da Silva, 2016). Functional expression of a heterologous cytosolic αKGDH complex could thus represent the first step towards efficient production of succinyl-CoA derived products in yeast.

## 5. FUNDING

This study was supported by the BE-Basic R&D Program, which was granted a FES subsidy from the Dutch Ministry of Economic Affairs, Agriculture and Innovation (EL&I).

## References

Abdou, A. M., Higashiguchi, S., Horie, K., Kim, M., Hatta, H., Yokogoshi, H., 2006. Relaxation and immunity enhancement effects of γ-aminobutyric acid (GABA) administration in humans. BioFactors. 26, 201-208. DOI: https://doi.org/10.1002/biof.5520260305

Angelides, K. J., Hammes, G. G., 1979. Structural and mechanistic studies of the α-ketoglutarate dehydrogenase multienzyme complex from *Escherichia coli*. Biochemistry. 18, 5531-5537. DOI: https://doi.org/10.1021/bi00592a001

Avalos, J. L., Fink, G. R., Stephanopoulos, G., 2013. Compartmentalization of metabolic pathways in yeast mitochondria improves the production of branched-chain alcohols. Nat Biotechnol. 31, 335-41. DOI: https://doi.org/10.1038/nbt.2509

Ben-Shem, A., Jenner, L., Yusupova, G., Yusupov, M., 2010. Crystal structure of the eukaryotic ribosome. Science. 330, 1203-1209. DOI: https://doi.org/10.1126/science.1194294

Bunik, V. I., 2003. 2-Oxo acid dehydrogenase complexes in redox regulation. European Journal of Biochemistry. 270, 1036-1042. DOI: https://doi.org/10.1046/j.1432-1033.2003.03470.x

Cardenas, J., Da Silva, N. A., 2016. Engineering cofactor and transport mechanisms in *Saccharomyces cerevisiae* for enhanced acetyl-CoA and polyketide biosynthesis. Metabolic Engineering. 36, 80-89. DOI: https://doi.org/10.1016/j.ymben.2016.02.009

Chen, W. L. A., Luo, Q., Williams, C. R., Zaikov, V., Compostible films and compostible labels. Vol. WO2015103239A1. Avery Dennison Corporation, 2015.

de Kok, S., Kozak, B. U., Pronk, J. T., van Maris, A. J. A., 2012. Energy coupling in *Saccharomyces cerevisiae*: selected opportunities for metabolic engineering. FEMS Yeast Research. 12, 387-397. DOI: https://doi.org/10.1111/j.1567-1364.2012.00799.x

Dickinson, J. R., Roy, D. J., Dawes, I. W., 1986. A mutation affecting lipoamide dehydrogenase, pyruvate dehydrogenase and 2-oxoglutarate dehydrogenase activities in *Saccharomyces cerevisiae*. Journal. 204, 103-107.

Drapeau, G. R., Boily, Y., Houmard, J., 1972. Purification and properties of an extracellular protease of *Staphylococcus aureus*. Journal. 247, 6720-6726.

Dudek, J., Rehling, P., van der Laan, M., 2013. Mitochondrial protein import: Common principles and physiological networks. Biochimica et biophysica acta. 1833, 274-285. DOI: https://doi.org/10.1016/j.bbamcr.2012.05.028

Ekas, H., Deaner, M., Alper, H. S., 2019. Recent advancements in fungal-derived fuel and chemical production and commercialization. Current Opinion in Biotechnology. 57, 1-9. DOI: https://doi.org/10.1016/j.copbio.2018.08.014

Entian, K.-D., Kötter, P., 2007. 25 Yeast genetic strain and plasmid collections. Methods in Microbiology. 36, 629-666. DOI: https://doi.org/10.1016/S0580-9517(06)36025-4

Galanie, S., Thodey, K., Trenchard, I. J., Filsinger Interrante, M., Smolke, C. D., 2015. Complete biosynthesis of opioids in yeast. Science. 349, 1095-1100. DOI: https://doi.org/10.1126/science.aac9373

Garcia, S. C., Moretti, M. B., Ramos, E., Batlle, A., 1997. Carbon and nitrogen sources regulate δ-aminolevulinic acid and γ-aminobutyric acid transport in *Saccharomyces cerevisiae*. The International Journal of Biochemistry & Cell Biology. 29, 1097-1101. DOI: 10.1016/s1357-2725(97)00047-2

Gietz, R. D., Woods, R. A., 2002. Transformation of yeast by lithium acetate/single-stranded carrier DNA/polyethylene glycol method. Methods in Enzymology. 350, 87-96. DOI: https://doi.org/10.1016/s0076-6879(02)50957-5

Gollub, E. G., Liu, K., Dayan, J., Adlersberg, M., Sprinson, D., 1977. Yeast mutants deficient in heme biosynthesis and a heme mutant additionally blocked in cyclization of 2,3-oxidosqualene. Journal. 252, 2846-2854.

Gorter de Vries, A. R., Couwenberg, L. G., van den Broek, M., de la Torre Cortés, P., ter Horst, J., Pronk, J. T., Daran, J.-M. G., 2018. Allele-specific genome editing using CRISPR–Cas9 is associated with loss of heterozygosity in diploid yeast. Nucleic Acids Research. 47, 1362-1372. DOI: https://doi.org/10.1093/nar/gky1216

Graham, L. D., Perham, R. N., 1990. Interactions of lipoyl domains with the E1p subunits of the pyruvate dehydrogenase multienzyme complex from *Escherichia coli*. FEBS Letters. 262, 241-244. DOI: https://doi.org/10.1016/0014-5793(90)80200-3

Hanna, D. A., Harvey, R. M., Martinez-Guzman, O., Yuan, X., Chandrasekharan, B., Raju, G., Outten, F. W., Hamza, I., Reddi, A. R., 2016. Heme dynamics and trafficking factors revealed by genetically encoded fluorescent heme sensors. Proceedings of the National Academy of Sciences. 113, 7539-7544. DOI: https://doi.org/10.1073/pnas.1523802113

Hoffman, M., Góra, M., Rytka, J., 2003. Identification of rate-limiting steps in yeast heme biosynthesis. Biochemical and Biophysical Research Communications. 310, 1247-1253. DOI: https://doi.org/10.1016/j.bbrc.2003.09.151

Hohmann, S., Meacock, P. A., 1998. Thiamin metabolism and thiamin diphosphate-dependent enzymes in the yeast *Saccharomyces cerevisiae*: genetic regulation. Biochimica et Biophysica Acta - Protein Structure and Molecular Enzymology. 1385, 201-219. DOI: https://doi.org/10.1016/S0167-4838(98)00069-7

Izard, T., Ævarsson, A., Allen, M. D., Westphal, A. H., Perham, R. N., de Kok, A., Hol, W. G., 1999. Principles of quasi-equivalence and Euclidean geometry govern the assembly of cubic and dodecahedral cores of pyruvate dehydrogenase complexes. Proceedings of the National Academy of Sciences. 96, 1240-1245. DOI: https://doi.org/10.1073/pnas.96.4.1240

Jansen, M. L. A., Heijen, J. J., Verwaal, R., Process for preparing dicarboxylic acids employing fungal cells. DSM IP Assets BV, 2017.

Köcher, T., Pichler, P., Swart, R., Mechtler, K., 2012. Analysis of protein mixtures from whole-cell extracts by single-run nanoLC-MS/MS using ultralong gradients. Nature Protocols. 7, 882-890. DOI: https://doi.org/10.1038/nprot.2012.036

Kozak, B. U., van Rossum, H. M., Luttik, M. A., Akeroyd, M., Benjamin, K. R., Wu, L., de Vries, S., Daran, J. M., Pronk, J. T., van Maris, A. J., 2014. Engineering acetyl coenzyme A supply: functional expression of a bacterial pyruvate dehydrogenase complex in the cytosol of *Saccharomyces cerevisiae*. mBio. 5, e01696-14. DOI: https://doi.org/10.1128/mBio.01696-14

Kuijpers, N. G., Solis-Escalante, D., Bosman, L., van den Broek, M., Pronk, J. T., Daran, J.-M., Daran-Lapujade, P., 2013. A versatile, efficient strategy for assembly of multi-fragment expression vectors in *Saccharomyces cerevisiae* using 60 bp synthetic recombination sequences. Microbial Cell Factories. 12. DOI: https://doi.org/10.1186/1475-2859-12-47

Leggett, D. S., Hanna, J., Borodovsky, A., Crosas, B., Schmidt, M., Baker, R. T., Walz, T., Ploegh, H., Finley, D., 2002. Multiple associated proteins regulate proteasome structure and function. Molecular Cell. 10, 495-507. DOI: https://doi.org/10.1016/S1097-2765(02)00638-X

Lian, J., Zhao, H., 2016. Functional reconstitution of a pyruvate dehydrogenase in the cytosol of *Saccharomyces cerevisiae* through lipoylation machinery engineering. ACS synthetic biology. 5, 689-697. DOI: https://doi.org/10.1021/acssynbio.6b00019

Lõoke, M., Kristjuhan, K., Kristjuhan, A., 2011. Extraction of genomic DNA from yeasts for PCR-based applications. Biotechniques. 50, 325-328. DOI: https://doi.org/10.2144/000113672

Luttik, M. A. H., Overkamp, K. M., Kötter, P., de Vries, S., van Dijken, J. P., Pronk, J. T., 1998. The *Saccharomyces cerevisiae NDE1* and *NDE2* genes encode separate mitochondrial NADH dehydrogenases catalyzing the oxidation of cytosolic NADH. Journal of Biological Chemistry. 273, 24529-24534. DOI: https://doi.org/10.1074/jbc.273.38.24529

Mans, R., van Rossum, H. M., Wijsman, M., Backx, A., Kuijpers, N. G., van den Broek, M., Daran-Lapujade, P., Pronk, J. T., van Maris, A. J., Daran, J. M., 2015. CRISPR/Cas9: a molecular Swiss army knife for simultaneous introduction of multiple genetic modifications in *Saccharomyces cerevisiae*. FEMS Yeast Research. 15. DOI: https://doi.org/10.1093/femsyr/fov004

Martin, D. P., Williams, S. F., 2003. Medical applications of poly-4-hydroxybutyrate: a strong flexible absorbable biomaterial. Biochemical Engineering Journal. 16, 97-105. DOI: https://doi.org/10.1016/S1369-703X(03)00040-8

Mikkelsen, M. D., Buron, L. D., Salomonsen, B., Olsen, C. E., Hansen, B. G., Mortensen, U. H., Halkier, B. A., 2012. Microbial production of indolylglucosinolate through engineering of a multi-gene pathway in a versatile yeast expression platform. Metabolic Engineering. 14, 104-111. DOI: https://doi.org/10.1016/j.ymben.2012.01.006

Moretti, M. B., García, S. C., Stella, C., Ramos, E., Batlle, A. M. d. C., 1993. δ-Aminolevulinic acid transport in *Saccharomyces cerevisiae*. International Journal of Biochemistry. 25, 1917-1924. DOI: https://doi.org/10.1016/0020-711X(88)90325-4

Morris, T. W., Reed, K. E., Cronan, J., 1995. Lipoic acid metabolism in *Escherichia coli*: the *lplA* and *lipB* genes define redundant pathways for ligation of lipoyl groups to apoprotein. Journal of Bacteriology. 177, 1-10. DOI: https://doi.org/10.1128/jb.177.1.1-10.1995

Pettit, F. H., Reed, L. J., 1967. α-keto acid dehydrogenase complexes. 8. Comparison of dihydrolipoyl dehydrogenases from pyruvate and α-ketoglutarate dehydrogenase complexes of *Escherichia coli*. Proceedings of the National Academy of Sciences of the United States of America. 58, 1126-1130. DOI: https://doi.org/10.1073/pnas.58.3.1126

Qiu, B., Xia, B., Zhou, Q., Lu, Y., He, M., Hasegawa, K., Ma, Z., Zhang, F., Gu, L., Mao, Q., 2018. Succinate-acetate permease from *Citrobacter koseri* is an anion channel that unidirectionally translocates acetate. Cell research. 28, 644-654. DOI: https://doi.org/10.1038/s41422-018-0032-8

Raab, D., Graf, M., Notka, F., Schödl, T., Wagner, R., 2010. The GeneOptimizer Algorithm: using a sliding window approach to cope with the vast sequence space in multiparameter DNA sequence optimization. Systems and synthetic biology. 4, 215-225. DOI: https://doi.org/10.1007/s11693-010-9062-3

Repetto, B., Tzagoloff, A., 1989. Structure and regulation of *KGD1*, the structural gene for yeast alpha-ketoglutarate dehydrogenase. Journal. 9, 2695-2705.

Saito, Y., Nakamura, S., Hiramitsu, M., Doi, Y., 1996. Microbial synthesis and properties of poly (3-hydroxybutyrate-co-4-hydroxybutyrate). Polymer International. 39, 169-174. DOI: https://doi.org/10.1002/(SICI)1097-0126(199603)39:3<169::AID-PI453>3.0.CO;2-Z

Schonauer, M. S., Kastaniotis, A. J., Kursu, V. S., Hiltunen, J. K., Dieckmann, C. L., 2009. Lipoic acid synthesis and attachment in yeast mitochondria. Journal of Biological Chemistry. 284, 23234-23242. DOI: https://doi.org/10.1074/jbc.M109.015594

Solis-Escalante, D., Kuijpers, N. G., Bongaerts, N., Bolat, I., Bosman, L., Pronk, J. T., Daran, J. M., Daran-Lapujade, P., 2013. *amdSYM*, a new dominant recyclable marker cassette for *Saccharomyces cerevisiae*. FEMS Yeast Research. 13, 126-139. DOI: https://doi.org/10.1111/1567-1364.12024

Tong, Z., 2011. Protocol for whole cell lysis of yeast. Bio-101. 1, e14. DOI: https://doi.org/10.21769/BioProtoc.14

van Rossum, H. M., Kozak, B. U., Niemeijer, M. S., Duine, H. J., Luttik, M. A., Boer, V. M., Kötter, P., Daran, J.-M. G., van Maris, A. J., Pronk, J. T., 2016a. Alternative reactions at the interface of glycolysis and citric acid cycle in *Saccharomyces cerevisiae*. FEMS Yeast research. 16. DOI: https://doi.org/10.1093/femsyr/fow017

van Rossum, H. M., Kozak, B. U., Pronk, J. T., van Maris, A. J. A., 2016b. Engineering cytosolic acetyl-coenzyme A supply in *Saccharomyces cerevisiae*: Pathway stoichiometry, free-energy conservation and redox-cofactor balancing. Metabolic Engineering. 36, 99-115. DOI: https://doi.org/10.1016/j.ymben.2016.03.006

Veit, A., Polen, T., Wendisch, V. F., 2007. Global gene expression analysis of glucose overflow metabolism in *Escherichia coli* and reduction of aerobic acetate formation. Appl Microbiol Biotechnol. 74, 406-21. DOI: 10.1007/s00253-006-0680-3

Verduyn, C., Postma, E., Scheffers, W. A., Van Dijken, J. P., 1992. Effect of benzoic acid on metabolic fluxes in yeasts: A continuous-culture study on the regulation of respiration and alcoholic fermentation. Yeast. 8, 501-517. DOI: https://doi.org/10.1002/yea.320080703

Weinert, Brian T., Schölz, C., Wagner, Sebastian A., Iesmantavicius, V., Su, D., Daniel, Jeremy A., Choudhary, C., 2013. Lysine Succinylation Is a Frequently Occurring Modification in Prokaryotes and Eukaryotes and Extensively Overlaps with Acetylation. Cell Reports. 4, 842-851. DOI: https://doi.org/10.1016/j.celrep.2013.07.024

Yim, H., Haselbeck, R., Niu, W., Pujol-Baxley, C., Burgard, A., Boldt, J., Khandurina, J., Trawick, J. D., Osterhout, R. E., Stephen, R., Estadilla, J., Teisan, S., Schreyer, H. B., Andrae, S., Yang, T. H., Lee, S. Y., Burk, M. J., Van Dien, S., 2011. Metabolic engineering of *Escherichia coli* for direct production of 1,4-butanediol. Nature Chemical Biology. 7, 445-452. DOI: https://doi.org/10.1038/nchembio.580

Zhang, Z., Tan, M., Xie, Z., Dai, L., Chen, Y., Zhao, Y., 2010. Identification of lysine succinylation as a new post-translational modification. Nature Chemical Biology. 7, 58. DOI: https://doi.org/10.1038/nchembio.495

## Supplementary data

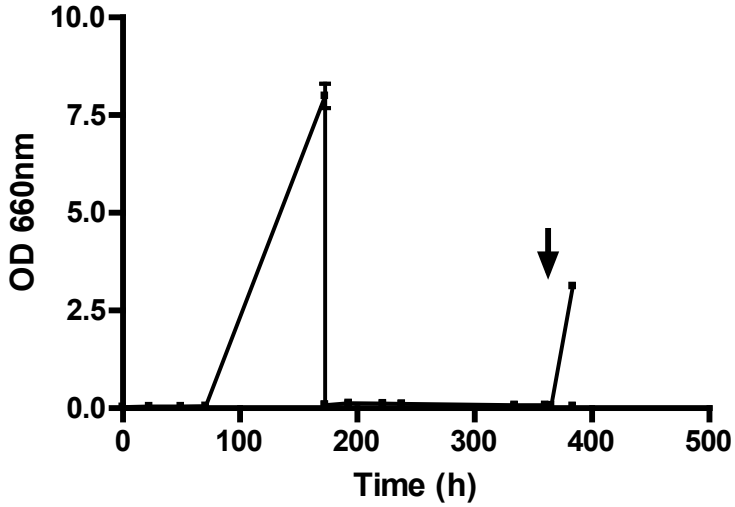


**Supplementary Figure 1 (S1):** growth profile in shake flask cultivation of IMX1190 (*hem1Δ*). Cells were pre-grown in SMD supplemented with 50 µg $mL^{-1}$ 5-aminolevulinic acid (not shown), washed and inoculated in SMD without supplementation. Growth for 5 to 10 generation occurred between timepoints 70h and 172h. At this latter time point, the cells were washed and inoculated in a new flasks containing SMD without supplementation. No growth was observed for 200 hours. To check the viability of the cells, one of the cultures was spiked with aminolevulinic acid (arrow) at a final concentration of 50 µg $mL^{-1}$. Growth observed after aminolevulinic acid addition indicated that cells were still viable.

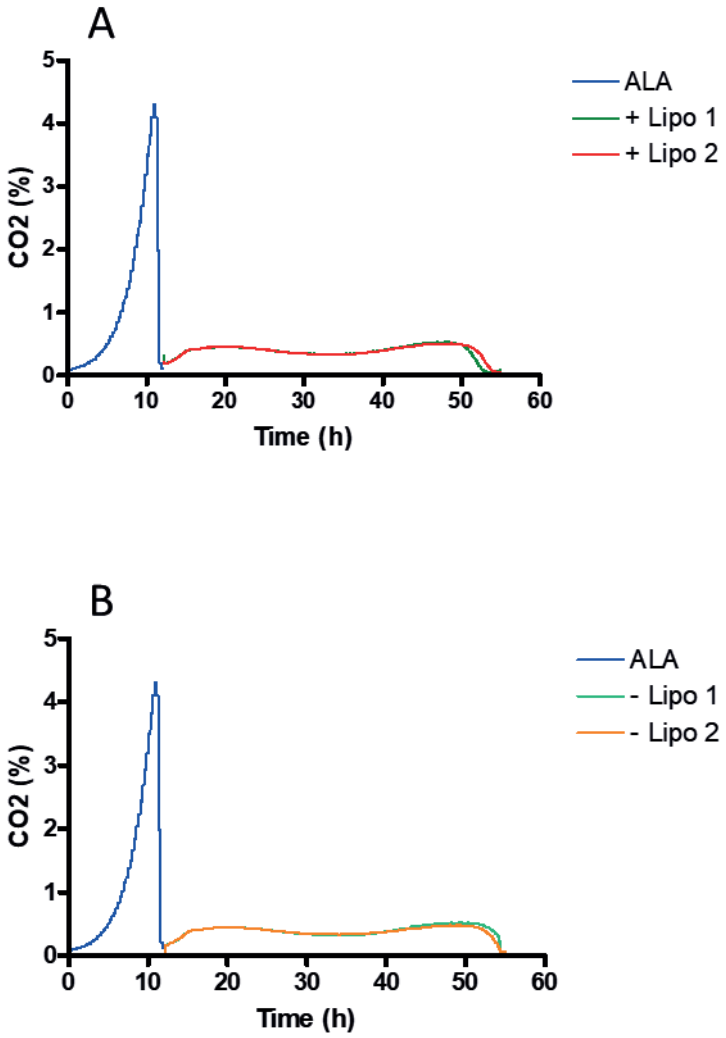


**Supplementary Figure 2 (S2):** growth profiles of IMX1230 in an SBR setup. The strain was inoculated in a single bioreactor with SMD 2% supplemented with 5-aminolevulinic acid (blue line in both graphs). Upon glucose depletion, the biomass was harvested and washed three times with sterile water. Subsequently it was used to inoculate four different bioreactors: two supplemented with lipoic acid (graph A, green and orange line) and two without supplementation (graph B, green and orange line). Growth was determined via readout of the $CO_2$ concentration in the offgas.

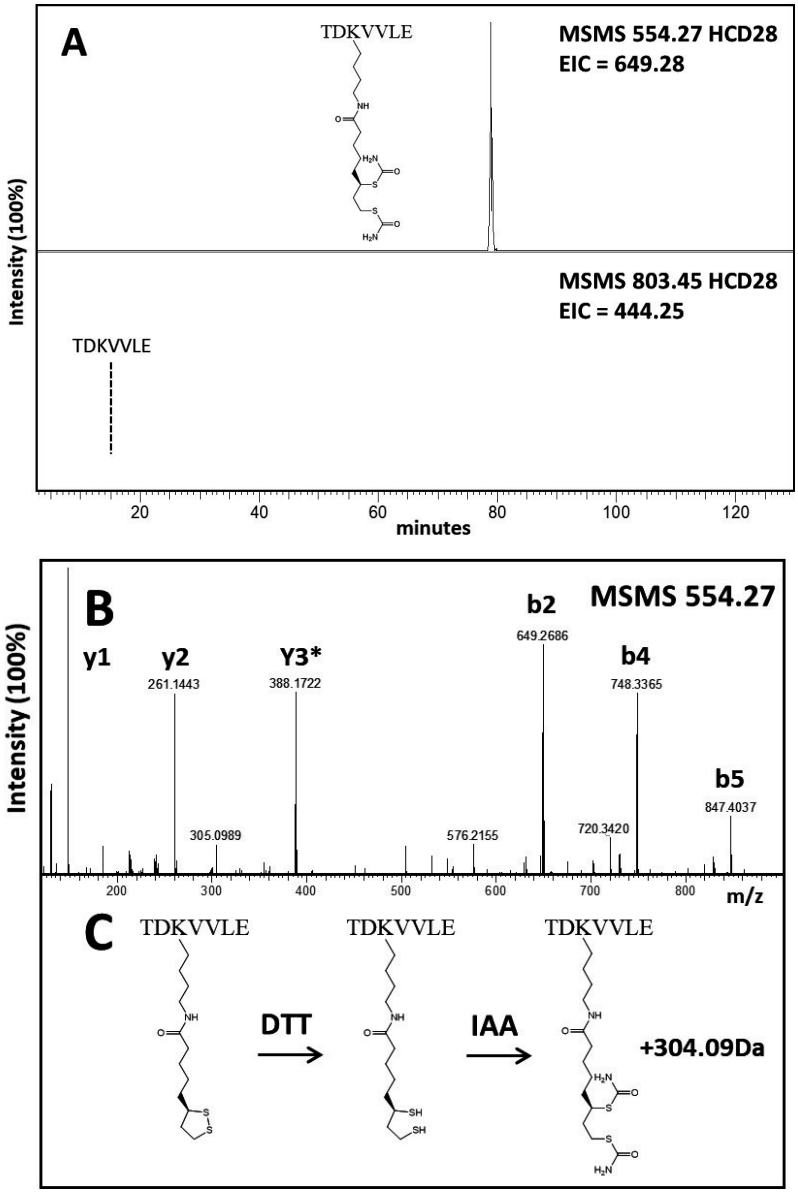


**Supplementary Figure 3 (S3)** Determination of the post translational mofidications on the subunit E2 of the *E. coli* α-ketoglutarate dehydrogenase complex following proteolytic digestion with GluC.
**Panel A:** Extracted ion chromatograms showing a strong signal for the lipoylated target peptide TDKVVLE. No signal was observed for the unmodified variant (lower trace). A synthetic, unmodified peptide was used as a standard to determine retention time of unmodified variant.
**Panel B.** HCD fragmentation spectrum of the lipoylated peptide TDKVVLE. Both, y and b series of ions indicate K as lipoylation site (+304Da).
**Panel C.** The dithiolane group of lipoic acid undergoes reduction and alkylation during sample preparation of the protein extract. This provides a final mass addition of 304.09 Da over the native peptide.
Abbreviations: DTT: Dithiothreitol; IAA: Iodoacetamide; HCD: High Energy collision Dissociation.

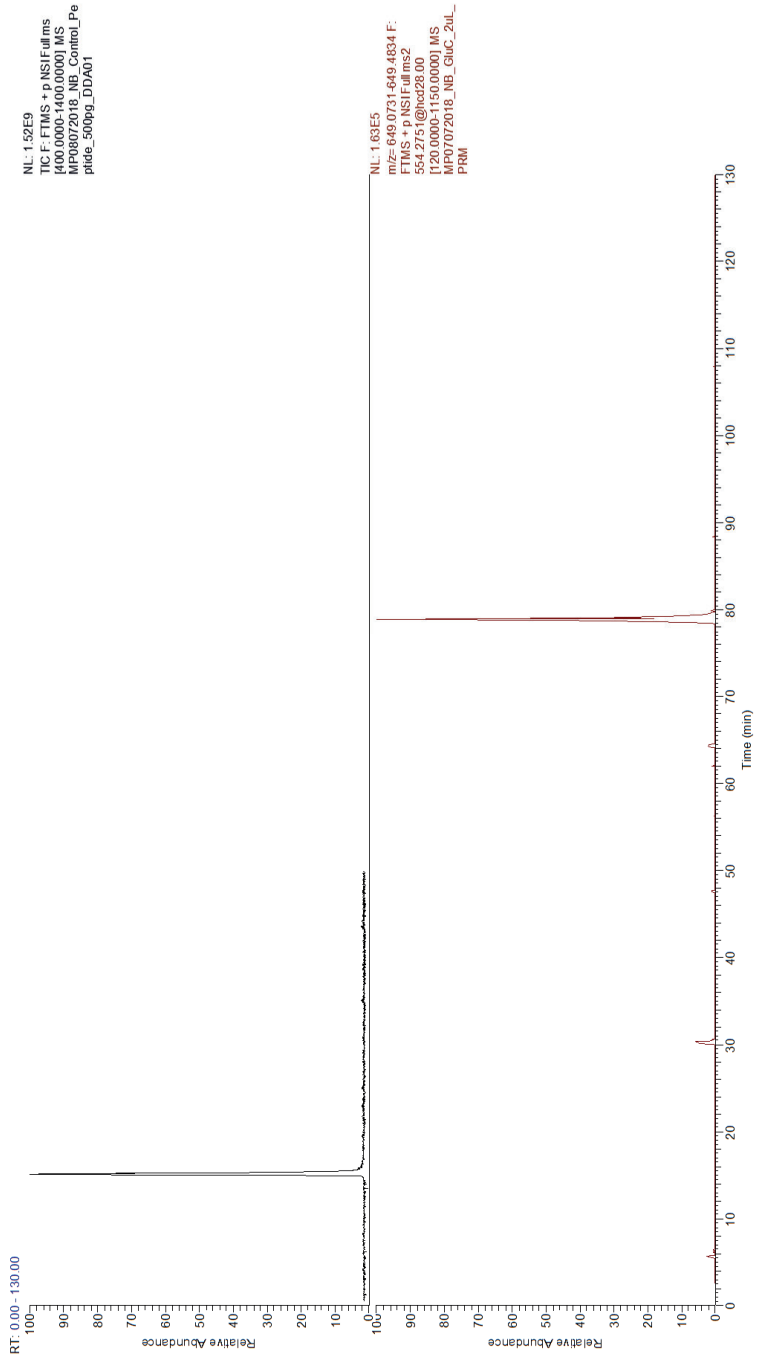


**Supplementary Figure 4 (SF4).** Extracted ion chromatogram comparing the retention times of an unmodified TDKVVLE peptide standard (top graph) against a digested protein sample of strain IMX1401 (*hem1Δ, sga1::Rs_hemA, X2::*{αKGDH}), in which the lysine residue is lipoylated (bottom graph).

**Supplementary Table 1:** Primers used in this study.

| Name | Number | Sequence | Purpose |
|---|---|---|---|
| bkdA_#_pTPI1 | 10540 | TGTTTGTATTCTTTTCTTGCTTAAATCTATAACTACAAAAAACACATACATAAACTAAAAGCGATACCCTGCGATCTTC | Construction of pUD614 |
| bkdA_*_tTEF1 | 10541 | AACTAATAGATAAGATTTAAATATAAAAGATATGCAACTAGAAAAGTCTTATCAATCTCCCGCGCAGATTAGCGAAGC | |
| Sc_TPI1_P_RV | 6486 | TTTTAGTTTATGTATGTGTTTTTTGTAGTTATAGATTTAAGCAAG | |
| tTEF1_fw | 10562 | GGAGATTGATAAGACTTTTCTAG | |
| bkdB_#_pTDH3 | 10542 | TTTTTTTAGTTTTAAAACACCAAGAACTTAGTTTCGAATAAACACACATAAACAAACAAAGCGATACCCTGCGATCTTC | Construction of pUD616 |
| bkdB_*_tCYC1 | 10543 | GCGTGAATGTAAGCGTGACATAACTAATTACATGATATCGACAAAGGAAAAGGGGCCTGTCGCGCAGATTAGCGAAGC | |
| tCYC1 fw | 3628 | ACAGGCCCCTTTTCCTTTG | |
| Sc_TDH3_P_FW | 6494 | TTTGTTTGTTTATGTGTGTTTATTCGAAACTAAG | |
| bkdC_#_pADH1 | 10544 | TTCTTTTTCTGCACAATATTTCAAGCTATACCAAGCATACAATCAACTATCTCATATACAGCGATACCCTGCGATCTTC | Construction of pUD618 |
| bkdC_*_tPGI1 | 10545 | GTATCTTTGCTTATAATATAGCTTTAATGTTCTTTAGGTATATATTTAAGAGCGATTTGTCGCGCAGATTAGCGAAGC | |
| PGI1t-fw | 4671 | ACAAATCGCTCTTAAATATATACCTAAAGAAC | |
| Sc_ADH1_P_FW | 6221 | TGTATATGAGATAGTTGATTGTATGCTTGGTATAG | |
| lpd_co_tag_# | 11303 | GCGATACCCTGCGATCTTCATGTCTACTGAAATCAAGACTCAAG | Construction of pUD625 |
| lpd_co_tag_* | 11304 | CGCGCAGATTAGCGAAGCTTACTTCTTCTTAGCCTTTGGGTTTGG | |
| tag_*_ol_tADH1 | 11219 | TACACTTATTTTTTTTATAACTTATTTAATAATAAAAATCATAAATCATAAGAAATTCGCCGCGCAGATTAGCGAAGC | |
| hemA_#_pTEF1 | 10561 | TTTTTTTACTTCTTGCTCATTAGAAAGAAAGCATAGCAATCTAATCTAAGTTTTAATTACGCGATACCCTGCGATCTTC | |
| tADH1 fw | 3903 | GCGAATTTCTTATGATTTATGATTTTTATTATTAAATAAG | |
| pTEF1 rv | 3904 | GTAATTAAAACTTAGATTAGATTGCTATGCTTTC | |
| pTEF1 rv | 3904 | GTAATTAAAACTTAGATTAGATTGCTATGCTTTC | Construction of pUD623 |
| tENO2_fw | 10563 | GGATCCTAACTCGAGAGTG | |
| hemA_*_tENO2 | 10560 | GAAAAAATAAGCAGAAAAGACTAATAATTCTTAGTTAAAAGCACTCTCGAGTTAGGATCCCGCGCAGATTAGCGAAGC | |
| hemA_#_pTEF1 | 10561 | TTTTTTTACTTCTTGCTCATTAGAAAGAAAGCATAGCAATCTAATCTAAGTTTTAATTACGCGATACCCTGCGATCTTC | |
| pCAS9 fw | 5792 | GTTTTAGAGCTAGAAATAGCAAGTTAAAATAAG | Construction of pUDR573 |
| stRNA_426_rv | 5980 | CGACCGAGTTGCTCTTG | |
| gRNA_426_fw | 5979 | TATTGACGCCGGGCAAGAGC | |
| RV-X-2_gRNA | 7374 | GTTGATAACGGACTAGCCTTATTTTAACTTGCTATTTCTAGCTCTAAAACCTACTCTCTTCCTAGTCGCCGAT-CATTTATCTTTCACTGCGGAGAAGTTTCGAACGCCGAAACATGCGCA | |

| Name | Number | Sequence | Purpose |
|---|---|---|---|
| C_FW_E3 | 5652 | AAGCTTACGTCTCACGGATCG | Construction of the αKGDH integration cassettes |
| D_RV_E3 | 5653 | AAGCTTAATCACTCTCCATACAGGG | |
| D_FW_E1a | 5654 | GAATTCACGCATCTACGACTG | |
| Fus Tag C rv | 3277 | CTAGCGTGTCCTCGCATAGTTCTTAGATTG | |
| Fus Tag J rv | 3284 | CGACGAGATGCTCAGACTATGTGTTC | |
| Fus Tag J fw | 3285 | GGCCGTCATATACGCGAAGATGTC | |
| X2 - tPGI1 | 8645 | TCACAGAGGGATCCCGTTACCCATCTATGCTGAAGATTTATCATACTATTCCTCCGCTCGTTAATTTTTAAAATTTTTACTTTTCGCG | |
| X2 - tTEF1 | 8646 | GTCATAACTCAATTTGCCTATTTCTTACGGCTTCTCATAAAACGTCCCACACTATTCAGGGGAGGCACTATTACTGATGTG | |
| hem1_gRNA_fw | 10534 | TGCGCATGTTTCGGCGTTCGAAACTTCTCCGCAGTGAAAGATAAATGATCCGTCATTAGTTAAAGATAGTGTTTTA-GAGCTAGAAATAGCAAGTTAAAATAAGGCTAGTCCGTTATCAAC | Construction of pUDR263 |
| hem1_gRNA_rv | 10535 | GTTGATAACGGACTAGCCTTATTTTAACTTGCTATTTCTAGCTCTAAAACACTATCTTTAACTAATGACGGAT-CATTTATCTTTCACTGCGGAGAAGTTTCGAACGCCGAAACATGCGCA | |
| p426 CRISP rv | 6005 | GATCATTTATCTTTCACTGCGGAGAAG | |
| p426 CRISP fw | 6006 | GTTTTAGAGCTAGAAATAGCAAGTTAAAATAAGGCTAGTC | |
| hem1_repair_fw | 10536 | CTAATAGAGCTAGTTGTTGTCCCTCAATAATCATAACAGTACTTAGGTTTTTTTTTCAGTAACAACCAATATATGCATGGGCT-GAGATAGAGGTACAAGGAATTTGTAAATCAGTAAAAA | hem1 repair fragment |
| hem1_repair_rv | 10537 | TTTTTACTGATTTACAAATTCCTTGTACCTCTATCTCAGCCCATGCATATATTGGTTGTTACTGAAAAAAAAACCTAAGTACTGT-TATGATTATTGAGGGACAACAACTAGCTCTATTAG | |
| hem1_dg_fwd | 10538 | TGCTCTGCTGTCTCTCAACC | Diagnostic hem1 |
| hem1_dg_rv | 10539 | CCTGTGTCTTCTACTGCCGG | |
| SGA1 KO ctrl FW | 7860 | GGCTCTGGATCCGTTATCTGTTC | Diagnostic sga1 |
| SGA1 KO ctrl RV | 7861 | TGCAAACGTGGTTGGGCTGG | |
| Kgd1_dg_fw | 10532 | CTTCGACCGTTTGCGATTCC | Diagnostic kgd1 |
| Kgd1_dg_rv | 10533 | CCACCGGATGAGGACAAGAG | |
| FW_x-2_outside | 7376 | GGTCTAGGCCTGCATAATCG | Diagnostic X-2 locus |
| RV_X-2_outside | 7377 | TGCGGCATCATGTCTACTTG | |

| Name | Number | Sequence | Purpose |
|---|---|---|---|
| Fus tag C rv | 3277 | CTAGCGTGTCCTCGCATAGTTCTTAGATTG | Diagnostic construction αKGDH |
| TPIp_control_fw | 3515 | CTGACAGGTGGTTTGTTACG | |
| PFL-plasmides p2 | 5387 | CTTTGGCTCGGCTGCTGTAAC | |
| Sc_TPI1_P_RV | 6486 | TTTTAGTTTATGTATGTGTTTTTTGTAGTTATAGATTTAAGCAAG | |
| VPR_seq_fwd | 6715 | CGGTAGGTATTGATTGTAATTC | |
| YAT2_2 | 7496 | CAGCTCTGGAACAACGACATCTG | |
| FW_#_seq | 7554 | GCGATACCCTGCGATCTTC | |
| RV_*_seq | 7555 | CGCGCAGATTAGCGAAGC | |
| ScCYCt_ver_rv | 11200 | ATGTTACATGCGTACACGCG | |
| sucA_co_FW_1 | 11253 | TGAAGTTGGGTGAACTGTTG | GeneStrings Sequencing primers |
| sucA_co_FW_2 | 11254 | GGTTTCACCACGTCTAATCC | |
| sucA_co_fw_3 | 11255 | ACCAGTCTAATGGTTCTAC | |
| sucA_co_FW_4 | 11256 | ATAAGGCTATGCAAGAAGTC | |
| sucA_co_RV_1 | 11257 | AGCGCACAACTGCAAGTATC | |
| sucA_co_RV_2 | 11258 | ACCAGCATCCAAAGCATCTC | |
| sucA_co_RV_3 | 11259 | TGTGGCTTCTTACCCAAGAC | |
| sucB_co_FW_1 | 11260 | GCCTCTGCTATCAAAGGTACTG | |
| sucB_co_RV_1 | 11261 | ACCGTATTGCTTTCTCAAGTC | |
| sucA_co_dg_RV | 11268 | TCTGGCTTAACACCAGTACC | |

# 4.

# Evolutionary engineering for lactic acid uptake reveals key amino acid residues involved in substrate specificity of *Saccharomyces cerevisiae* carboxylic acid transporters

Nicolò Baldi[1]*,Sophie de Valk[1]*, Maria Sousa-Silva[2,3], Margarida Casal[2,3], Isabel Soares-Silva[2,3] & Robert Mans[1]

[1]Department of Biotechnology, Delft University of Technology, Delft, The Netherlands
[2]Centre of Molecular and Environmental Biology (CBMA), University of Minho, Campus de Gualtar, Braga, Portugal
[3]Institute of Science and Innovation for Bio-Sustainability (IB-S), University of Minho, Campus de Gualtar, Braga, Portugal

*Shared-first authorship
Corresponding author: Robert Mans, r.mans@tudelft.nl

Essentially as published in **FEMS Yeast Research**

## ABSTRACT

Lactic acid is one of the most commonly produced organic acids, with uses in medicine, polymer chemistry and the food industry. Although the pathways connecting this organic acid to the central carbon metabolism are well known, its export from microbial cells remains elusive. In *Saccharomyces cerevisiae*, adaptive laboratory evolution of a strain lacking *JEN1*, known to mediate lactic acid uptake, previously led to the identification of a gene involved in acetate transport (*ADY2*), which was also able to transport lactate. In this study, selection for growth on lactic acid of a strain lacking both these transporters lead to the identification of two genes, *ATO2* and *ATO3*, involved in lactate import. In a *jen1Δ*, *ady2Δ*, *ato2Δ* and *ato3Δ* strain background, the overexpression of *JEN1* and *ADY2* allowed growth on lactic acid, as previously reported. For *ATO2* and *ATO3*, growth under these conditions was observed only when the mutated alleles of these genes were overexpressed. The mutations in *ADY2*, *ATO2* and *ATO3* that allow for efficient transport of lactic acid often occur in one of three amino acid residues that comprise the hydrophobic constriction of the anion channel. We propose that an increased size of the constriction present in these transporters may allow facilitated diffusion of lactic acid.

## 1. INTRODUCTION

Carboxylic acids are widely applied as platform molecules in the chemical, pharmaceutical, food and beverage industries. Some organic acids, like succinic and lactic acid, are currently produced on industrial scale using biotechnological processes (Abdel-Rahman et al., 2013; Jansen et al., 2017; Verwaal et al., 2007). Advantages of bioprocesses are their potential sustainability compared to their petrochemical counterparts and, in the case of chiral compounds, their ability to selectively produce one of the enantiomers. The latter is of importance for the production of biodegradable polymers, which requires the precursors to be optically pure (Borodina and Nielsen, 2014). One of these optically active molecules is lactic acid, which is used as a preservative in the dairy industry and as precursor for bioplastic formation. The demand for lactic acid was 1.220.000 tons in 2016 and is expected to further increase by 16.2% by 2025 (Singhvi et al., 2018). At present, lactic acid is mostly produced by prokaryotic hosts (reviewed by Es et al. (2018) and McKinlay et al. (2007)), with titers reaching upwards of 182 g $L^{-1}$ in fed-batch cultures (Subramanian et al., 2015). The limited tolerance of these hosts to low pH implicates that neutralizing agents must be added during microbial fermentation under industrial conditions. Subsequent retrieval of the undissociated acid requires acidification of the broth, with concomitant production of gypsum, resulting in additional costs in downstream processing (Lopez-Garzon and Straathof, 2014).

Despite exhibiting the highest growth rate at pH 5.0-5.5 (Verduyn et al., 1990), the yeast *Saccharomyces cerevisiae* is known for its tolerance to low pH, and could therefore be an interesting production host for carboxylic acids (Abbott et al., 2009; Carmelo et al., 1996; Della-Bianca and Gombert, 2013). Early attempts to engineer this organisms for industrial production of lactic acid have been successful (Dequin and Barre, 1994; Porro et al., 1995) and, more recently, fed-batch cultures of engineered *S. cerevisiae* strains reached titers of 82 g $L^{-1}$ and 142 g $L^{-1}$ for the D and L isomer, respectively (Baek et al., 2017; Song et al., 2016). Despite our ability to engineer the production several organic acids in *S. cerevisiae*, little is known about their transport across the yeast membrane (Abbott et al., 2009; Borodina, 2019). Transport of carboxylic acids forms an important optimization target for metabolic engineering, to stimulate product export (increasing productivity and titers) and to increase tolerance to weak organic acid stress (Abbott et al., 2009; Casal et al., 2008). Although diffusion of undissociated lactic acid across yeast cell membranes has been described (Gabba et al., 2020), it is unlikely to be the main mechanism for lactic acid export under physiological conditions (Cassio et al., 1987; Mans et al., 2017; van Maris et al., 2004). Therefore, further investigation of the genes involved in lactic acid export in yeast remains important to enable the design and construction of future industrial cell factories.

Two genes encoding transporters for monocarboxylic acids have been identified in *S. cerevisiae*: *JEN1* and *ADY2*. Jen1 is a member of the Major Facilitator Superfamily (MFS) which enables uptake of lactic, acetic and pyruvic acid, while Ady2 has been described to function predominantly as an acetate transporter (Akita et al., 2000; Casal et al., 1999; Paiva

et al., 2004). While deletion of both genes abolished growth on lactic acid as the sole carbon source, export of lactic acid in an engineered *S. cerevisiae* strain remained unaffected by combined deletion of *JEN1* and *ADY2* (Kok et al., 2012; Pacheco et al., 2012). The difficulty of identifying the export system(s) for lactic acid was further illustrated by a recent study, in which the combined deletion of 25 (putative) transporter-encoding genes in a single yeast strain did not affect the rate of lactic acid export (Mans et al., 2017).

A powerful strategy to identify genes involved in a specific physiological function is the use of adaptive laboratory evolution. Application of a selective pressure is used to enrich for mutants with the phenotype of interest, which can subsequently be analysed by whole genome sequencing to identify mutated genes related to the evolved phenotype (Mans et al., 2018). Whereas the use of this strategy to select for mutants with altered lactic acid export remains a challenge, adaptive evolution can be directly applied to select for improved lactic acid uptake. This concept was demonstrated in a previous study, in which laboratory evolution of a *jen1Δ* strain in culture medium with lactic acid as sole carbon source led to the identification of mutated *ADY2* alleles that had an increased uptake capacity for lactic acid (de Kok et al., 2012).

In this study, we use adaptive laboratory evolution to identify additional transporters, which upon mutation can efficienty catalyze lactic acid uptake in *S. cerevisiae*. Subsequently, we overexpress the complete suite of native and evolved lactic acid transporters and characterize the ability of the resulting strains to grow on a variety of organic acids. Finally, we identify specific amino acid residues in a conserved motive of the evolved transporters which play a key role in determining their ability to transport lactic acid.

## 2. MATERIALS AND METHODS

### 2.1 Strains and maintenance

The *S. cerevisiae* strains used in this study (Table 2) share the CEN.PK113-7D or the CEN.PK2-1C genetic backgrounds (Entian and Kötter, 2007). Stock cultures of *S. cerevisiae* were grown aerobically in 500 mL round-bottom shake flasks containing 100 mL synthetic medium (SM) (Verduyn et al., 1992) or YP medium (10 g $L^{-1}$ Bacto yeast extract, 20 g $L^{-1}$ Bacto peptone) supplemented with 20 g $L^{-1}$ glucose. When needed, auxotrophic requirements were complemented via addition of 150 mg $L^{-1}$ uracil, 100 mg $L^{-1}$ histidine, 500 mg $L^{-1}$ leucine and/or 75 mg $L^{-1}$ tryptophan (Pronk, 2002). For plate cultivation, 2% (w/v) agar was added to the medium prior to heat sterilization. Stock cultures of *E. coli* XL1-Blue Subcloning Grade Competent Cells (Agilent, Santa Clara, CA, USA) that were used for plasmid propagation were grown in LB medium (5 g $L^{-1}$ Bacto yeast extract, 10 g $L^{-1}$ Bacto tryptone, 10 g $L^{-1}$ NaCl) supplemented with 100 mg $L^{-1}$ ampicillin. Media were autoclaved at 121°C for 20 min and supplements and antibiotics were filter sterilized and added to the media prior to use. Frozen culture stocks were prepared by addition of sterile glycerol (to a final concentration of 30% v/v) to exponentially growing shake flask cultures of *S. cerevisiae* or overnight cultures of *E. coli* and 1 mL aliquots were stored at -80°C.

### 2.2 Molecular biology techniques

Phusion High-Fidelity DNA Polymerase (Thermo Fisher Scientific, Waltham, MA, USA) was used for PCR amplification for cloning purposes. Diagnostic PCRs were performed using DreamTaq PCR Master Mix (2X) (Thermo Fisher Scientific). In both cases, the manufacturer's protocol was followed, with the exception of the use of lower primer concentrations (0.2 µM each). Desalted (DST) oligonucleotide primers were used, except for primers binding to coding regions, which were PAGE purified. Primers were purchased from Sigma Aldrich (Saint Louis, MO, USA), with the exception of primers 17453 and 17453, which were purchased from Ella Biotech (Planegg, Germany). For diagnostic PCR, yeast genomic DNA was isolated as described by Lõoke et al. (2011). Commercial kits for DNA extraction and purification were used for small-scale DNA isolation (Sigma Aldrich), PCR cleanup (Sigma Aldrich), and gel extraction (Zymo Research, Irvine, CA, USA). Restriction analysis of constructed plasmids was performed using FastDigest restriction enzymes (Thermo Scientific). Gibson assembly of linear DNA fragments was performed using NEBuilder HiFi DNA Assembly Master Mix (New England Biolabs, Ipswich, MA, USA) in a total reaction volume of 5 µL. Transformation of chemically competent *E. coli* XL1-Blue (Agilent) was performed according to the manufacturer's protocol.

### 2.3 Plasmid construction

The plasmids and oligonucleotide primers used in this study are listed in Table 1 and Supplementary Table 1, respectively. All plasmids were constructed by Gibson assembly of two linear fragments. With the exception of the fragments used for the construction of plasmid pUDR420, all fragments were PCR-amplified from either a template plasmid or from

genomic DNA. A detailed description of the parts used to make each plasmid can be found in Supplementary Table 2.

Plasmid pUDR405 was constructed by Gibson assembly of two linear fragments, both obtained via PCR amplification of plasmid pROS13 using primers 8664 and 6262 (for the *JEN1*-gRNA_2µ_*ADY2*-gRNA insert) and 6005 (for the plasmid backbone), as previously described by Mans et al. (2015). Plasmid pUDR420 was constructed by Gibson assembly of a double-stranded DNA fragment, obtained by annealing the complementary single-stranded oligonucleotides 8691 and 13552, and a vector backbone amplified from plasmid pMEL13 using primers 6005 and 6006. For construction of pUDE813, the linear p426-TEF plasmid backbone was amplified from plasmid p426-TEF using primers 5921 and 10547 and the *ATO3* open reading frame (ORF) was amplified from yeast strain CEN.PK113-7D genomic DNA using primers 13513 and 13514. Subsequently, Gibson assembly of the linear p426-TEF plasmid backbone and the *ATO3* insert yielded pUDE813. pUDE814, pUDE1001, pUDE1002, pUDE1003, pUDE1004, pUDE1021 and pUDE1022 were constructed similar to pUDE813, using primers 5921 and 10547 to amplify the linear p427-TEF plasmid backbone. The inserts were amplified from genomic DNA of strain CEN.PK113-7D (for wildtype genes) or from genomic DNA of the corresponding evolved strain (for mutated genes) using primers 13513 and 13514 (pUDE814), 17170 and 17171 (pUDE1001), 17168 and 17169 (pUDE1002, pUDE1003 and pUDE1004) or 17452 and 17453 (pUDE1021 and pUDE1022). For construction of pUDC319, plasmid p426-TEF was amplified using primers 2949 and 17741 and the CEN6 origin of replication was amplified from pUDC156 using primers 17742 and 17743. Subsequently, Gibson assembly of the linear p426-TEF plasmid fragment and the CEN6 fragment yielded pUDC319. pUDC320, pUDC321, pUDC322, pUDC323, pUDC324, pUDC325, pUDC326 and pUDC327 were constructed in a similar way using the same primers, but the linear plasmid fragment was amplified from pUDE813, pUDE814, pUDE1001, pUDE1002, pUDE1003, pUDE1004, pUDE1021 and pUDE1022, respectively.

**Table 1:** Plasmids used in this study.

| Name | Relevant characteristic | Origin |
|---|---|---|
| pROS13 | *2µ*m ampR *kanMX gRNA-CAN1 gRNA-ADE2* | (Mans et al., 2015) |
| pMEL13 | *2µ*m ampR *kanMX gRNA-CAN1* | (Mans et al., 2015) |
| pUDR405 | *2µ*m ampR *kanMX gRNA-JEN1 gRNA-ADY2* | This study |
| pUDR420 | *2µ*m ampR *kanMX gRNA-ATO3* | This study |
| p426-TEF | *2µ*m *URA3 pTEF1-tCYC1* | (Mumberg et al., 1995) |
| pUDE813 | *2µ*m *URA3 pTEF1-ATO3-tCYC1* | This study |
| pUDE814 | *2µ*m *URA3 pTEF1-ATO3$^{T284C}$-tCYC1* | This study |
| pUDE1001 | *2µ*m *URA3 pTEF1-JEN1-tCYC1* | This study |
| pUDE1002 | *2µ*m *URA3 pTEF1-ADY2-tCYC1* | This study |
| pUDE1003 | *2µ*m *URA3 pTEF1- ADY2$^{C755G}$ -tCYC1* | This study |
| pUDE1004 | *2µ*m *URA3 pTEF1- ADY2$^{C655G}$-tCYC1* | This study |
| pUDE1021 | *2µ*m *URA3 pTEF1-ATO2-tCYC1* | This study |
| pUDE1022 | *2µ*m *URA3 pTEF1-ATO2$^{T653C}$-tCYC1* | This study |

| Name | Relevant characteristic | Origin |
|---|---|---|
| pUDC156 | *CEN6 URA3 pTEF-CAS9-tCYC1* | (Marques et al., 2017) |
| pUDC319 | *CEN6 URA3 pTEF-tCYC1* | This study |
| pUDC320 | *CEN6 URA3 pTEF1-ATO3-tCYC1* | This study |
| pUDC321 | *CEN6 URA3 pTEF1-ATO3$^{T284C}$-tCYC1* | This study |
| pUDC322 | *CEN6 URA3 pTEF1-JEN1-tCYC1* | This study |
| pUDC323 | *CEN6 URA3 pTEF1-ADY2-tCYC1* | This study |
| pUDC324 | *CEN6 URA3 pTEF1- ADY2$^{C755G}$ -tCYC1* | This study |
| pUDC325 | *CEN6 URA3 pTEF1- ADY2$^{C655G}$-tCYC1* | This study |
| pUDC326 | *CEN6 URA3 pTEF1-ATO2-tCYC1* | This study |
| pUDC327 | *CEN6 URA3 pTEF1-ATO2$^{T653C}$-tCYC1* | This study |

**2.4 Strain construction**

*S. cerevisiae* strains were transformed with the LiAc/ssDNA method (Gietz and Woods, 2002). For transformations with a dominant marker, the transformation mixture was plated on YP plates, containing glucose (20 g $L^{-1}$) as carbon source, and supplemented with 200 mg $L^{-1}$ G418 (Invitrogen, Carlsbad, CA, USA). Gene deletions were performed as previously described (Mans et al., 2015). For transformation of plasmids harboring an auxotrophic marker, transformed cells were plated on SM medium with glucose (20 g $L^{-1}$) as a carbon source and when needed, appropriate auxotrophic requirements were supplemented.

The tryptophan auxotrophy of IMX1000 was the result of a single point mutation in the *TRP1* gene (*trp1-289*) (Botstein et al., 1979) and was spontaneously reverted by plating the strain on SM medium supplemented with uracil, histidine and leucine, and picking a tryptophan prototrophic colony, yielding strain IMX2486. Strain IMX2487 was constructed by transforming IMX2486 with a linear fragment, obtained by PCR amplification of the *LEU2* gene from CEN.PK113-7D, using primers 1742 and 1743. Strain IMX2488 was constructed by transforming IMX2487 with a linear fragment, obtained by PCR amplification of the *HIS3* gene from CEN.PK113-7D, using primers 1738 and 3755. Strain IMK875 was constructed by transforming the Cas9-expressing strain IMX585 with plasmid pUDR405 and two double stranded repair oligonucleotides obtained by annealing oligonucleotides 8597 to 8598 and 8665 to 8666. Strain IMK876 was constructed by transforming the Cas9-expressing strain IMX581 with plasmid pUDR405 and two double stranded repair oligonucleotides obtained by annealing oligonucleotides 8597 to 8598 and 8665 to 8666. Strains IMK882 and IMK883 were obtained by transforming strains IMK875 and IMK876, respectively, with plasmid pUDR420 and a double stranded repair oligonucleotide obtained by annealing oligonucleotides 14120 and 14121. Plasmids p426-TEF, pUDE813, pUDE814, pUDE1001, pUDE1002, pUDE1003, pUDE1004, pUDE1021, pUDE1022, pUDC319, pUDC320, pUDC321, pUDC322, pUDC323, pUDC324, pUDC325, pUDC326 and pUDC327 were transformed in strain IMX2488, yielding IME581, IME582, IME583, IME584, IME585, IME586, IME587, IME588, IME589, IMC164, IMC165, IMC166, IMC167, IMC168, IMC169, IMC170, IMC171 and IMC172, respectively. Single colony isolates from evolution cultures ('IMS'-strains) were

obtained by plating the evolved culture on solid medium and restreaking a grown colony to a fresh plate three consecutive times.

**Table 2** *Saccharomyces cerevisiae* strains used in this study

| Strain name | Relevant genotype [a] | Origin |
|---|---|---|
| CEN.PK113-7D | Prototrophic reference, *MAT*a | (Entian and Kötter, 2007) |
| IMX581 | *MAT*a *ura3-52 can1Δ::cas9-natNT2* | (Mans et al., 2015) |
| IMX585 | *MAT*a *can1Δ::cas9-natNT2* | (Mans et al., 2015) |
| IMK341 | *MAT*a *ura3Δ::loxP ady2Δ::loxP-hphNT1-loxP jen1Δ::loxP* | (Kok et al., 2012) |
| IMW004 | *MAT*a *URA3 ADY2$^{C755G}$ jen1Δ::loxP-KanMX4-loxP* | (Kok et al., 2012) |
| IMW005 | *MAT*a *URA3 ADY2$^{C655G}$ jen1Δ::loxP-KanMX4-loxP* | (Kok et al., 2012) |
| IMX1000 | *MAT*a *ura3-52 trp1-289 leu2-3112 his3Δ can1Δ::cas9-natNT2 mch1Δ mch2Δ mch5Δ aqy1Δ itr1Δ pdr12Δ mch3Δ mch4Δ yil166cΔ hxt1Δ jen1Δ ady2Δ aqr1Δ thi73Δ fps1Δ aqy2Δ yll053cΔ ato2Δ ato3Δ aqy3Δ tpo2Δ yro2Δ azr1Δ yhl008cΔ tpo3Δ* | (Mans et al., 2017) |
| IMK875 | *MAT*a *can1Δ::cas9-natNT2 jen1Δ ady2Δ* | This study |
| IMK876 | *MAT*a *can1Δ::cas9-natNT2 ura3-52 jen1Δ ady2Δ* | This study |
| IMK882 | *MAT*a *can1Δ::cas9-natNT2 jen1Δ ady2Δ ato3Δ* | This study |
| IMK883 | *MAT*a *can1Δ::cas9-natNT2 ura3-52 jen1Δ ady2Δ ato3Δ* | This study |
| IMS807 | IMK341 evolved for growth on lactate, evolution line A | This study |
| IMS808 | IMK341 evolved for growth on lactate, evolution line A | This study |
| IMS809 | IMK341 evolved for growth on lactate, evolution line A | This study |
| IMS810 | IMK341 evolved for growth on lactate, evolution line B | This study |
| IMS811 | IMK341 evolved for growth on lactate, evolution line B | This study |
| IMS1122 | IMK882 evolved for growth on lactate | This study |
| IMS1123 | IMK882 evolved for growth on lactate | This study |
| IMS1130 | IMK882 evolved for growth on lactate | This study |
| IMX2486 | IMX1000 *ura3-52 TRP1, leu2-3112, his3Δ* | This study |
| IMX2487 | IMX1000 *ura3-52 TRP1, LEU2, his3Δ* | This study |
| IMX2488 | IMX1000 *ura3-52 TRP1, LEU2, HIS3* | This study |
| IME581 | IMX2488 p426-*TEF* (2*μ*m) | This study |
| IME582 | IMX2488 pUDE813 (2*μ*m *ATO3*) | This study |
| IME583 | IMX2488 pUDE814 (2*μ*m *ATO3$^{T284C}$*) | This study |
| IME584 | IMX2488 pUDE1001 (2*μ*m *JEN1*) | This study |
| IME585 | IMX2488 pUDE1002 (2*μ*m *ADY2*) | This study |
| IME586 | IMX2488 pUDE1003 (2*μ*m *ADY2$^{C755G}$*) | This study |
| IME587 | IMX2488 pUDE1004 (2*μ*m *ADY2$^{C655G}$*) | This study |
| IME588 | IMX2488 pUDE1021 (2*μ*m *ATO2*) | This study |
| IME589 | IMX2488 pUDE1022 (2*μ*m *ATO2$^{T653C}$*) | This study |
| IMC164 | IMX2488 pUDC319 (*CEN6*) | This study |
| IMC165 | IMX2488 pUDC320 (*CEN6 ATO3*) | This study |
| IMC166 | IMX2488 pUDC321 (*CEN6 ATO3$^{T284C}$*) | This study |
| IMC167 | IMX2488 pUDC322 (*CEN6 JEN1*) | This study |
| IMC168 | IMX2488 pUDC323 (*CEN6 ADY2*) | This study |
| IMC169 | IMX2488 pUDC324 (*CEN6 ADY2$^{C755G}$*) | This study |
| IMC170 | IMX2488 pUDC325 (*CEN6 ADY2$^{C655G}$*) | This study |
| IMC171 | IMX2488 pUDC326 (*CEN6 ATO2*) | This study |
| IMC172 | IMX2488 pUDC327 (*CEN6 ATO2$^{T653C}$*) | This study |

**2.5 Media and cultivation**

Evolution experiments were performed in 500 mL shake-flask cultures containing 100 mL synthetic medium (Verduyn et al., 1992) with 84 mM lactic acid as sole carbon source. The pH of the medium was set at 5.0 and the cultures were incubated at 30°C in an Innova incubator shaker (New Brunswick Scientific, Edison, NJ, USA) set at 200 rpm. Auxotrophic requirements were supplemented as needed.

Strains were characterized in SM supplemented with different carbon sources. To achieve an initial carbon concentration of 250 mM, the culture media contained either 42 mM glucose, 83 mM lactic acid, 125 mM acetic acid or 83 mM pyruvic acid. The characterization was performed in a Growth-Profiler system (EnzyScreen, Heemstede, The Netherlands) equipped with 96-well plates in a culture volume of 250 µL, set at 250 rpm and 30°C. The measurement interval was set at 30 minutes. Raw green values were corrected for well-to-well variation using measurements of a 96-well plate containing a culture with an externally determined optical density of 3.75 in all wells. Optical densities were calculated by converting green values (corrected for well-to-well variation) using a calibration curve that was determined by fitting a third-degree polynomial through 22 measurements of cultures with known OD values between 0.1 and 20. Growth rates were calculated using the calculated optical densities of at least 15 points in the exponential phase. Exponential growth was assumed when an exponential curve could be fitted with an $R^2$ of at least 0.985.

**2.6 Analytical methods**

Culture optical density at 660 nm was measured with a Libra S11 spectrophotometer (Biochrom, Cambridge, United Kingdom). In order to measure within the linear range of the instrument (OD between 0.1 and 0.3), cultures were diluted in an appropriate amount of demineralized water. Metabolite concentrations in culture supernatants and media were analyzed using an Agilent 1260 Infinity HPLC system equipped with a Bio-rad Aminex HPX-87H ion exchange column, operated at 60°C with 5 mM $H_2SO_4$ as mobile phase at a flow rate of 0.600 mL $min^{-1}$.

**2.7 DNA extraction and whole genome sequencing**

Strain IMK341 and the evolved single colony isolates (IMS-strains) were grown in 500 mL shake flasks containing 100 mL YP medium supplemented with glucose (20 g $L^{-1}$) as a carbon source. The cultures were incubated at 30°C until the strains reached stationary phase and genomic DNA was isolated using the Qiagen 100/G kit (Qiagen, Hilden, Germany) according to the manufacturer's instructions and quantified using a Qubit® Fluorometer 2.0 (Thermo Fisher Scientific). The isolated DNA was sequenced in-house on a MiSeq (Illumina, San Diego, CA, USA) with 300 bp paired-end reads using TruSeq PCR-free library preparation (Illumina). For all the strains, the reads were mapped onto the *S. cerevisiae* CEN.PK113-7D genome (Salazar et al., 2017) using the Burrows–Wheeler Alignment tool (BWA) and further processed using SAMtools and Pilon for variant calling (Li and Durbin, 2010; Li et al., 2009; Walker et al., 2014).

### 2.8 3D modelling and molecular docking of Ato1, Ato2 and Ato3

The three-dimensional modelling analysis was performed for the protein sequences of Ato1, Ato1$^{L219V}$, Ato1$^{A252G}$, Ato2, Ato2$^{L218S}$, Ato3 and Ato3$^{F95S}$. The amino acid sequences were retrieved from the *Saccharomyces* Genome Database (Cherry et al., 2012). To determine the predicted transporter 3D structures, the amino acid sequences were threaded through the PDB library using LOMETS (Local Meta-Threading-Server) (Zheng et al., 2019). LOMETS was used to generate a 3D model using high-scoring target-to-template alignments from 11 locally installed threading programs (FFAS-3D, HHpred, Neff-MUSTER, MUSTER, CEthreader, HHsearch, PPAS, PRC, PROSPECTOR2, SP3 and Sparks-X). The *Citrobacter koseri* succinate acetate permease (CkSatP, PDB 5YS3) was the top ranked template threading identified in LOMETS for Ato1, Ato2 and Ato3 (Qui et al. 2018).

## 3. RESULTS

### 3.1 Laboratory evolution on lactic acid leads to point mutations in Ato2 or Ato3.

In an attempt to identify additional transporters able to catalyze uptake of lactic acid transport after gaining point mutations, we incubated strains IMK341 and IMX1000 in duplicate shake flasks cultures containing synthetic medium with lactic acid as the sole carbon source. In IMK341 the known carboxylic acid transporters *JEN1* and *ADY2* are knocked out (*jen1Δ*, *ady2Δ*), whereas IMX1000 contains a further 23 deletions in putative lactic acid transporter-encoding genes (Mans et al., 2017). After 9 weeks, growth was observed in both cultures of IMK341 whereas no growth was observed after 12 weeks of incubation of IMX1000. Whole-genome sequencing of evolved IMK341 (*jen1Δ*, *ady2Δ*) cell lines, isolated after transfer to fresh medium, revealed three to seven non-synonymous SNPs in each mutant and no chromosomal duplications or rearrangements (Table 3). Strikingly, all evolved isolates shared an identical mutation in *ATO3* (*ATO3$^{T284C}$*), which encodes a protein described to be involved in ammonium transport (Palková et al., 2002). To investigate the role of *ATO3* in lactic acid uptake, we overexpressed both the native and evolved *ATO3* in IMK883 (*jen1Δ*, *ady2Δ*, *ato3Δ*) and tested the strains for growth on SM lactic acid plates. After 5 days, only the reference strain CEN.PK113-7D and the strain carrying the *ATO3$^{T284C}$* allele were able to grow (Supplementary Figure 1), indicating that the T284C mutation in *ATO3* was responsible for the evolved phenotype. We then combined the deletion of *JEN1*, *ADY2* and *ATO3* in strain IMK882 (*jen1Δ, ady2Δ, ato3Δ*) and repeated the evolution. After 5 and 12 days, growth was observed in two of the cultures from which strains IMS1122 and IMS1123 were isolated after transfer to a flask with fresh medium. In both single colony isolates, five SNPs were present (Table 3), including a common mutation in *ATO2*, (*ATO2$^{T653C}$*), which has also been described as an ammonium transporter together with *ATO3* and *ADY2* (Palková et al., 2002).

**Table 3** Amino acid changes identified by whole-genome sequencing of single colony isolates evolved for growth in medium containing lactic acid as sole carbon source. Isolates IMS807 to IMS811 are derived from IMK341 (*jen1Δ, ady2Δ*) and IMS1122 and IMS1123 are derived from IMK882 (*jen1Δ, ady2Δ, ato3Δ*)). IMS807, IM808 and IMS809 are isolates from evolution line #1 and IMS810 and IMS811 are isolates from evolution line #2. The mutation Sip5$^{*490Q}$ indicates the loss of the stop codon.

| IMK341 evolution #1 | | | IMK341 evolution #2 | | IMK822 evolution #1 | IMK822 evolution #2 |
|---|---|---|---|---|---|---|
| **IMS807** | **IMS808** | **IMS809** | **IMS810** | **IMS811** | **IMS1122** | **IMS1123** |
| Ato3$^{F95S}$ | Ato3$^{F95S}$ | Ato3$^{F95S}$ | Ato3$^{F95S}$ | Ato3$^{F95S}$ | Ato2$^{L218S}$ | Ato2$^{L218S}$ |
| Mms2$^{Y58C}$ | Mms2$^{Y58C}$ | Mms2$^{Y58C}$ | Sip5$^{*490Q}$ | Sip5$^{*490Q}$ | Lrg1$^{H979N}$ | Whi2$^{E119*}$ |
| Pih1$^{D147Y}$ | Pih1$^{D147Y}$ | Pih1$^{D147Y}$ | Ssn2$^{M1280R}$ | Lip5$^{R4L}$ | Ykr051w$^{Y285H}$ | Ykr051w$^{Y285H}$ |
| Uba1$^{L952F}$ | | Drn1$^{P213L}$ | | | Jjj1$^{H356Q}$ | Jjj1$^{H356Q}$ |
| Stv1$^{L275F}$ | | | | | Trm10$^{A49V}$ | Trm10$^{A49V}$ |
| Whi2$^{E187*}$ | | | | | | |
| Vba4$^{P198L}$ | | | | | | |

### 3.2 Overexpression of mutated transporters enables rapid growth in liquid medium with lactic acid as sole carbon source.

Strikingly, the evolved transporters able to catalyze uptake of lactic acid (*ATO2* and *ATO3* in this study, and *ADY2* in work by de Kok et al., 2012) represent all members of the Acetate Uptake Transporter Family (TCDB 2.A.96). To characterize impact of the mutations on the ability of the mutated transport proteins to catalyze uptake of organic acids, we individually overexpressed *JEN1, ADY2, ATO2* and *ATO3* and their mutated alleles via centromeric vectors in IMX2488, a strain background in which 25 (putative) organic acid transporters were deleted (Table 2). Whereas no viable cultures could be obtained with strains overexpressing wildtype *ATO2* in liquid medium with 42 mM glucose as carbon source, all other IMX2488-derived transporter expressing strains had similar growth rates compared to the empty vector control (IMC164), indicating no major physiological adaptations of the overexpression of the transporters when grown on glucose (Figure 1, top left panel). Overexpression of the transporter variants from multicopy vectors resulted in a growth rate reduction of up to 66% compared to the empty vector reference when grown on glucose and were therefore not tested further (Supplementary Figure 2). In accordance with previous research, strains overexpressing *ADY2*, *ADY2*$^{C755G}$ and *ADY2*$^{C655G}$ showed a maximum specific growth rate of 0.02 ± 0.01 $h^{-1}$, 0.08 ± 0.01 $h^{-1}$ and 0.10 ± 0.01 $h^{-1}$ when grown in medium containing 83 mM lactic acid as carbon source, respectively (de Kok et al., 2012). Surprisingly, strains expressing the evolved *ATO2*$^{T653C}$ and *ATO3*$^{T284C}$ alleles outperformed all the other tested strains, with a maximum specific growth rate of 0.11 ± 0.01 $h^{-1}$ and 0.15 ± 0.01 $h^{-1}$, respectively (Figure 1, top right panel and Supplementary Figure 5). These represent the highest reported growth rates reported for *S. cerevisiae* on this carbon source and indicate that the mutations in Ato2 are responsible for the evolved phenotypes observed in IMS1122 and IMS1123 (Table 3).

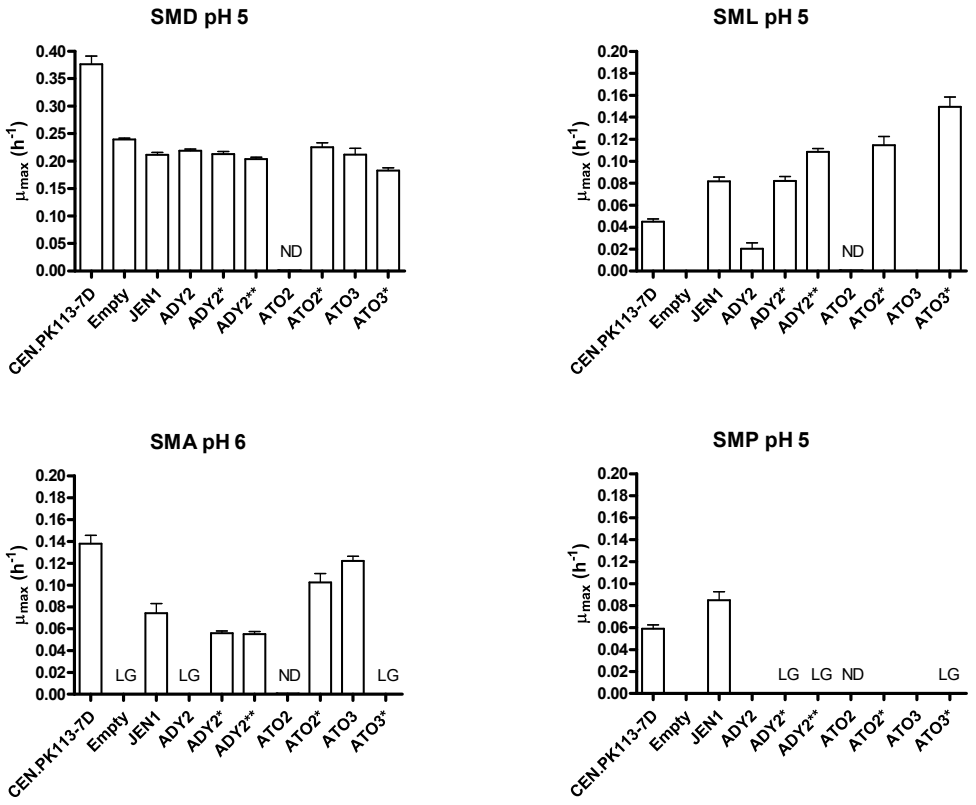


**Figure 1** Growth rates on different carbon sources of *S. cerevisiae* reference strain CEN.PK113-7D and the 25-transporter deletion strain IMX2488 expressing an empty vector or a vector carrying the indicated organic acid transporter. Bars and error bars represent the average and standard deviation of three independent experiments. SMD: synthetic medium with 42 mM glucose. SML: synthetic medium with 83 mM lactic acid. SMA: synthetic medium with 125 mM acetic acid. SMP: synthetic medium with 83 mM pyruvic acid. Empty: empty plasmid. ADY2*: *ADY2*$^{C755G}$ allele. ADY2**: *ADY2*$^{C655G}$ allele. ATO2*: *ATO2*$^{T653C}$ allele. ATO3*: *ATO3*$^{T284C}$ allele. For some experiments, a linear increase in optical density was observed, which impeded the determination of an exponential growth rate (indicated by L.G.). N.D.: not determined.

### 3.3 Mutations in *ATO2* and *ATO3* change the uptake capacity of acetate and pyruvate

After demonstrating that the point mutations increased the catalytic activity of Ato2, Ato3 and Ady2 for lactic acid transport, we also investigated their ability to transport acetic and pyruvic acid (Figure 1, bottom panels and Supplementary Figures 6 and 7). In liquid medium at pH 5.0 with 125 mM acetic acid (p$K_a$ of 4.75), no growth was observed for any of the strains with the 25-deletion background, likely caused by acetic acid toxicity due to the absence of essential acetic acid exporters (Supplementary Figure 3). However, at pH 6.0 different growth characteristics were observed in strains expressing *ADY2* and *ATO3* compared to their evolved counterparts. Whereas expression of native *ADY2* resulted in slow non-exponential growth, expression of *ADY2*$^{C755G}$ or *ADY2*$^{C655G}$ improved growth performance. The opposite

behavior was observed in strains expressing *ATO3* (exponential growth) and the evolved *ATO3*$^{T284C}$ variant (slow non-exponential growth). In medium containing 83 mM pyruvic acid, no exponential growth was observed for any of the strains expressing Ato2, Ato3 or Ady2 variants. However, slow, non-exponential growth was observed for strains expressing any variant of *ADY2* or *ATO2*$^{T653C}$ which could indicate a minor change in affinity for this substrate caused by the point mutations.

**3.4 Protein modelling reveals mutations in the central hydrophobic constriction site as important factor in determining substrate specificity**

In order to establish a link between the mutated amino acid residues and the molecular mechanism of the studied transporters, the putative protein structures of Ady2, Ato2 and Ato3, and of their mutated alleles, were modelled *in silico*. To this end, the amino acid sequences of Ady2, Ato2 and Ato3 were aligned against the crystal structure of the *Citrobacter koseri* acetate anion channel SatP (PDB 5YS3), which obtained the best score for protein structure prediction. This alignment showed that the Leu219Val mutation in Ady2, the Leu218Ser mutation in Ato2 and the Phe95Ser mutation in Ato3 are amongst three amino acid residues that were previously identified to be essential for the formation of the central narrowest hydrophobic constriction of the anion pathway in *C. koseri* SatP (Qiu et al., 2018) (Figure 2 and Figure 3). Specifically, these changes result in the substitution of the amino acid side group with a smaller (and in the case of Ato2 and Ato3 a more hydrophilic) alternative (Ato3 is shown in Figure 3 and the models for Ady2 and Ato2 can be found in Supplementary Figure 8-9). Based on these models, we estimated the distance between these three hydrophobic residues and found an increased distance in the *ADY2*$^{C655G}$, *ATO3*$^{T284C}$ and *ATO2*$^{T653C}$ encoded mutants compared to their corresponding wildtype protein, leading to a larger aperture in the middle of the channel (Figure 3). We hypothesize that this increased size of the hydrophobic constriction may allow larger substrates to pass through, thus increasing substrate specificity and transport capacity.

To investigate if the mutations affected the presence and affinity of binding sites for acetate, lactate and pyruvate, docking of ligands in the protein structures was simulated using AutoDock Vina (Supplementary Figure 10, Supplementary Table 3). In all proteins, both wildtype and mutated, four binding sites were identified for acetate, which is in accordance with what has previously been reported for the homolog CkSatP (Qiu et al., 2018). Of these four binding sites, two, which are located closest to the hydrophobic constriction, also consistently bind lactate and pyruvate. Strikingly, mutations in Ady2, Ato2 and Ato3 led to an increased lactate affinity of at least one of these two sites closest to the hydrophobic constriction, which might have contributed to the increased lactate transport capacity. On the other hand, no clear correlation was found between the physiology observed for strains overexpressing the different protein variants when grown on acetate and pyruvate and the corresponding binding affinities of these two ligands.

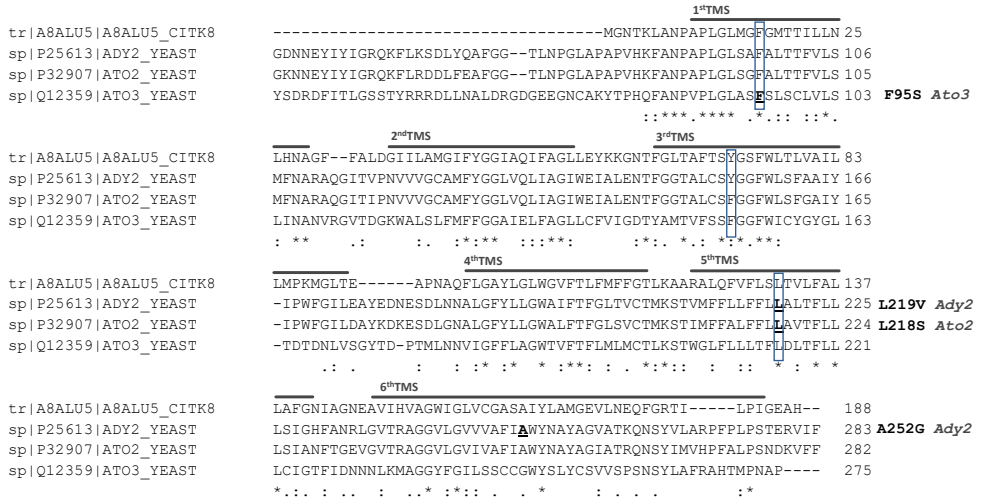


**Figure 2** Multiple sequence alignment of *Citrobacter koseri* SatP and *Saccharomyces cerevisiae* Ady2, Ato2 and Ato3. The multiple sequence alignment was built with ClustalOmega (https://www.ebi.ac.uk/Tools/msa/clustalo/). Localization of the transmembrane segments (TMS) was done using PSI/TM-Coffee (http://tcoffee.crg.cat/apps/tcoffee/do:tmcoffee). Blue rectangles indicate the residues of the narrowest constriction site F98-Y155-L219 (amino acid numbers referred to Ady2) (Qiu et al., 2018). Bold, underlined letters indicate the mutated residue.

**Table 4** Average distances (in Å) between different amino acids in the constriction pore of Ady2, Ato2 Ato3 and mutated alleles, calculated using the corresponding protein model. Bold values in the table indicate distances which are at least 1 Å larger than the one calculated in the reference structure.

| Protein | Amino acid residues | | | Protein | Amino acid residues | | | Protein | Amino acid residues | | |
|---|---|---|---|---|---|---|---|---|---|---|---|
| | 219&98 | 98&155 | 155&219 | | 218&97 | 97&154 | 154&218 | | 215&95 | 95&152 | 152&215 |
| Ady2 | 4,57 | 6,85 | 3,96 | Ato2 | 4,16 | 5,74 | 4,37 | Ato3 | 4,04 | 4,60 | 4,11 |
| Ady2 L219V | 4,37 | 6,94 | 5,34 | Ato2 L218S | 5,94 | 5,64 | 5,57 | Ato3 F95S | 7,69 | 8,50 | 4,51 |
| Ady2 A252G | 4,49 | 6,74 | 3,89 | | | | | | | | |

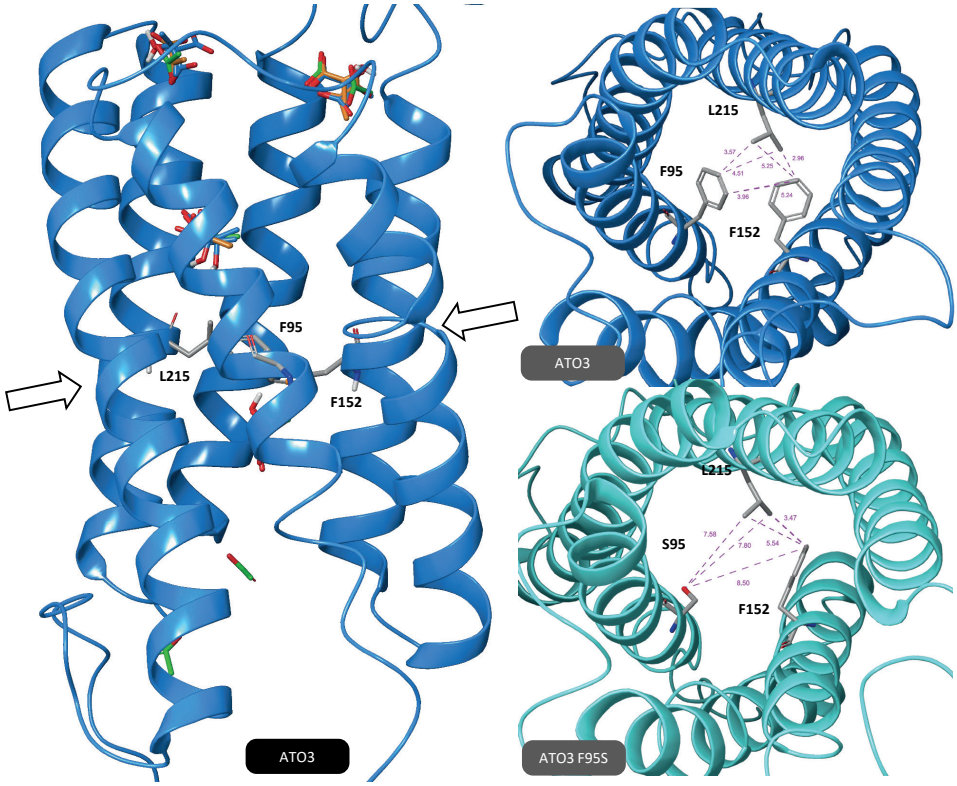


**Figure 3:** 3D models of the transporters Ato3 (dark blue) and Ato3 F95S (light blue). Left: side view of Ato3. Arrows indicate the hydrophobic constriction site, consisting of F95, L215 and F152. Right, top view of either Ato3 (top) or Ato3F95S (bottom). The amino acids involved in the constriction site are shown. Purple lines and values indicate distances (in Å) between different anchor points of amino acids.

## 4. DISCUSSION

In this study, we report the identification and characterization of a family of transporter genes which, upon mutation, are able to efficiently catalyze import of lactic acid in *S. cerevisiae*. As rational engineering to identify lactic acid transporters remains elusive (Borodina, 2019; Mans et al., 2017), we used adaptive laboratory evolution to select for mutants capable of consuming lactic acid, which led to the identification of mutations in *ATO3* (*ATO3*$^{T284C}$) and *ATO2* (*ATO2*$^{T653C}$). Together with *ADY2*, *ATO2* and *ATO3* were previously described to code for ammonium transporters (Ammonium Transport Outwards) based on two observations: the high expression of these genes during ammonia production by *S. cerevisiae,* and the presence of a motif associated with ammonium transport in these proteins (Palková et al., 2002). However, the function of *ADY2* was later reassessed by Rabitsch et al. (2001), who identified it as a gene required for correct spore formation, and thus renamed it as *ADY2* (Accumulation of DYads). In view of the observations in our study, where *ADY2*, *ATO2* and *ATO3* and their evolved variants catalyzed uptake of lactic and acetic acid, and the absence of mechanistic studies aimed at illustrating the phenomenon of ammonium export, we support the recent proposition by Alves et al. (2020) to rename these genes, present in *S. cerevisiae* and other yeasts, as "Acetate Transporter Ortholog".

When studying the effect of the transporter overexpression on strain physiology when grown on glucose (Figure 1; growth curves can be found in Supplementary Figure 4), IMC164 (empty vector) exhibited a ~36% decreased growth rate (0.24 ± 0.00 $h^{-1}$) compared to the reference laboratory strain CEN.PK113-7D (0.38 ± 0.02 $h^{-1}$), which is in accordance to the previously described effect of the 25 deletions on the growth rate (Mans et al., 2017). As expected, no growth was observed for the strain carrying the empty vector, indicating that the 25-deletion strain is unable to import lactate and therefore a suitable background to test the transport capacity of the different transporters. When grown on acetic acid at pH 6.0, IMC164 (empty plasmid) exhibited non-exponential linear growth (Supplementary Figure 6), suggesting acetic acid diffusion, or the presence of at least one gene involved in acetate transport in the IMX2488 background. The strains were also tested for their ability to grow on SM with pyruvate as the sole carbon source, where IMC164 (empty vector) did not exhibit growth, suggesting that all genes responsible for pyruvate uptake were amongst the 25 deleted genes.

It was reported by Kok et al. (2012) that the overexpression of *ADY2*, under the control of the strong glycolytic promoter *TEF1*, was sufficient to enable slow growth ($\mu_{max}$ ~ 0.02 $h^{-1}$) in medium containing lactic acid as sole carbon source. Despite a high amino acid sequence similarity with *ADY2* (36% sequence identity), the overexpression of the native allele of *ATO3* did not enable growth on lactic acid. Moreover, overexpression of the native *ATO2*, which displays an even higher sequence identity with *ADY2*, (77% at the protein level) was detrimental to cell growth on glucose, and thus could not be tested. These observations indicate the differences in substrate specificity and uptake capacity between *ADY2*, *ATO2* and *ATO3*, hinting at distinct physiological roles of each of these transporters.

While the native alleles of *ATO3* and likely *ATO2* were not able to sustain growth on lactic acid medium, their mutated versions (*ATO2*$^{T653C}$ and *ATO3*$^{T284C}$) enabled high growth rates, with the highest growth rate determined at 0.15 ± 0.01 $h^{-1}$ for the strain harboring *ATO3*$^{T284C}$. This is, to the best of our knowledge, the highest reported growth rate of *S. cerevisiae* grown on lactic acid, and close to the growth rate observed by de Kok et al. (2012) of 0.14 $h^{-1}$ by a strain expressing *ADY2*$^{C655G}$. This 3-fold increase in growth rate of the engineered strain compared to the reference strain CEN.PK113-7D indicates that, in non-engineered *S. cerevisiae* strains, growth on lactic acid is likely limited by its transport into the cell, and not the capacity to be further metabolized. Therefore, for future work that requires fast consumption of lactic acid, overexpression of *ATO3*$^{T284C}$ can be considered.

To infer the function of the newly identified mutations we performed an *in-silico* analysis. As the 3D structures of neither Ady2 (Ato1), Ato2 nor Ato3 have been determined, we used the known structure of a homologous transporter as a scaffold, on which a 3D model of Ady2, Ato2 and Ato3 was built. Because of the high degree of homology of our proteins of interest with *Citrobacter koseri* SucP, the crystal structure of this protein was used for the construction of said models. Out of the four identified mutations in the evolved transporters, three modified one of the three amino acids in the hydrophobic constriction of the protein, allowing for a larger aperture to be formed. This observation is in line with previous research, in which changes in these three hydrophobic residues have been associated with a change of substrate specificity in different homologs of SatP (Sá-Pessoa et al., 2013; Sun et al., 2018). Simulation of ligand docking in the predicted protein structures showed that the identified mutations led to an increased binding affinity of lactate in the core of the protein, whereas a similar consistent change in binding affinity for acetate and pyruvate was not observed. We postulate that an increased binding affinity upon mutation may contribute to increased transport capacity by facilitating passage of the ligand through the hydrophobic constriction, although the increased size of the hydrophobic constriction is probably the main contributor to the evolved phenotype.

In this study, we show that laboratory evolution is a powerful tool for the identification genes involved in substrate transporter and resulted in the identification of Ato3$^{F95S}$, which, to the best of our knowledge, enables the highest growth rate on lactic acid by *S. cerevisiae* reported thus far. In addition, the presented data on transporter sequence, structure and function identified important amino-acid residues that dictate substrate specificity of *S. cerevisiae* carboxylic acid transporters, which could potentially aid in future rational engineering and annotation of additional organic acid transport proteins.

## 5. REFERENCES


Abbott, D. A., Zelle, R. M., Pronk, J. T., van Maris, A. J. A., 2009. Metabolic engineering of *Saccharomyces cerevisiae* for production of carboxylic acids: current status and challenges. FEMS Yeast Research. 9, 1123-1136. DOI: https://doi.org/10.1111/j.1567-1364.2009.00537.x

Abdel-Rahman, M. A., Tashiro, Y., Sonomoto, K., 2013. Recent advances in lactic acid production by microbial fermentation processes. Biotechnol Adv. 31, 877-902. DOI: https://www.doi.org/10.1016/j.biotechadv.2013.04.002

Akita, O., Nishimori, C., Shimamoto, T., Fujii, T., Iefuji, H., 2000. Transport of Pyruvate in *Saccharomyces cerevisiae* and Cloning of the Gene Encoded Pyruvate Permease. Bioscience, Biotechnology, and Biochemistry. 64, 980-984. DOI:

Alves, R., Sousa-Silva, M., Vieira, D., Soares, P., Chebaro, Y., Lorenz, M. C., Casal, M., Soares-Silva, I., Paiva, S., 2020. Carboxylic Acid Transporters in *Candida* Pathogenesis. mBio. 11, e00156-20. DOI: https://www.doi.org/10.1128/mBio.00156-20

Baek, S. H., Kwon, E. Y., Bae, S. J., Cho, B. R., Kim, S. Y., Hahn, J. S., 2017. Improvement of d-Lactic Acid Production in *Saccharomyces cerevisiae* Under Acidic Conditions by Evolutionary and Rational Metabolic Engineering. Biotechnology journal. 12. DOI: https://www.doi.org/10.1002/biot.201700015

Borodina, I., 2019. Understanding metabolite transport gives an upper hand in strain development. Microb Biotechnol. 12, 69-70. DOI: https://www.doi.org/10.1111/1751-7915.13347

Borodina, I., Nielsen, J., 2014. Advances in metabolic engineering of yeast *Saccharomyces cerevisiae* for production of chemicals. Biotechnology journal. 9, 609-620. DOI: https://www.doi.org/10.1002/biot.201300445

Botstein, D., Falco, S. C., Stewart, S. E., Brennan, M., Scherer, S., Stinchcomb, D. T., Struhl, K., Davis, R. W., 1979. Sterile host yeasts (SHY): a eukaryotic system of biological containment for recombinant DNA experiments. Gene. 8, 17-24. DOI: https://www.doi.org/10.1016/0378-1119(79)90004-0

Carmelo, V., Bogaerts, P., Sa-Correia, I., 1996. Activity of plasma membrane H+-ATPase and expression of *PMA1* and *PMA2* genes in *Saccharomyces cerevisiae* cells grown at optimal and low pH. Archives of microbiology. 166, 315-320. DOI: https://doi.org/10.1007/s002030050389

Casal, M., Paiva, S., Andrade, R. P., Gancedo, C., Leão, C., 1999. The Lactate-Proton Symport of *Saccharomyces cerevisiae* Is Encoded by *JEN1*. Journal of Bacteriology. 181, 2620-2623. DOI: https://www.doi.org/10.1128/JB.181.8.2620-2623.1999

Casal, M., Paiva, S., Queirós, O., Soarez-Silva, I., 2008. Transport of carboxylic acids in yeasts. FEMS microbiology reviews. 32, 974–994. DOI: https://www.doi.org/10.1111/j.1574-6976.2008.00128.x

Cassio, F., Leao, C., van Uden, N., 1987. Transport of lactate and other short-chain monocarboxylates in the yeast *Saccharomyces cerevisiae*. Appl Environ Microbiol. 53, 509-13. DOI: https://doi.org/10.1128/AEM.53.3.509-513.1987

Cherry, J. M., Hong, E. L., Amundsen, C., Balakrishnan, R., Binkley, G., Chan, E. T., Christie, K. R., Costanzo, M. C., Dwight, S. S., Engel, S. R., 2012. Saccharomyces Genome Database: the genomics resource of budding yeast. Nucleic acids research. 40, D700-D705. DOI: https://doi.org/10.1093/nar/gkr1029

de Kok, S., Nijkamp, J. F., Oud, B., Roque, F. C., de Ridder, D., Daran, J.-M. G., Pronk, J. T., van Maris, A. J. A., 2012. Laboratory evolution of new lactate transporter genes in a *jen1Δ* mutant of *Saccharomyces cerevisiae* and their identification as *ADY2* alleles by whole-genome resequencing and transcriptome analysis. FEMS Yeast Research. 12, 359-374. DOI: https://doi.org/10.1111/j.1567-1364.2011.00787.x

Della-Bianca, B. E., Gombert, A. K., 2013. Stress tolerance and growth physiology of yeast strains from the Brazilian fuel ethanol industry. Antonie Van Leeuwenhoek. 104, 1083-95. DOI: https://www.doi.org/10.1007/s10482-013-0030-2

Dequin, S., Barre, P., 1994. Mixed lactic acid–alcoholic fermentation by *Saccharomyes cerevisiae* expressing the *Lactobacillus casei* L (+)–LDH. Bio/Technology. 12, 173-177. DOI: https://doi.org/10.1038/nbt0294-173

Entian, K.-D., Kötter, P., 2007. 25 Yeast genetic strain and plasmid collections. Methods in Microbiology. 36, 629-666. DOI: https://doi.org/10.1016/S0580-9517(06)36025-4

Es, I., Mousavi Khaneghah, A., Barba, F. J., Saraiva, J. A., Sant'Ana, A. S., Hashemi, S. M. B., 2018. Recent advancements in lactic acid production - a review. Food Res Int. 107, 763-770. DOI: https://www.doi.org/10.1016/j.foodres.2018.01.001

Gabba, M., Frallicciardi, J., van 't Klooster, J., Henderson, R., Syga, L., Mans, R., van Maris, A. J. A., Poolman, B., 2020. Weak Acid Permeation in Synthetic Lipid Vesicles and Across the Yeast Plasma Membrane. Biophys J. 118, 422-434. DOI: https://www.doi.org/10.1016/j.bpj.2019.11.3384

Gietz, R. D., Woods, R. A., 2002. Transformation of yeast by lithium acetate/single-stranded carrier DNA/polyethylene glycol method. Methods Enzymol. 350, 87-96. DOI: https://doi.org/10.1016/s0076-6879(02)50957-5

Jansen, M. L. A., Heijen, J. J., Verwaal, R., Process for preparing dicarboxylic acids employing fungal cells. DSM IP Assets BV, 2017.

Kok, S., Nijkamp, J. F., Oud, B., Roque, F. C., Ridder, D., Daran, J.-M., Pronk, J. T., Maris, A. J. A., 2012. Laboratory evolution of new lactate transporter genes in a *jen1Δ* mutant of *Saccharomyces cerevisiae* and their identification as *ADY2* alleles by whole-genome resequencing and transcriptome analysis. FEMS Yeast Research. 12, 359-374. DOI: https://www.doi.org/10.1111/j.1567-1364.2011.00787.x

Li, H., Durbin, R. J. B., 2010. Fast and accurate long-read alignment with Burrows–Wheeler transform. 26, 589-595. DOI: https://doi.org/10.1093/bioinformatics/btp698

Li, H., Handsaker, B., Wysoker, A., Fennell, T., Ruan, J., Homer, N., Marth, G., Abecasis, G., Durbin, R., Genome Project Data Processing, S., 2009. The Sequence Alignment/Map format and SAMtools. Bioinformatics. 25, 2078-9. DOI: https://doi.org/10.1093/bioinformatics/btp352

Lõoke, M., Kristjuhan, K., Kristjuhan, A., 2011. Extraction of genomic DNA from yeasts for PCR-based applications. Biotechniques. 50, 325-8. DOI: https://doi.org/10.2144/000113672

Lopez-Garzon, C. S., Straathof, A. J., 2014. Recovery of carboxylic acids produced by fermentation. Biotechnol Adv. 32, 873-904. DOI: https://www.doi.org/10.1016/j.biotechadv.2014.04.002

Mans, R., Daran, J.-M. G., Pronk, J. T., 2018. Under pressure: evolutionary engineering of yeast strains for improved performance in fuels and chemicals production. Current Opinion in Biotechnology. 50, 47-56. DOI: https://doi.org/10.1016/j.copbio.2017.10.011

Mans, R., Hassing, J.-E., Wijsman, M., Giezekamp, A., Pronk, J. T., Daran, J.-M. G., Van Maris, A. J. A., 2017. A CRISPR/Cas9-based exploration into the elusive mechanism for lactate export in *Saccharomyces cerevisiae*. FEMS Yeast Research. 17, 1-12. DOI: https://doi.org/10.1093/femsyr/fox085

Mans, R., van Rossum, H. M., Wijsman, M., Backx, A., Kuijpers, N. G., van den Broek, M., Daran-Lapujade, P., Pronk, J. T., van Maris, A. J., Daran, J. M., 2015. CRISPR/Cas9: a molecular Swiss army knife for simultaneous introduction of multiple genetic modifications in *Saccharomyces cerevisiae*. FEMS Yeast Res. 15. DOI: https://doi.org/10.1093/femsyr/fov004

Marques, W. L., Mans, R., Marella, E. R., Cordeiro, R. L., van den Broek, M., Daran, J. G., Pronk, J. T., Gombert, A. K., van Maris, A. J., 2017. Elimination of sucrose transport and hydrolysis in *Saccharomyces cerevisiae*: a platform strain for engineering sucrose metabolism. FEMS Yeast Res. 17, fox006. DOI: https://www.doi.org/10.1093/femsyr/fox006

McKinlay, J. B., Vieille, C., Zeikus, J. G., 2007. Prospects for a bio-based succinate industry. Appl Microbiol Biotechnol. 76, 727-40. DOI: https://www.doi.org/10.1007/s00253-007-1057-y

Mumberg, D., Muller, R., Funk, M., 1995. Yeast vectors for the controlled expression of heterologous proteins in different genetic backgrounds. Gene. 156, 119-22. DOI: https://www.doi.org/10.1016/0378-1119(95)00037-7

Pacheco, A., Talaia, G., Sa-Pessoa, J., Bessa, D., Goncalves, M. J., Moreira, R., Paiva, S., Casal, M., Queiros, O., 2012. Lactic acid production in *Saccharomyces cerevisiae* is modulated by expression of the monocarboxylate transporters Jen1 and Ady2. FEMS Yeast Res. 12, 375-81. DOI: https://www.doi.org/10.1111/j.1567-1364.2012.00790.x

Paiva, S., Devaux, F., Barbosa, S., Jacq, C., Casal, M., 2004. Ady2p is essential for the acetate permease activity in the yeast *Saccharomyces cerevisiae*. Yeast. 21, 201-210. DOI:

Palková, Z., Devaux, F., Icicova, M., Minarikova, L., Le Crom, S., Jacq, C., 2002. Ammonia pulses and metabolic oscillations guide yeast colony development. Mol Biol Cell. 13, 3901-14. DOI: https://www.doi.org/10.1091/mbc.e01-12-0149

Porro, D., Brambilla, L., Ranzi, B. M., Martegani, E., Alberghina, L., 1995. Development of metabolically engineered *Saccharomyces cerevisiae* cells for the production of lactic acid. Biotechnol Prog. 11, 294-8. DOI: https://www.doi.org/10.1021/bp00033a009

Pronk, J. T., 2002. Auxotrophic yeast strains in fundamental and applied research. Appl Environ Microbiol. 68, 2095-100. DOI: https://www.doi.org/10.1128/aem.68.5.2095-2100.2002

Qiu, B., Xia, B., Zhou, Q., Lu, Y., He, M., Hasegawa, K., Ma, Z., Zhang, F., Gu, L., Mao, Q., 2018. Succinate-acetate permease from *Citrobacter koseri* is an anion channel that unidirectionally translocates acetate. Cell research. 28, 644-654. DOI: https://doi.org/10.1038/s41422-018-0032-8

Rabitsch, K. P., Toth, A., Galova, M., Schleiffer, A., Schaffner, G., Aigner, E., Rupp, C., Penkner, A. M., Moreno-Borchart, A. C., Primig, M., Esposito, R. E., Klein, F., Knop, M., Nasmyth, K., 2001. A screen for genes required for meiosis and spore formation based on whole-genome expression. Curr Biol. 11, 1001-9. DOI: https://www.doi.org/10.1016/s0960-9822(01)00274-3

Sá-Pessoa, J., Paiva, S., Ribas, D., Silva, I. J., Viegas, S. C., Arraiano, C. M., Casal, M., 2013. SATP (YaaH), a succinate–acetate transporter protein in *Escherichia coli*. Biochemical journal. 454, 585-595. DOI: https://www.doi.org/10.1042/BJ20130412

Salazar, A. N., Gorter de Vries, A. R., van den Broek, M., Wijsman, M., de la Torre Cortes, P., Brickwedde, A., Brouwers, N., Daran, J. G., Abeel, T., 2017. Nanopore sequencing enables near-complete de novo assembly of *Saccharomyces cerevisiae* reference strain CEN.PK113-7D. FEMS Yeast Res. 17. DOI: https://doi.org/10.1093/femsyr/fox074

Singhvi, M., Zendo, T., Sonomoto, K., 2018. Free lactic acid production under acidic conditions by lactic acid bacteria strains: challenges and future prospects. Appl Microbiol Biotechnol. 102, 5911-5924. DOI: https://www.doi.org/10.1007/s00253-018-9092-4

Song, J. Y., Park, J. S., Kang, C. D., Cho, H. Y., Yang, D., Lee, S., Cho, K. M., 2016. Introduction of a bacterial acetyl-CoA synthesis pathway improves lactic acid production in *Saccharomyces cerevisiae*. Metab Eng. 35, 38-45. DOI: https://www.doi.org/10.1016/j.ymben.2015.09.006

Subramanian, M. R., Talluri, S., Christopher, L. P., 2015. Production of lactic acid using a new homofermentative *Enterococcus faecalis* isolate. Microb Biotechnol. 8, 221-9. DOI: https://www.doi.org/10.1111/1751-7915.12133

Sun, P., Li, J., Zhang, X., Guan, Z., Xiao, Q., Zhao, C., Song, M., Zhou, Y., Mou, L., Ke, M., 2018. Crystal structure of the bacterial acetate transporter SatP reveals that it forms a hexameric channel. Journal of Biological Chemistry. 293, 19492-19500. DOI: https://www.doi.org/10.1074/jbc.RA118.003876

van Maris, A. J., Winkler, A. A., Porro, D., van Dijken, J. P., Pronk, J. T., 2004. Homofermentative lactate production cannot sustain anaerobic growth of engineered *Saccharomyces cerevisiae*: possible consequence of energy-dependent lactate export. Appl Environ Microbiol. 70, 2898-905. DOI: https://www.doi.org/10.1128/aem.70.5.2898-2905.2004

Verduyn, C., Postma, E., Scheffers, W. A., van Dijken, J. P., 1990. Physiology of *Saccharomyces cerevisiae* in anaerobic glucose-limited chemostat culturesx. Microbiology. 136, 395-403. DOI: https://www.doi.org/10.1099/00221287-136-3-395

Verduyn, C., Postma, E., Scheffers, W. A., Van Dijken, J. P., 1992. Effect of benzoic acid on metabolic fluxes in yeasts: a continuous-culture study on the regulation of respiration and alcoholic fermentation. Yeast. 8, 501-17. DOI: https://doi.org/10.1002/yea.320080703

Verwaal, R., Wu, L., Damveld, R. A., Sagt, C. M. J., Succinic acid production in a eukaryotic cell In: WIPO, (Ed.). Dsm Ip Assets B.V., 2007.

Walker, B. J., Abeel, T., Shea, T., Priest, M., Abouelliel, A., Sakthikumar, S., Cuomo, C. A., Zeng, Q., Wortman, J., Young, S. K., Earl, A. M., 2014. Pilon: an integrated tool for comprehensive microbial variant detection and genome assembly improvement. PLoS One. 9, e112963. DOI: https://doi.org/10.1371/journal.pone.0112963

Zheng, W., Zhang, C., Wuyun, Q., Pearce, R., Li, Y., Zhang, Y., 2019. LOMETS2: improved meta-threading server for fold-recognition and structure-based function annotation for distant-homology proteins. Nucleic acids research. 47, W429-W436. DOI: https://doi.org/10.1093/nar/gkz384

# SUPPLEMENTARY DATA

**Supplementary Table 1:** Primers used in this study

| Number | Name | Sequence (5' -> 3') | Purpose |
|---|---|---|---|
| 8664 | JEN1_targetRNA FW SspI | TGCGCATGTTTCGGCGTTCGAAACTTCTCCGCAGTGAAAGATAAATGATCGTCACTCAATATTAATTTAC-GTTTTAGAGCTAGAAATAGCAAGTTAAAATAAGGCTAGTCCGTTATCAAC | Construction of pUDR405 |
| 6262 | CrRNA insert ADY2 fw | TGCGCATGTTTCGGCGTTCGAAACTTCTCCGCAGTGAAAGATAAATGATCCCCACCGTAAGAACATAATG-GTTTTAGAGCTAGAAATAGCAAGTTAAAATAAGGCTAGTCCGTTATCAAC | Construction of pUDR405 |
| 6005 | p426 CRISP rv | GATCATTTATCTTTCACTGCGGAGAAG | Construction of pUDR405 – pUDR420 |
| 8691 | ATO3_targetRNA FW SspI | TGCGCATGTTTCGGCGTTCGAAACTTCTCCGCAGTGAAAGATAAATGATCGAGTATATCTCTT-GAATATTGTTTTAGAGCTAGAAATAGCAAGTTAAAATAAG | Construction of pUDR420 |
| 13552 | ATO3_targetRNA_RV_ SspI | CTTATTTTAACTTGCTATTTCTAGCTCTAAAACAATATTCAAGAGATATACTCGATCATTTATCTTTCACTGC-GGAGAAGTTTCGAACGCCGAAACATGCGCA | Construction of pUDR420 |
| 6006 | p426 CRISP fw | GTTTTAGAGCTAGAAATAGCAAGTTAAAATAAGGCTAGTC | Construction of pUDR420 |
| 5921 | Primer_pTEF1_rv | AAAACTTAGATTAGATTGCTATGCTTTCTTTCTAATGAGC | Linear p426-TEF backbone amplification |
| 10547 | p426-GPD backbone rv | TCATGTAATTAGTTATGTCACGC | Linear p426-TEF backbone amplification |
| 13513 | pTEF1_ATO3 | TACAACTTTTTTTACTTCTTGCTCATTAGAAAGAAAGCATAGCAATCTAATCTAAGTTTTATGACATCGTCT-GCTTCTTC | Construction of pUDE813 and pUDE814 |
| 13514 | tCYC1_ATO3 | CGGTTAGAGCGGATGTGGGGGGAGGGCGTGAATGTAAGCGTGACATAACTAATTACATGATTAAGGAG-CATTTGGCATTG | Construction of pUDE813 and pUDE814 |
| 17168 | pTEF1_ADY2_fw | TACAACTTTTTTTACTTCTTGCTCATTAGAAAGAAAGCATAGCAATCTAATCTAAGTTTTATGTCTGACAAG-GAACAAACG | Construction of pUDE1002, pUDE1003 and pUDE1004 |
| 17169 | tCYC1_ADY2_rv | CGGTTAGAGCGGATGTGGGGGGAGGGCGTGAATGTAAGCGTGACATAACTAATTACATGATTA-AAAGATTACCCTTTCAGTAG | Construction of pUDE1002, pUDE1003 and pUDE1004 |
| 17170 | pTEF1_JEN1_fw | TACAACTTTTTTTACTTCTTGCTCATTAGAAAGAAAGCATAGCAATCTAATCTAAGTTTTATGTCGTCGT-CAATTACAGATG | Construction of pUDE1001 |
| 17171 | tCYC1_JEN1_rv | CGGTTAGAGCGGATGTGGGGGGAGGGCGTGAATGTAAGCGTGACATAACTAATTACATGATTAAACG-GTCTCAATATGCTCC | Construction of pUDE1001 |
| 17452 | pTEF1_ATO2_fw | TACAACTTTTTTTACTTCTTGCTCATTAGAAAGAAAGCATAGCAATCTAATCTAAGTTTTATGTCTGACA-GAGAACAAAGC | Construction of pUDE1021 and pUDE1022 |
| 17453 | tCYC1_ATO2_rv | CGGTTAGAGCGGATGTGGGGGGAGGGCGTGAATGTAAGCGTGACATAACTAATTACATGATT-AGAAGAACACCTTATCATTGC | Construction of pUDE1021 and pUDE1022 |
| 17742 | p426_CENARS_fw | TAGAAAAATAAACAAATAGGGGTTCCGCGCACATTTCCCCGAAAAGTGCCACCTGAACGAACGGATC-GCTTGCCTGTAAC | Amplification of CEN6 from pUDC156 |

| Number | Name | Sequence (5' -> 3') | Purpose |
|---|---|---|---|
| 17743 | p426_CENARS_rv | GATAATATCACAGGAGGTACTAGACTACCTTTCATCCTACATAAATAGACGCATATAAGTTC-CCCGAAAAGTGCCACCTG | Amplification of CEN6 from pUDC156 |
| 2949 | F Tag Episomal Rev | CGTTCAGGTGGCACTTTTCG | Construction of pUDC319-pUDC327 |
| 17741 | p426_originremoval | ACTTATATGCGTCTATTTATGTAGGATG | Construction of pUDC319-pUDC327 |
| 1742 | LEU2 check fw | GGTCGCCTGACGCATATACC | *LEU2* amplification |
| 1743 | LEU2 check rv | TAAGGCCGTTTCTGACAGAG | *LEU2* amplification |
| 1738 | HIS3 check fw | GCAGGCAAGATAAACGAAGG | *HIS3* amplification |
| 3755 | his3 outside rv (B) | CACTTGTTCGCTCAGTTCAG | *HIS3* amplification |
| 8597 | JEN1_repair oligo fw | AAGAAGAGTAACAGTTTCAAAAGTTTTTCCTCAAAGAGATTAAATACTGCTACTGAAAAT-TCACTTTTCATTGCTCTCTAGGGCGTGTTCGCTTCTCTATGTAACTGCATTTCACATATA | Deletion of *JEN1* |
| 8598 | JEN1_repair oligo rv | TATATGTGAAATGCAGTTACATAGAGAAGCGAACACGCCCTAGAGAGCAATGAAAAGTGAATTTTCAG-TAGCAGTATTTAATCTCTTTGAGGAAAAACTTTTGAAACTGTTACTCTTCTT | Deletion of *JEN1* |
| 8665 | ADY2_repair oligo fw | CGACAGCTAACACAGATATAACTAAACAACCACAAAACAACTCATATACAAACAAATAATGAGCAC-GACCTACTAATAACGAGAACTATTGAAATAAAAAAGAGTAGTTTTTTATTTTTC | Deletion of *ADY2* |
| 8666 | ADY2_repair oligo rv | GAAAAATAAAAAACTACTCTTTTTTATTTCAATAGTTCTCGTTATTAGTAGGTCGTGCTCATTATTTGTTTG-TATATGAGTTGTTTTGTGGTTGTTTAGTTATATCTGTGTTAGCTGTCG | Deletion of *ADY2* |
| 14120 | ATO3_repair_syn_fw | ATTGAGACGCTCCCCCAGCAGGGTTCGATTGCAGGCGTTTCGCAGGGCAGTAGAATTTCACCTAGACGT-GGCCTTCTTGATGTTGATGTGTACATTGAAGAGCACGTGGGGTTTGTTCT | Deletion of *ATO3* |
| 14121 | ATO3_repair_syn_fw | AGAACAAACCCCACGTGCTCTTCAATGTACACATCAACATCAAGAAGGCCACGTCTAGGTGAAATTC-TACTGCCCTGCGAAACGCCTGCAATCGAACCCTGCTGGGGGAGCGTCTCAAT | Deletion of *ATO3* |

## Plasmid construction

**Supplementary Table 2:** Plasmid construction. Each plasmid was constructed via Gibson assembly of two linear DNA fragments. The template and the primers used to generate those fragments are indicated for each constructed plasmid.

| Name | Relevant characteristic | First fragment | Second fragment | Origin |
|---|---|---|---|---|
| pROS13 | 2µm ampR *kanMX* gRNA-*CAN1* gRNA-*ADE2* | | | (Mans et al., 2015) |
| pMEL13 | 2µm ampR *kanMX* gRNA-*CAN1* | | | (Mans et al., 2015) |
| pUDR405 | 2µm ampR *KAN-MX* gRNA-*JEN1* gRNA-*ADY2* | pROS13<br>8664+6262 | pROS13<br>6005 (binds twice) | This study |
| pUDR420 | 2µm ampR *kanMX* gRNA-*ATO3* | pMEL13<br>6005+6006 | dsDNA oligo formed by:<br>8691+13552 | This study |
| p426-TEF | 2µ URA3 pTEF1-tCYC1 | | | (Mumberg et al., 1995) |
| pUDE813 | 2µ URA3 pTEF1-ATO3-tCYC1 | p426-TEF<br>5921+10547 | CEN.PK113-7D<br>13513+13514 | This study |
| pUDE814 | 2µ URA3 pTEF1-ATO3$^{T284C}$-tCYC1 | p426-TEF<br>5921+10547 | IMS807<br>13513+13514 | This study |
| pUDE1001 | 2µ URA3 pTEF1-JEN1-tCYC1 | p426-TEF<br>5921+10547 | CEN.PK113-7D<br>17170+17171 | This study |
| pUDE1002 | 2µ URA3 pTEF1-ADY2-tCYC1 | p426-TEF<br>5921+10547 | CEN.PK113-7D<br>17168+17169 | This study |
| pUDE1003 | 2µ URA3 pTEF1- ADY2$^{C755G}$ -tCYC1 | p426-TEF<br>5921+10547 | IMW004<br>17168+17169 | This study |
| pUDE1004 | 2µ URA3 pTEF1- ADY2$^{C655G}$-tCYC1 | p426-TEF<br>5921+10547 | IMW005<br>17168+17169 | This study |
| pUDE1021 | 2µ URA3 pTEF1-ATO2-tCYC1 | p426-TEF<br>5921+10547 | CEN.PK113-7D<br>17452+17453 | This study |
| pUDE1022 | 2µ URA3 pTEF1-ATO2$^{T653C}$-tCYC1 | p426-TEF<br>5921+10547 | IMS1122<br>17452+17453 | This study |
| pUDC156 | CEN6 URA3 pTEF-CAS9-tCYC1 | | | Marques *et al.* 2017 |
| pUDC319 | CEN6 URA3 pTEF-tCYC1 | p426-TEF<br>2949+17741 | pUDC156<br>17742+17743 | This study |
| pUDC320 | CEN6 URA3 pTEF1-ATO3-tCYC1 | pUDE813<br>2949+17741 | pUDC156<br>17742+17743 | This study |
| pUDC321 | CEN6 URA3 pTEF1-ATO3$^{T284C}$-tCYC1 | pUDE814<br>2949+17741 | pUDC156<br>17742+17743 | This study |

| Name | Relevant characteristic | First fragment | Second fragment | Origin |
|---|---|---|---|---|
| pUDC322 | CEN6 URA3 pTEF1-JEN1-tCYC1 | pUDE1001<br>2949+17741 | pUDC156<br>17742+17743 | This study |
| pUDC323 | CEN6 URA3 pTEF1-ADY2-tCYC1 | pUDE1002<br>2949+17741 | pUDC156<br>17742+17743 | This study |
| pUDC324 | CEN6 URA3 pTEF1- ADY2$^{C755G}$ -tCYC1 | pUDE1003<br>2949+17741 | pUDC156<br>17742+17743 | This study |
| pUDC325 | CEN6 URA3 pTEF1- ADY2$^{C655G}$-tCYC1 | pUDE1004<br>2949+17741 | pUDC156<br>17742+17743 | This study |
| pUDC326 | CEN6 URA3 pTEF1-ATO2-tCYC1 | pUDE1021<br>2949+17741 | pUDC156<br>17742+17743 | This study |
| pUDC327 | CEN6 URA3 pTEF1-ATO2$^{T653C}$-tCYC1 | pUDE1022<br>2949+17741 | pUDC156<br>17742+17743 | This study |

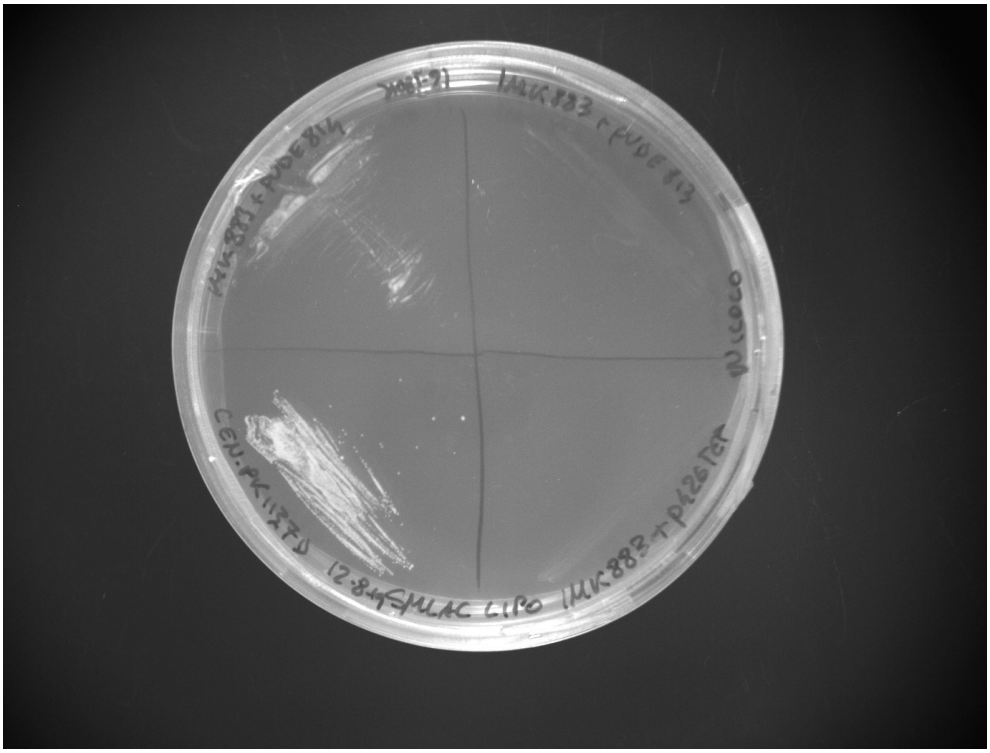

**Supplementary Figure 1:** Growth of different strains on SM media with lactic acid as the sole carbon source. Bottom left quadrant: prototrophic strain CEN.PK113-7D. Bottom right quadrant: IMK883 (*ura3-52, jen1Δ, ady2Δ, ato3Δ*) carrying an empty p426-pTEF plasmid. Top right quadrant: IMK883 carrying pUDE813 (p426-p*TEF-ATO3*). Top left quadrant: IMK883 carrying pUDE814 (p426-p*TEF- ATO3*$^{T284C}$). Cells were streaked from a single colony and the plate was incubated at 30 °C for 5 days.

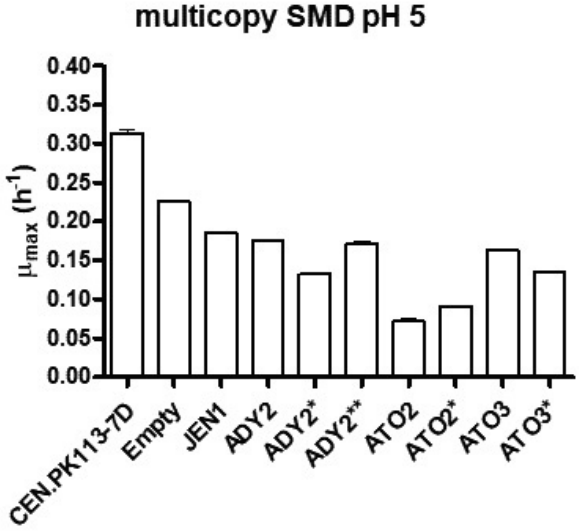


**Supplementary Figure 2:** Growth rates on SMD of *S. cerevisiae* reference strain CEN.PK113-7D and the 25-transporter deletion strain IMX2488 expressing an empty multicopy vector or a multicopy vector containing the indicated organic acid transporter gene. Bars and error bars represent the average and standard deviation of three independent experiments. Empty: empty plasmid. ADY2*: *ADY2*$^{C755G}$ allele. ADY2**: *ADY2*$^{C655G}$ allele. ATO2*: *ATO2*$^{T653C}$ allele. ATO3*: *ATO3*$^{T284C}$ allele.

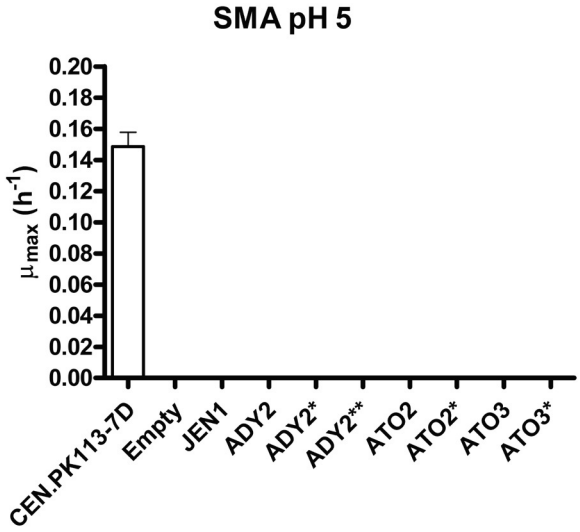


**Supplementary Figure 3:** Growth rates of *S. cerevisiae* reference strain CEN.PK113-7D and the 25-transporter deletion strain IMX2488 expressing an empty centromeric vector or a centromeric vectors containing the indicated organic acid transporter gene. Growth on SMA medium set at pH5. Bars and error bars represent the average and standard deviation of three independent experiments.Empty: empty plasmid. ADY2*: *ADY2*$^{C755G}$ allele. ADY2**: *ADY2*$^{C655G}$ allele. ATO2*: *ATO2*$^{T653C}$ allele. ATO3*: *ATO3*$^{T284C}$ allele.

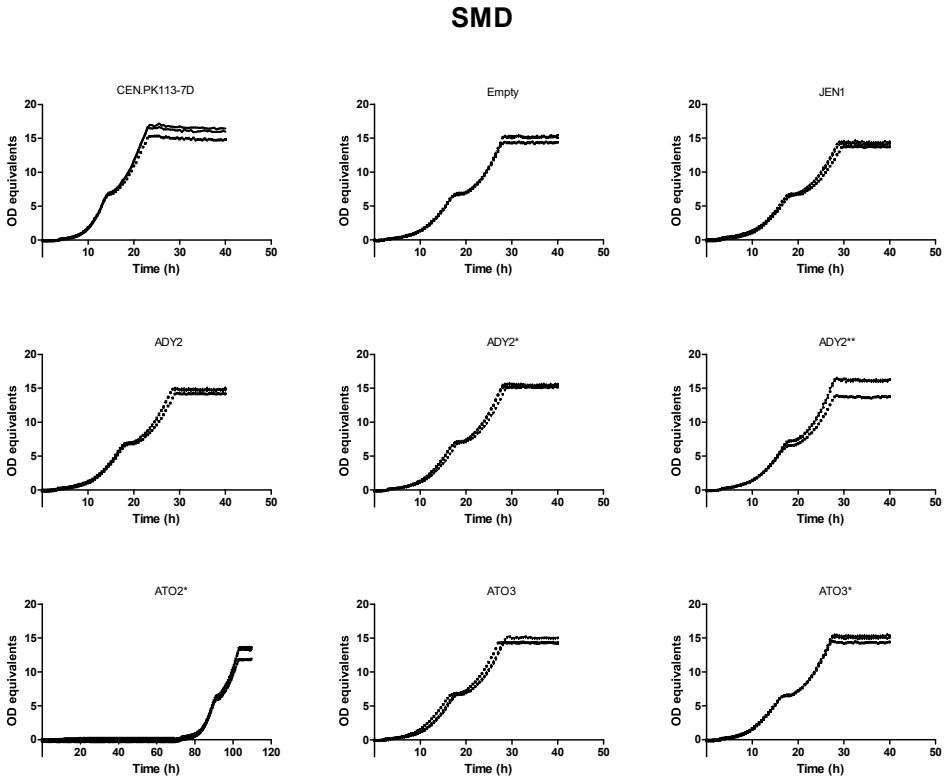


**Supplementary Figure 4:** Growth profiles in synthetic medium (pH 5.0) with glucose as the sole carbon source of CEN.PK113-7D and the 25-transporter deletion strain IMX2488 expressing an empty multicopy vector or a multicopy vector containing the indicated organic acid transporter gene. Empty: empty plasmid. ADY2*: *ADY2*$^{C755G}$ allele. ADY2**: *ADY2*$^{C655G}$ allele. ATO2*: *ATO2*$^{T653C}$ allele. ATO3*: *ATO3*$^{T284C}$ allele.

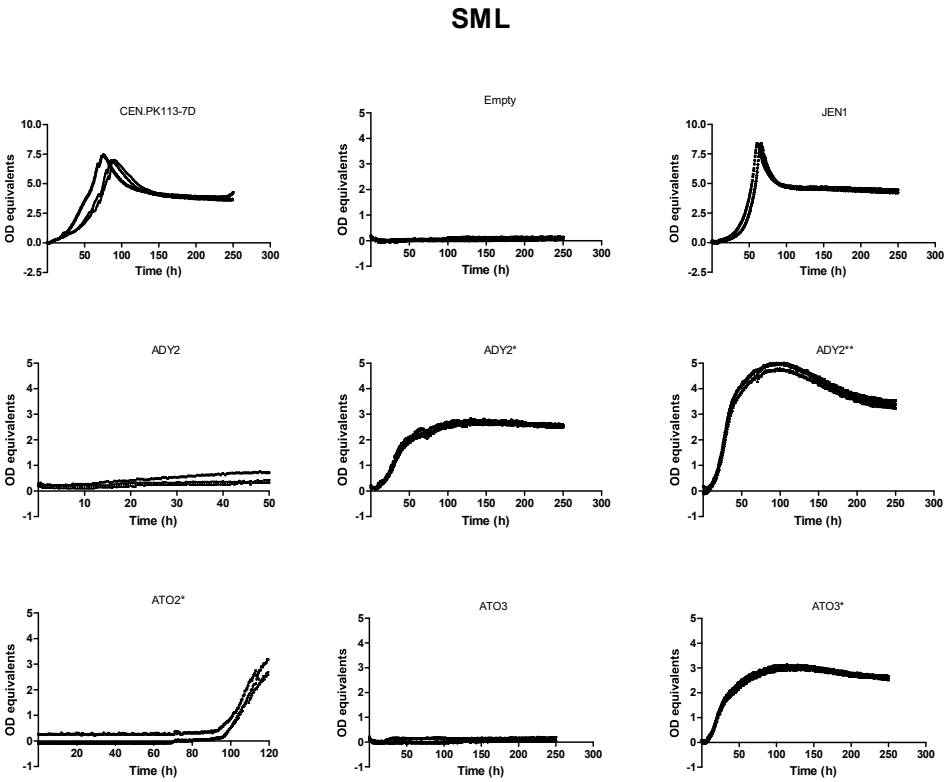


**Supplementary Figure 5:** Growth profiles in synthetic medium (pH 5.0) with lactate as the sole carbon source of CEN.PK113-7D and the 25-transporter deletion strain IMX2488 expressing an empty multicopy vector or a multicopy vector containing the indicated organic acid transporter gene. Empty: empty plasmid. ADY2*: *ADY2*$^{C755G}$ allele. ADY2**: *ADY2*$^{C655G}$ allele. ATO2*: *ATO2*$^{T653C}$ allele. ATO3*: *ATO3*$^{T284C}$ allele.

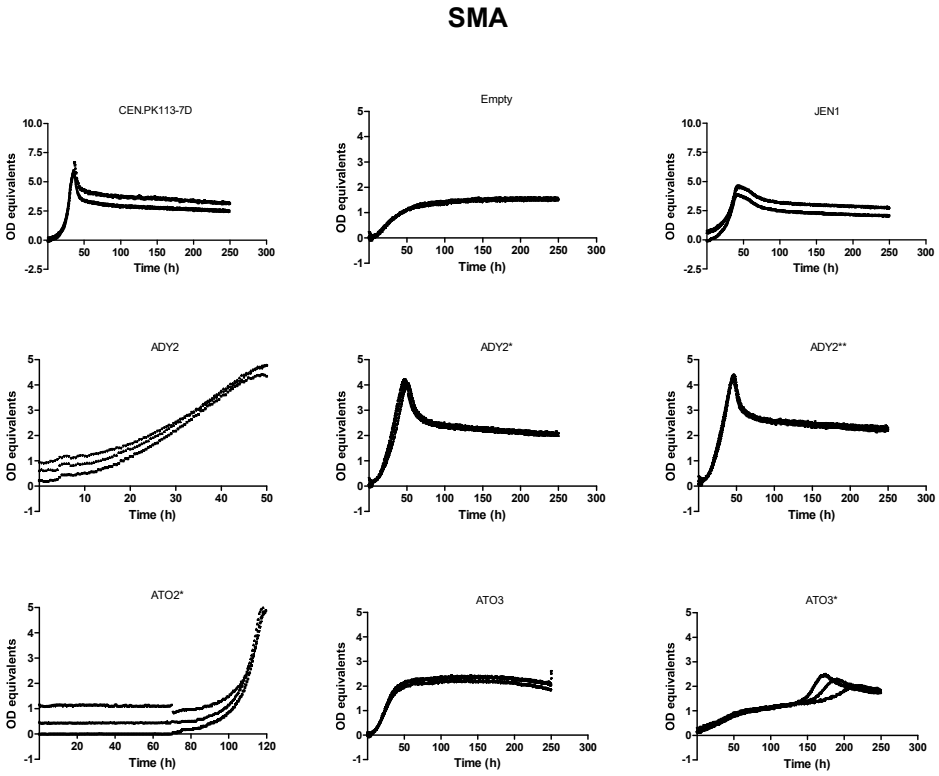


**Supplementary Figure 6:** Growth profiles in synthetic medium (pH 6.0) with acetate as the sole carbon source of CEN.PK113-7D and the 25-transporter deletion strain IMX2488 expressing an empty multicopy vector or a multicopy vector containing the indicated organic acid transporter gene. Empty: empty plasmid. ADY2*: *ADY2*$^{C755G}$ allele. ADY2**: *ADY2*$^{C655G}$ allele. ATO2*: *ATO2*$^{T653C}$ allele. ATO3*: *ATO3*$^{T284C}$ allele.

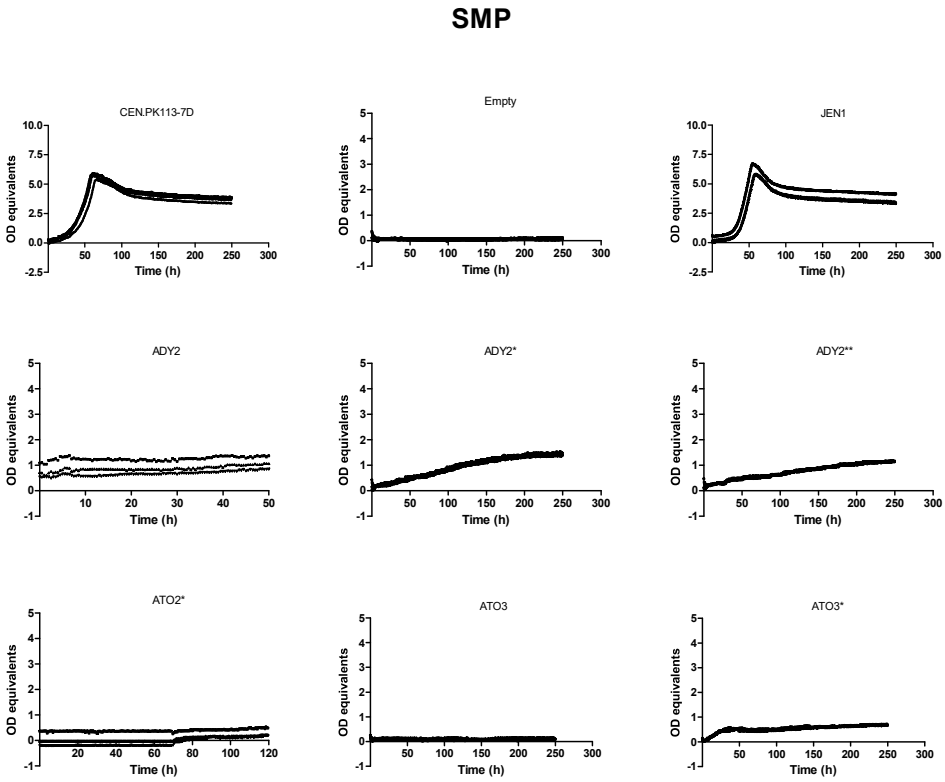


**Supplementary Figure 7:** Growth profiles in synthetic medium (pH 5) with pyruvate as the sole carbon source of CEN.PK113-7D and the 25-transporter deletion strain IMX2488 expressing an empty multicopy vector or a multicopy vector containing the indicated organic acid transporter gene. Empty: empty plasmid. ADY2*: *ADY2*$^{C755G}$ allele. ADY2**: *ADY2*$^{C655G}$ allele. ATO2*: *ATO2*$^{T653C}$ allele. ATO3*: *ATO3*$^{T284C}$ allele.

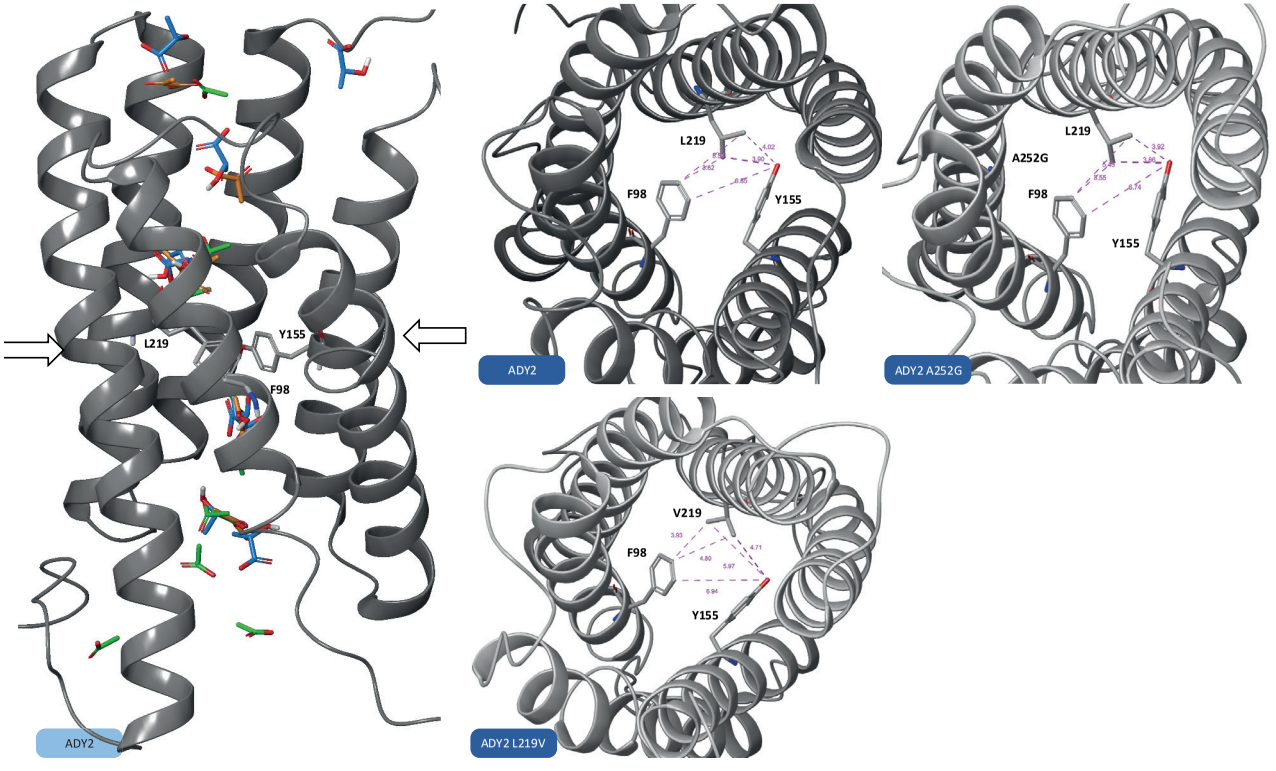


**Supplementary Figure 8:** 3D model of Ady2 and different mutants (as indicated in the blue boxes). Left, side view of Ady2. Arrows indicate the hydrophobic constriction site. Right, top view of either Ady2 or different mutants (as indicated). The amino acids involved in the hydrophobic constriction site are shown. Purple lines and values indicate distances (in Å) between different anchor points of amino acids.

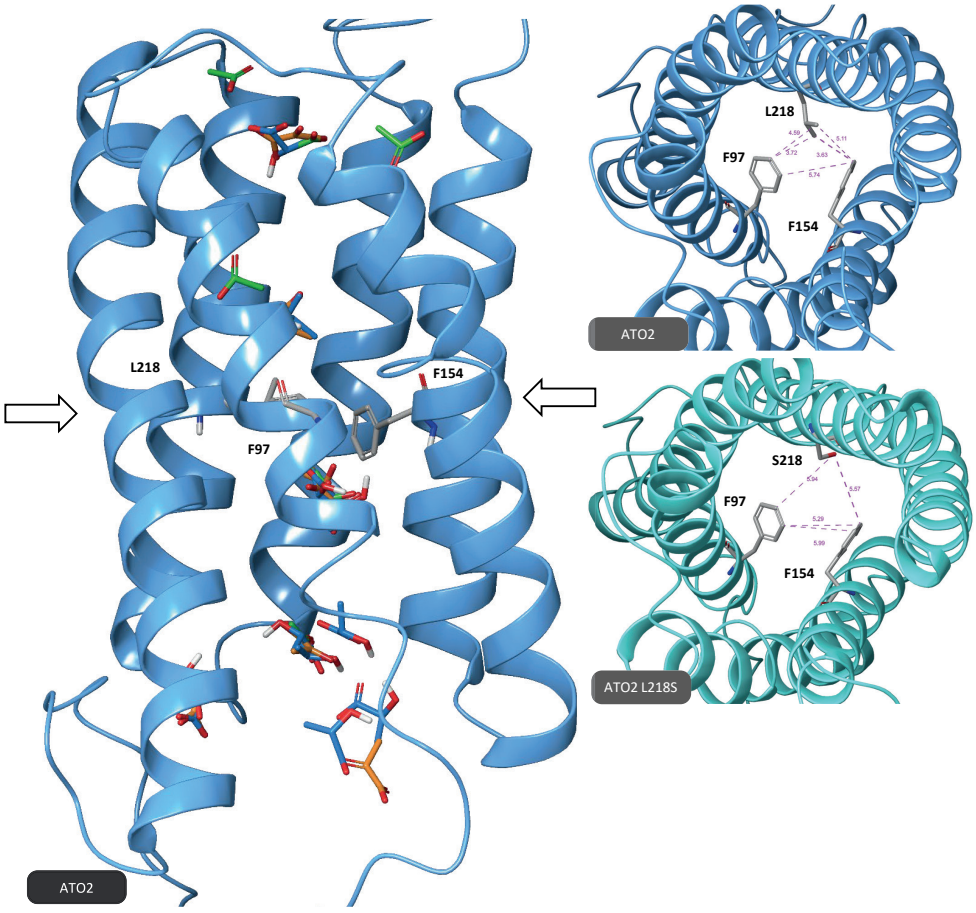


**Supplementary Figure 9:** 3D model of Ato2 and different alleles (as indicated in the blue boxes). Left, side view of Ato2. Arrows indicate the constriction site. Right, top view of either Ato2 or different alleles (as indicated). The amino acids involved in the constriction site are shown. Purple lines and values indicate distances (in Å) between different anchor points of different amino acids.

| 3D-Protein templates | Average of binding affinities (kcal/mol) at different binding sites | | | | | | | | |
|---|---|---|---|---|---|---|---|---|---|
| | Acetate | | | | | | | | |
| | 1 | | | 2 | 3 | 4 | | | |
| | a | b | c | | | a | b | c | |
| Ady2 | -2,1 | -2,4 | -2,3 | -2,7 | -3,1 | -2,7 | - | - | |
| Ady2 A252G | -2,3 | -2,2 | -2,1 | -3,1 | -3,1 | -2,6 | -2,7 | - | |
| Ady2 L219V | -2,4 | - | - | -3,0 | -3,0 | -2,5 | -2,7 | - | |
| Ato2 | -2,5 | -2,6 | - | -3,1 | -2,9 | -2,8 | -2,9 | -3 | |
| Ato2 L218S | -2,7 | - | - | -2,7 | -3,1 | -3,3 | -2,6 | -2,5 | |
| Ato3 | -2,3 | -2,2 | - | -2,9 | -3,0 | -2,2 | - | -2,4 | |
| Ato3 F95S | -2,6 | -2,4 | - | -3,0 | -2,9 | -2,4 | -2,4 | -2,4 | |
| | Lactate | | | | | | | | |
| | 1 | | | 2 | 3 | 4 | | | |
| | a | b | c | | | a | b | c | d |
| Ady2 | - | -3,1 | -3,0 | -3,6 | -4,3 | -3,5 | -3,1 | -3,1 | - |
| Ady2 A252G | -2,9 | -2,8 | -2,7 | -3,7 | -4,4 | -3,3 | -3,4 | - | -2,1 |
| Ady2 L219V | -3,4 | - | - | -3,9 | -4,4 | - | -3,8 | - | - |
| Ato2 | -3,2 | -3,1 | -3,2 | -3,9 | -3,8 | - | -2,9 | - | - |
| Ato2 L218S | -3,5 | - | - | -3,8 | -4,2 | -3,6 | - | -3,4 | - |
| Ato3 | - | - | - | -3,4 | -3,8 | -3,1 | - | -3,2 | - |
| Ato3 F95S | -3,3 | - | - | -4,2 | -4,0 | -3,2 | -3,2 | -3,2 | - |
| | Pyruvate | | | | | | | | |
| | 1 | | | 2 | 3 | 4 | | | |
| | a | b | c | | | a | b | c | |
| Ady2 | - | -3,1 | - | -3,7 | -4,2 | -3,2 | -3,3 | - | |
| Ady2 A252G | -3,0 | - | -2,7 | -3,9 | -4,3 | -3,3 | -3,3 | - | |
| Ady2 L219V | -3,2 | - | - | -4,0 | -4,2 | - | -3,5 | - | |
| Ato2 | -3,3 | -3,3 | -3,1 | -3,9 | -4,1 | - | -3,6 | - | |
| Ato2 L218S | -3,5 | - | - | -3,9 | -4,3 | - | - | -3,3 | |
| Ato3 | - | - | - | -3,6 | -4,0 | -3,0 | - | -3,2 | |
| Ato3 F95S | -3,4 | - | - | -4,2 | -3,9 | - | -3,4 | - | |

**Supplementary Table 3:** Average of the binding affinity values [kcal/mol] calculated with PyRx software for the docking of ligand in the predicted structures of wildtype and mutated Ady2, Ato2 and Ato3.

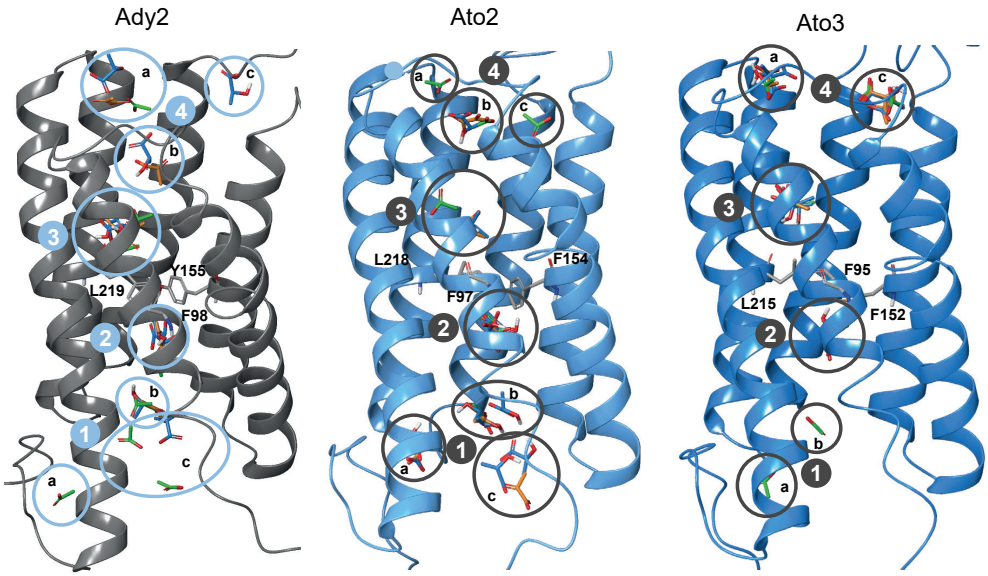


**Supplementary Figure 10** Molecular docking sites of acetate (green ligand), lactate (blue ligand) and pyruvate (orange ligand) in the predicted structure of Ady2, Ato2 and Ato3, identified using Autodock Vina.

**Supplementary Table 4:** Residues identified by molecular docking analysis as being involved in the establishment of strong intramolecular interactions with the indicated ligand.

| 3D-Protein templates | Acetate | Lactate | Pyruvate |
|---|---|---|---|
| Ady2 | N89, N145, S208, T222, H23O (IL), T262 | N89, T102, S106, Q133, E140, N145, D182, S208, T222, G229, H230, T238 | N145, S208, T222, H230, T238 |
| Ady2 L219V | Y176, T209, T222, H230, T238, N255 | T102, N109, Y176, T209, T222, H230, N255 | N109, Y166, Y176, T222, T209, H230, N255 |
| Ady2 A252G | N109, R111(IL), Q133, N145, Y176, T209, T222, H230 (IL), T238, N255, | K86, T102, N109, R111(IL), Q133, N145, Y176, T209, T222, H230(IL), T238, N255, G259, T262 | Y176, R111(IL), T209, T238, T222, H230, N255, T262 |
| Ato2 | Q132, N229, K176(IL), Y175, T237, T221, S207 | T101, Q132, N144, S207, T221, N229, T237, N254, T261, R262(IL) | H84, K85(IL), Q132, S207, T221, N229, T237, T261, N254 |
| Ato2 L218S | K176, S180, T208, S218, T221, N229, T237 | S105, Q132, D173, A174, K176, D177, S180, L182, T208, T221 | D173, K176, S180, L182, T208, T221 |
| Ato3 | N106, Y173, T205, T218, M271 | C99, N106, G162, Y173, T218, N230 | N106, Y173, T218 |
| Ato3 F95S | S95, N106, T218, K234, S258 | S95, N106, C158, Y159, T218, D229, N231, K234, S244, S251 | S95, N106, T218, K234, S258 |

# Outlook

Currently, cost-competitive production of commodity chemicals by means of microbial biotechnology is possible for only a small number of compounds. Many potential products remain in the proof-of-concept phase because product titer, production rate and yield are too low to justify an investment in full-scale processes. In addition to balanced expression of enzymes that couple product formation to the central carbon metabolism of the microbial host, sufficient and efficient supply of precursors derived from central carbon metabolism is a key prerequisite for optimal product formation. The research presented in this thesis has led to new insights in modification of the central carbon metabolism of *Saccharomyces cerevisiae* to improve production of two of these precursors, acetyl-CoA and succinyl-CoA, in the yeast cytosol. In addition, new information was obtained on the impact of mutator genotypes in laboratory evolution experiments and on the genetic plasticity of lactate transport in *S. cerevisiae*.

Chapter 2 investigates re-routing the entire dissimilatory carbon flux through acetyl-CoA via a cytosolically expressed bacterial pyruvate dehydrogenase, by a combination of metabolic engineering and prolonged adaptive laboratory evolution. Strains in which dissimilatory metabolism was re-routed through this novel pathway were obtained in evolved, lactate-grown cultures. This result demonstrated that fluxes through this ATP-independent pathway for cytosolic acetyl-CoA synthesis in *S. cerevisiae* can be increased to levels relevant for product formation. However, before this concept can be flexibly applied in industrial strains that produce cytosolic-acetyl-CoA-dependent products, it is essential to elucidate the molecular basis for fast *in vivo* operation of the pyruvate dehydrogenase. Unfortunately, the molecular mechanism underlying the fast growth of the evolved strains remains elusive. This was to a large extent caused by the emergence, in multiple instances, of a mutator phenotype, which strongly increased by the number of mutations found in the genomes of cultures subjected to prolonged laboratory evolution, in some cases to over 500 per genome.

The emergence of a rare mutator phenotype in several independently evolved strains indicated that multiple, simultaneous mutations are likely to be needed for the establishment of an efficiently functioning pathway. Both from the viewpoint of industrial relevance and because the results described in Chapter 2 represent an intriguing metabolic and genomic puzzle, identification of the relevant mutations and their reverse engineering into industrial strains remains a highly relevant goal. The use of high-throughput strain engineering systems and/or backcrossing of evolved strains to 'dilute' non-causal mutations can be relevant experimental strategies to achieve this objective.

Despite the challenge in the unraveling a possible mechanism solely based on genome sequence data, we hypothesized that faster growth of the evolved strains may be due to a partial location of Ach1 in the yeast cytosol. Cytosolic Ach1 might contribute to provision of small amounts of cytosolic acetate which, after mitochondrial import and subsequence transfer of CoA from succinyl-CoA by mitochondrial Ach1, could provide mitochondrial acetyl-CoA for essential biosynthetic reactions. Although Ach1 is generally described to be a mitochondrial enzyme, the data on Ach1 localization provided by (Buu et al., 2003) do not completely exclude its presence in the cytosol. Therefore, accurate localization studies should be performed in order to clearly establish the intracellular localization of Ach1 and its potential role of acetyl-CoA 'shuttling' between cytosol and mitochondria.

Although hardly a welcome result in the context of this thesis, the mutator genotypes found in Chapter 2 are of scientific interest in their own right. While in the majority of cases an increased mutation rate was attributed to loss-of-function mutations in *MSH6*, three strains eluded efforts to explain their high mutation frequency. Further analysis of these elusive mutator phenotypes may enable identification of novel DNA-repair or DNA-damaging mechanisms. While hampering the reverse engineering of industrially relevant traits, purposefully inducing a mutator phenotype could be used to aid or accelerate the selection of new metabolic features in adaptive laboratory evolution experiments, especially where previous attempts have not succeeded in selecting advantageous phenotypes.

The results shown in **Chapter 2** were aimed at reducing the ATP cost associated with acetyl-CoA biosynthesis via a pathway that had previously already been shown to sustain low rates *in vivo* rates of cytosolic acetyl-CoA production. In contrast, the research showed in **Chapter 3** describes the first demonstration of the synthesis of cytosolic succinyl-CoA in *S. cerevisiae*. This result expanded the potential the product range for this already versatile microbial host. Our proof-of-principle results demonstrated formation of the small amounts of the heme precursor aminolevulinic acid. Further research can now explore additional metabolic engineering strategies for producing industrially relevant product levels, not only of aminolevulinic acid, but also of industrially relevant compounds such as 1,4-butanediol, γ-aminobutyrate and γ-hydroxybutyric acid. Although not included in this thesis, preliminary research was performed into further engineering of the succinyl-CoA producing strains to synthesize of 4-hydroxybutyric acid. Although trace amounts of this compound were detected by mass spectrometry, concentrations were below quantification

limit (low µM range). Oxygen sensitivity of the introduced heterologous 4-hydroxybutyrate dehydrogenase may well explain this low attained product concentration. In future research, it may be attempted to circumvent this problem by growing engineered yeasts in an oxygen-limited chemostat cultures.

Related to the subject discussed in Chapter 3, succinyl-CoA metabolism in yeast still presents a metabolic conundrum: what is the source of the succinyl-CoA which, according to Weinert et al. (2013) is used for succinylation of yeast? A large body of experiments, which were not included in this thesis, were aimed at establishing the possible presence of a succinyl-CoA pool in the cytosol of non-engineered *S. cerevisiae* strains. Preliminary results do indeed strongly point in this direction, but refuting a commonly held assumption that succinyl-CoA is exclusively located in the mitochondria and identifying the source of cytosolic succinyl-CoA in wild-type *S. cerevisiae* requires further research. If successful, it will be intriguing to investigate the condition-dependent effect of eliminating cytosolic succinyl-CoA production and, thereby, protein succinylation in yeasts and, perhaps, even in human cell lines.

The research described in **Chapter 4** gives insights into the genetic plasticity of lactate transport in *S. cerevisiae*, and illustrates how adaptive laboratory evolution experiments can shed light on novel or extended gene functions. In this study, we identified and characterized evolved alleles of the genes *ATO2* and *ATO3* as novel lactate transporters by means of whole-genome sequencing, reverse engineering and strain characterization. In an inspiring collaboration with researchers from the University of Minho, it was possible to infer how the observed mutations affected the three-dimensional structures of the Ato2 and Ato3 proteins to change their substrate specificities. This combination of genome resequencing and reverse engineering with structural analysis is a powerful approach for adaptive laboratory evolution strategies, which can even help predict additional, industrially relevant alleles that have not (yet) been observed in laboratory evolution experiments.

Despite having identified two new lactate transporters, Chapter 4 did not yet solve the longstanding question by which mechanism *S. cerevisiae* exports lactate. Further laboratory evolution experiments, perhaps with the induction of a mutator phenotype, may provide further clues on this riddle, which has eluded yeast researchers for almost 20 years.

## References

Buu, L. M., Chen, Y. C., Lee, F. J., 2003. Functional characterization and localization of acetyl-CoA hydrolase, Ach1p, in *Saccharomyces cerevisiae*. J Biol Chem. 278, 17203-9. DOI: https://doi.org/10.1074/jbc.M213268200

Weinert, B. T., Scholz, C., Wagner, S. A., Iesmantavicius, V., Su, D., Daniel, J. A., Choudhary, C., 2013. Lysine succinylation is a frequently occurring modification in prokaryotes and eukaryotes and extensively overlaps with acetylation. Cell Rep. 4, 842-51. DOI: https://doi.org/10.1016/j.celrep.2013.07.024

# Acknowledgments

The journey to get to this moment was a long and challenging one. Along the way, I had the privilege to meet brilliant, amazing and inspiring people, and I hope to convey my gratitude to you.

**Ton**, thank you for taking me on board in IMB, and for still saying “no problem” after I told you that, at the earliest, I could start in eight months’ time from the moment you offered me the position. Despite having a short overlap of our stays at TU Delft, I very much enjoyed your supervision.

**Jack**, there are so many things to thank you for. Despite you moving higher and higher in the academic/managerial ladder, you always found the time to have a chat, and more often than not within the day! If that’s not a superpower, I do not know what is! After weeks of failed experiments, with strains either refusing to grow or growing at 0.00-nooo rates (read “o-point-o-o-nooo”), I would come battered to your office, and yet, you would boost my morale, with your endless optimism and your ability to see the bright into the (scientifically or else) darkest hours. Despite filled with failed experiments, science is also fun! And you never missed an occasion to remind me (or anybody) of that, didn’t matter if it was just a simple, already proven experiment, or if a scientific breakthrough just happened: science is fun! And when breakthroughs came, they were often accompanied by your joyous giggle and excitement. Working together with you was a great honor Jack!

This project about yeast energetic metabolism would have not gone far without you, **Robert**. The jump from “ancient PhDer” to “baby PI” happened swiftly, and in the same swift way you demonstrated that the adjective “baby” had no place there. You also showed that science was a fun business, and more often than not you were peeking into the lab, popping out of thin air and curiously looking around when a new machine arrived or when the time to take a critical sample came. Inadvertently, when you moved to Denmark for your sabbatical, you gave Aafke, Sophie, Hannes and me a taste of what a life with regular online meetings would look like. When the whole world switched to home-based working,

we definitively had an edge there[5]! And even if you were in Denmark for quite a while, it never felt like you were gone. You would always reply within the day, and if necessary, you would set up a meeting within the hour. I really admire that and I am deeply grateful for the care you put in the development of your newly formed group. That energy and care was not only put into science, but also into people, something that is to be admired! And post-its… oh didn't you put some care in post-its!?

**Anna**, there are many things I am thankful for! From our dinners and boardgames nights, to the awesome time we had skiing down the slopes. I am deeply honored to have you as my paranymph, and for having had the opportunity to get to know you. More than a colleague or an office mate, you are a friend, a confidant, and a dispenser of relationship advice which I regret to not have followed. I promise you, that you can trust me.

**Charlotte**, I think the world's meme collection has gone through our phones. We had a kick for giving a fabulous vibe to equipment in the lab, and for making puns which would cause by-standers to perform a 10/10 facepalm. I feel privileged for having you as my paranymph, and also a little bit terrified, given the number of pictures and stories you have. You are a dear friend, and I am lucky to have met you! Also, thank you for teaching me that being weak can also not be too bad.

**Marijke**, a lot of the work contained in this thesis would not have been possible without you. We spent days and nights full of action, isolating mitochondria like there was no tomorrow, having dinner with pizza and coffee, sharing "mini heart attack" moments when I thought I injected the cell extract in the waste stream… You taught me so much, and I don't mean scientifically (well, also that!). This journey, from colleagues to friends, has been amazing, and I loved sharing it with you. In the same way that we went on to share many things, from coffee cups, to chocolate cookies (a big shoutout to **Laura**), to many long and deep conversations… to so many memes!

**Pilar**, your help in the past years has been essential! More often than not, when it was not going great, you were there to cheer me up, reminding me that a PhD is not all there is to life. Working together with you has been amazing, and I already miss our chats in the sequencing lab, between one sample and another. In truth, I already miss you!

**The Energetics**… Thank you for these fantastic years of discussion on the inner workings of, guess what, the energetics of cerevisiae and 'Hannesula' (para)polymorpha (this is the only occasion our little buddies may be mentioned in such writing style). **Robert** and **Hannes**, thank you for helplessly giggling at the slightest mention of *Enterococcus faecalis*, and for providing incredibly detailed explanations for my questions about P/O ratios, substrate consumption rates and more. **Hannes**, your expertise in fermentation and data analysis ("it's invisible!") was always appreciated! As were the walks to the sport center to have

5 This thesis was written between February and August 2020, at the height of the COVID-19 pandemic

dinner, where we would stay for too long, and we would then go back home rather than continue working. I am still waiting for you to send me pictures of 'strange planet'! **Sophie**, you inherited the lactic acid research line, but saying that alone would not do you justice. You were an integral part of this work, and quite possibly all the data of the growth studies would not have come to light if it wasn't for your perseverance in making the growth profiler work! I am sure that, with your number 5, you get a step closer to unraveling the mystery of lactic acid transport. **Aafke**, you are a perfect fit for this group, and it was a pleasure working with you.

**Arthur**, despite you being one of the most hard-working people I know, you showed me (and us all!) that doing a PhD does not automatically imply a ban from partying and from having a social life. You are the catalyst that brings a group together towards doing something fun! But more than a catalyst, you are a great scientist, a great consultant, and a great friend. Thank you for letting me stay at your place that fateful party night in Den Haag, and for then letting me stay in as a housemate. Thanks for listening to what troubled me, and for feeling confident to share with me what troubles you.

**Xavier**, thank you for never answering 'yes' or 'no' to a simple question, and for proceeding instead to unraveling the inner workings of metabolism and microbial physiology. Nog meer, heel veel dank voor het niet meteen teruggaan naar Engels, als ik probeer om in het Nederlands te praten. Je gaf me het vertrouwen om Nederlands te beginnen spreken. Also, thank you for practically demonstrating what not to do in case you are stuck at the top of a ski slope.

**Susan**, given the energy that you emanate, you should have been in Energetics! Thank you for making the time for helping me when the HPLC would, for one reason or another, stop working, for the countless beers at the botanical garden, and for all the fun we had on the ski slopes and on our beach retreats!! Your wonderful son Jorre is lucky to have such a great mom!

**Jasmine**, I can still imagine you inexplicably bursting into laughter moments before the plane would take off (inexplicably, that is, from the point of view of the passengers). That must have creeped out the passengers right next to you! Thank you for giving me moments like that, were we would laugh at the simple funny things. Also thank you to host so many fondue-based parties, and for entrusting me to be your paranymph, despite knowing my sense of humor and how much material I gathered in the past.

**Jasmijn**, you are one of the fires fueling the spirit of IMB. You bring so much energy! Between technical discussions over the role of the PDCs in *S. cerevisiae*, and the various dinners and wine tastings, there has not been a boring moment around you. You have been a source of inspiration, and I am looking forward to read your manuscript! Also, you are the best conference companion one might hope to have, and you definitively rose the bar with your presentation!

Dear **Mark**, Mr. Baldi here. I must say, I never wanted to participate in the competition for the slowest yeast strain, but yet, I am glad you won! I don't think many people can claim that their strains have growth rates with two zeros after the comma… we are part of an exclusive club! I will miss our coffee breaks in your office, which would come included with insightful discussions over the inner workings of *S. cerevisiae*, and with lots of laughter over terrible, terrible jokes.

**Erik**, despite you being a bit-bloody-cynical at times (your words!) you are on top of it! You make sure everyone has what they need, whether that is in the lab or in the office. Thank you for your help in setting up my reactors, in accommodating my runs in the planning (a herculean task, with strains capable of having a month-long lag phase) and for introducing me to climbing!

**Jean-Marc**, thank you for stepping in during my promovendus meetings! You always had those out-of-the-box solutions to help me get unstuck. I see that, under your direction, IMB is set on a path to do some great work!

**Pascale**, teaching alongside you was a wonderful experience! I really enjoyed the opportunity to give lectures, and to be part of the MR groupworks. I will miss the long days and late nights correcting exams with you, **Anna** and **Eline**. We made quite the team!

**Kirsten** and **Liang**, thank you for the fruitful discussions we had. I much enjoyed our collaboration.

To **Marc Strampraad**, **Martin Pabst**, **André Vente**, **Maria**, **Margarida**, **Isabel** and all the other colleagues that were part of my project, thank you for the great collaboration!

I was fortunate enough to have a group of wonderful students to join me in this quest. **Fieke**, **James**, **Siem**, **Damien**, **Demi**, **Remon**, **Thijs** and **David**, you might think I taught you something, but truth is you taught me much more than you can imagine! Not many of the research lines you worked on ended up in this thesis, but rest assured, the insights you generated were fundamental in shaping it, and for that I am deeply grateful!

**Apilena**, **Astrid** and **Jannie**, IMB would collapse if it wasn't for you! Thank you for being always so supporting, for your snacks, your hugs!

To all you current and past IMBers, **Ioannis**, **Francine**, **Sofia**, **Paola**, **Christiaan**, **Flip**, **Aurin**, **Maria**, **Thomas**, **Mario**, **Jordi**, **Ewout**, **Jasper**, **Eline**, **Wijb**, **Sanne**, **Jonna**, **Anja**, **Wesley**, **Michelle**, **Melanie**, thank you for making IMB the great place it is! Working together with such brilliant minds has been an honor! And it's almost inevitable that I might have forgotten someone, but if I did, please rest assure that I was honored to work with you!

Stepping outside of the people working directly or indirectly with me, it is now time to acknowledge some who were there for me behind the scenes.

**Enrico**, you have been, in these past years, a friend, a role model, and a person who I know I could confide to. Thank you for listening to me, and for sharing with me things that troubled you. But most of all, I want to thank you for the advice you gave me on that fateful night in summer 2016… You, quite literally, saved my life there.

Too often the role of psychologists in the development of a PhD candidate goes unnoticed. **Jack C.**, thank you for helping me out in, quite possibly, the most obscure part of my life. What we discussed was not necessarily related to doing a PhD, but it most definitively helped in that. **Barlas**, you have been pivotal in my development as a researcher, but most importantly as a person. You taught me the value of compassion and self-forgiveness, and you helped me in accepting myself, my limitations, and taught me that being a perfectionist does more harm than good. But also, you taught me that, despite the fact that the things I worked on might be relevant for the public in a distant future, they are utterly irrelevant in what concerns my personal life. Learning to detach myself has been one of the most helpful skills you could teach me to stay sane, and I deeply thank you for that.

Lastly, I want to thank my family, for their continuous support for these 7 years I have been far away from home. **Mamma**, **Papà**, thank you for believing in me when I first left for college. Without your love and support, I would not have made it where I am now.

# Biography

Nicolò Baldi was born in Rome, in 1991. In 2010, he started attendance at the University of Bologna to pursue a BSc in biotechnology. Granted an Erasmus Mundus scholarship, he spent a semester abroad in Madrid, Spain, to perform his Bachelor thesis in the laboratory of Maria Gomez, where he studied the relationship between the position of nucleosomes on the DNA and the initiation sites of DNA replication. After graduating *cum laude* in 2010, he moved to the Netherlands to pursue a Master in cellular and molecular biotechnology at Wageningen University and Research. Here he performed a first Master end project under the supervision of Ruud Weusthuis, attempting at engineering the metabolism of *Escherichia coli* for $CO_2$ fixation. After that, he performed a second Master end project under the supervision of Stan Brouns, where he studied the mechanism of DNA glucosylation of the bacteriophage T4. In 2016, he joined the Industrial Microbiology group (IMB) in Delft to pursue a PhD, the results of which are contained in this dissertation.

# List of publications

**Baldi, N.**, Dykstra, J. C., Luttik, M. A., Pabst, M., Wu, L., Benjamin, K. R., Vente, A., Pronk, J. T. & Mans, R. (2019). Functional expression of a bacterial α-ketoglutarate dehydrogenase in the cytosol of *Saccharomyces cerevisiae*. Metabolic engineering, 56, 190-197.

**Baldi, N.**, de Valk, S., Sousa-Silva, M., Casal, M., Soares-Silva, I. & Mans, R. (2021). Evolutionary engineering reveals amino acid substitutions in Ato2 and Ato3 that allow improved growth of *Saccharomyces cerevisiae* on lactic acid. FEMS Yeast Research.

ISBN: 978-94-6423-270-7